

**Advancing Boron Mediated Fluoroalkylation Reactions**

by

Michael McCreery Wade Wolfe

A dissertation submitted in partial fulfillment  
of the requirements for the degree of  
Doctor of Philosophy  
(Chemistry)  
in the University of Michigan  
2022

Doctoral Committee:

Professor Nathaniel Szymczak, Chair  
Professor Melanie Sanford  
Professor Peter Scott  
Professor Corey Stephenson

Michael M. Wade Wolfe

[mwadewo@umich.edu](mailto:mwadewo@umich.edu)

ORCID iD: [0000-0002-3464-3237](https://orcid.org/0000-0002-3464-3237)

© Michael M. Wade Wolfe 2022

## **Dedication**

This dissertation is dedicated to Dr. Shari L. Wade, Dr. Christopher R. Wolfe  
and Dr. Donald M. Wolfe

## Acknowledgments

When I started a summer rotation in the Szymczak in 2016, a mere 4 weeks after graduating from college, I was still in many ways a kid. For me, graduate school can be best summarized as *growth*; exciting, excruciating and yet extremely rewarding growth. While this is not a comprehensive list, I wanted to thank some of the key people who have helped me grow over the past 6 years.

I want to start by thanking my adviser Nathaniel Szymczak (Nate) who has been an excellent mentor to me. Nate gave me a second chance by letting me do a spring rotation in his lab, and I will always be grateful for that opportunity. Over the years I've found that Nate has always been in my corner, even when I didn't deserve it. Importantly, I've learned how to critically approach scientific problem solving from Nate directly and indirectly from spending time in subgroups and group meetings. The *chemical intuition* I've gained over the past 6 years in Nate's lab is invaluable to me, and the main reason that I feel confident moving forward with a career in research. I enjoyed talking with Nate at least once every day about science or just life in general during my later years in grad school. Thank you, for putting countless hours into making me a better scientist.

I want to thank my other committee members Melanie Sanford, Corey Stephenson and Peter Scott. Your expertise on fluoroalkylation, organometallics and medicine has been very useful over the years serving on my committee. Additionally I want to thank Liz Oxford and Katie Foster in the front office for being extremely well organized and helping me navigate the doctoral

program devoid of administrative headaches. I also want to thank the NSF (CHE 1955284) and a Rackham Graduate Student Research Grant (MMWW) for supporting my doctoral research.

Hai Dong was a day-one friend for me in graduate school as we rotated through the Szymczak lab at the same time in the summer of 2016. We went to lunch together at least 3 times per week and Hai helped me get through some of my roughest spots during graduate school. Through all of the good times and the bad times, I consider Hai a lifelong friend and it was a privilege to get to spend so much time with him in grad school.

Ryan Dodson has been another one of my best friends since the beginning of grad school. Ryan, his wife, Susan Nussbaum and I have spent countless hours watching silly Danny McBride shows, playing board games and hanging out. I was honored to take part in their wedding and I considered their apartment as a home away from home throughout my time in Ann Arbor. I also want to thank Brad Musselman and Sibin Wang who were excellent friends to me during grad school. I will always remember the dim sum excursions and legendary boardgame nights.

I want to thank Jacob Geri for getting me started on the fluoroalkylation project and teaching me how to do low temperature NMR experiments. I thank John Kiernicki for teaching me rigorous air-free purifications and also inspiring me to get into better physical shape. I also want to thank Jim Shanahan for being a fantastic coauthor with an eye to meticulous detail.

I'm glad that I had Jessi Wilson as a lab mate from my year. It was fantastic to have her for moral support, going through the same struggles as me (482, candidacy, etc...). Lucy Yu was the greatest mentee that I could ask for. It was a real pleasure working with her and seeing her learn, and I appreciate her taking me to my first Michigan football game. Emily Norwine is one of the most reliable people I know. She has been a fantastic lab mate and friend and I will definitely miss our weekly lunch at Totoro. I want to thank Wei Sun for having insightful conversations

about fluoroalkylation with me. I want to thank Andrew LaDuca for always being excited about science and bringing fresh bread into lab. I want to thank Dan Beagan, Chris Seo and Alyssa Cabelof for helpful scientific discussions and just being cool people to get a drink or a cigar with. Alice Atkins (Goatlice) was the best desk mate I had during grad school. During the last semester of grad school she was a great friend and I'm sad we didn't overlap more.

Finally, I want to thank my parents Shari Wade and Chris Wolfe for providing me the foundation and inspiration to get a Ph.D. During the height of the pandemic when laboratory research was shut down I went back to live with my parents for 2.5 months. It was an extremely productive time for me as I finished my first first-author paper, data meeting, and departmental seminar in large part due to their love and support for me. I love coming home for the holidays and going on family vacations. Finally, I want to thank my younger brother Patrick Wade Wolfe. I can always have a 3-hour video call with him even if we haven't spoken in a while. It's been amazing seeing him grow up during my time in grad school.

## Table of Contents

<b>Dedication .....</b>	<b>ii</b>
<b>Acknowledgments .....</b>	<b>iii</b>
<b>Table of Contents .....</b>	<b>vi</b>
<b>List of Tables .....</b>	<b>xi</b>
<b>List of Figures.....</b>	<b>xii</b>
<b>Abstract.....</b>	<b>xvii</b>
<b>Chapter 1 Introduction .....</b>	<b>1</b>
1.1 Importance of Fluorine .....	1
1.2 Methods to Directly Install Fluorine Into Organic Molecules.....	3
1.2.1 Xenon Difluoride .....	3
1.2.2 Diethylaminosulfur Trifluoride (DAST) and Other Deoxygenative Fluorination Strategies.....	3
1.2.3 Pyridine•HF and Other Basic Adducts of Hydrogen Fluoride .....	4
1.2.4 Selectfluor .....	5
1.3 Methods to Directly Install –CF <sub>3</sub> .....	5

1.3.1 Nucleophilic Trifluoromethylation .....	6
1.3.2 Radical Trifluoromethylation.....	7
1.3.3 Electrophilic Trifluoromethylation .....	8
1.4 Methods to Directly Install $-\text{CF}_2\text{R}$ .....	8
1.4.1 Deprotonation of $\text{H}-\text{CF}_2\text{R}$ and Subsequent Transfer.....	8
1.4.2 $\text{Br}-\text{CF}_2\text{R}$ as a “ $\text{CF}_2\text{R}$ ” Source .....	11
1.4.3 $\text{R}'\text{O}_2\text{S}-\text{CF}_2\text{R}$ as a “ $\text{CF}_2\text{R}$ ” Source.....	12
1.4.4 $\text{F}-\text{CF}_2\text{R}$ as a “ $\text{CF}_2\text{R}$ ” Source.....	12
1.5 Boron Fluoroalkyl Species.....	13
1.5.1 Potassium Trimethoxy(trifluoromethyl)borate .....	13
1.5.2 Potassium Trifluoro(trifluoromethyl)borate .....	14
1.5.3 Hexamethylborazine Fluoroalkyl Adducts .....	15
1.6 Metal Fluorocarbenes.....	15
<b>Chapter 1 Bibliography .....</b>	<b>18</b>
<b>Chapter 2 Lewis Acid Stabilized Fluoroalkyl and Fluoroalkenyl Anions .....</b>	<b>21</b>
2.1 Introduction.....	21
2.2 Mechanistic Insights into Borazine Based $\cdot\text{CF}_3$ Reagents .....	22
2.3 Comparison to Trimethoxy(trifluoromethyl)borate .....	24
2.4 Neutral Fluoroalkyl Borane Species .....	29
2.5 Deprotonation/Adduct Formation with More Complex Fluoroalkanes.....	33
2.6 Zweifel Olefination.....	36



2.7 Conclusions.....	42
2.8 Experimental Details.....	42
2.8.1 Preparation of 2b Hexamethylborazine-CF <sub>3</sub> Cs[18-crown-6] <sub>2</sub> .....	42
2.8.2 Kinetic Measurements of CF <sub>3</sub> Transfer and Decomposition.....	44
2.8.3 Kinetic Measurements of CF <sub>3</sub> Transfer with (MeO) <sub>3</sub> BCF <sub>3</sub> K.....	50
2.8.4 Synthesis and Characterization of HBPInCF <sub>2</sub> Ph K(18-crown-6).....	51
2.8.5 Reactions with HBPInCF <sub>2</sub> PhK(18-crown-6).....	53
2.8.6 Synthesis and Characterization of Pentamethylborazine-CF <sub>2</sub> Ph.....	60
2.8.7 Synthesis and Characterization of Pentamethylborazine-CF <sub>2</sub> H.....	63
2.8.8 Synthesis and Characterization of Hexamethylborazine-CF=CH <sub>2</sub> Adduct.....	66
2.8.9 Deprotonation of Polyfluroethane and Polyfluoropropane Substrates.....	67
2.8.10 Synthesis and Characterization of VinylBPInCF <sub>2</sub> Ph K(18-crown-6).....	73
2.8.11 Zweifel Olefination Reactions.....	76
<b>Bibliography .....</b>	<b>85</b>
<b>Chapter 3 Defluorinative Functionalization of Pd (II) Fluoroalkyl Complexes .....</b>	<b>87</b>
3.1 Introduction.....	87
3.2 Synthesis and Reactivity of the [Pd]-CF <sub>2</sub> Ph Complex.....	89
3.3 Synthesis and Reactivity of the [Pd]-CF <sub>3</sub> Complex.....	93
3.4 Computational Analysis of [Pd]=CF <sub>2</sub> .....	98
3.5 Defluorinative Arylation of [Pd]-CF <sub>3</sub> .....	99
3.6 One-pot Strategy for Defluorinative Arylation of [Pd]-CF <sub>3</sub> .....	103

3.7 Conclusions.....	105
3.8 Experimental Details.....	105
3.8.1 Synthesis of Pd Fluoroalkyl Complexes (1a-1c) .....	105
3.8.2 Organic Molecules Derived from 1a.....	107
3.8.3 Selective Formation of (3a-3c) or (4a-4c) from 1b with p-Substituted Triaryl Boranes .....	110
3.8.4 Defluorinative Arylation from 1b Optimization of Equivalents of PPh <sub>3</sub> Added .....	112
3.8.5 Defluorinative Arylation Scope from 1b (5a-5j) .....	112
3.8.6 One-pot Defluorinative Arylation Scope in Aryl/Heteroaryl Bromide (6a-6c).....	122
<b>Chapter 3 Bibliography .....</b>	<b>127</b>
<b>Chapter 4 Synthetic Approaches to Construct C–CF<sub>2</sub>Ph Bonds Using a Nucleophilic Borazine–CF<sub>2</sub>Ph Reagent.....</b>	<b>130</b>
4.1 Introduction.....	130
4.2 Difluorobenzyl C(sp <sup>2</sup> )-C(sp <sup>3</sup> ) Coupling through S <sub>N</sub> Ar and Pd Cross-coupling .....	131
4.3 Difluorobenzyl C(sp <sup>3</sup> )-C(sp <sup>3</sup> ) Coupling through S <sub>N</sub> 2.....	136
4.4 Conclusions.....	138
4.5 Experimental Details.....	139
4.5.1 Optimization of Pd Catalysis .....	139
4.5.2 Scope in sp <sup>2</sup> -sp <sup>3</sup> Coupling (2a-2k).....	142
4.5.3 Scope in S <sub>N</sub> Ar Reactions (3a-3d).....	149
4.5.4 Scope in S <sub>N</sub> 2 Reactions (4a-4g).....	151

<b>Chapter 4 Bibliography .....</b>	<b>155</b>
<b>Chapter 5 Summary and Future Outlook .....</b>	<b>157</b>
5.1 Summary .....	157
5.2 Future Outlook .....	158

## List of Tables

<b>Table 2.1</b> Relative reaction rates for 0.02 M of benzaldehyde with varying equivalents of (MeO) <sub>3</sub> BCF <sub>3</sub> K .....	25
<b>Table 2.2</b> Relative reaction rates for 0.02 M of (MeO) <sub>3</sub> BCF <sub>3</sub> K with varying equivalents of benzaldehyde.....	26
<b>Table 2.3</b> Suppression of <sup>-</sup> CF <sub>3</sub> transfer in the presence of alkali cation.....	27
<b>Table 2.4</b> Reported crystal structure of (MeO) <sub>3</sub> BCF <sub>3</sub> K and increased reactivity in the presence of crown ether.....	28
<b>Table 2.5</b> Attempts to optimize Zweifel olefination. <sup>a</sup> Reactions were tumbled in screwcap NMR tubes using isolated vinylBPinCF <sub>2</sub> Ph. <sup>b</sup> VinylBPinCF <sub>2</sub> Ph was generated in situ in quantitative yield with 1.2 eq with vinylBPin, then immediately use as a stock solution for further reactions that were stirred in 8 mL vials. (Yield after 3 days) .....	40
<b>Table 2.6</b> Reaction rates with uncertainty in mM/s for 0.04 M of electrophile with varying equivalents of <b>2</b> .....	45
<b>Table 2.7</b> Reaction rates with uncertainty in mM/s for 0.025 M of <b>2</b> with varying equivalents of electrophile (electrophile=E) .....	47
<b>Table 2.8</b> k values for Eyring analysis .....	49
<b>Table 3.1</b> Influence of (B(4-R-Ph) <sub>3</sub> ) identity on the formation of <b>3</b> and <b>4</b> from <b>1b</b> . BAr' <sub>3</sub> and <b>1b</b> were allowed to react at 65 °C for 24 h. *Yields determined by <sup>19</sup> F NMR integration with respect to C <sub>6</sub> H <sub>5</sub> F or C <sub>6</sub> H <sub>5</sub> OCF <sub>3</sub> internal standard. Entries 1-3 = 0.008 M, entries 4 and 5 = 0.01 M.....	93
<b>Table 3.2</b> Percent of <b>1b</b> remaining in the presence of 1 eq. borane .....	100
<b>Table 3.3</b> In situ yields of <b>3</b> and <b>4</b> across three trials .....	111
<b>Table 3.4</b> Yield dependence on equivalents of PPh <sub>3</sub> added .....	112
<b>Table 4.1</b> Optimization of Pd catalyzed sp <sup>2</sup> -sp <sup>3</sup> cross coupling. In situ yields were measured by <sup>19</sup> F NMR with respect to an internal standard, trifluoromethyl anisole or by GC-FID. <sup>a</sup> Reaction run in triplicate, error bars reported as 3 standard deviations from the mean. ....	134
<b>Table 4.2</b> Reaction optimization for sp <sup>2</sup> -sp <sup>3</sup> coupling.....	139

## List of Figures

<b>Figure 1.1</b> The medicinal relevance of fluorine a) the first fluorinated drug b) bioisosteres .....	2
<b>Figure 1.2</b> Retrosynthetic strategies to synthesize a difluorobenzyl containing molecule with a) xenon difluoride b) DAST c) Olah's reagent d) Selectfluor.....	4
<b>Figure 1.3</b> Trifluoromethylation strategies a) nucleophilic trifluoromethylation b) radical trifluoromethylation c) electrophilic trifluoromethylation.....	6
<b>Figure 1.4</b> Different ways to directly install $-CF_2R$ and the pros and cons to each $-CF_2R$ precursor: a) deprotonation of $ArCF_2H$ b) cross-coupling with $ArCF_2Br$ c) cross-coupling with $ArCF_2SO_2CF_3$ d) cross-coupling with $ArCF_3$ .....	9
<b>Figure 1.5</b> Kanai's direct trifluoromethylation of 2-substituted N-oxide heterocycles derived from $KF_3BCF_3$ .....	15
<b>Figure 1.6</b> Reactions of metal difluorocarbenes a) adduct formation b) 1,1-insertion c) fluoride rebound .....	16
<b>Figure 2.1</b> a) Possible mechanisms for $^-CF_3$ transfer. b) Cation effects on $^-CF_3$ stability/reactivity. In 7, $Ar=4-F-Ph$ .....	23
<b>Figure 2.2</b> Plot of log of reaction rate vs. log concentration of $(MeO)_3BCF_3K$ , slope 1.04 (benzaldehyde as substrate) .....	25
<b>Figure 2.3</b> Plot of log of reaction rate vs. log concentration of benzaldehyde, slope 0.01 .....	26
<b>Figure 2.4</b> a) Synthesis of $HBPi nCF_2Ph K(18-crown-6)$ b) X-ray crystal structure. Key bond metrics; $B_1-C_1$ : 1.65 Å, $K_1-F_1$ : 3.04 Å, $K_1-O_1$ : 2.68 Å c) Reactions with $HBPi nCF_2Ph K(18-crown-6)$ .....	30
<b>Figure 2.5</b> Proposed pathway to form pentamethyl $CF_2R$ borazine species.....	32
<b>Figure 2.6</b> a) Observed $\beta$ -fluoride elimination. b) Stability of borazine fluoroethylene adducts.	34
<b>Figure 2.7</b> Deprotonation of trifluoroethane with and without hexamethylborazine and 18-crown-6 .....	35
<b>Figure 2.8</b> Reactivity trends of fluoroalkyl(enyl) borazine adducts .....	36

<b>Figure 2.9</b> Boron mediated, metal-free C-C coupling reactions a) $\alpha$ -Fluoroalkylation strategies b) $\beta$ -Fluoroalkylation strategies. c) Zweifel ofelination mechanism. d) This work. ....	37
<b>Figure 2.10</b> Scope in Zweifel olefination and formation of undesired iodinated side products ..	39
<b>Figure 2.11</b> Stability of <b>2b</b> at 25 °C in Solid State .....	44
<b>Figure 2.12</b> Stability of <b>2b</b> at 25 °C in solution.....	44
<b>Figure 2.13</b> Example linear fit .....	45
<b>Figure 2.14</b> Plot of log of reaction rate vs. log concentration of <b>7</b> (4-fluorobenzaldehyde), slope 0.06.....	46
<b>Figure 2.15</b> Plot of log of reaction rate vs. log concentration of <b>8</b> (perfluorotoluene): slope 0.09 .....	47
<b>Figure 2.16</b> Plot of log of reaction rate vs. log concentration of <b>2</b> , slope 0.89 ( <b>7</b> , 4-fluorobenzaldehyde as substrate).....	48
<b>Figure 2.17</b> Plot of log of reaction rate vs. log concentration of <b>2</b> , slope 0.83 ( <b>8</b> , perfluorotoluene as substrate).....	48
<b>Figure 2.18</b> Eyring plot for reaction of <b>2</b> and <b>7</b> , (4-fluorobenzaldehyde).....	49
<b>Figure 2.19</b> Kinetic traces for thermal decomposition of <b>2</b> , <b>2a</b> and <b>2b</b> 60 °C and second order fit .....	50
<b>Figure 2.20</b> $^{-}\text{CF}_3$ transfer to <b>7</b> from <b>2</b> , <b>2b</b> , and <b>2b</b> activated with $\text{K}^+$ at 10 °C .....	50
<b>Figure 2.21</b> $^1\text{H}$ NMR spectrum of $\text{HBPi nCF}_2\text{Ph K(18-crown-6)}$ in $\text{C}_6\text{D}_6$ .....	52
<b>Figure 2.22</b> $^{11}\text{B}$ NMR spectrum of $\text{HBPi nCF}_2\text{Ph K(18-crown-6)}$ in $\text{C}_6\text{D}_6$ .....	52
<b>Figure 2.23</b> $^{19}\text{F}$ NMR spectrum of $\text{HBPi nCF}_2\text{Ph K(18-crown-6)}$ in $\text{C}_6\text{D}_6$ .....	53
<b>Figure 2.24</b> $^1\text{H}$ NMR of $\text{PinBCF}_2\text{Ph}$ in $\text{C}_6\text{D}_6$ .....	54
<b>Figure 2.25</b> $^{11}\text{B}$ NMR of $\text{PinBCF}_2\text{Ph}$ in $\text{C}_6\text{D}_6$ (TMSI used instead of $\text{TMSCl}$ ) .....	54
<b>Figure 2.26</b> $^{19}\text{F}$ NMR of $\text{PinBCF}_2\text{Ph}$ in $\text{C}_6\text{D}_6$ .....	55
<b>Figure 2.27</b> $^1\text{H}$ NMR $\text{HBPi nCF}_2\text{Ph K(18-crown-6)}$ with benzophenone in THF .....	56
<b>Figure 2.28</b> $^{19}\text{F}$ NMR $\text{HBPi nCF}_2\text{Ph K(18-crown-6)}$ with benzophenone in THF .....	56
<b>Figure 2.29</b> $^1\text{H}$ NMR of $\text{HBPi nCF}_2\text{Ph K(18-crown-6)}$ with chalcone in THF .....	58
<b>Figure 2.30</b> $^{11}\text{B}$ NMR of $\text{HBPi nCF}_2\text{Ph K(18-crown-6)}$ with chalcone in THF (unreferenced) ..	58

<b>Figure 2.31</b> $^{19}\text{F}$ NMR of HBPInCF <sub>2</sub> Ph K(18-crown-6) with chalcone in THF .....	58
<b>Figure 2.32</b> $^{19}\text{F}$ NMR of HBPInCF <sub>2</sub> Ph K(18-crown-6) with Pd(II)Br(3,5-(CF <sub>3</sub> ) <sub>2</sub> Ph)(PPh <sub>3</sub> ) <sub>2</sub> in THF .....	59
<b>Figure 2.33</b> $^1\text{H}$ NMR of difluorobenzyl pentamethylborazine in C <sub>6</sub> D <sub>6</sub> .....	61
<b>Figure 2.34</b> $^{19}\text{F}$ NMR of difluorobenzyl pentamethylborazine in C <sub>6</sub> D <sub>6</sub> .....	61
<b>Figure 2.35</b> $^1\text{H}$ NMR of pentane insoluble material in C <sub>6</sub> D <sub>6</sub> .....	62
<b>Figure 2.36</b> $^{19}\text{F}$ NMR of pentane insoluble material in C <sub>6</sub> D <sub>6</sub> .....	62
<b>Figure 2.37</b> $^{31}\text{P}$ NMR of pentane insoluble material in C <sub>6</sub> D <sub>6</sub> .....	63
<b>Figure 2.38</b> $^1\text{H}$ NMR of pentamethylborazine-CF <sub>2</sub> H in THF .....	64
<b>Figure 2.39</b> $^{11}\text{B}$ NMR of pentamethylborazine-CF <sub>2</sub> H in THF .....	65
<b>Figure 2.40</b> $^{19}\text{F}$ NMR of pentamethylborazine-CF <sub>2</sub> H in THF .....	65
<b>Figure 2.41</b> $^1\text{H}$ NMR of the hexamethylborazine-CF=CH <sub>2</sub> adduct in DMSO-d <sub>6</sub> .....	66
<b>Figure 2.42</b> $^{19}\text{F}$ NMR of the hexamethylborazine-CF=CH <sub>2</sub> adduct in THF .....	67
<b>Figure 2.43</b> Deprotonation of 1,1,1,2-tetrafluoroethane (no borazine) $^{19}\text{F}$ NMR array .....	68
<b>Figure 2.44</b> Deprotonation of 1,1,1,2-tetrafluoroethane (with borazine) $^{19}\text{F}$ NMR array .....	69
<b>Figure 2.45</b> Deprotonation of 1,1,1-trifluoroethane (no borazine) $^{19}\text{F}$ NMR array .....	69
<b>Figure 2.46</b> Deprotonation of 1,1,1-trifluoroethane (with borazine) $^{19}\text{F}$ NMR array .....	70
<b>Figure 2.47</b> Deprotonation of 1,1,1,3,3-pentafluoropropane (no borazine) $^{19}\text{F}$ NMR array .....	70
<b>Figure 2.48</b> Deprotonation of 1,1,1,3,3-pentafluoropropane (with borazine) $^{19}\text{F}$ NMR array ....	71
<b>Figure 2.49</b> Deprotonation of 1,1,1,3,3,3-hexafluoropropane (no borazine) $^{19}\text{F}$ NMR array.....	71
<b>Figure 2.50</b> Deprotonation of 1,1,1,3,3,3-hexafluoropropane (with borazine) $^{19}\text{F}$ NMR array ..	72
<b>Figure 2.51</b> Deprotonation of 2-H-heptafluoropropane (no borazine) $^{19}\text{F}$ NMR array .....	72
<b>Figure 2.52</b> Deprotonation of 2-H-heptafluoropropane (with borazine) $^{19}\text{F}$ NMR array .....	73
<b>Figure 2.53</b> $^1\text{H}$ NMR spectrum of vinylBPInCF <sub>2</sub> Ph K(18-crown-6) in THF-d <sub>8</sub> .....	74
<b>Figure 2.54</b> $^{11}\text{B}$ NMR spectrum of vinylBPInCF <sub>2</sub> Ph K(18-crown-6) in THF-d <sub>8</sub> .....	75
<b>Figure 2.55</b> $^{19}\text{F}$ NMR spectrum of vinylBPInCF <sub>2</sub> Ph K(18-crown-6) in THF-d <sub>8</sub> .....	75

<b>Figure 2.56</b> $^{19}\text{F}$ NMR spectrum of 8-(difluoromethyl)-1,4-dioxaspiro[4.5]dec-7-ene (54% yield)	76
<b>Figure 2.57</b> $^{19}\text{F}$ NMR spectrum of 8-(trifluoromethyl)-1,4-dioxaspiro[4.5]dec-7-ene (5% yield)	77
<b>Figure 2.58</b> $^{19}\text{F}$ NMR (THF) spectrum of 8-(1-fluorovinyl)-1,4-dioxaspiro[4.5]dec-7-ene (26% yield)	79
<b>Figure 2.59</b> $^1\text{H}$ NMR ( $\text{CDCl}_3$ ) spectrum of 8-(1-fluorovinyl)-1,4-dioxaspiro[4.5]dec-7-ene	79
<b>Figure 2.60</b> $^{13}\text{C}$ NMR ( $\text{CDCl}_3$ ) spectrum of 8-(1-fluorovinyl)-1,4-dioxaspiro[4.5]dec-7-ene	80
<b>Figure 2.61</b> $^1\text{H}$ - $^1\text{H}$ COSY ( $\text{CDCl}_3$ ) spectrum of 8-(1-fluorovinyl)-1,4-dioxaspiro[4.5]dec-7-ene	80
<b>Figure 2.62</b> $^1\text{H}$ - $^{13}\text{C}$ HSQC ( $\text{CDCl}_3$ ) spectrum of 8-(1-fluorovinyl)-1,4-dioxaspiro[4.5]dec-7-ene	81
<b>Figure 2.63</b> $^1\text{H}$ - $^{13}\text{C}$ HMBC ( $\text{CDCl}_3$ ) spectrum of 8-(1-fluorovinyl)-1,4-dioxaspiro[4.5]dec-7-ene	81
<b>Figure 2.64</b> $^{19}\text{F}$ NMR spectrum of 8-(difluoro(phenyl)methyl)-1,4-dioxaspiro[4.5]dec-7-ene (36% yield)	82
<b>Figure 2.65</b> $^{19}\text{F}$ NMR Spectrum of 4-(Difluoro(1,4-dioxaspiro[4.5]dec-7-en-8-yl)methyl)pyridine (3% Yield)	83
<b>Figure 2.66</b> $^{19}\text{F}$ NMR spectrum of 8-(1,2,2-trifluorovinyl)-1,4-dioxaspiro[4.5]dec-7-ene (15% yield)	84
<b>Figure 3.1</b> Prior work demonstrating defluorination induced 1,1-insertion (top), and Lewis acid-mediated defluorinative arylation (bottom). In the Sanford example, $\text{CsF}$ was added 30 min. after $\text{Me}_3\text{SiOTf}$ . <sup>41</sup>	88
<b>Figure 3.2</b> a) Preparation of <b>1a</b> . b) X-ray structure of <b>1a</b> , $\text{Pd}_1\text{-C}_1$ distance 2.0735(19) Å, ellipsoids shown at 50%, H-atoms removed and non-essential aryl rings wireframed for clarity. c) Diversification of <b>1a</b> : i) 1 eq. $\text{AgSbF}_6$ at 0 °C (1 h) affords <b>2a</b> , ii) 1 eq. $\text{BPh}_3$ (5 min), followed by 1 eq. $\text{PPh}_3$ (17 h) at RT affords <b>2b/2b'</b> and iii) 1 eq. $\text{BPh}_3$ (15 min), followed by 1 eq. $\text{KHBET}_3$ at RT for 17 h affords <b>2c</b> .	90
<b>Figure 3.3</b> Proposed mechanism for formation of <b>2b/2b'</b> and <b>2c</b>	92
<b>Figure 3.4</b> Preparation and X-ray structure of <b>1c</b> . Elongation of $\text{Pd}_1\text{-C}_1$ observed <b>1b</b> : 2.068(9) Å vs. <b>1c</b> : 2.176(8) Å, ellipsoids shown at 30%, H-atoms removed and non-essential aryl rings wireframed for clarity.	95



<b>Figure 3.5</b> $^{19}\text{F}$ NMR (500 MHz, THF, -80 to 25 °C) overlay of fluoride abstraction from <b>1b</b> (-80 °C bottom, 25 °C top) .....	97
<b>Figure 3.6</b> $^{31}\text{P}$ NMR (500 MHz, THF, -80 to 25 °C) Overlay of Fluoride Abstraction from <b>1b</b> (-80 °C bottom, 25 °C top) .....	97
<b>Figure 3.7</b> Fluoride ion affinity (FIA) scale for Lewis acids and defluorinated fluoroalkyl products. FIA reported as the $\Delta\text{G}$ of fluoride abstraction from $\text{CF}_3\text{O}^-$ to form $\text{CF}_2\text{O}$ (i.e. $\text{CF}_2\text{O}$ FIA = 0 kcal/mol). .....	98
<b>Figure 3.8</b> Scope in boronic acid <sup>1</sup> /pinacol ester <sup>2</sup> . <b>1b</b> mixed with $\text{B}(\text{C}_6\text{F}_5)_3$ for 5 min, then 1 eq. $\text{PPh}_3$ added, followed by 1 eq. $(\text{RO})_2\text{BR}$ and 2 eq. $\text{NMe}_4\text{F}$ at 23 °C. Reactions were stirred at 1000 rpm at 80 °C for 16 h. Isolated reported, and (in situ) yields determined by $^{19}\text{F}$ NMR integration against $\text{PhOCF}_3$ internal standard. All reactions refer to 0.1 mmol scale unless otherwise noted. <sup>a</sup> : 1 eq. $\text{B}(\text{C}_6\text{F}_5)_3$ , dioxane solvent. <sup>b</sup> : 1.1 eq. $\text{B}(\text{C}_6\text{F}_5)_3$ , THF solvent. *0.005 mmol scale. **94 °C. ....	101
<b>Figure 3.9</b> Scope in aryl bromide. 1) $\text{Pd}(\text{PPh}_3)_4$ was stirred with 1.2 eq. aryl bromide at 80 °C for 4 h in THF. 2) 2 eq. $\text{TMSCF}_3$ added with 18-crown-6 and $\text{KO}^t\text{Bu}$ and stirred at 23 °C for 2-3 h. 3) $\text{B}(\text{C}_6\text{F}_5)_3$ added at 23 °C for 5 min. 4) 1 eq. $(\text{HO})_2\text{B}(4\text{-X-Ph})$ and 2 eq. $\text{NMe}_4\text{F}$ added and stirred at 1000 rpm at 80 °C for 18 h. Isolated reported, and (in situ) yields determined by $^{19}\text{F}$ NMR integration against $\text{PhOCF}_3$ internal standard. All reactions refer to 0.15 mmol scale unless otherwise noted. *0.004 mmol scale with 2 eq. of $\text{B}(\text{C}_6\text{F}_5)_3$ used in step 3. ....	104
<b>Figure 4.1</b> a) Previous work: cross-coupling reactions of aryl and alkyl $\text{CF}_2\text{X}$ . b) This work: nucleophilic strategies to form C-C <sub>F</sub> bonds .....	131
<b>Figure 4.2</b> i) Electronic trends with Pd catalyzed cross-coupling and $\text{S}_{\text{N}}\text{Ar}$ . ii) Scope in cross coupling and $\text{S}_{\text{N}}\text{Ar}$ . In situ yields measured by $^{19}\text{F}$ NMR with respect to an internal standard, trifluoromethyl anisole. Mass purity of isolated samples measured by $^{19}\text{F}$ NMR with respect to an internal standard, trifluoromethyl anisole. <sup>a</sup> Conditions: reactions performed in toluene (0.02M) at 25 °C, 16h with 5 mol% $\text{Pd}(\text{PPh}_3)_4$ . <sup>b</sup> Conditions: reactions performed in THF (0.02M) at 25 °C, 18h. ....	133
<b>Figure 4.3</b> Mercury poisoning experiment.....	135
<b>Figure 4.4</b> $\text{S}_{\text{N}}2$ reactions with alkyl halides. Reactions performed on 0.01-0.02 mmol scale In situ yields measured by $^{19}\text{F}$ NMR with respect to an internal standard, trifluoromethyl anisole. <sup>a</sup> Reaction performed at 90 °C, 30 min in toluene. <sup>b</sup> After formation of <b>4d</b> , solids removed by filtration and allyl bromide removed by vacuum. <b>4d</b> heated to 80 °C in 1.2 mL THF in the presence of pinacol borane (2eq.) and $\text{RhCl}(\text{PPh}_3)_3$ for 14 h. ....	137
<b>Figure 5.1</b> Strategy to make fluoroalkyl boronic acids and esters from $\text{BH}_3$ .....	158
<b>Figure 5.2</b> Difunctionalization catalysis with $\text{K}[\text{HB}(\text{OR})_2\text{CF}_2\text{Ph}]$ .....	159

## Abstract

Discovering new methods to form carbon-fluorine bonds is of great interest to the scientific community. Fluorinated motifs play a key role in medicinal chemistry specifically because they exhibit desirable properties: increased lipophilicity, metabolic stability and biological activity compared to their non-fluorinated counterparts. Chemists have developed two general routes to install C–F bonds: direct fluorination and installation of preassembled larger fluoroalkyl units. The work in this dissertation focuses on the second route, more generally referred to as *fluoroalkylation*. We use boron Lewis-acids to form stable adducts with reactive fluoroalkyl anions. These adducts can subsequently release potent fluoroalkyl nucleophiles to further react with organic and inorganic electrophiles including palladium(II). We employ the palladium(II)-fluoroalkyl complexes in both catalytic cross-coupling and defluorinative functionalization reactions.

In Chapter 2, we discuss how hexamethylborazine- $\text{CF}_3$  adducts and potassium trimethoxy(trifluoromethyl)borate both operate through dissociative  $\text{CF}_3^-$  transfer. Alkali metal additives enhance the rate of  $\text{CF}_3^-$  transfer from borazine, while the opposite effect is observed for  $(\text{MeO})_3\text{BCF}_3\text{K}$  which is likely due to the Lewis-basic methoxide groups on the latter. In order to generate fluoroalkylation reagents that are more specifically suited towards catalysis, we synthesized and characterized 3 neutral fluoroalkyl borane species ( $\text{PinBCF}_2\text{Ph}$ ,  $\text{B}_3\text{N}_3\text{Me}_5\text{CF}_2\text{Ph}$  and  $\text{B}_3\text{N}_3\text{Me}_5\text{CF}_2\text{Ph}$ ).  $\text{PinBCF}_2\text{Ph}$  was shown to be competent in a stoichiometric Suzuki cross coupling, demonstrating the important proof of principle that these reagents have catalytic

application. More chemically complex polyfluoroethane substrates also formed adducts with borazine in the presence of base, however  $\beta$ -fluoride elimination was operative, forming polyfluorovinyl borazine adducts. Finally, we assessed the generality of fluoroalkyl anions stabilized by borazine and their ability to transfer  $\text{R}_\text{F}^-$  to vinyl BPin compounds. Iodine and base could be used to induce metal-free C–C coupling of these fluoroalkylated vinyl boronate species.

In Chapter 3, we demonstrated that when subjected to arylboranes, anionic trifluoromethyl and difluorobenzyl palladium(II) complexes undergo fluoride abstraction followed by 1,1-migratory insertion. The resulting intermediate fluoroalkyl species can be induced to undergo a subsequent transmetalation and reductive elimination from either an *in situ* formed fluoroboronate ( $\text{FB}(\text{Ar}_3)^-$ ) or an exogenous boronic acid/ester ( $\text{ArB}(\text{OR})_2$ ) and nucleophilic activator, representing a net defluorinative arylation reaction. The latter method enabled a structurally diverse substrate scope to be prepared in one pot from a representative aryl palladium- $\text{CF}_3$  complex either discretely isolated or generated *in situ* from  $\text{Pd}(\text{PPh}_3)_4$  and other commercially available reagents.

In Chapter 4, we demonstrate C–C bond formation through nucleophilic addition reactions to prepare molecules containing internal  $-\text{CF}_2-$  linkages using a hexamethylborazine- $\text{CF}_2\text{Ph}$  reagent. We were able to achieve metal-free  $\text{C}(\text{sp}^2)\text{-C}(\text{sp}^3)$  coupling with electron-deficient nitroarenes using an  $\text{S}_\text{N}\text{Ar}$  strategy. Palladium catalyzed  $\text{C}(\text{sp}^2)\text{-C}(\text{sp}^3)$  cross-coupling allowed for access of electron-rich and neutral aryl iodides to provide a complimentary scope of diaryl difluoromethyl products. Finally,  $\text{C}(\text{sp}^3)\text{-C}(\text{sp}^3)$  bonds are forged using operationally simple  $\text{S}_\text{N}2$  reactions that tolerate medicinally-relevant motifs and functional groups that are amenable to further functionalization. To demonstrate the utility of the method, allyl bromide could undergo nucleophilic substitution and with an experimentally facile intermediate removal of solvent and unreacted starting materials subsequent rhodium catalyzed hydroboration reaction.

## Chapter 1 Introduction

Fluoroalkylation, and more generally, installation of carbon–fluorine bonds, represents one of the most popular and rapidly expanding fields in all of synthetic chemistry over the past 50 years. The products of such transformations are prominently used in medicine,<sup>1</sup> agriculture<sup>2</sup> and materials.<sup>3</sup> When we think about how to generate a molecule with a R–CF<sub>2</sub>–R' motif, two main retrosynthetic disconnections can be considered. The first disconnection is direct fluorination of a R–CX–R' synthon, a strategy that has been exploited since the early 1970's with reagents such as diethylaminosulfur trifluoride (DAST) and Olah's reagent.<sup>4,5</sup> The other choice of disconnection is directly installing a CF<sub>2</sub>R unit onto a R'-containing substrate. Over the past decade, this second strategy has blossomed, especially when cross-coupling with a transition metal catalyst is employed.<sup>6-8</sup> My PhD work has focused on installing these preassembled CF<sub>2</sub>R motifs into more complex, fluoroalkylated molecules. Specifically, I have focused on using boranes for the capture and transfer of reactive, transient <sup>-</sup>CF<sub>2</sub>R anions (Chapters 2 and 4) and for fluoride abstraction from Pd–CF<sub>2</sub>R complexes to ultimately induce transformative defluorinative functionalization reactions (Chapter 3).

### 1.1 Importance of Fluorine

One of the main, overarching motivations for synthesizing fluoroalkylated compounds is the application to the field of medicine.<sup>1</sup> In 1955, the first fluorinated drug, fludrocortisone, was approved and exhibited the same effectiveness as hydrocortisone in one tenth the concentration (**Figure 1.1 a**).<sup>9, 10</sup> Since then, the biological implications of fluorine in pharmaceutical targets

have remained in high interest to the medicinal community. Comparatively, when examining the list of drugs approved by the United States Food and Drug Administration in 2020, 13 out of 53 contain fluorine.<sup>11</sup>

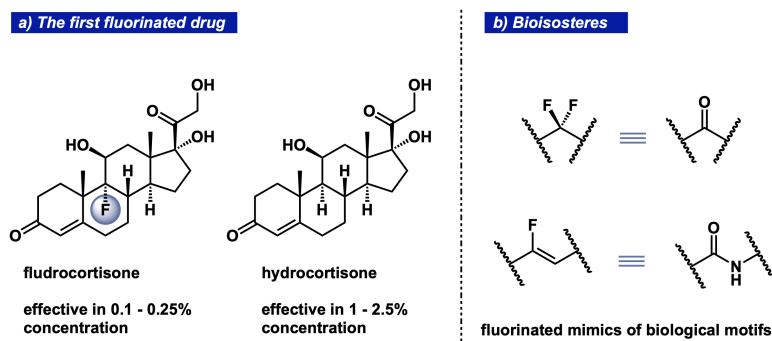


**Figure 1.1** The medicinal relevance of fluorine a) the first fluorinated drug b) bioisosteres

Due to the size and dipole moment of C–F bonds, they are considered to be C=O bioisosteres, or moieties that mimic a functional group in terms of size, polarity or biological activity (**Figure 1.1 a**).<sup>12</sup> In many instances, fluorinated drug candidates display enhancement of lipophilicity, metabolic stability and enzyme binding affinity.<sup>1</sup> In vivo, C–F containing substrates are shown to hydrogen-bond with the acidic moieties inside of the active site (lysine  $-\text{NH}_3^+$ , cysteine  $-\text{SH}$ , general peptide  $-\text{NH}-$  for example).<sup>12</sup> Electron-rich anionic moieties such as carboxylate are even shown to participate in tetrel bonding with the  $\sigma$ -hole of  $-\text{CF}_3$ .<sup>12</sup>

The general increase in lipophilicity is another key motivator for installing fluorine into drug molecules. When comparing the organic solubility of two simple molecules, (benzene and fluorobenzene) the Log P values are 2.13 and 2.27 respectively.<sup>13</sup> When rotation is possible about a C–C bond, fluorinated alkanes favor gauche interactions, allowing hyperconjugation between the C–F  $\sigma^*$  and C–H  $\sigma$  bonds.<sup>1</sup> Recently, an in depth study revealed that gem-difluoromethylene containing molecules are even more lipophilic than their vic-difluoromethylene counterparts, which further motivates chemists to install multiple fluorine atoms on the same carbon.<sup>14</sup>

## 1.2 Methods to Directly Install Fluorine Into Organic Molecules

### 1.2.1 Xenon Difluoride

Discovered in 1962, XeF<sub>2</sub> is one of the oldest and most chemically simplistic fluorination reagents.<sup>15</sup> The chemical was rationally synthesized by Weeks et. al., mixing stoichiometric ratios of xenon and fluorine gas and irradiating with a 1000-watt mercury pressure arc.<sup>16</sup> After the initial discovery, this powerful fluorinative oxidant has been demonstrated to react with alkyl iodides, carboxylic acids, and famously alkenes to form the corresponding fluoroalkanes (**Figure 1.2 a**).<sup>15</sup> Decarboxylative fluorination using XeF<sub>2</sub> invokes a radical mechanism, which was demonstrated by reacting 6-heptenoic acid and XeF<sub>2</sub> through observation of the ring-closed, (fluoromethyl)cyclopentane in 25% yield.<sup>17</sup> Interestingly, in the presence of HF, XeF<sub>2</sub> can induce not only fluorination, but also atom rearrangement of benzaldehyde substrates to the corresponding difluoromethoxyl phenyl ethers.<sup>18</sup> The skeletal rearrangement reactions serve as a distinction for aldehydes and ketones substrates, when compared to esters that do not easily react with XeF<sub>2</sub>, and carboxyl acids that undergo decarboxylative fluorination.<sup>15</sup>

### 1.2.2 Diethylaminosulfur Trifluoride (DAST) and Other Deoxygenative Fluorination

#### *Strategies*

In contrast to the reactivity of XeF<sub>2</sub>, diethylaminosulfur trifluoride, *DAST*, is known for deoxygenative fluorination reactions.<sup>4</sup> Aldehydes, ketones and carboxylic acids are transformed into the corresponding difluoromethyl, gemdifluoromethylene and acyl fluoride products in the presence of *DAST* (**Figure 1.2 b**).<sup>4</sup> For decades, this powerful methodology remained one of the only ways to install an internal –CF<sub>2</sub>– linkage into organic molecules,<sup>4, 5</sup> and has been utilized in the synthesis of many pharmaceutical targets.<sup>14, 19</sup> The key drawback of using *DAST* as a

fluorination reagent is a high risk of an explosion,<sup>20</sup> which is, in many cases, prohibitive to industrial scale reactions.<sup>21</sup>

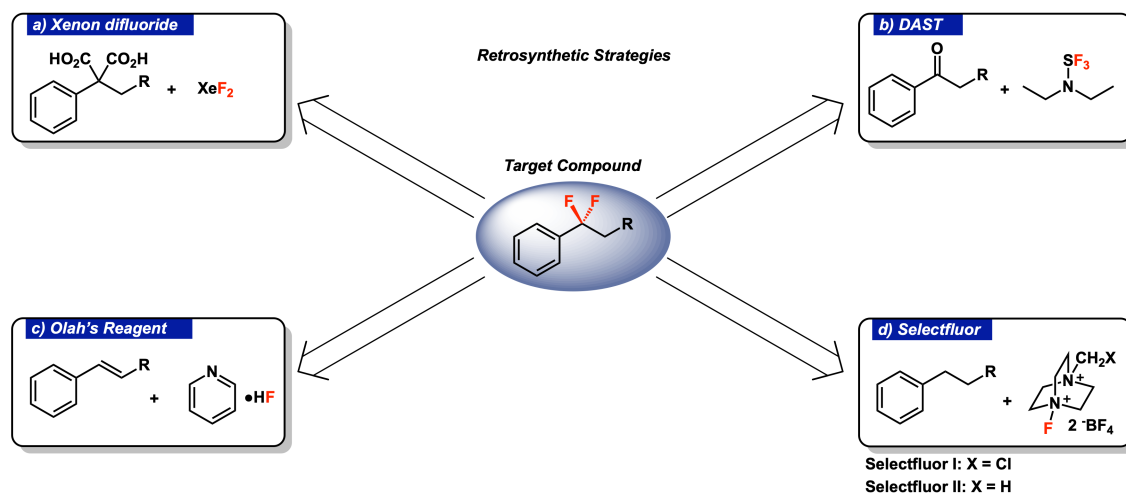


**Figure 1.2** Retrosynthetic strategies to synthesize a difluorobenzyl containing molecule with a) xenon difluoride b) DAST c) Olah's reagent d) Selectfluor

In more recent years, other deoxygenative fluorination methodologies have been developed to evade the explosion hazard of DAST.<sup>22</sup> Sanford and coworkers demonstrated that sulfonyl fluoride and tetramethyl ammonium fluoride could effectively fluorinate aldehydes and  $\alpha$ -keto esters.<sup>23</sup> Sulfonyl fluoride offers higher thermal stability when compared to DAST, and the corresponding deoxyfluorination reactions resulted in even higher yields in certain cases.<sup>23</sup>

### 1.2.3 Pyridine•HF and Other Basic Adducts of Hydrogen Fluoride

One alternative strategy for installation of a  $-\text{CF}_2-$  linkage is via a mixture of pyridine and hydrofluoric acid (30:70) developed by Olah and coworkers.<sup>5</sup> Like other HX acids, pyridine•HF adds across double and triple C–C bonds to form the corresponding mono and gemdifluoro alkane products (**Figure 1.2 c**).<sup>5</sup> Pyridine•HF offers distinct advantages over hydrofluoric acid, which is volatile (bp = 19.6 °C) and highly dangerous to work with as it can dissolve flesh and bone. Alcohols can also be converted to alkyl fluoride products via an acid promoted nucleophilic

substitution.<sup>5</sup> One of the main concerns with this class of reagent is that the conjugate base can coordinate to transition metals and inhibit catalysis. Hammond and Xu recently showed a method to overcome this problem, by tuning the pKa and ability of the base-HF motif to accept a hydrogen-bond.<sup>24</sup> They demonstrated that adducts of DMPU and HF can be utilized in Au(I) catalyzed selective mono and difluorination reactions without having DMPU coordinate irreversibly to the cationic gold species.<sup>24</sup>

#### ***1.2.4 Selectfluor***

To overcome the outstanding challenge of selective fluorination without using toxic or explosive reagents, a series of quaternary alkyl ammonium fluoride salts were synthesized and trademarked as Selectfluor reagents.<sup>25</sup> In the initial report, directed 1,2 and 1,4 C–H monofluorination of ketones was disclosed as well as aryl fluorination.<sup>25</sup> Since then, Selectfluor has been widely used for monofluorination, especially in formation of glycosylfluoride molecules.<sup>26</sup> In 2013, the more synthetically challenging benzylic C–H mono and difluorination was achieved using either Selectfluor I or II and a photocatalyst (**Figure 1.2 d**).<sup>27</sup> Two separate sets of conditions (Selectfluor I and 9-fluorenone or Selectfluor II and xanthone) afforded selectively mono or difluorinated products at the benzylic position upon exposure to visible light.<sup>27</sup> Reaction progress was completely arrested in the dark demonstrating the requirement of light.<sup>27</sup> While degree of fluorination can be regulated with Selectfluor and other direct fluorination reagents, convergent syntheses will require preassembled fluoroalkyl building blocks.

### **1.3 Methods to Directly Install –CF<sub>3</sub>**

The breadth and depth of methods to install a trifluoromethyl group from reagents containing a preassembled –CF<sub>3</sub> unit are unparalleled compared to any other fluoroalkyl group.



The plethora of information on trifluoromethylation can be catalogued by mechanism of  $-\text{CF}_3$  transfer into 3 categories (nucleophilic, radical and electrophilic) (**Figure 1.3**). These categories dictate the types of transformations the trifluoromethylation reagents can invoke.

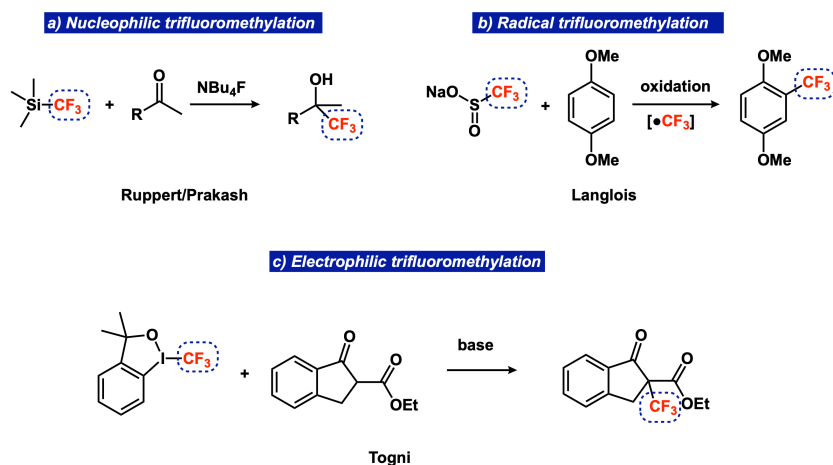


**Figure 1.3** Trifluoromethylation strategies a) nucleophilic trifluoromethylation b) radical trifluoromethylation c) electrophilic trifluoromethylation

### 1.3.1 Nucleophilic Trifluoromethylation

The most widely used reagent to perform nucleophilic trifluoromethylation reactions is trifluoromethyltrimethylsilane ( $\text{TMSCF}_3$ ).<sup>28</sup> This versatile building block was first synthesized in 1984 by Ruppert and coworkers by reducing  $\text{BrCF}_3$  in the presence of  $\text{TMSCl}$  with tris(dimethylamino)phosphine as a reductant.<sup>29</sup> Five years later, Prakash demonstrated trifluoromethylation ketones and aldehydes with  $\text{TMSCF}_3$  and a catalytic fluoride source (**Figure 1.3 a**).<sup>30</sup> Fluoride was only required for the initial activation of the silane, and subsequent nucleophilic activation was propagated by the trifluoromethyl alkoxide products.<sup>30</sup> Mechanistic NMR studies revealed that  $\text{TMSCF}_3$  forms a transient reactive pentacoordinate silicate species, which is the key intermediate responsible for  $-\text{CF}_3$  transfer.<sup>31</sup>

Over the past three decades, a massive variety of trifluoromethylation reactions have been uncovered and optimized with trifluoromethyl silanes.<sup>28</sup> Importantly, Buchwald and coworkers

employed triethyl(trifluoromethyl)silane in palladium catalyzed cross-coupling with aryl chlorides to afford trifluoromethyl arenes; substrates that are generally difficult to synthesize through traditional electrophile/nucleophile chemistry.<sup>6</sup> Another key advancement was the synthesis of  $\text{TMSCF}_3$  from fluoroform, a cheap byproduct of the Teflon industry, using potassium hexamethyldisilazide as a base for deprotonation.<sup>32</sup> While other reagents such as trifluoromethyl borates<sup>33</sup> and trifluoromethyl hemiaminals<sup>34</sup> exist as alternatives to  $\text{TMSCF}_3$ , they are not used as frequently and do not offer the same bevy of potential reactions.

The Szymczak lab reported a Lewis acid/base strategy to deprotonate fluoroform and stabilize an adduct of hexamethylborazine and the trifluoromethyl anion.<sup>35</sup> Treatment of benzyl potassium with hexamethylborazine and 18-crown-6 affords a highly basic Lewis acid/base adduct, which can subsequently deprotonate  $\text{HCF}_3$  to form a borazine- $\text{CF}_3$  adduct.<sup>35</sup> After  $-\text{CF}_3$  capture, transfer to  $\text{TMSCl}$  and  $\text{B}(\text{OMe})_3$  affords established reagents,  $\text{TMSCF}_3$  and  $(\text{MeO})_3\text{BCF}_3\text{K}$  in nearly quantitative yields at room temperature.<sup>35</sup> Subsequently, borazine- $\text{CF}_3$  was shown to transfer trifluoromethanide to 18 different elements as well as a wide variety of carbon based electrophiles including ketones, aldehydes, nitroarenes and activated N-heterocycles.<sup>36</sup> To differentiate the approach from  $\text{TMSCF}_3$ , which extrudes  $\text{TMSF}$  as a stoichiometric, thermodynamic sink, 0.1 equivalents of hexamethyl borazine were cycled 10 total times with sodium hydride as a base to convert  $\text{TMSCl}$  to  $\text{TMSCF}_3$  in 49% yield.<sup>35</sup>

### ***1.3.2 Radical Trifluoromethylation***

In situ generation of a  $\bullet\text{CF}_3$  radical unlocks an entirely different set of reactions that are inaccessible with nucleophilic methodology.<sup>37</sup> N-trifluoromethyl-N-nitrosobenzenesulfonamide induces the C-H activation of arenes and heteroarenes to form the corresponding trifluoromethylated products.<sup>38</sup> Potassium trifluoromethanesulfinate can trifluoromethylate olefins

and electron rich arenes under electrochemical oxidation (**Figure 1.3 b**).<sup>39</sup> Additionally, copper and silver salts can effect dehalogenative or decarboxylative trifluoromethylation of alkanes.<sup>37</sup>

### 1.3.3 Electrophilic Trifluoromethylation

In contrast to the above nucleophilic and radical trifluoromethylation strategies, electrophilic trifluoromethylation allows for reaction with classic C, N, O, and S nucleophiles.<sup>40</sup> Umemoto developed a series of (trifluoromethyl) dibenzothiophenium and (trifluoromethyl) dibenzoselenophenium reagents.<sup>41</sup> Enolates, aniline and acetylide nucleophiles displaced dibenzothiophene or the related uncharged selenium compound to form trifluoromethyl ketones, aniline and alkynes.<sup>41</sup> Hypervalent iodide trifluoromethyl species undergo similar transformations with nucleophiles.<sup>42</sup> Togni and coworkers effectively used an umpolung approach by transforming TMSCF<sub>3</sub>, a nucleophilic –CF<sub>3</sub> source into a potent electrophile.<sup>42</sup> The ortho benzyl alcohol moiety of aryl iodides allowed for stabilization of the *I*-trifluoromethyl group in a T-shaped geometry.<sup>42</sup> Finally a β-keto ester was used as a nucleophilic substrate in the presence of base, affording the α-trifluoromethylated dione product (**Figure 1.3 c**).<sup>42</sup> Ultimately, these electrophilic, nucleophilic and radical trifluoromethylation strategies laid the ground-work for direct installation of more complex fluoroalkyl nucleophiles.

## 1.4 Methods to Directly Install –CF<sub>2</sub>R

### 1.4.1 Deprotonation of H–CF<sub>2</sub>R and Subsequent Transfer

The Szymczak lab found that the deprotonation/Lewis acid stabilization methodology discussed in Chapter 1.3 could be expanded to other fluoroalkyl groups with the estimated pK<sub>a</sub> of 28-40 (**Figure 1.4 a**).<sup>43</sup> Difluoromethylbenzene is activated under completely analogous conditions to fluorobenzene (formation of benzyl–hexamethylborazine adduct, followed by addition

of fluoroalkane).<sup>35, 43</sup> Unlike the borazine–CF<sub>3</sub> species,<sup>35, 36</sup> borazine–CF<sub>2</sub>Ph proved to be stable as an isolable solid or as a concentrated THF stock solutions.<sup>43</sup>

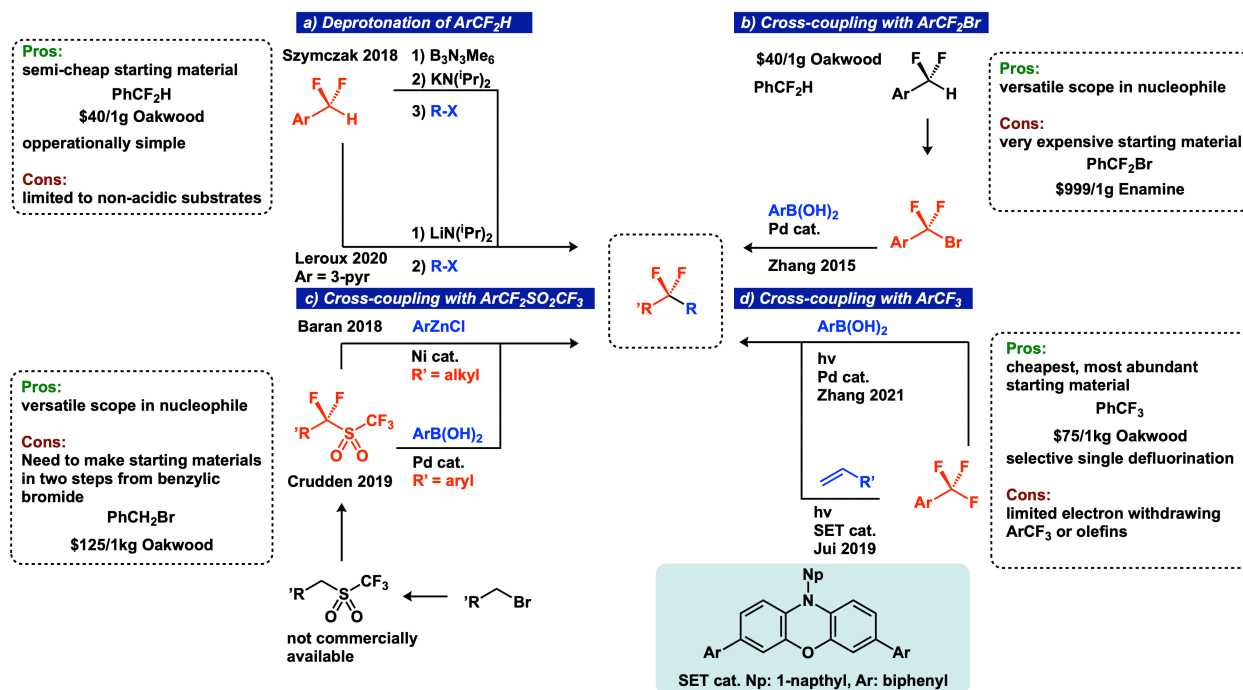


**Figure 1.4** Different ways to directly install –CF<sub>2</sub>R and the pros and cons to each –CF<sub>2</sub>R precursor: a) deprotonation of ArCF<sub>2</sub>H b) cross-coupling with ArCF<sub>2</sub>Br c) cross-coupling with ArCF<sub>2</sub>SO<sub>2</sub>CF<sub>3</sub> d) cross-coupling with ArCF<sub>3</sub>

Order of addition and selection of base proved to be important for deprotonation and adduct formation for difluoromethyl heteroarenes.<sup>43</sup> Unlike difluoromethyl benzene, other HCF<sub>2</sub>Ar substrates did not react when benzyl potassium was used as a base.<sup>43</sup> Potassium diisopropyl amide (KDA) had to be added *last* to a mixture of Lewis acid and HCF<sub>2</sub>Ar at -78 °C to ensure formation of the desired borazine–CF<sub>2</sub>Ar adduct.<sup>43</sup> Due to the bulky nature of the diisopropyl amide group, borazine–amide adducts are inaccessible, leading to reactions with lower kinetic barriers to form borazine–CF<sub>2</sub>Ar when KDA is used as a base. The corresponding borazine–CF<sub>2</sub>Ar is quenched with an electrophile at -78 °C and warmed to room temperature. Benzophenone, a tosylated imine, benzaldehyde, diphenyl disulfide and pyridine were demonstrated as electrophilic reagents

competent for reactivity with borazine–CF<sub>2</sub>Ar (11 examples) species to form C–CF<sub>2</sub>Ar or S–CF<sub>2</sub>Ar bonds.<sup>43</sup>

One alternative to using a strong base like benzyl potassium or KDA to deprotonate a difluoromethyl aryl species is lowering the pK<sub>a</sub> of the HCF<sub>2</sub>Ar precursor. Difluoromethyltriazoles represent a unique class of difluoromethyl heteroaryl compounds that are sufficiently acidic to be deprotonated by potassium tert-butoxide.<sup>44</sup> In contrast to a lithium base, LHMDS, which induces rapid formation of difluorocarbene, KHMDS and KO<sup>t</sup>Bu can successfully deprotonate difluoromethyltriazole compounds.<sup>44</sup> The resulting difluoromethanide species further reacts with carbonyl electrophiles to form the corresponding fluorinate alcohol products.<sup>44</sup>

While lithium bases have been widely cited to induce  $\alpha$ -fluoride elimination when deprotonating fluoroalkanes,<sup>45, 46</sup> there are select instances when strong lithium bases can be utilized to successfully deprotonate fluoroalkanes with use of cryogenic temperatures and rapid quenching with an electrophile.<sup>47</sup> Leroux and coworkers found that at -78 °C or -100 °C, lithium diisopropyl amide could be used to deprotonate 3-difluoromethyl pyridine and subsequently transfer the resulting anion to electrophilic halosilane, stannane or alkane substrates (**Figure 1.4 a**).<sup>47</sup> The resulting silane reagents could successfully transfer the difluoromethylpyridyl group to a larger selection of electrophiles than the original lithiate.<sup>47</sup>

Ultimately direct deprotonation is a powerful strategy to generate powerful nucleophiles from relatively inert fluoroalkyl precursors. The crucial limitation is the inherent basicity of the corresponding aryl/alkyl difluoromethanide anions.<sup>43</sup> Reactions that invoke even mildly acidic reagents or solvents will be challenging if not impossible when using direct deprotonation methodology.

### 1.4.2 Br-CF<sub>2</sub>R as a “CF<sub>2</sub>R” Source

Metal catalyzed cross-coupling reactions typically involve an electrophilic and nucleophilic partner, invoking oxidative addition and transmetalation/reductive elimination respectively.<sup>48</sup> Due to the comparatively low numbers of B-CF<sub>2</sub>R<sup>49</sup> and Si-CF<sub>2</sub>R,<sup>47, 50</sup> the corresponding Suzuki and Hiyama coupling reactions with organic electrophiles remain largely underdeveloped. Consequently, research efforts have focused more on the use of bromodifluoromethyl arenes in conjunction with the standard organonucleophiles used in cross-coupling.

Zhang and coworkers employed a Pd(II) acetate precatalyst with exogenous diadamantyl butyl phosphine ligand to induce cross-coupling between bromodifluoromethyl benzene and boronic acids (**Figure 1.4 b**).<sup>51</sup> Inhibition of catalysis with 1,4-dinitrobenzene and radical trapping experiments suggest a single electron transfer pathway to form a transient difluorobenzyl radical during catalysis.<sup>51</sup> In addition to bromodifluoromethyl arenes, heteroarenes, alkenes and alkynes have been utilized in similar Pd, Ni and Cu cross coupling systems.<sup>7</sup> While this class of electrophilic -CF<sub>2</sub>R reagent is versatile in catalytic reactions, it suffers from being expensive to synthesize. The main synthetic route to access these useful precursors is a radical bromination of difluoromethyl arenes, N-bromo succinimide and light.<sup>52</sup> This is arguably the biggest draw-back to using bromodifluoromethyl arenes as reagents in cross-coupling reactions, as even the precursory difluoromethyl arenes would require either DAST<sup>4</sup> or a difluoromethyl cross-coupling strategy to synthesize.<sup>7</sup>

### 1.4.3 $R'O_2S-CF_2R$ as a “ $CF_2R$ ” Source

Aryl difluoromethyl sulfones are similar to bromodifluoromethyl arenes (Chapter 1.4.2) in that they can act as electrophilic cross coupling partners.<sup>8</sup> However, the difluoromethyl sulfonyl group offers one distinct advantage over its brominated counterpart in terms of ease of synthesis.<sup>8</sup> Benzylic sulfone precursors contain activated C–H bonds, which can be fluorinated under mild conditions using *N*-fluorobenzenesulfonimide as an electrophilic fluorination source.<sup>8</sup> For the aforementioned reasons, high-impact studies on desulfonylative difluoromethyl aryl and alkyl coupling reactions have been published (**Figure 1.4 c**).<sup>53, 54</sup> The Baran group<sup>53</sup> recently demonstrated Negishi coupling reactions between fluoroalkyl sulfones and aryl zinc organonucleophiles using a nickel bipyridine catalyst.<sup>53</sup> A complementary method to install doubly benzylic difluoromethylene linkages was established by Crudden and coworkers, leveraging aryl difluoromethyl sulfones with aryl boronic acid coupling partners and a palladium catalyst.<sup>54</sup> While mild, late-stage fluorination of benzylic sulfones offers a distinct advantage over the harsh late-stage bromination of difluoromethyl arenes, initial installation of benzylic sulfone still presents its own synthetic challenges.<sup>55</sup>

### 1.4.4 $F-CF_2R$ as a “ $CF_2R$ ” Source

The trifluoromethyl group is the most ubiquitous of all fluoroalkyls. Consequently, selective mono-defluorinative functionalization reactions from aryl and alkyl trifluoromethyl precursors are of high interest to the synthetic community. Selective defluorination of trifluoromethyl arenes presents a unique challenge, however, due to these substrates possessing comparatively high C–F bond dissociation energy (BDE).<sup>56</sup> Indeed, the C–F BDE of  $PhCF_3$ , (111 kcal/mol) is higher than that of the potential singly-defluorinated products, [ $PhCF_2H$  (101 kcal/mol),  $PhCF_2Ph$  (95 kcal/mol),  $PhCF_2Me$  (102 kcal/mol)], indicating that it is

thermodynamically easier to defluorinate multiple times.<sup>56</sup> To circumvent this inherent selectivity issue, light promoted catalysis has been employed in recent years.<sup>56, 57</sup>

Given the infrastructure of Pd cross-coupling with bromodifluoromethyl arenes and aryl boronic acids,<sup>51</sup> The Zhang group was uniquely situated to expand their system to include trifluoromethyl arenes as substrates for defluorinative cross-coupling reactions (**Figure 1.4 d**).<sup>56</sup> C–F oxidative addition was induced with the use of a blue LED lamp and a palladium catalyst with bulky phosphine ligands.<sup>56</sup> Proceeding transmetalation of a boronic acid and reductive elimination afforded a series of diaryl difluoromethane products.<sup>56</sup> In spite of the synthetic advantage of using cheap, widely available trifluoromethyl arenes, the scope was electronically limited. Only trifluoromethyl arenes and heteroarenes with reduction potentials between -2.68 and -2.55 volts were successful substrates for cross-coupling and subsequent isolation.<sup>56</sup>

By using a phenoxazine photo catalyst,<sup>58</sup> Jui and coworkers were able to effectively defluorinate and functionalize an electronically diverse series of trifluoromethyl arenes (**Figure 1.4 d**).<sup>57</sup> By photo-inducing single electron transfer with a blue LED, an ArCF<sub>2</sub>· equivalent can insert into a carbon–carbon double bond, ultimately leading to ArCF<sub>2</sub>–alkyl products in the presence of an H-atom donor.<sup>57</sup> While having access to electron neutral and donating ArCF<sub>3</sub> substrates is a clear advantage of Jui's methodology over Zhang's, terminal olefins are inherently less stable than boronic acids as coupling partners, which could lead to problems in application of this methodology to more complex syntheses.<sup>56, 57</sup>

## 1.5 Boron Fluoroalkyl Species

### 1.5.1 Potassium Trimethoxy(trifluoromethyl)borate

Potassium trimethoxy(trifluoromethyl)borate, (MeO)<sub>3</sub>BCF<sub>3</sub>K, was initially synthesized from TMSCF<sub>3</sub> and proposed to have application in Suzuki coupling and Petasis reactions.<sup>49</sup> In



2011, nearly a decade later, copper catalyzed cross-coupling of aryl and heteroaryl iodides using  $(\text{MeO})_3\text{BCF}_3\text{K}$  were reported.<sup>59</sup> In the same year, Tartakovsky and coworkers published  $-\text{CF}_3$  transfer from  $(\text{MeO})_3\text{BCF}_3\text{K}$  to a series of imines, aldehydes and ketones, as well as trifluorovinyl and pentafluoroethyl transfer from the related trimethoxy(fluoroalkyl)borates.<sup>33</sup> While  $(\text{MeO})_3\text{BCF}_3\text{K}$  offers the advantage of not requiring a nucleophilic activator over  $\text{TMSCF}_3$ , the scope in nucleophilic and catalytic reactivity is severely limited.<sup>6, 30, 33, 59</sup>

### 1.5.2 Potassium Trifluoro(trifluoromethyl)borate

In general organotrifluoroborate salts are extremely deactivated and robust to reaction conditions, and require water to participate in Suzuki cross-coupling reactions with electrophiles.<sup>60</sup> Therefore, the electron-deficient trifluoro(trifluoromethyl)borate,  $\text{F}_3\text{BCF}_3\text{K}$ , does not possess the same nucleophilic properties as  $(\text{MeO})_3\text{BCF}_3\text{K}$ , and no analogous trifluoromethylation reactions of standard electrophiles (ketones/aldehydes) have been reported.<sup>33</sup> However, selective  $-\text{CF}_3$  additions to pyridine and quinoline N-oxides have been uncovered using trifluoromethyl-difluoroborane,  $\text{F}_2\text{BCF}_3$ , as an activator and/or a  $-\text{CF}_3$  source.<sup>61, 62</sup> Upon fluoride abstraction with  $\text{BF}_3 \cdot \text{OEt}_2$ ,  $\text{F}_3\text{BCF}_3\text{K}$  is converted to the neutral  $\text{F}_2\text{BCF}_3$  species, which thereby coordinates to and activates pyridine and quinoline N-oxides.<sup>61</sup> The activated N-oxides are primed for ortho-trifluoromethylation using  $\text{TMSCF}_3$  followed by rearomatization.<sup>61</sup> The next year, Kanai and coworkers discovered using  $\text{TMSCF}_3$  as an exogenous  $-\text{CF}_3$  source is not required for 2-methyl or benzyl trifluoromethylborate N-oxides (**Figure 1.5**).<sup>62</sup> They propose deprotonation of the benzylic C–H bond, followed by a 6-membered concerted trifluoromethyl transfer as the operative mechanism.<sup>62</sup> These transformations offered a novel route to aromatic and benzylic C–H trifluoromethylation of N-heterocycles.<sup>61, 62</sup>

Direct C-H trifluoromethylation derived from  $F_3BCF_3K$

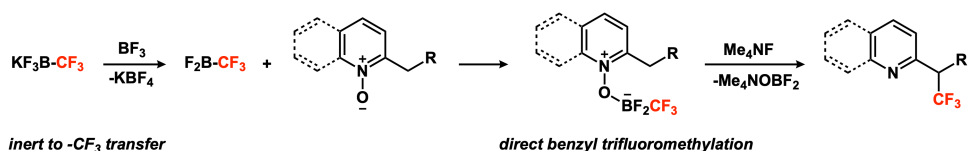


**Figure 1.5** Kanai's direct trifluoromethylation of 2-substituted N-oxide heterocycles derived from  $KF_3BCF_3$

### 1.5.3 Hexamethylborazine Fluoroalkyl Adducts

Hexamethylborazine- $CF_2R$  adducts ( $R = F, Ph, \text{hetAr}$ ) can be generated from fluoroalkanes in the presence of hexamethylborazine, a strong base, and crown ether (*See sections 1.3.1 and 1.4.1 for greater detail*).<sup>35, 36, 43</sup> This class of reagent does not require a nucleophilic activator, like  $TMSCF_3$ ,<sup>30</sup> to induce  $-CF_2R$  transfer.<sup>35, 36, 43</sup> Moreover, the conditions for fluoroalkyl transfer ( $25\text{ }^\circ\text{C}$ )<sup>35, 36, 43</sup> are much milder than  $(MeO)_3BCF_3K$  which typically requires heating.<sup>33</sup> A key feature of these  $-CF_2R$  adducts is the stabilization of potassium using a crown-ether, which increases both their stability and solubility.<sup>35, 36, 43</sup> Indeed, K1-F1 interactions are present in the crystal structures:  $2.697\text{ \AA}$  for borazine- $CF_3$  and  $2.782\text{ \AA}$  for borazine- $CF_2Ph$ .<sup>35, 43</sup> In the later case, recrystallization of the adduct affords white crystalline material that can be stored and weighed out for subsequent reactions.<sup>43</sup>

## 1.6 Metal Fluorocarbenes

The difluorocarbene is an attractive building block for installation of a difluoromethylene unit into more complex chemical structures.<sup>63</sup> Many non-fluorinated metal carbenes are generated from diazo compounds.<sup>64-66</sup> This strategy does not directly translate to the difluorocarbene, as the corresponding difluorodiazomethane compound is not formed experimentally and the related difluorodiazirine is extremely limited in synthesis.<sup>67, 68</sup> Alternatively, mono and

dihalodifluoromethane species ( $\text{CF}_2\text{X}_2/\text{CF}_2\text{XH}$ ) as well as  $\text{TMSCF}_2\text{X}$  are utilized to generate a difluorocarbene equivalent in situ.<sup>63</sup>

For generation of metal difluorocarbenes in particular,  $\alpha$ -fluoride elimination of a discrete metal trifluoromethyl complex is a commonly used strategy.<sup>63</sup> A set of isostructural P-O-C-O-P pincer Ni and Pd difluorocarbenes were synthesized in the Baker lab from the metal- $\text{CF}_3$  precursor complexes with  $\text{B}(\text{C}_6\text{F}_5)_3$  as a fluoride abstractor (**Figure 1.6 a**).<sup>69</sup> These electrophilic carbenes react with pyridine, forming  $\text{M}-\text{CF}_2$ -pyr adducts.<sup>69</sup> Phenyl substitution at the 2-position of pyridine proved to be too sterically encumbered for analogous adduct formation with the metal difluorocarbenes, instead resulting in regeneration on the  $\text{M}-\text{CF}_3$  precursor.<sup>69</sup>

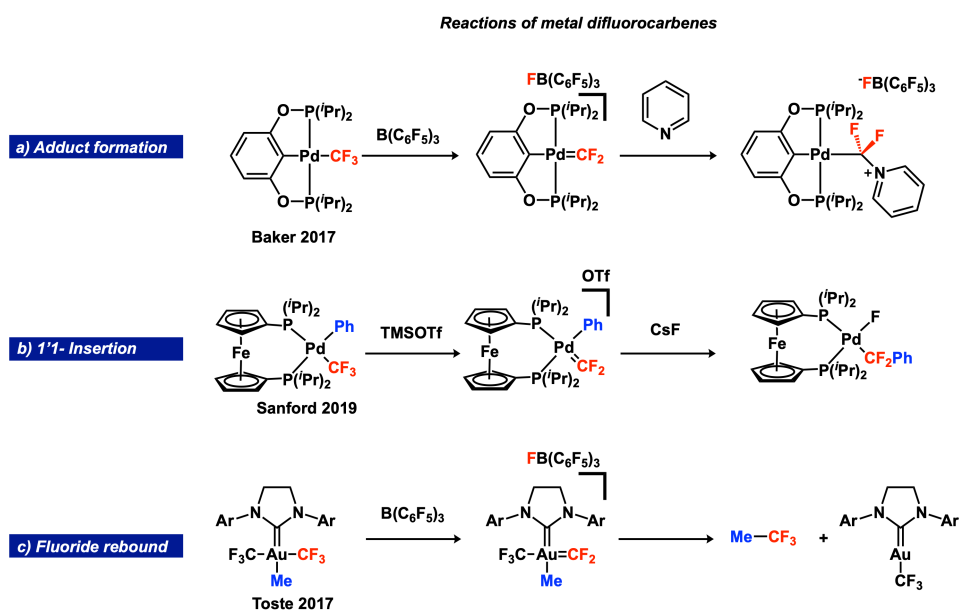


**Figure 1.6** Reactions of metal difluorocarbenes a) adduct formation b) 1,1-insertion c) fluoride rebound

In addition to reactions with nitrogen nucleophiles, metal difluorocarbenes can also undergo 1,1-insertion into metal-carbon bonds.<sup>63</sup> In catalytic Pd cross-coupling of  $\text{TESCF}_3$  and aryl chlorides, difluorodiphenyl methane was observed as a homo-coupled side-product by Sanford and coworkers.<sup>70</sup> In the presence of excess  $\text{TMSCF}_3$ , their T-shaped Pd-phenyl- $\text{CF}_3$

complex decomposed at room temperature into a new complex featuring a CF<sub>2</sub>-Ph unit.<sup>70</sup> Two years later in a detailed study of Pd-CF<sub>3</sub> complexes, they found that TMS triflate could be used to abstract a fluoride and induce 1,1-migratory insertion of the CF<sub>2</sub> carbene into a Pd-Ph bond (**Figure 1.6 b**).<sup>71</sup>

In addition to 1,1-insertion chemistry, fluoride rebound of gold difluorocarbene species can allow for difficult formal C(sp<sup>3</sup>)-CF<sub>3</sub> reductive elimination reactions.<sup>72</sup> The Toste lab demonstrated catalytic B(C<sub>6</sub>F<sub>5</sub>)<sub>3</sub> can be used to abstract fluoride from gold(III) trifluoromethyl alkyl complexes, and also redeliver fluoride to the transient gold difluoroalkyl species, forming trifluoromethyl alkanes (**Figure 1.6 c**).<sup>72</sup> Finally, the isolable gold difluoroalkyl intermediates can be treated with radio-labeled K<sup>18</sup>F-cryptand to form positron emission tomography tracers via a late-stage fluorination strategy.<sup>72</sup>

The goal of my PhD work is to establish new methods to directly install -CF<sub>2</sub>R groups using boron-based reagents. As discussed in Chapters 1.2 and 1.4, installation of a preassembled fluoroalkyl group can mitigate some of the compatibility issues with direct fluorination of C-H or C-O bonds.

## Chapter 1 Bibliography

1. Gillis, E. P.; Eastman, K. J.; Hill, M. D.; Donnelly D. J.; Meanwell, N. A. *J. Med. Chem.*, 2015, 58, 8315-8359.
2. Jeschke, P. in *Organofluorine Chemistry*, Wiley-VCH, Weinheim, 2021, pp. 363-395.
3. Jaye, J. A.; Sletten, E. M. *Polym. Chem.*, 2021, 12, 6515-6526.
4. Markovskij, L. N.; Pashinnik, V. E.; Kirsanov, A. V. *Synthesis*, 1973, 1973, 787-789.
5. Olah, G. A.; Welch, J. T.; Vankar, Y. D.; Nojima, M.; Kerekes, I.; Olah, J. A. *J. Org. Chem.*, 1979, 44, 3872-3881.
6. Cho, E. J.; Senecal, T. D.; Kinzel, T.; Zhang, Y.; Watson, D. A.; Buchwald, S. L. *Science*, 2010, 328, 1679-1681.
7. Feng, Z.; Xiao, Y.-L.; Zhang, X. *Acc. Chem. Res.*, 2018, 51, 2264-2278.
8. Nambo, M.; Crudden, C. M. *Chem. Rec.*, 2021, 21, 3978-3989.
9. Fried, J.; Sabo, E. F. *J. Am. Chem. Soc.*, 1954, 76, 1455-1456.
10. Lubowe, I. I. *A.M.A. Archives of Dermatology*, 1955, 72, 164-170.
11. Yu, Y.; Liu, A.; Dhawan, G.; Mei, H.; Zhang, W.; Izawa, K.; Soloshonok, V. A.; Han, J. *Chin. Chem. Lett.*, 2021, 32, 3342-3354.
12. Meanwell, N. A. *J. Med. Chem.*, 2018, 61, 5822-5880.
13. Murphy, C. D.; Sandford, G. *Expert Opin. Drug Metab. Toxicol.*, 2015, 11, 589-599.
14. Huchet, Q. A.; Kuhn, B.; Wagner, B.; Kratochwil, N. A.; Fischer, H.; Kansy, M.; Zimmerli, D.; Carreira, E. M.; Müller, K. *J. Med. Chem.*, 2015, 58, 9041-9060.
15. Tius, M. A. *Tetrahedron*, 1995, 51, 6605-6634.
16. Weeks, J. L.; Chernick, C. L.; Matheson, M. S. *J. Am. Chem. Soc.*, 1962, 84, 4612-4613.
17. Patrick, T. B.; Khazaeli, S.; Nadji, S.; Hering-Smith, K.; Reif, D. *J. Org. Chem.*, 1993, 58, 705-708.
18. Stavber, S.; Koren, Z.; Zupan, M. *Synlett*, 1994, 1994, 265-266.
19. Bilska-Markowska, M.; Szwajca, A.; Marciniak, B. *J. Fluor. Chem.*, 2019, 227, 109364.
20. Messina, P. A.; Mange, K. C.; Middleton, W. J. *J. Fluor. Chem.*, 1989, 42, 137-143.
21. Gustafsson, T.; Gilmour, R.; Seeberger, P. H. *Chem. Commun.*, 2008, 3022-3024.
22. Iashin, V.; Wirtanen, T.; Perea-Buceta, J. E. *Catalysts*, 2022, 12, 233.
23. Melvin, P. R.; Ferguson, D. M.; Schimmler, S. D.; Bland, D. C.; Sanford, M. S. *Org. Lett.*, 2019, 21, 1350-1353.
24. Okoromoba, O. E.; Han, J.; Hammond, G. B.; Xu, B. *J. Am. Chem. Soc.*, 2014, 136, 14381-14384.
25. Banks, R. E.; Mohialdin-Khaffaf, S. N.; Lal, G. S.; Sharif, I.; Syvret, R. G. *J. Chem. Soc., Chem. Commun.*, 1992, 595-596.
26. Nyffeler, P. T.; Durón, S. G.; Burkart, M. D.; Vincent, S. P.; Wong, C.-H. *Angew. Chem. Int. Ed.*, 2005, 44, 192-212.
27. Xia, J.-B., Zhu, C.; Chen, C. *J. Am. Chem. Soc.*, 2013, 135, 17494-17500.
28. Liu, X.; Xu, C.; Wang, M.; Liu, Q. *Chem. Rev.*, 2015, 115, 683-730.

29. Ruppert, I.; Schlich, K.; Volbach, W. *Tetrahedron Lett.*, 1984, 25, 2195-2198.
30. Prakash, G. K. S.; Krishnamurti, R.; Olah, G. A. *J. Am. Chem. Soc.*, 1989, 111, 393-395.
31. Maggiorosa, N.; Tyrra, W.; Naumann, D.; Kirij, N. V.; Yagupolskii, Y. L. *Angew. Chem. Int. Ed.*, 1999, 38, 2252-2253.
32. Prakash, G. K.; Jog, P. V.; Batamack, P. T.; Olah, G. A. *Science*, 2012, 338, 1324-1327.
33. Levin, V. V.; Dilman, A. D.; Belyakov, P. A.; Struchkova, M. I.; Tartakovskiy, V. A. *Tetrahedron Lett.*, 2011, 52, 281-284.
34. Billard, T.; Langlois, B. R.; Blond, G. *Eur. J. Org. Chem.*, 2001, 2001, 1467-1471.
35. Geri, J. B.; Szymczak, N. K. *J. Am. Chem. Soc.*, 2017, 139, 9811-9814.
36. Geri, J. B.; Wade Wolfe, M. M.; Szymczak, N. K. *Angew. Chem. Int. Ed.*, 2018, 57, 1381-1385.
37. Xiao, H.; Zhang, Z.; Fang, Y.; Zhu, L.; Li, C. *Chem. Soc. Rev.*, 2021, 50, 6308-6319.
38. Umemoto, T.; Miyano, O. *Tetrahedron Lett.*, 1982, 23, 3929-3930.
39. Tommasino, J.-B.; Brondex, A.; Médebielle, M.; Thomalla, M.; Langlois, B. R.; Billard, T. *Synlett*, 2002, 2002, 1697-1699.
40. Barata-Vallejo, S.; Lantaño, B.; Postigo, A. *Chem. Eur. J.*, 2014, 20, 16806-16829.
41. Teruo, U.; Sumi, I. *Tetrahedron Lett.*, 1990, 31, 3579-3582.
42. Eisenberger, P.; Gischig, S.; Togni, A. *Chem. Eur. J.*, 2006, 12, 2579-2586.
43. Geri, J. B.; Wade Wolfe, M. M.; Szymczak, N. K. *J. Am. Chem. Soc.*, 2018, 140, 9404-9408.
44. Chai, J. Y.; Cha, H.; Kim, H. B.; Chi, D. Y. *Tetrahedron*, 2020, 76, 131370.
45. Lishchynskiy, A.; Miloserdov, F. M.; Martin, E.; Benet-Buchholz, J.; Escudero-Adán, E. C.; Konovalov, A. I.; Grushin, V. V. *Angew. Chem. Int. Ed.*, 2015, 54, 15289-15293.
46. Prakash, G. K. S.; Wang, F.; Zhang, Z.; Haiges, R.; Rahm, M.; Christe, K. O.; Mathew, T.; Olah, G. A.; *Angew. Chem. Int. Ed.*, 2014, 53, 11575-11578.
47. Santos, L.; Panossian, A.; Donnard, M.; Vors, J.-P.; Pazenok, S.; Bernier, D.; Leroux, F. R. *Org. Lett.*, 2020, 22, 8741-8745.
48. Hassan, J.; Sévignon, M.; Gozzi, C.; Schulz, E.; Lemaire, M. *Chem. Rev.*, 2002, 102, 1359-1470.
49. Kolomeitsev, A. A.; Kadyrov, A. A.; Szczepkowska-Sztolcman, J.; Milewska, M.; Koroniak, H.; Bissky, G.; Barten, J. A.; Röschenthaler, G.-V. *Tetrahedron Lett.*, 2003, 44, 8273-8277.
50. Clavel, P.; Léger-Lambert, M. P.; Biran, C.; Serein-Spirau, F.; Bordeau, M.; Roques, N.; Marzouk, H. *Synthesis*, 1999, 1999, 829-834.
51. Gu, J.-W.; Guo, W.-H.; Zhang, X. *Org. Chem. Front.*, 2015, 2, 38-41.
52. He, J.; Fittman, C. U. *Synth. Commun.*, 1999, 29, 855-862.
53. Merchant, R. R.; Edwards, J. T.; Qin, T.; Kruszyk, M. M.; Bi, C.; Che, G.; Bao, D.-H.; Qiao, W.; Sun, L.; Collins, M. R.; Fadeyi, O. O.; Gallego, G. M.; Mousseau, J. J.; Nuhant, P.; Baran, P. S. *Science*, 2018, 360, 75-80.
54. Nambo, M.; Yim, J. C. H.; Freitas, L. B. O.; Tahara, Y.; Ariki, Z. T.; Maekawa, Y.; Yokogawa, D.; Crudden, C. M. *Nat. Commun.*, 2019, 10, 4528.
55. Hendrickson, J. B.; Giga, A.; Wareing, J. *J. Am. Chem. Soc.*, 1974, 96, 2275-2276.
56. Luo, Y.-C.; Tong, F.-F.; Zhang, Y.; He, C.-Y.; Zhang, X. *J. Am. Chem. Soc.*, 2021, 143, 13971-13979.
57. Vogt, D. B.; Seath, C. P.; Wang, H.; Jui, N. T. *J. Am. Chem. Soc.*, 2019, 141, 13203-13211.

58. Pearson, R. M.; Lim, C.-H.; McCarthy, B. G.; Musgrave, C. B.; Miyake, G. M. *J. Am. Chem. Soc.*, 2016, 138, 11399-11407.
59. Knauber, T.; Arikan, F.; Röschenthaler, G.-V.; Gooßen, L. J. *Chem. Eur. J.*, 2011, 17, 2689-2697.
60. Molander, G. A.; Ellis, N. *Acc. Chem. Res.*, 2007, 40, 275-286.
61. Nishida, T.; Ida, H.; Kuninobu, Y.; Kanai, M. *Nat. Commun.*, 2014, 5, 3387.
62. Kuninobu, Y.; Nagase, M.; Kanai, M. *Angew. Chem. Int. Ed.*, 2015, 54, 10263-10266.
63. Zhou, W.; Pan, W.-J.; Chen, J.; Zhang, M.; Lin, J.-H.; Cao, W.; Xiao, J.-C. *Chem. Commun.*, 2021, 57, 9316-9329.
64. Davies, H. M. L.; Morton, D. *Chem. Soc. Rev.*, 2011, 40, 1857-1869.
65. Maas, G. *Chem. Soc. Rev.*, 2004, 33, 183-190.
66. Pei, C.; Yang, Z.; Koenigs, R. M. *Org. Lett.*, 2020, 22, 7300-7304.
67. Boldyrev, A. I.; Schleyer, P. v. R.; Higgins, D.; Thomson, C.; Kramarenko, S. S. *J. Comput. Chem.*, 1992, 13, 1066-1078.
68. Moss, R. A.; Wang, L.; Krogh-Jespersen, K. *J. Am. Chem. Soc.*, 2009, 131, 2128-2130.
69. Lee, G. M.; Korobkov, I.; Baker, R. T.; *J. Organomet. Chem.*, 2017, 847, 270-277.
70. Ferguson, D. M.; Bour, J. R.; Canty, A. J.; Kampf, J. W.; Sanford, M. S. *J. Am. Chem. Soc.*, 2017, 139, 11662-11665.
71. Ferguson, D. M.; Bour, J. R.; Canty, A. J.; Kampf, J. W.; Sanford, M. S. *Organometallics*, 2019, 38, 519-526.
72. Levin, M. D.; Chen, T. Q.; Neubig, M. E.; Hong, C. M.; Theulier, C. A.; Kobylanskii, I. J.; Janabi, M.; O'Neil, J. P.; Toste, F. D. *Science*, 2017, 356, 1272-1276.

## Chapter 2 Lewis Acid Stabilized Fluoroalkyl and Fluoroalkenyl Anions

Portions of this chapter have been published:

Geri, J. B.; Wade Wolfe, M. M.; Szymczak, N. K. *Angew. Chem. Int. Ed.* **2018**, *57*, 1381-1385.

### 2.1 Introduction

Strategies to install C–F bonds are of great interest to the medicinal community, due to the increased biological activity, metabolic stability and lipophilicity found in fluorinated drug-molecules when compared to their non-fluorinated counterparts.<sup>1</sup> Specifically, bioisosteres, or fluorinated functional groups that mimic non-fluorinated moieties in terms of size, electronegativity, and bioactivity have been established as templates for advancing drug discovery.<sup>2</sup> The –CF<sub>3</sub> group, for instance, can replace –CH<sub>3</sub> to produce drug candidates of similar size and polarity, but with increased biological activity.<sup>2</sup> Akenyl fluorides possess a similar size a dipole moment to enols, which are a common motif in biological systems.<sup>2</sup> Since fluoroalkyl(enyl) groups have been established as potent bioisosteres, new methods to synthesize pharmacophores containing these motifs are valuable.

Trimethyl(trifluoromethyl)silane, TMSCF<sub>3</sub>, is the most prolific trifluoromethylation reagent in synthetic chemistry.<sup>3-5</sup> While stable as a neat liquid at room temperature,<sup>5</sup> TMSCF<sub>3</sub> is activated with anionic ligands such as fluoride or alkoxide to form a reactive pentacoordinate silicate species that is competent for <sup>-</sup>CF<sub>3</sub> transfer.<sup>6</sup> Consequently, the identity of the counter cation of the activator and presence or absence of crown ethers dramatically changes the reactivity of TMSCF<sub>3</sub>.<sup>7</sup> While it is indeed possible to transfer <sup>-</sup>CF<sub>3</sub> from TMSCF<sub>3</sub> to boranes to create the



corresponding trifluoromethyl borate species,<sup>8</sup> boranes are also known to react with fluoride and alkoxide activators,<sup>9</sup> and undesired borane quenching side-reactions a challenge to overcome.

Recently, Geri and Szymczak reported a Lewis acid/base strategy to capture and transfer  $\text{CF}_3^-$  with hexamethylborazine.<sup>10</sup> The borazine- $\text{CF}_3$  adduct was able to quantitatively transfer a trifluoromethyl group to both  $\text{TMSCl}$  and  $\text{B(OMe)}_3$  at room temperature without the use of any exogenous activator.<sup>10</sup> We sought to understand the mechanism of  $\text{CF}_3^-$  transfer from hexamethyl borazine and how it differs from commercially available trifluoromethylation reagents,  $\text{TMSCF}_3$  and  $(\text{MeO})_3\text{BCF}_3\text{K}$ .

## 2.2 Mechanistic Insights into Borazine Based $\text{CF}_3^-$ Reagents

To interrogate whether  $\text{CF}_3^-$  transfer occurs through an associative or dissociative pathway, we determined the rate law for  $\text{CF}_3^-$  transfer from **2** ( $\text{B}_3\text{N}_3\text{Me}_6\text{CF}_3 \text{K(18-crown-6)}$ ) to representative electrophiles ( $\text{E} = \mathbf{7}$  (4-fluorobenzaldehyde), **8** (perfluorotoluene)). In an associative mechanism, the rate dependence for both **2** and  $\text{E}$  would be 1<sup>st</sup> order with a negative  $\Delta\text{S}^\ddagger$ . In a dissociative mechanism, the rate dependence for **2** and  $\text{E}$  would be 1<sup>st</sup>/zero order, with a positive  $\Delta\text{S}^\ddagger$ . Orders consistent with a dissociative mechanism were observed in  $\text{CF}_3^-$  transfer to **7/8**, with a positive  $\Delta\text{S}^\ddagger$  (+12(3) e.u.) value for **7** (**Figure 2.1 a**).

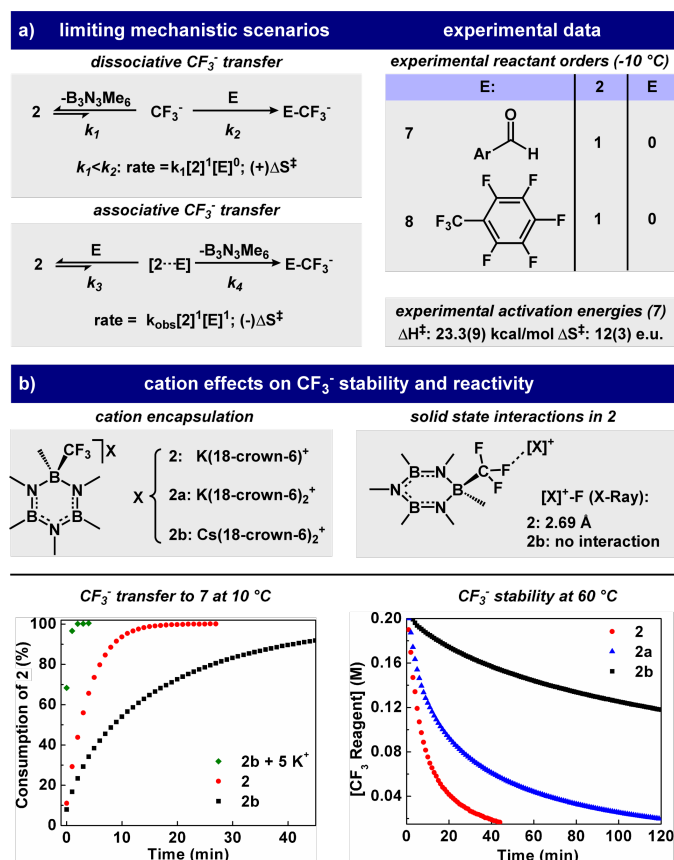


**Figure 2.1** a) Possible mechanisms for <sup>-</sup>CF<sub>3</sub> transfer. b) Cation effects on <sup>-</sup>CF<sub>3</sub> stability/reactivity. In 7, Ar=4-F-Ph

In addition to establishing the rate law for CF<sub>3</sub><sup>-</sup> transfer, we also found that thermal decomposition of **2** followed second order kinetics, suggesting that an encounter between [K(18-crown-6)]<sup>+</sup> and CF<sub>3</sub><sup>-</sup> units promote CF<sub>3</sub><sup>-</sup> defluorination.<sup>11</sup> This is supported by the presence of an intermolecular K-F interaction in the solid state structure of **2**, which elongates a single C-F bond.<sup>10</sup> Accordingly, cation Lewis acidity was found to directly influence the stability of **2**. Encapsulation of K<sup>+</sup> with 2 equiv 18-crown-6 improved the solution half-life at 60 °C (0.2 M) from 7 min to 18 min. Replacing K<sup>+</sup> in **2a** with less Lewis acidic Cs<sup>+</sup> provided even higher stability (180 min) (**Figure 2.1 b**). The latter variant exhibits high stability at 25 °C, with a daily decomposition rate of 1% in solution (0.2 M THF) and 3% as a solid, and showed *no* decomposition after one month

at -30 °C. The higher stability of **2b** is consistent with the absence of Cs-CF<sub>3</sub> interactions in its solid state structure.

The alkali metal dependence on the decomposition of **2** suggested that Lewis acids could also be used to facilitate dissociative CF<sub>3</sub><sup>-</sup> transfer. We hypothesized that the B<sub>3</sub>N<sub>3</sub>Me<sub>6</sub>(CF<sub>3</sub>)-cation interaction would labilize the B-CF<sub>3</sub> bond by reducing electron density at the carbon atom of CF<sub>3</sub>. Reagents **2** and **2b**, in which a cation-fluorine interaction is either present or absent, allowed us to clearly interrogate this hypothesis. In nucleophilic CF<sub>3</sub><sup>-</sup> transfer to aldehyde **7**, **2** was 3x faster than **2b**, indicating that the cation likely assists in rate-determining CF<sub>3</sub><sup>-</sup> dissociation. This mechanistic insight suggested that **2b** could be activated by the addition of exogenous Lewis acids: addition of 5 equiv. K[B(C<sub>6</sub>F<sub>5</sub>)<sub>4</sub>] to **2b** lead to a >40x increase in rate with no reduction in yield. This provides a complementary strategy to SiR<sub>3</sub>CF<sub>3</sub> reagents: activity is enhanced by addition of cationic, rather than anionic, activators.

### 2.3 Comparison to Trimethoxy(trifluoromethyl)borate

Chengyuan Peng helped contribute to this subchapter.

To better understand the generality of the effect of alkali metal additives on CF<sub>3</sub> transfer from boron-CF<sub>3</sub> adducts, we examined a known nucleophilic reagent, potassium trimethoxy(trifluoromethyl)borate [(MeO)<sub>3</sub>BCF<sub>3</sub>K].<sup>8, 12</sup> Since (MeO)<sub>3</sub>BCF<sub>3</sub>K has established reactivity with benzaldehyde<sup>12</sup> at 25 and 50 °C, we chose the 1,2-nucleophilic addition reaction for comparative mechanistic studies. First, we established operative dissociative kinetics, observing first-order dependence in (MeO)<sub>3</sub>BCF<sub>3</sub>K (**Figure 2.2**) and zero-order dependence in benzaldehyde (**Figure 2.3**) by comparing the logarithm of the concentration to the logarithm of the reaction rate. These data confirm that <sup>-</sup>CF<sub>3</sub> dissociation is the rate limiting step, which happens prior to trifluoromethylation of the substrate.

**Table 2.1** Relative reaction rates for 0.02 M of benzaldehyde with varying equivalents of  $(\text{MeO})_3\text{BCF}_3\text{K}$



$(\text{MeO})_3\text{BCF}_3\text{K}$ (M)	0.08	0.04	0.02	0.01	0.005
Rate (M/s)	$5.1(8) \times 10^{-6}$	$2.7(6) \times 10^{-6}$	$1.5(3) \times 10^{-6}$	$5(2) \times 10^{-7}$	$3.2(9) \times 10^{-7}$

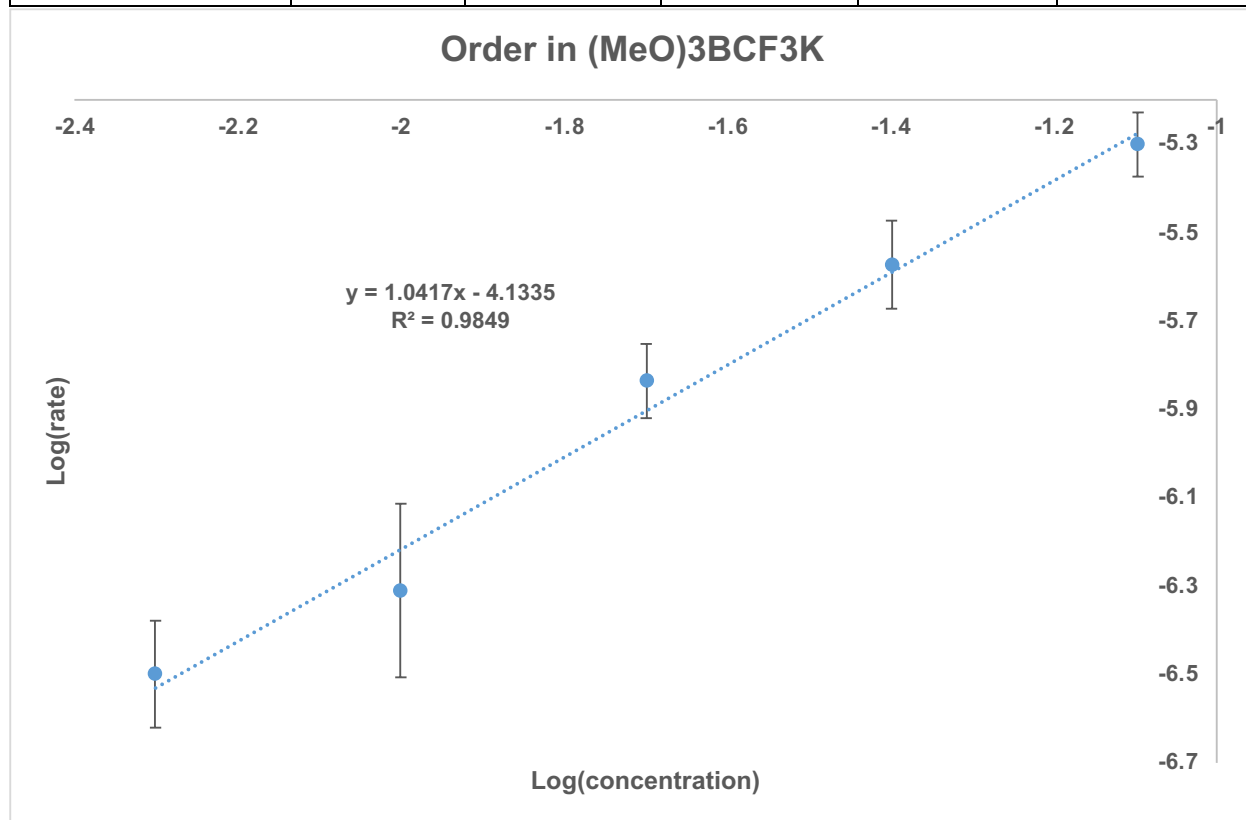


**Figure 2.2** Plot of log of reaction rate vs. log concentration of  $(\text{MeO})_3\text{BCF}_3\text{K}$ , slope 1.04 (benzaldehyde as substrate)

**Table 2.2** Relative reaction rates for 0.02 M of  $(\text{MeO})_3\text{BCF}_3\text{K}$  with varying equivalents of benzaldehyde



Benzaldehyde (M)	0.08	0.04	0.02	0.01	0.005
Rate (M/s)	$1.9(4) \times 10^{-6}$	$1.65(9) \times 10^{-6}$	$1.8(4) \times 10^{-6}$	$1.8(4) \times 10^{-6}$	$1.8(1) \times 10^{-6}$

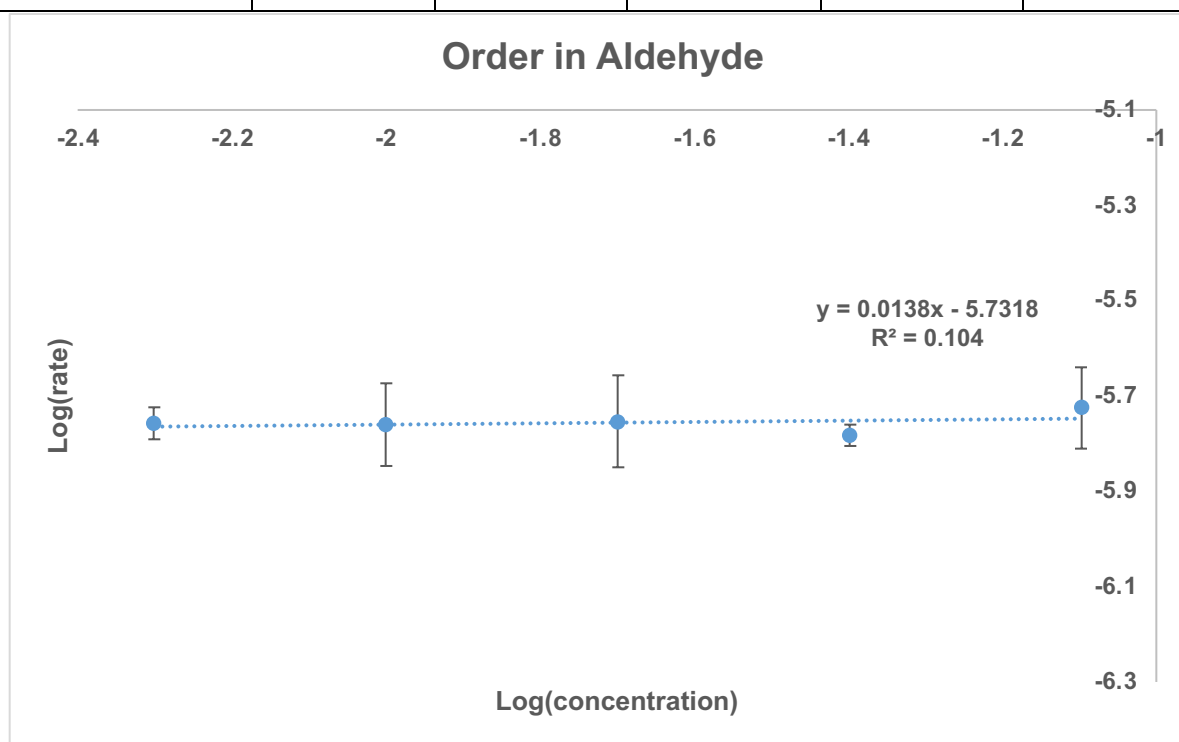
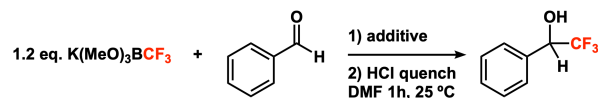


**Figure 2.3** Plot of log of reaction rate vs. log concentration of benzaldehyde, slope 0.01

We first examined the 1,2-addition reaction in the presence of a series of alkali metals with non-coordinating counter anions. Surprisingly, we observed suppression of  $-\text{CF}_3$  transfer in the presence of alkali cations unlike the observed trends with **2**. We observed an inverse correlation between the chemical yield of 1-phenyl-2,2,2-trifluoroethanol and the amount of exogenous  $\text{K}^+$  added to the reaction. Additionally, smaller and harder cations suppressed the reaction further, as

5 eq. of K<sup>+</sup>, Na<sup>+</sup> and Li<sup>+</sup> resulted in 5%, 3% and 0% yield of the desired product respectively (Table 2.1).

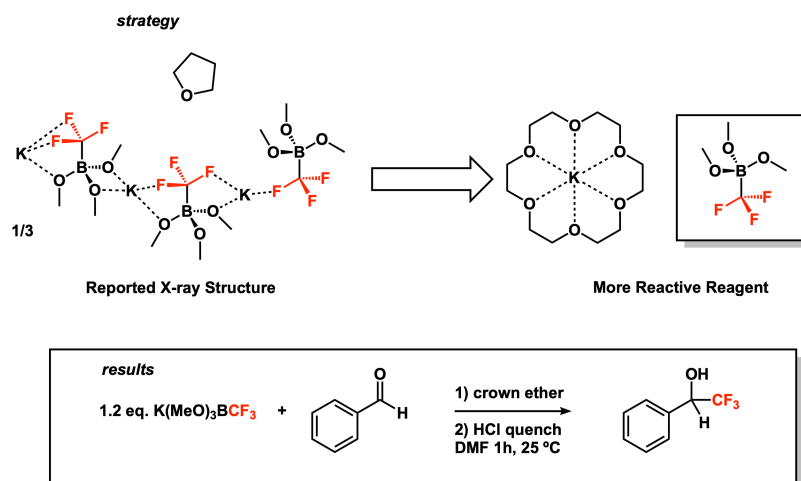
**Table 2.3** Suppression of <sup>-</sup>CF<sub>3</sub> transfer in the presence of alkali cation



Equivalents	KBPh <sub>4</sub>	NaBPh <sub>4</sub>	LiB(C <sub>6</sub> F <sub>5</sub> ) <sub>4</sub>
0	31%	31%	31%
1	17%	9%	N/A
3	9%	N/A	N/A
5	5%	3%	0%
10	2%	1%	N/A

We hypothesized that alkali metal cations were stabilizing the [(MeO)<sub>3</sub>BCF<sub>3</sub>]<sup>-</sup> anion in solution, leading to an overall decrease in reactivity. This trend in reactivity lead us to investigate the reported crystal structure of (MeO)<sub>3</sub>BCF<sub>3</sub>K.<sup>13</sup> We noted the oligomeric form of (MeO)<sub>3</sub>BCF<sub>3</sub>K in the solid state and the presence of interactions between K and F as well as K and O.<sup>13</sup> We postulated that similar aggregations could exist in solution, and have a profound effect on reactivity (Table 2.4), a phenomenon that has been well established for Grignard reagents.<sup>14</sup> To test this hypothesis further, we examined the extent of <sup>-</sup>CF<sub>3</sub> transfer in the presence of crown ethers. Indeed, a 6% increase in yield was observed when 1 equivalents of 18-crown-6 was added to the reaction mixture and a 20% increase in yield was observed with two 2 equivalents. Similarly, having 2 equivalents of 15-crown-5 or 1 equivalents of 2.2.2-cryptand afforded 8% and 18% increase in yield respectively.

**Table 2.4** Reported crystal structure of  $(\text{MeO})_3\text{BCF}_3\text{K}$  and increased reactivity in the presence of crown ether



Additive	none	1 eq. 18-crown-6	2 eq. 18-crown-6	2 eq. 15-crown-5	1 eq. cryptand
Yield	31%	37%	51%	39%	49%

The observed trends in reactivity in the presence of alkali cations and crown ethers support the hypothesis that alkali cations can modulate the nucleophilicity of trimethoxy(trifluoromethyl)borate by reinforcing aggregates in solution and crown ethers can break up said aggregates. An alternative hypothesis could be that there is an equilibrium between  $(\text{MeO})_3\text{BCF}_3\text{K}$  and  $(\text{MeO})_2\text{BCF}_3 + \text{KOME}$  that is dramatically shifted to the right with alkali cations and to the left with crown ethers. Methoxide has been established as a competing nucleophile for  $(\text{MeO})_3\text{BCF}_3\text{K}$ , and can be selectively abstracted from boron using trimethylsilyl chloride to form  $(\text{MeO})_2\text{BCF}_3$ .<sup>8</sup> Ultimately, the presence of methoxide ligands, which are Lewis basic and potentially nucleophilic differentiates  $\text{B}(\text{OMe})_3$  from  $\text{B}_3\text{N}_3\text{Me}_6$  as Lewis acid scaffolds to stabilize fluoroalkyl anions. These two Lewis acids have a very similar  $\text{CF}_3$  anion affinity,<sup>10</sup> and both operate through a dissociative mechanism and yet exhibit opposing reactivity trends in when exposed to exogenous Lewis acids or crown ethers. For future studies, chloride and fluoride

additives with inert counter cations (e.g. tetramethyl ammonium) should be examined with  $(\text{MeO})_3\text{BCF}_3\text{K}$  reactions, as formation of KCl or KF could be a driving force to accelerate  $^-\text{CF}_3$  transfer as well.

## 2.4 Neutral Fluoroalkyl Borane Species

Lucy S. Yu helped contribute to this subchapter.

The dissociative transfer of fluoroalkyl borate salts discussed in Chapters 2.2 and 2.3 is well suited for traditional electrophiles such as aldehydes and imines.<sup>15, 16</sup> While transition metal cross-coupling with these reagents can be achieved with iodoarenes,<sup>17, 13</sup> the thermal instability of these reagents discussed in Chapter 2.2 remains a challenge for reactions at elevated temperatures. We hypothesize that neutral fluoroalkyl boranes can undergo intramolecular transmetalation in the presence of anionic activators akin to traditional organoboronic acids and esters.<sup>18</sup> This strategy in principle can be utilized to overcome the challenge of competitive decomposition of fluoroalkyl borazine reagents. We targeted the syntheses of a series of neutral fluoroalkyl borane reagents that we hope will have application to catalysis at elevated temperatures.

Since pinacol boronic esters are commonly used as templates for Suzuki coupling reactions,<sup>19</sup> we targeted difluorobenzyl pinacol borane as a reagent suitable for cross-coupling.  $\text{B}_3\text{N}_3\text{Me}_6\text{CF}_2\text{Ph K}(18\text{-crown-}6)$  readily reacts with 2 eq. of pinacol borane in THF at 50 °C to form  $\text{HBPi nCF}_2\text{Ph K}(18\text{-crown-}6)$  in 98% yield (**Figure 2.4 a**). Excess borane and THF can be removed under vacuum to afford the desired product as a white powder, which can be recrystallized by layering a saturated THF solution with pentane. Analysis of the x-ray crystal structure (**Figure 2.4 b**),  $^{19}\text{F}$ ,  $^{11}\text{B}$  and  $^1\text{H}$  NMR unequivocally displayed the formation of the desired adduct.



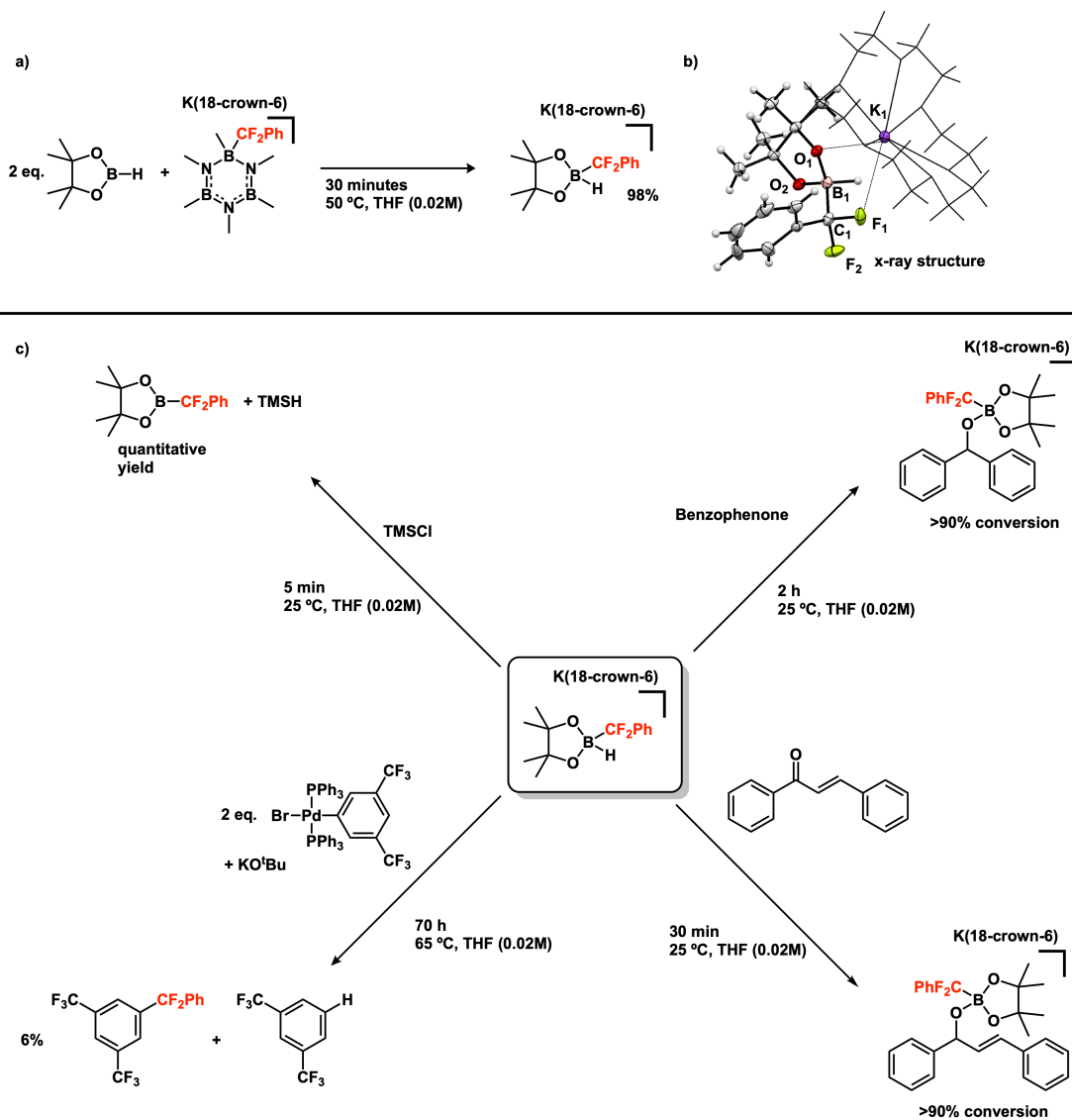


**Figure 2.4** a) Synthesis of HBPInCF<sub>2</sub>Ph K(18-crown-6) b) X-ray crystal structure. Key bond metrics; B<sub>1</sub>-C<sub>1</sub>: 1.65 Å, K<sub>1</sub>-F<sub>1</sub>: 3.04 Å, K<sub>1</sub>-O<sub>1</sub>: 2.68 Å c) Reactions with HBPInCF<sub>2</sub>Ph K(18-crown-6)

Since HBPInCF<sub>2</sub>Ph K(18-crown-6) contains at least two potentially nucleophilic groups, (-H and -CF<sub>2</sub>Ph), we investigated the nucleophilic reactivity of the reagent with a series of electrophiles to discern if hydride or difluorobenzyl anion transfer is preferential (**Figure 2.4 c**). Hydride transfer was experimentally found to be preferential, reducing the carbonyl group of benzophenone as well as chalcone in 90% conversion or greater. In the case of the latter, heating to 80 °C for an extended period of time did not induce an intramolecular 1,4-difluorobenzyl

addition. In order to achieve the goal of synthesizing a neutral difluorobenzyl BPin reagent, the hydridic reactivity of HBPInCF<sub>2</sub>Ph K(18-crown-6) was leveraged to form the desired compound, BPinCF<sub>2</sub>Ph, in the presence of TMSCl to extrude TMSH and KCl 18-crown-6. Unfortunately, KCl 18-crown-6 was found to be a persistent impurity in the desired compound and efforts to remove KCl 18-crown-6, such as pentane extraction were unsuccessful as the impurity was also pentane soluble. BPinCF<sub>2</sub>Ph was found to be unstable to neutral alumina rendering purification by column chromatography intractable. Vacuum distillation may be achievable under extremely low pressure, however BPinCF<sub>2</sub>Ph also decomposes at 100 °C, so our attempts at distillation under static vacuum were unsuccessful as well. The mixture of HBPInCF<sub>2</sub>PhK(18-crown-6) and 2 equivalents of Pd(II)(3,5-(CF<sub>3</sub>)<sub>2</sub>Ph)Br(PPh<sub>3</sub>)<sub>2</sub> and KO<sup>t</sup>Bu forms (3,5-(CF<sub>3</sub>)<sub>2</sub>Ph)CF<sub>2</sub>Ph in 6% yield as well as 3,5-(CF<sub>3</sub>)<sub>2</sub>Ph as the side product from initial hydride transfer providing the proof of principle that BPinCF<sub>2</sub>Ph is indeed competent for transmetalation to palladium(II) and further reductive elimination.

From the results of attempting stoichiometric cross-coupling with B<sub>3</sub>N<sub>3</sub>Me<sub>6</sub>CF<sub>2</sub>Ph K(18-crown-6) and cyclohexenyl triflate, a serendipitous discovery was made; formation of pentamethyl difluorobenzyl borazine (B<sub>3</sub>N<sub>3</sub>Me<sub>5</sub>CF<sub>2</sub>Ph) in 90% chemical yield. This product could be extracted into pentane with PPh<sub>3</sub> as the sole persistent impurity. By <sup>1</sup>H NMR, in addition to 2 equivalents of free PPh<sub>3</sub>, diagnostic borazine methyl resonances integrating to 3:6:6 and 5 aromatic resonances were observed. Moreover, the –CF<sub>2</sub>– group exhibited a <sup>19</sup>F NMR signal at -93.3 ppm, downfield of the parent difluorobenzyl borazine adduct (-102.7 ppm).<sup>16</sup> These spectroscopic features in addition to the notable solubility changes lead us to the assignment of the difluorobenzyl pentamethylborazine. Hexamethylborazine fluoroalkyl adducts exclusively transfer the fluoroalkyl group (instead of methyl) via a dissociative mechanism as discussed in Chapter 2.2. In

contrast to the known reactivity of these fluoroalkyl borazine adducts, we hypothesized that only an *associative mechanism* could support methyl transfer (**Figure 2.5**). We propose that cationic Pd(II) triflate species can effectively turn on associative pathway for borazine reagents to coordinate to Pd via the slightly Lewis basic nitrogen atom. The more sterically accessible side is *syn* with respect to the methyl group, allowing for facile  $\beta$ -methyl elimination, which results in the formation of pentamethyl difluorobenzyl borazine and cyclohexenyl-Pd(II)Me(PPh<sub>3</sub>)<sub>2</sub>. The reaction generalizable and also works with B<sub>3</sub>N<sub>3</sub>Me<sub>6</sub>CF<sub>2</sub>H K(18-crown-6) to form B<sub>3</sub>N<sub>3</sub>Me<sub>5</sub>CF<sub>2</sub>H. Unfortunately these borazine species are unstable to air and silica, making separation from PPh<sub>3</sub> challenging.

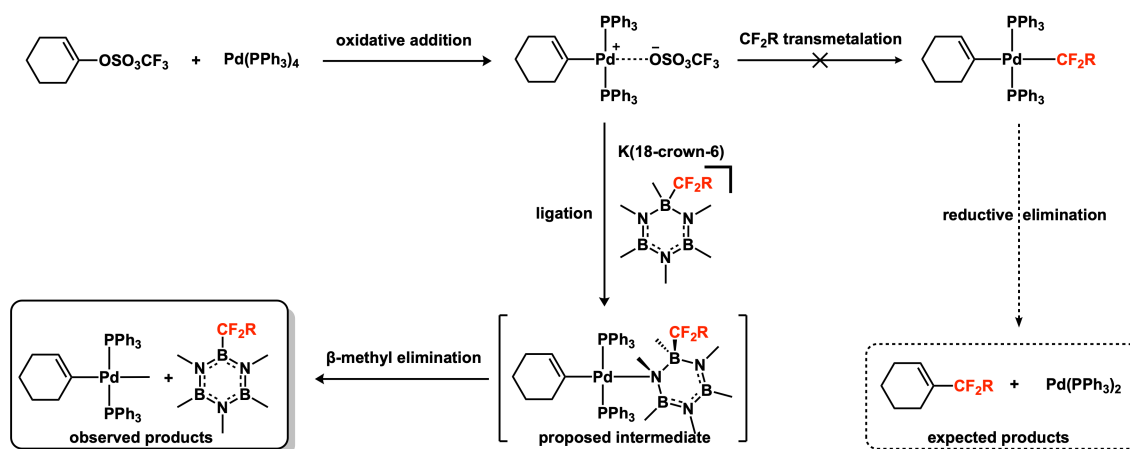


**Figure 2.5** Proposed pathway to form pentamethylCF<sub>2</sub>R borazine species

Previously, tris(trifluorovinyl) trimethylborazine and trifluorovinyl pentamethylborazine were synthesized with trifluorovinyl lithium and the corresponding chloroborazine precursor.<sup>20</sup> We anticipate that the use of chloroborazine precursors, potassium diisopropyl amide and fluoroalkane would be a more facile and straight-forward route to access these compounds. While we did not explore subsequent reactivity of the neutral fluoroalkyl borazine reagents, we hypothesize that they can be activated for <sup>-</sup>CF<sub>2</sub>R transfer when exposed to nucleophilic activators. This concept, in principle, would allow for fine-tuning of the nucleophilicity of the borazine

reagent. For example, use of fluoride anion would likely form a less nucleophilic source of  $^{-}\text{CF}_2\text{R}$  as the conjugate Lewis acid  $\text{B}_3\text{N}_3\text{Me}_5\text{F}$  would be more Lewis acidic than hexamethylborazine. Alternatively, a bulky activator such as isopropyl anion, would make a more nucleophilic source of  $^{-}\text{CF}_2\text{R}$ .

## 2.5 Deprotonation/Adduct Formation with More Complex Fluoroalkanes

Considering the observation of hexamethylborazine stabilizing borazine- $\text{CF}_2\text{R}$  adducts from undesired  $\alpha$ -fluoride elimination,<sup>10, 16</sup> we wondered if  $\beta$ -fluoride elimination of polyfluoroethyl and propyl anions could also be suppressed, making for more chemically complex fluoroalkyl transfer reagents. We selected 1,1-difluoroethane as an initial fluoroalkane to study, anticipating that it would have a similar pKa to difluoromethane and that the corresponding borazine adduct would exhibit similar reactivity.<sup>21</sup> When 1,1-difluoroethane gas (5 equiv.) was bubbled through a THF solution of benzyl potassium (2 equiv.),<sup>22</sup> hexamethyl borazine (1 equiv.) and 18-crown-6 (1 equiv.) and then stirred at 25 °C for 22 h, a new broad  $^{19}\text{F}$  NMR resonance is observed at -92.7 ppm, (26% in situ yield). We also observed a doublet of doublet of doublets at -114.95 ppm by  $^{19}\text{F}$  NMR, indicating fluoroethylene. The new borazine adduct was washed with pentane and dissolved in DMSO- $d_6$ , revealing two diagnostic doublet peaks in the  $^1\text{H}$  NMR spectrum (3.91 ppm,  $J_{\text{H-F}} = 64.7$  Hz) and (4.25 ppm,  $J_{\text{H-F}} = 32.0$  Hz). These spectroscopic features did not reflect the presence of a  $-\text{CF}_2\text{CH}_3$  unit, which we anticipated would have a triplet in the  $^1\text{H}$  NMR spectrum and a quartet in  $^{19}\text{F}$  NMR. Instead, the observed  $^1\text{H}$  NMR characteristics aligned much better with a borazine- $\text{CF}=\text{CH}_2$  adduct, possessing two chemically inequivalent protons.

Interestingly, in the absence of hexamethylborazine and 18-crown-6, fluoroethylene was only formed in 4%. Upon this observation, we hypothesized that borazine helps facilitate rather than suppress  $\beta$ -fluoride elimination. Thereafter, we began to systematically study deprotonation

and borazine-adduct formation of a series of polyfluoroethane and polyfluoropropane substrates (Figure 2.6). We examined the reaction profile of the deprotonation of 1,1,1,2-tetrafluoroethane in the presence and absence of borazine and 18-crown-6 by variable temperature  $^{19}\text{F}$  NMR. At  $-35\text{ }^\circ\text{C}$  and higher temperatures, 3 new resonances appear at  $-105\text{ ppm}$ ,  $-127\text{ ppm}$  and  $-182\text{ ppm}$ . Upon warming the instrument to  $10\text{ }^\circ\text{C}$ , the 3 peaks resolve as clear doublet of doublets at the same chemical shifts, indicating  $\beta$ -fluoride elimination and subsequent adduct formation. The stability of the borazine- $\text{CF}=\text{CF}_2$  adduct is dramatically reduced compared to borazine- $\text{CF}=\text{CH}_2$ . Borazine- $\text{CF}=\text{CF}_2$  begins to decompose into trifluoroethylene at  $10\text{ }^\circ\text{C}$  and upon warming to  $25\text{ }^\circ\text{C}$  for 16 h, no borazine- $\text{CF}=\text{CF}_2$  remains in solution. When comparing the reaction profiles, the borazine and 18-crown-6 free reaction only produced trifluoroethylene in 7% compared to 30% with Lewis acid and crown ether after warming to  $25\text{ }^\circ\text{C}$ . Moreover, 6% of trifluoroethylene was already present at the initial timepoint at  $-65\text{ }^\circ\text{C}$  in the control system.

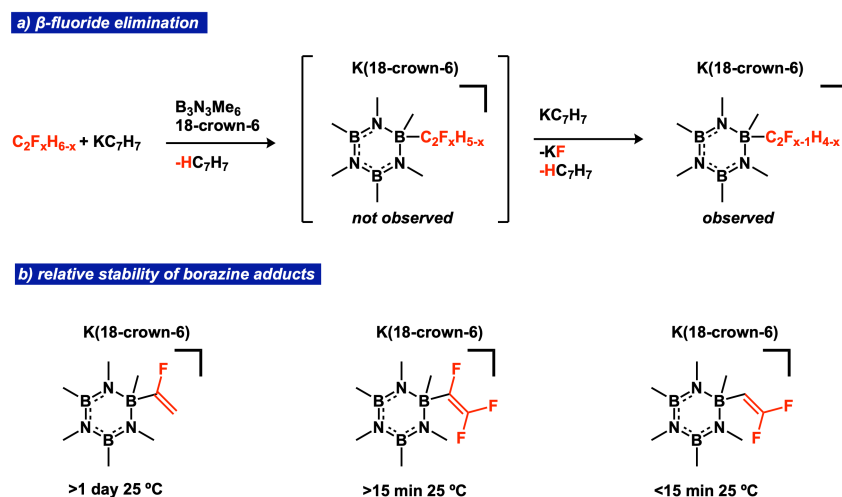


**Figure 2.6** a) Observed  $\beta$ -fluoride elimination. b) Stability of borazine fluoroethylene adducts.

When examining a substrate with only  $\beta$ -fluorine atoms, 1,1,1-trifluoroethane, the observed phenomenon of borazine and 18-crown-6 inducing  $\beta$ -fluoride elimination is even more pronounced. In the borazine-free control reaction, no new fluorinated products are formed even at

25 °C (**Figure 2.7**). In the presence of borazine, 1,1-difluoroethylene is visible in the reaction mixture at -82 ppm in  $^{19}\text{F}$  NMR spectra even at -65 °C. When warmed to -20 °C, two new  $^{19}\text{F}$  NMR resonances appear at -78 ppm and -92 ppm, indicating the probable formation of borazine- $\text{CH}=\text{CF}_2$  species. When the sample is warmed to 10 °C, a maximum of 8% of the adduct is formed. However, upon warming to 25 °C, this adduct completely decomposes.

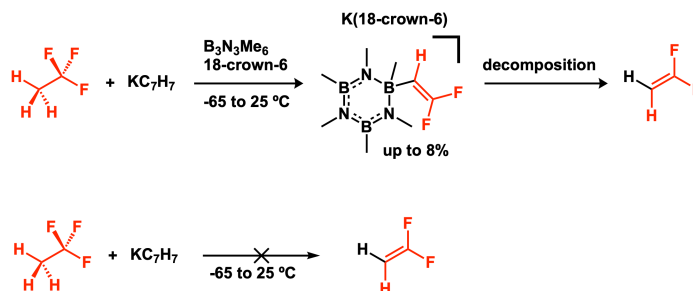


**Figure 2.7** Deprotonation of trifluoroethane with and without hexamethylborazine and 18-crown-6

We also studied 1,1,1,3,3-pentafluoropropane, 1,1,1,3,3,3-hexafluoropropane and 2-H-heptafluoropropane as well, however, decomposition had begun at -50 °C by the time the first NMR spectrum was collected. Moreover, the product profile was too complex for concrete analysis by NMR spectroscopy alone. Perhaps complementary GCMS analysis could help elucidate some of these fluoroalkyl species. The instability of the borazine adducts with hexafluoropropane and heptafluoropropane likely stems from these fluoroalkanes having lower  $\text{pK}_a$  values than fluoroform making for less Lewis and Brønsted basic anions. Moreover, there is a considerable degree more steric strain when considering polyfluoropropyl(enyl)-borazine adducts compared to a trifluoromethyl adduct. The formation of Lewis acid/base adducts with polyfluoropropyl anions and boron Lewis acids may in fact be intractable. The solution of increasing the Lewis acidity of the borane to generate a stronger Lewis pair would likely result in even faster rates of defluorination.

The general reactivity trend is; the higher degree of fluorination, the lower the  $pK_a$  and the less stable the borazine fluoroalkyl(enyl) adduct will be (**Figure 2.8**). The one interesting exception to this trend is the 2,2-difluorovinyl borazine adduct being less stable than the trifluorovinyl borazine adduct. Future studies involving 1,2-difluorovinyl borazine adducts and NBO analysis could help elucidate how  $\alpha$ -fluorination can help stabilize borazine adducts.

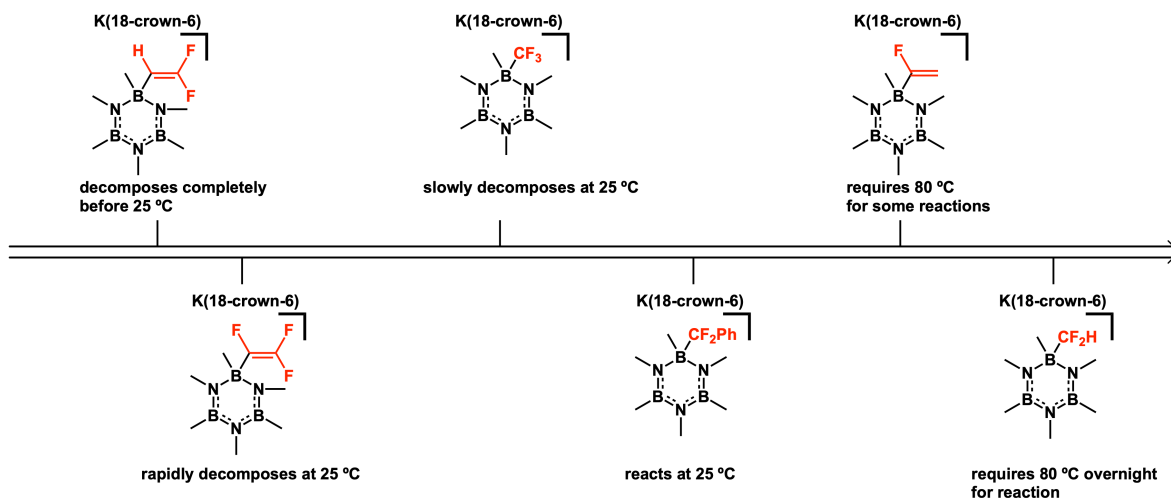


**Figure 2.8** Reactivity trends of fluoroalkyl(enyl) borazine adducts

## 2.6 Zweifel Olefination

Dr. Shuo Guo helped contribute to this subchapter.

Carbon-carbon bond forming reactions represent a powerful class of chemical transformations. Fluorinated olefins in particular are of high interest because of their application to materials,<sup>23, 24</sup> agrochemicals,<sup>25</sup> and pharmaceuticals.<sup>2</sup> Palladium catalyzed Suzuki coupling reactions of trifluorovinyl borate salts and aryl bromides has been implemented as one strategy to form these valuable chemical commodities.<sup>26</sup> Vinyl borate reagents can also be induced to undergo metal-free C-C bond forming reactions. Fluoroalkyl iodides can be irradiated with light to add across the C-C double bond of the vinyl borate, introducing the fluoroalkyl group at the  $\beta$ -carbon and iodide at the  $\alpha$ -carbon (**Figure 2.9 b**).<sup>27, 28</sup> Alternatively, borane Lewis acids can

facilitate the same class of addition reactions in the absence of light.<sup>29</sup> Conversely,  $\alpha$ -fluoroalkylation of vinyl boranes is much rarer and typically involves an umpolung strategy to achieve the desired stereochemistry.<sup>30, 31</sup> For instance, trifluoromethyl epoxides are electrophilic at the  $\alpha$  position and will undergo  $S_N2$  ring opening when a vinyl-BPin substrate is lithiated (Figure 2.9 a).<sup>30</sup> Diazo fluoroalkanes can also react with vinyl boroximes to achieve the desired  $\alpha$ -trifluoromethylation.<sup>31</sup> Thus, there is an unmet need to develop new strategies to install fluoroalkyl units to the  $\alpha$ -position of vinyl boranes without the use of a transition metal catalyst.

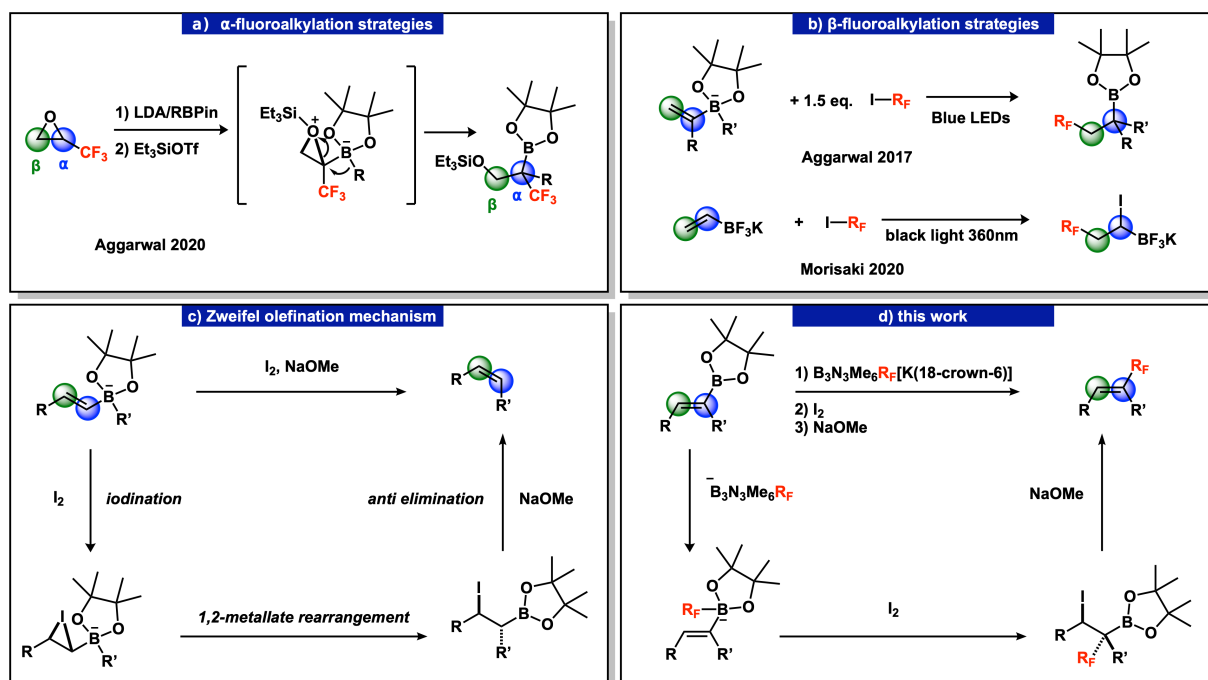


**Figure 2.9** Boron mediated, metal-free C-C coupling reactions a)  $\alpha$ -Fluoroalkylation strategies b)  $\beta$ -Fluoroalkylation strategies. c) Zweifel olefination mechanism. d) This work.

One powerful strategy to functionalize olefins without utilizing an expensive transition metal catalyst is through the Zweifel olefination reaction.<sup>32</sup> An alkyl borane can be reacted with an vinyl anion in the form of a lithiate or Grignard to form a vinyl borate. The olefin can be oxidized with a chemical oxidant such as molecular iodine and the nucleophilic alkyl group will undergo a 1,2 metallate rearrangement to the  $\alpha$ -carbon. Finally a base such as an alkoxide can



induce elimination forming the desired olefinic product (**Figure 2.9 c**).<sup>32</sup> With the use of an anionic fluoroalkyl synthon, Zweifel olefination can grant access to the opposite stereochemistry that is common with fluoroalkyl iodide electrophiles. The Szymczak group previously established that fluoroalkyl borazine adducts were competent in transferring fluoroalkyl anions to boranes with higher Lewis acidity than the parent borazine in quantitative yield.<sup>10, 16</sup> On this basis, we hypothesized that nucleophilic borazine fluoroalkyl species would be ideal substrates for a) the transfer of fluoroalkyl anions to vinyl pinacol boronic ester, and b) subsequent Zweifel olefination reactions to form novel  $\alpha$ -fluoroalkylated products (**Figure 2.9 d**).

As predicted, difluorobenzyl hexamethylborazine reacted with vinyl-BPin in near quantitative yield after 30 minutes of heating to 50 °C in THF. Subsequent introduction of iodine and sodium methoxide produced the desired product (1,1-difluoroallyl) benzene in 37% yield. However, several competitive reactions persisted including iodination of the two nucleophilic groups to form vinyl iodide and difluoroiodomethyl benzene as well as protonation of the difluorobenzyl group to form difluoromethyl benzene. We hypothesized that dissociation of the vinyl and difluorobenzyl anions lead to these undesired products and that more basic/nucleophilic fluoroalkyl anions would be more likely to participate in the intramolecular 1,2-shift.

We examined several other fluoroalkyl and fluoroalkenyl borazine reagents to probe this hypothesis in conjunction with a heavier olefin, to support less volatile and possibly isolable products. The fluoroalkyl or fluoroalkenyl anions could easily be transferred from borazine to a vinyl BPin compound [1,4-Dioxa-spiro[4,5]dec-7-en-8-boronic acid, pinacol ester] in high yield. Oxidation with I<sub>2</sub> and NaOMe induced elimination formed a series of C-C<sub>F</sub> coupled olefins. Over 3 steps, the fluorinated olefin products were formed in 3-54% yield (**Figure 2.10**). We observed a trend of the more basic fluoroalkyl(enyl) anions affording the desired product in higher yield;

CF<sub>2</sub>H: 54%, CF<sub>2</sub>Ph: 36% and CF=CH<sub>2</sub>: 26% yield, while the less basic anions formed the coupled products in much lower yield; CF=CF<sub>2</sub>: 15%, CF<sub>3</sub>: 5%, CF<sub>2</sub>-4pyr: 3%. These data supported the hypothesis that more basic and more nucleophilic anions like <sup>-</sup>CF<sub>2</sub>H were more likely to participate in the desired, concerted 1,2-metallate rearrangement, while less nucleophilic anions like <sup>-</sup>CF<sub>2</sub>-4-pyr are more likely to dissociate completely and undergo undesired side reactions with I<sub>2</sub>, forming ICF<sub>2</sub>-4pyr. Given the relatively poor stability of the borazine-CF=CF<sub>2</sub> adduct, we were not surprised by the low overall conversion to trifluoroethenylated products.

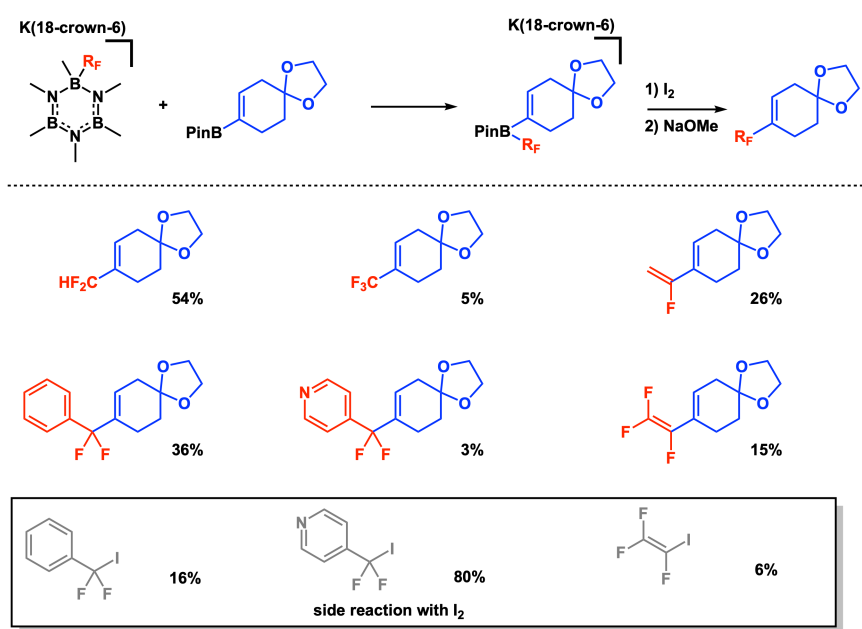
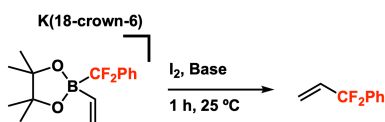


**Figure 2.10** Scope in Zweifel olefination and formation of undesired iodinated side products

Unfortunately, other attempts to further optimize the Zweifel olefination reaction outside of changing nucleophile were unsuccessful (**Table 2.5**), although some useful insights into the reaction were gleaned. Order of addition proved to be crucial for maximizing the yield of the olefinated product. (1,1-difluoroallyl)benzene is formed in 29% in situ yield (Entry 1) under the standard conditions: stirring VinylBPi<sub>n</sub>CF<sub>2</sub>Ph and I<sub>2</sub> together for 5-10 minutes followed by addition the base (NaOMe) last after. However, when I<sub>2</sub> is added last, the yield drops to 13% (Entry 2), and further modification of the order of addition to add vinylBPi<sub>n</sub>CF<sub>2</sub>Ph last results in 0%

formation of the desired product (Entry 3). This likely means that there is a competitive quenching reaction between I<sub>2</sub> and NaOMe that completely inhibits further reactivity.

**Table 2.5** Attempts to optimize Zweifel olefination. <sup>a</sup>Reactions were tumbled in screwcap NMR tubes using isolated vinylBPinCF<sub>2</sub>Ph. <sup>b</sup>VinylBPinCF<sub>2</sub>Ph was generated in situ in quantitative yield with 1.2 eq with vinylBPin, then immediately use as a stock solution for further reactions that were stirred in 8 mL vials. (Yield after 3 days)



Entry	Base	Order of Addition	Yield %
1 <sup>a</sup>	NaOMe	Standard	29%
2 <sup>a</sup>	NaOMe	I <sub>2</sub> last	13%
3 <sup>a</sup>	NaOMe	BPin last	0%
4 <sup>a</sup>	NaOH	Standard	5% (24)
5 <sup>a</sup>	NaOH (2 eq.)	Standard	5% (22)
6 <sup>b</sup>	NaOMe	Standard	26%
7 <sup>b</sup>	LiO <sup>t</sup> Bu	Standard	22%
8 <sup>b</sup>	NaO <sup>t</sup> Bu	Standard	27%
9 <sup>b</sup>	KO <sup>t</sup> Bu	Standard	23%
10 <sup>b</sup>	none	Standard	14%

The use of in situ-prepared vinylBPinCF<sub>2</sub>Ph had little effect on reaction yield (26%) when compared to reactions that used discretely isolated starting materials (29%) (Entries 6 and 1). When examining different sodium bases, bulkier tert-butoxide anions had a negligible effect on the reaction yield (Entry 8) while smaller hydroxide anions resulted in low (5%) yield after 1 hour (Entry 4). After 3 days, the reaction with sodium hydroxide converted to 24% yield, which is

comparable to reactions with NaOMe and NaO<sup>t</sup>Bu. We anticipate that the observed difference in reaction profile is due to the poor solubility of NaOH in THF. Finally, sodium bases proved to be more effective than lithium or potassium bases (Entries 7-9) albeit only by 4-5%. Interestingly, in the absence of base, the reaction still proceeds in 14% yield in 1 hour (Entry 10). This observation implies that either the anti-elimination step can proceed to some extent without a base, or I<sup>-</sup> or some other non-alkoxide anion can facilitate the reaction as well.

Electronic tuning of the vinylBPin precursor resulted in the prevalence of undesired side reactions instead of increased yield of Zweifel olefination. Under reaction conditions, incorporation of an electron-donating group (OMe) in (E)-1-ethoxyethene-2-boronic acid pinacol ester did not form the desired C-C coupled product, and instead formed PinBCF<sub>2</sub>Ph in around 86% yield. This implies that C-B oxidation is preferential to C=C oxidation when EDG's are incorporated. The same product profile was observed when the electron withdrawing (4-Cl-Ph) group was used. Conversely, when another electron-withdrawing group (COOEt) in (E)-2-ethoxycarbonylvinylboronic acid pinacol ester is used, mostly unreacted starting material remains.

In conclusion, the Zweifel olefination reaction with fluoroalkyl vinylborates persists in a very small window of chemical space. Use of less nucleophilic/basic fluoroalkyl groups results in lower reaction yields and in some cases, a dramatic increase of iodinated fluoroalkane products, likely due to dissociation of <sup>-</sup>R<sub>F</sub> being favored to an intramolecular shift. Electronic tuning of the olefin group can result in dissociation of the vinylic group to form PinBCF<sub>2</sub>Ph when either EDG or EWG are utilized. Tuning the Lewis acidity of boron with the non-participating ligand(s) is likely the best path forward in optimizing the Zweifel olefination reaction beyond 30-40% yield. Using catechol instead of pinacol would increase the Lewis acidity at boron, which in principle would make competitive ligand dissociation reactions become unfavorable. A few unsuccessful

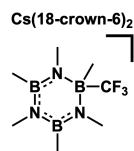
reactions were tried with hydroborated phenyl acetylene (styrylBCat and styrylBBN) however, as established earlier, the favorability of the Zweifel olefination is dramatically different when comparing a styryl group to a vinyl group.

## 2.7 Conclusions

We demonstrated that borazine trifluoromethyl adducts transfer  $-\text{CF}_3$  through a dissociative mechanism, which is also operative for  $(\text{MeO})_3\text{BCF}_3\text{K}$ . However, when alkali metal cations are introduced to the reaction, the opposite effects are observed: rate enhancement for borazine- $\text{CF}_3$  and reaction yield suppression for  $(\text{MeO})_3\text{BCF}_3\text{K}$ . These effects were amplified proportional to the amount of alkali metal or crown ether additive, unlike for  $\text{TMSCF}_3$  where only identity and presence of additive changed the reaction profile.<sup>7</sup> Fluoroalkanes containing  $\beta$ -fluorine atoms rapidly undergo  $\beta$ -fluoride elimination in the presence of base, hexamethylborazine and 18-crown-6 to form borazine-fluoroethylene adducts. The products from these transformations can be transformed into more chemically complex  $\text{C}-\text{C}_\text{F}$  coupled olefin species through a metal-free coupling strategy.

## 2.8 Experimental Details

### 2.8.1 Preparation of 2b Hexamethylborazine- $\text{CF}_3\text{Cs}[18\text{-crown-6}]_2$



Hexamethylborazine (3.15 mmol, 0.518 g), 18-crown-6 (6.30 mmol, 1.668 g) and cesium fluoride (3.00 mmol, 0.455 g) were combined in 10 mL THF. The mixture was stirred at 0 °C for 50 minutes.  $\text{SiMe}_3\text{CF}_3$  (3.6 mmol, 0.53 mL), cooled to 0 °C, was slowly added to the mixture and the

reaction stirred for 1.5 hours. Volatiles were removed under vacuum, and the resulting solid dissolved in 10 mL of THF and filtered. The filtrate was layered with 115 mL of Et<sub>2</sub>O, and allowed to stand for 3 days at -30 °C to afford large crystals. Solvent was decanted from the crystals, which were then washed with pentane (5 x 15 mL). The residual solvent was allowed to evaporate at ambient pressure for 90 minutes to afford crystalline **2b** (1.215g, 45%). A single crystal for structural analysis was prepared by layering Et<sub>2</sub>O on a concentrated THF solution of **2b** at -30 °C. <sup>1</sup>H-NMR (DMSO-d<sub>6</sub>): 3.49 (ω, 48H, s), 2.47 (α, 3H, s), 2.42 (ε, 6H, s), -0.05 (β, 6H, s), -0.38 (γ, 3H, s). <sup>11</sup>B-NMR: 32.94 (2B), -5.77 (1B). <sup>19</sup>F-NMR: -64.50 (3F (dd, *J*<sub>11B-19F</sub>: 56, 22)). HRMS (ES<sup>+</sup>): 191.0195 (M<sup>+</sup>: 191.0194). Anal. Calcd for C<sub>31</sub>H<sub>66</sub>B<sub>3</sub>CsF<sub>3</sub>N<sub>3</sub>O<sub>12</sub>: C, 41.59; H, 7.43; N, 4.69. Found: C, 41.09; H, 6.95; N, 4.46. Samples were aged for 30 days at either 25 °C, during which time greater than 80% of the sample decomposed, or at or -30 °C, during which no decomposition was observed. The samples were subjected to elemental analysis (Anal. Calcd for C<sub>31</sub>H<sub>66</sub>B<sub>3</sub>CsF<sub>3</sub>N<sub>3</sub>O<sub>12</sub>: C, 41.59; H, 7.43; N, 4.69. Found (30 days at 25 °C): C, 41.67; H, 7.62; N, 4.45), found (30 days at -30 °C): C, 41.42; H, 7.24; N, 4.66). Elemental analysis of the decomposed sample still closely matched the expected values for pure **2b**, indicating that HCF<sub>3</sub> gas is not a decomposition product.

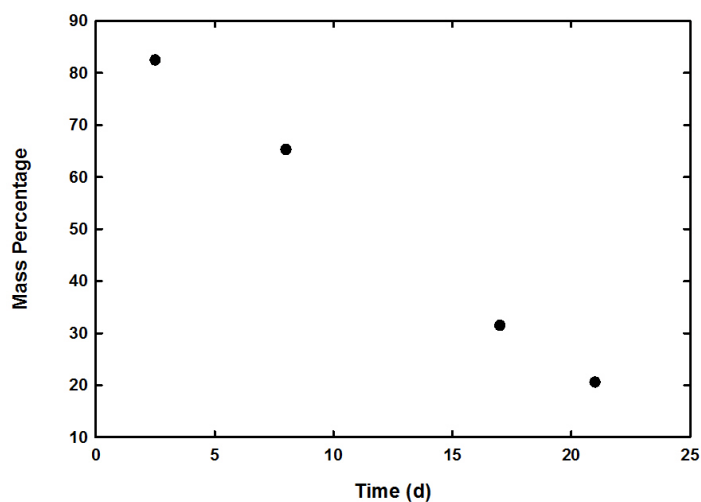


**Figure 2.11** Stability of **2b** at 25 °C in Solid State

**2b** decomposes at a rate of 3.4% per day ( $R^2 = 0.998$ ). Samples of pure solid (10-15 mg) were weighed into sealed vials and allowed to stand at 25°C for a desired amount of time. Mass percentage was determined by comparing the original mass of the sample to the number of moles of **2b** determined by dissolving the sample and integrating its resonance in the  $^{19}\text{F}$  NMR spectrum against 10.0  $\mu\text{L}$  added fluorobenzene standard.

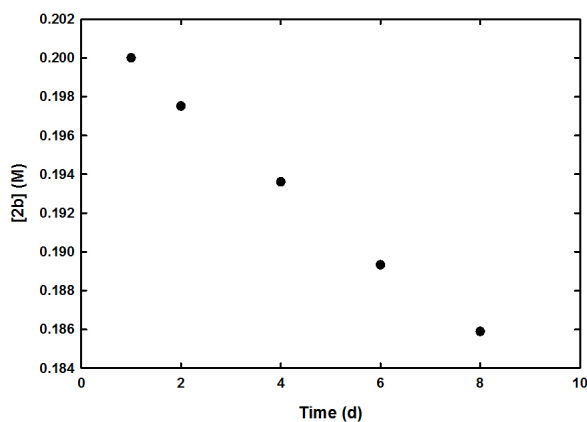


**Figure 2.12** Stability of **2b** at 25 °C in solution

A 0.2 M sample of **2b** was prepared in an NMR tube and periodically monitored by  $^{19}\text{F}$  NMR spectroscopy at room temperature. Rate of decomposition: 0.00201 M/d  $R^2 = 0.998$

**2.8.2 Kinetic Measurements of  $\text{CF}_3$  Transfer and Decomposition**

**General Protocol:**

**2** (dispensed as a -78 °C 0.2 M stock solution in THF) was added to a solution of electrophile at -78 °C in a glovebox cold well to give desired concentrations of **2** and electrophile. A 0.7 mL sample of this reaction mixture was then transferred into a -78 °C NMR tube, and the tube rapidly (<30 s) transferred to a -78 °C dry ice acetone bath outside the glovebox. The NMR samples were then inserted into an NMR spectrometer probe held at the desired reaction temperature, and the

reaction progress monitored by  $^{19}\text{F}$  NMR spectroscopy (spectra were taken at the rate of 1 spectrum per minute to provide kinetic traces.  $d1 = 2.5$  s,  $pw = 2.958$   $\mu\text{s}$ ,  $aq = 602.931$  ms; interpulse delay: 3.1 s). For determination of reactant order, initial rates were measured through a linear fit of the first 30 minutes of the reaction, or of data encompassing the first 15% of reaction progress, whichever was shorter. In all other cases, reaction profiles were obtained through at least 75% reaction progress. Concentrations were calculated by integration against a known concentration of fluorobenzene internal standard.

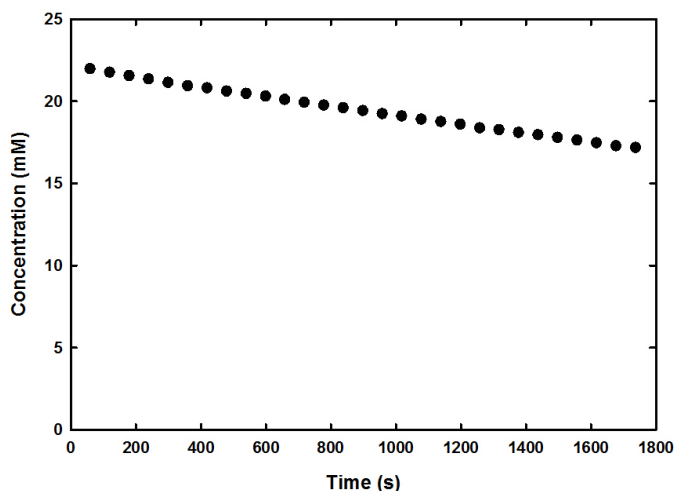
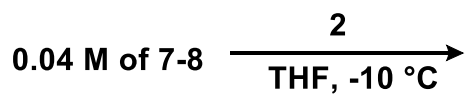


**Figure 2.13** Example linear fit

0.025 M **2** with 0.025 M **7** at  $-10$   $^{\circ}\text{C}$  in THF. Rate:  $-0.00283$  mM/s for consumption of **2**;  $R^2 = 0.999$ .

### Order in **2** for $\text{CF}_3^-$ transfer to **7-8**

**Table 2.6** Reaction rates with uncertainty in mM/s for 0.04 M of electrophile with varying equivalents of **2**





2 (M)	0.16 M	0.08 M	0.04 M	0.02 M	0.01 M
7 (rate)	$1.8(3) \cdot 10^{-2}$	$1.0(1) \cdot 10^{-2}$	$5.2(7) \cdot 10^{-3}$	$3.0(3) \cdot 10^{-3}$	$1.5(2) \cdot 10^{-3}$
8 (rate)	$1.9(3) \cdot 10^{-2}$	$1.0(2) \cdot 10^{-2}$	$5.8(1) \cdot 10^{-3}$	$3.5(6) \cdot 10^{-3}$	$1.8(1) \cdot 10^{-3}$

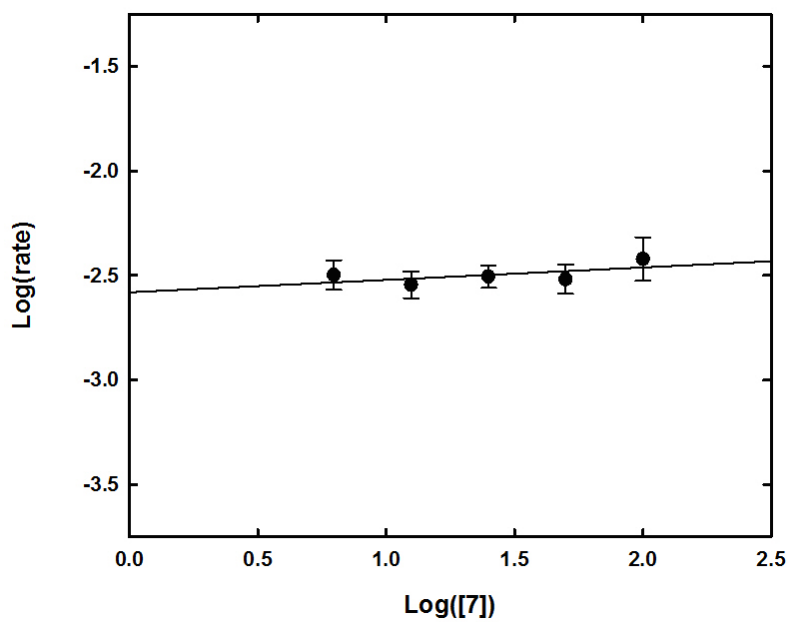


**Figure 2.14** Plot of log of reaction rate vs. log concentration of 7 (4-fluorobenzaldehyde), slope 0.06

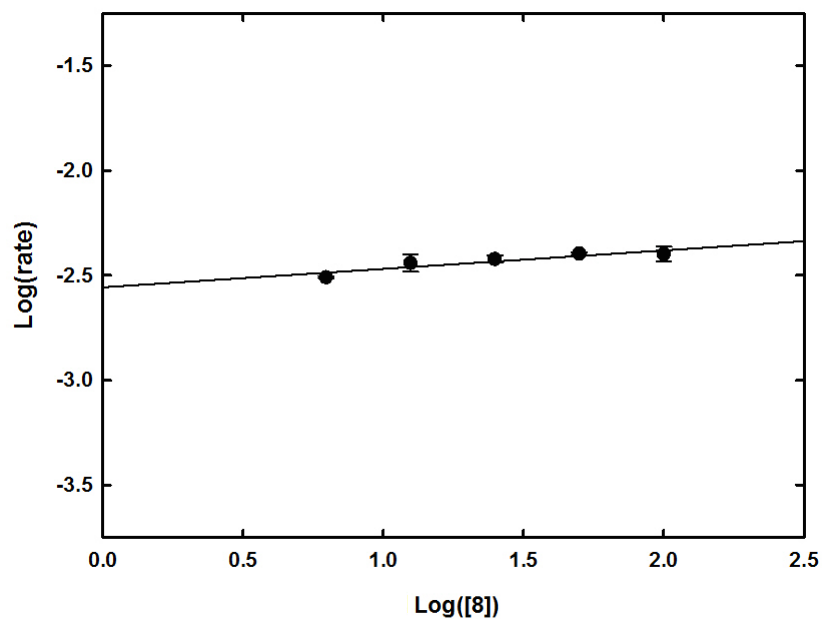
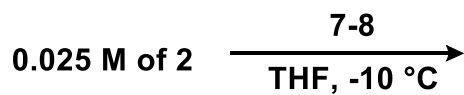


**Figure 2.15** Plot of log of reaction rate vs. log concentration of **8** (perfluorotoluene): slope 0.09

**Order in 7-8 for  $\text{CF}_3^-$  transfer from 2**

**Table 2.7** Reaction rates with uncertainty in mM/s for 0.025 M of **2** with varying equivalents of electrophile (electrophile=E)



E (M)	0.1 M	0.05 M	0.025 M	0.0125 M	0.00625 M
<b>7</b> (rate)	$4(1) \cdot 10^{-3}$	$3.1(5) \cdot 10^{-3}$	$3.1(4) \cdot 10^{-3}$	$2.9(4) \cdot 10^{-3}$	$3.2(5) \cdot 10^{-3}$
<b>8</b> (rate)	$4.0(3) \cdot 10^{-3}$	$4.01(7) \cdot 10^{-3}$	$3.8(1) \cdot 10^{-3}$	$3.6(4) \cdot 10^{-3}$	$3.10(3) \cdot 10^{-3}$

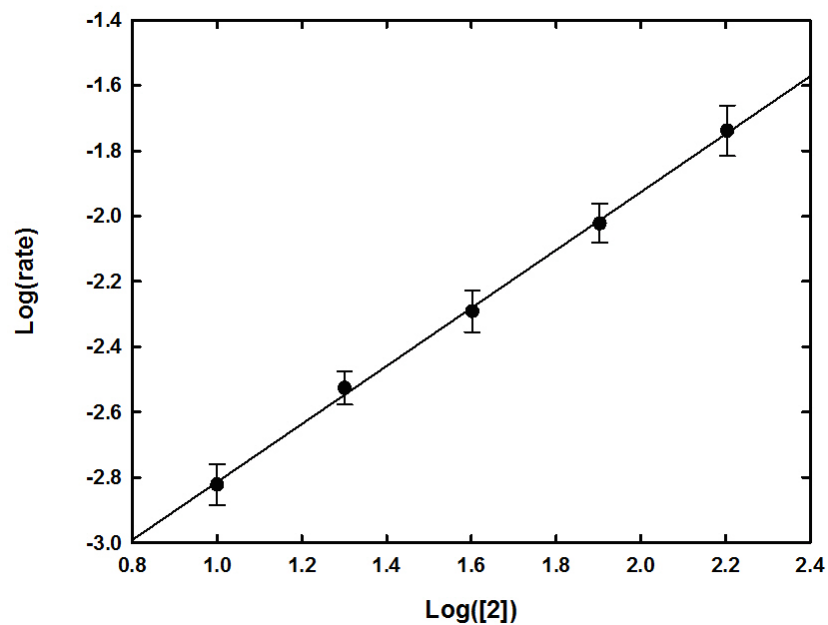


**Figure 2.16** Plot of log of reaction rate vs. log concentration of **2**, slope 0.89 (**7**, 4-fluorobenzaldehyde as substrate)

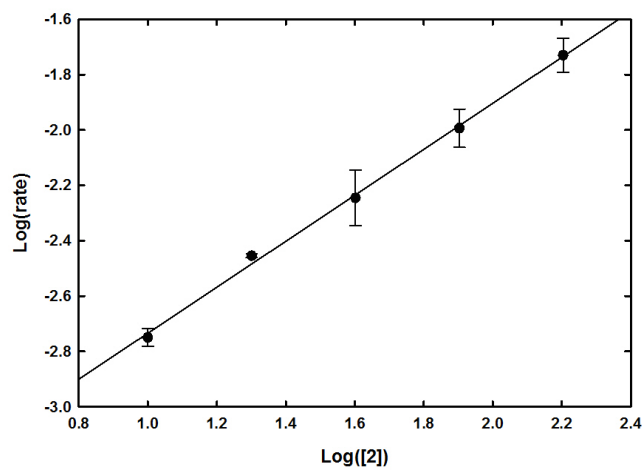


**Figure 2.17** Plot of log of reaction rate vs. log concentration of **2**, slope 0.83 (**8**, perfluorotoluene as substrate)

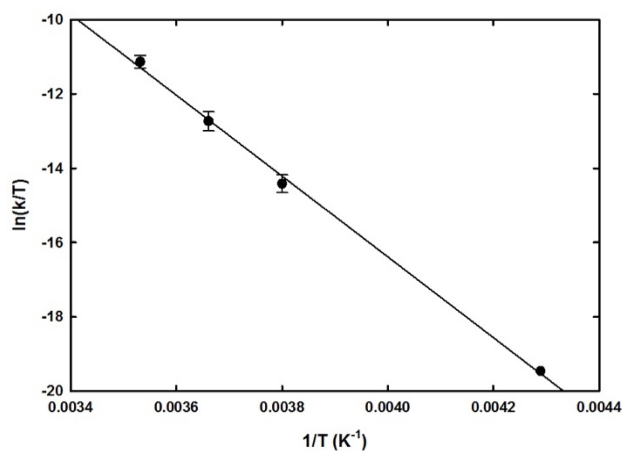


**Figure 2.18** Eyring plot for reaction of **2** and **7**, (4-fluorobenzaldehyde)

**Table 2.8** k values for Eyring analysis

Temperature	-40 °C	-10 °C	0 °C	10 °C
k (s <sup>-1</sup> )	8.3*10 <sup>-7</sup>	1.5(3)*10 <sup>-4</sup>	8(2)*10 <sup>-4</sup>	4.2(7)*10 <sup>-3</sup>

Linear fit parameters:

Slope: -11700(479); Intercept: 30(1)

Enthalpy of activation: 23.3(9) kCal/mol; Entropy of activation: 12(3) eu.

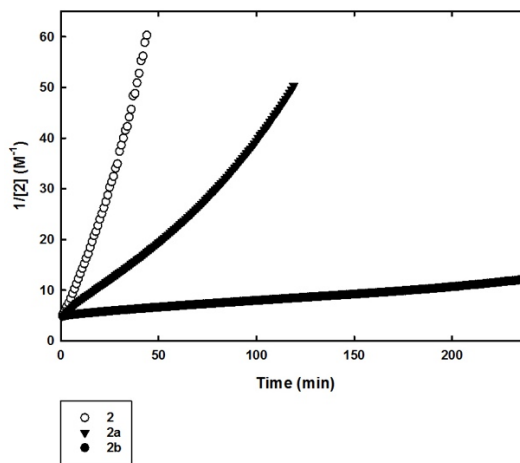
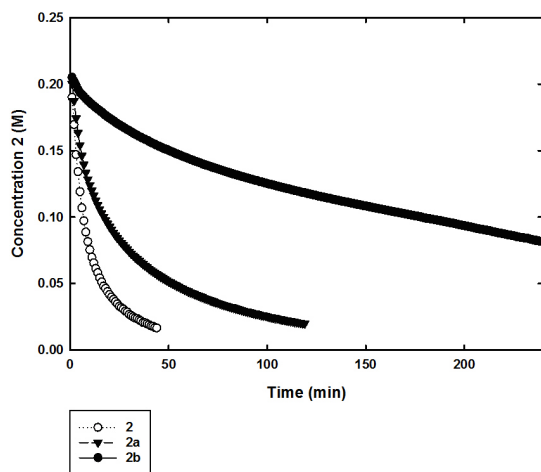


**Figure 2.19** Kinetic traces for thermal decomposition of **2**, **2a** and **2b** 60 °C and second order fit **2a** was prepared in-situ by addition of one equiv. 18-crown-6 to solutions of **2**.

**2**:  $k=1.25 \text{ M}^{-1}\text{s}^{-1}$ , linear fit  $R^2=0.986$ .

**2a**:  $k=0.364 \text{ M}^{-1}\text{s}^{-1}$ , linear fit  $R^2=0.983$ .

**2b**:  $k=0.0280 \text{ M}^{-1}\text{s}^{-1}$ , linear fit  $R^2=0.996$ .

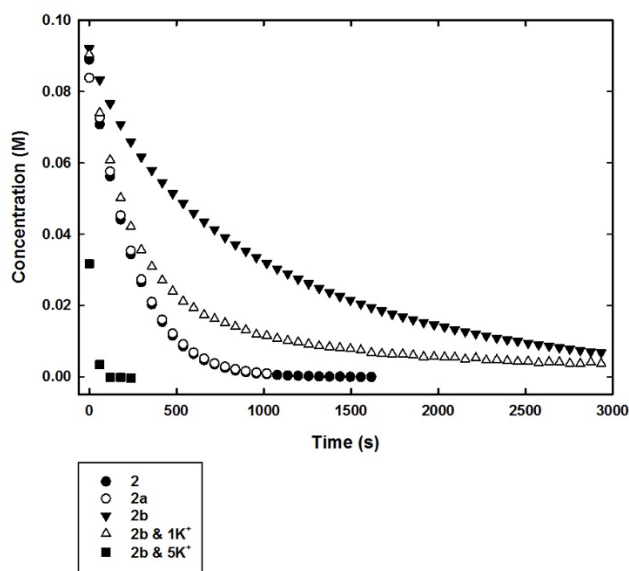


**Figure 2.20** <sup>-</sup>CF<sub>3</sub> transfer to **7** from **2**, **2b**, and **2b** activated with K<sup>+</sup> at 10 °C

0.1 M **2** and 0.1 M **7**, 10 °C. One equiv. KB(C<sub>6</sub>F<sub>5</sub>)<sub>4</sub> (K<sup>+</sup>) was added last as a THF solution at -78 °C to activate **2b** prior to kinetic measurements at 10 °C in **2b & 1K<sup>+</sup>** and 5 equiv. added in **2b & 5K<sup>+</sup>**.

### 2.8.3 Kinetic Measurements of CF<sub>3</sub> Transfer with (MeO)<sub>3</sub>BCF<sub>3</sub>K

#### General Protocol for Reaction Orders:

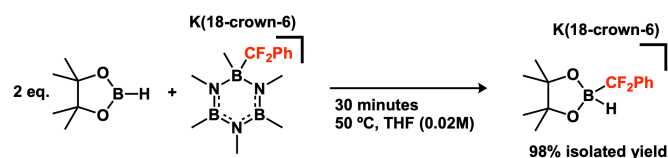
(MeO)<sub>3</sub>BCF<sub>3</sub>K was added to a DMF solution of benzaldehyde at 0 °C in a glovebox cold well to give desired concentrations. A 0.45 mL sample of this reaction mixture was then transferred into

a 0 °C NMR tube, and the tube rapidly (<30 s) transferred to a 0 °C ice bath outside the glovebox. The NMR samples were then inserted into an NMR spectrometer probe held at the desired reaction temperature, and the reaction progress monitored by  $^{19}\text{F}$  NMR spectroscopy.

### General Protocol for Reactions with Alkali Salts and Crown Ether Additives

In 1 mL of DMF  $(\text{MeO})_3\text{BCF}_3\text{K}$  (0.024 mmol), benzaldehyde (0.02 mmol) and fluorobenzene (0.06 mmol) were combined with the desired amount of either alkali metal salt or crown ether. After 1 h, the reactions were quenched with  $\text{HCl}(\text{aq})$ . Reaction yields were assessed by  $^{19}\text{F}$  NMR.

#### 2.8.4 Synthesis and Characterization of HBPInCF<sub>2</sub>Ph K(18-crown-6)



Hexamethylborazine- $\text{CF}_2\text{Ph}$  K(18-crown-6) (0.30 mmol, 181 mg) and HBPIn (0.60, 87  $\mu\text{L}$ ) were dissolved in 15 mL of THF in a 20 mL scintillation vial charged with a magnetic stir bar. The reaction mixture was heated to 50 °C and stirred for 30 minutes. THF and excess HBPIn were removed under vacuum and the remaining solid residue was washed with 3 x 5 mL of pentane to afford 166.4 mg of HBPInCF<sub>2</sub>Ph K(18-crown-6), 98% yield. Crystals suitable for X-ray diffraction were grown by layering diethyl ether onto a concentrated THF solution at 25 °C.

$^1\text{H-NMR}$  ( $\text{C}_6\text{D}_6$ ): 1.48 ( $\text{H}_a$ , 6H, OL), 1.49 ( $\text{H}_b$ , 6H, OL), 3.16 ( $\text{H}_c$ , 24H, s), 7.18 ( $\text{H}_d$ , 1H, OL), 7.35 ( $\text{H}_e$ , 2H, t(apparent),  $J_{\text{H-H}} = 7.7$  Hz), 8.16 ( $\text{H}_f$ , 2H, d,  $J_{\text{H-H}} = 8.3$  Hz).  $^{11}\text{B-NMR}$ : 3.67 (d,  $J_{\text{B-H}} = 91.3$  Hz)  $^{19}\text{F-NMR}$ : -108.15 (2F, broad).

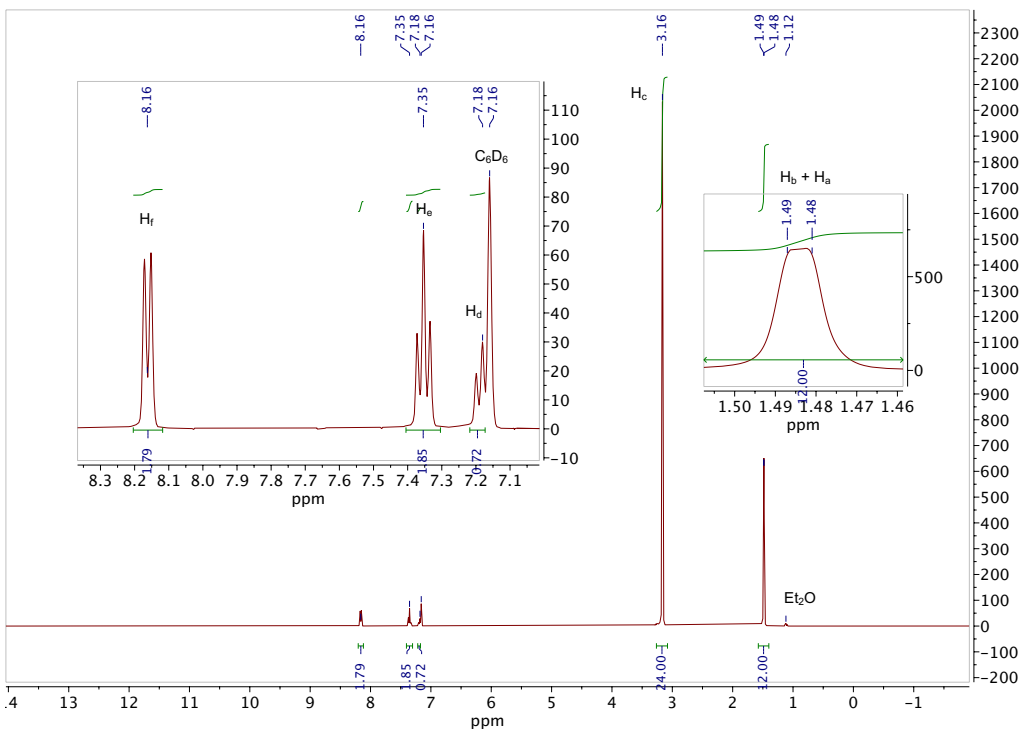


**Figure 2.21**  $^1\text{H}$  NMR spectrum of HBPInCF<sub>2</sub>Ph K(18-crown-6) in C<sub>6</sub>D<sub>6</sub>

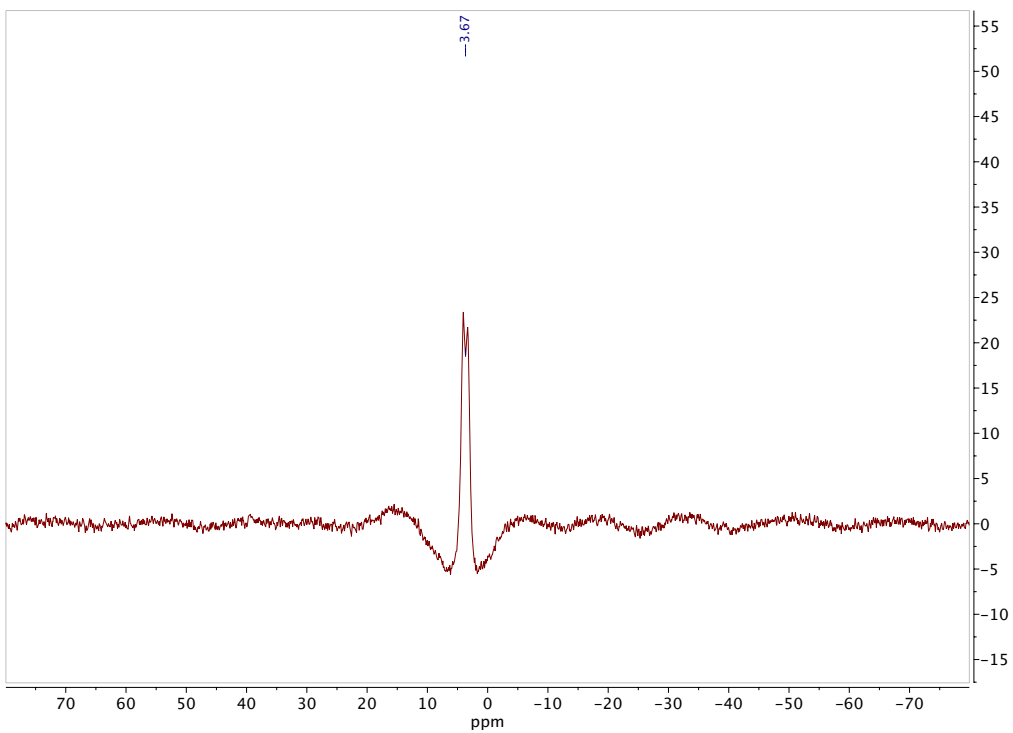


**Figure 2.22**  $^{11}\text{B}$  NMR spectrum of HBPInCF<sub>2</sub>Ph K(18-crown-6) in C<sub>6</sub>D<sub>6</sub>

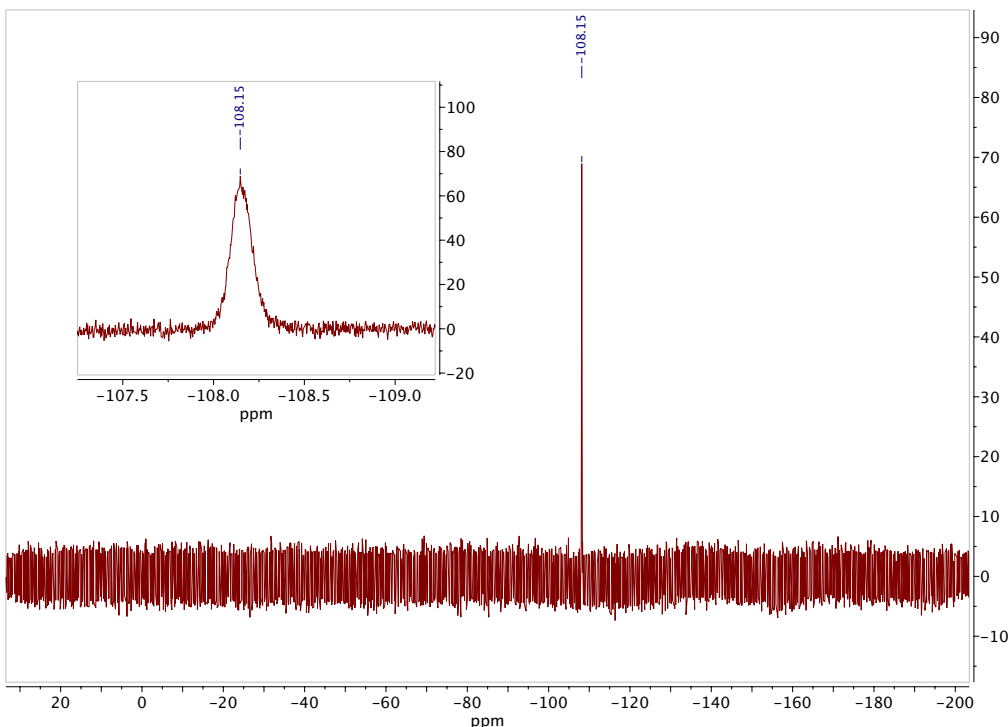
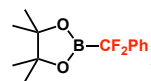


**Figure 2.23**  $^{19}\text{F}$  NMR spectrum of  $\text{HBPinCF}_2\text{Ph K}(18\text{-crown-6})$  in  $\text{C}_6\text{D}_6$

### 2.8.5 Reactions with $\text{HBPinCF}_2\text{PhK}(18\text{-crown-6})$

#### TMSCl



$\text{HBPinCF}_2\text{Ph K}(18\text{-crown-6})$  (0.1 mmol) was dissolved in 5 mL of THF in a 20 mL scintillation vial and  $\text{TMSCl}$  (0.2 mmol, 26  $\mu\text{L}$ ) were added to the reaction mixture. After 5 minutes the reaction solvent, unreacted  $\text{TMSCl}$  and  $\text{TMSH}$  were removed under vacuum.  $\text{PinBCF}_2\text{Ph}$  was extracted into 3 x 1.5 mL of pentane. Both the methyl resonances on the pinacol group (0.89 ppm) and the ortho protons (7.74 ppm) were shifted upfield with respect to the starting material by  $^1\text{H}$  NMR. The  $^{11}\text{B}$  NMR exhibited a trigonal planar borane resonance at 28.64 ppm and the  $^{19}\text{F}$  NMR resonance shifted upfield to -110.12 ppm. It should be noted that the reaction also works with  $\text{TMSI}$  but goes to a lower conversion.



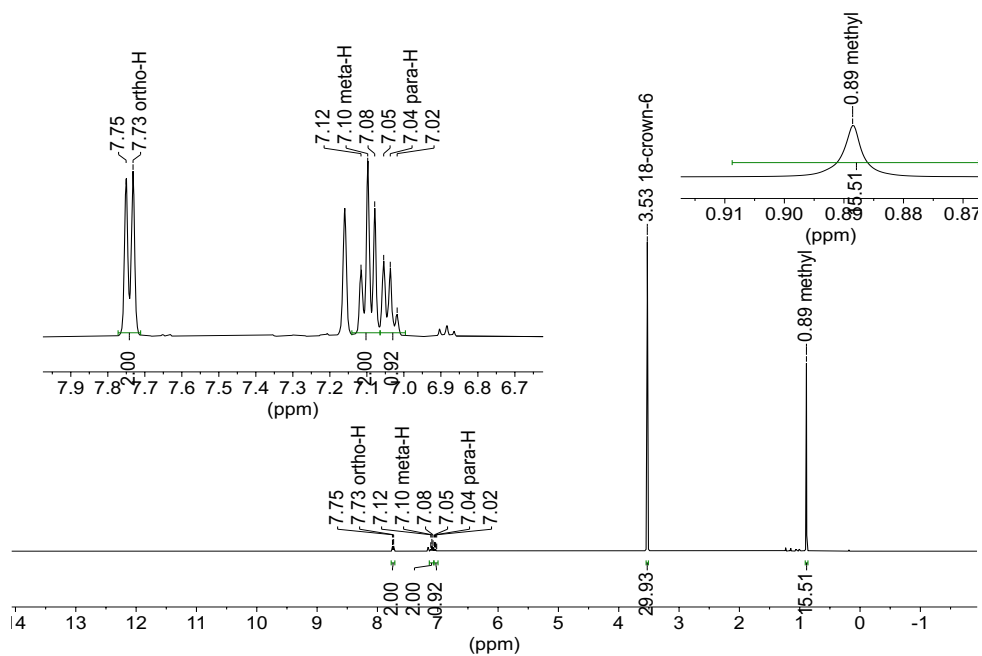


**Figure 2.24**  $^1\text{H}$  NMR of PinBCF<sub>2</sub>Ph in C<sub>6</sub>D<sub>6</sub>

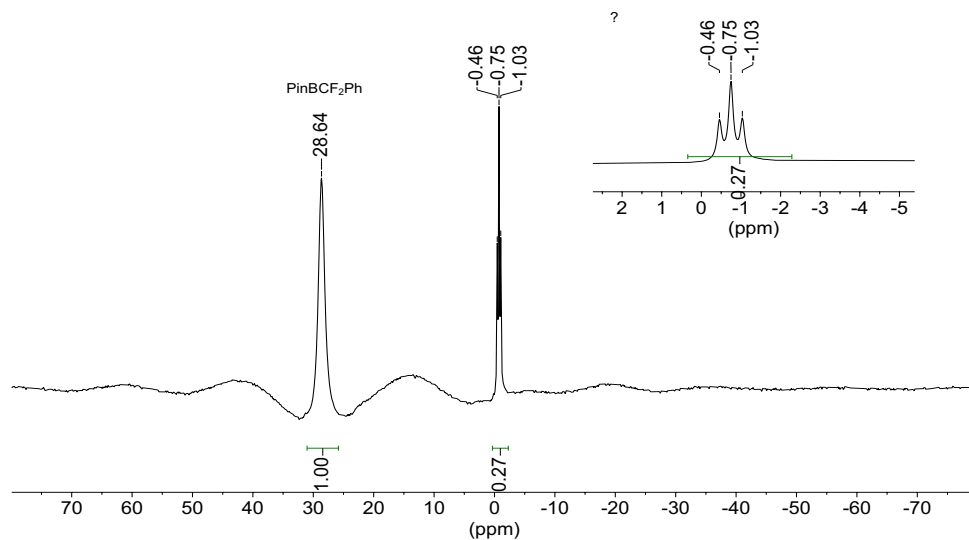


**Figure 2.25**  $^{11}\text{B}$  NMR of PinBCF<sub>2</sub>Ph in C<sub>6</sub>D<sub>6</sub> (TMSI used instead of TMSCl)

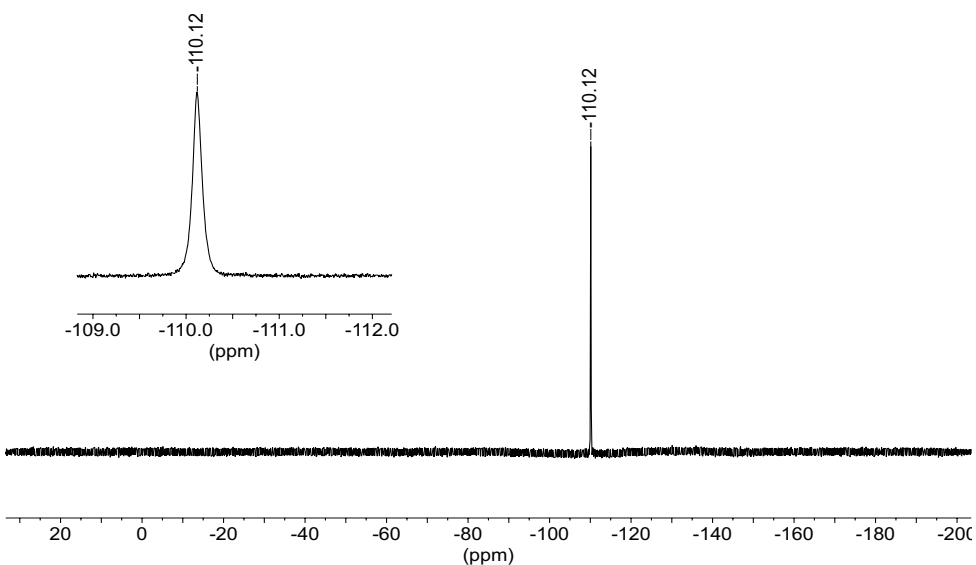
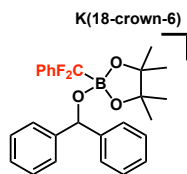


**Figure 2.26**  $^{19}\text{F}$  NMR of PinBCF<sub>2</sub>Ph in C<sub>6</sub>D<sub>6</sub>

### Benzophenone



HBPInCF<sub>2</sub>Ph K(18-crown-6) (0.01 mmol, 5.8 mg) was dissolved in 0.4 mL of THF.

A stock solution was made by dissolving benzophenone (0.05 mmol, 9.3 mg) and fluorobenzene (0.1 mmol, 9.4  $\mu\text{L}$ ) in 0.5 mL of THF. A 0.1 mL aliquot of the benzophenone solution was transferred to the HBPInCF<sub>2</sub>Ph solution and the reaction was monitored by  $^1\text{H}$  and  $^{19}\text{F}$  NMR. After 2 hours, >90% of the starting material had converted to a new  $^{19}\text{F}$  NMR resonance at -106.7 ppm. Importantly, a singlet appeared by  $^1\text{H}$  NMR at 5.67 ppm, which was diagnostic of a doubly benzylic proton rather than a borohydride. These data indicate preferential hydridic reactivity of HBPInCF<sub>2</sub>Ph.

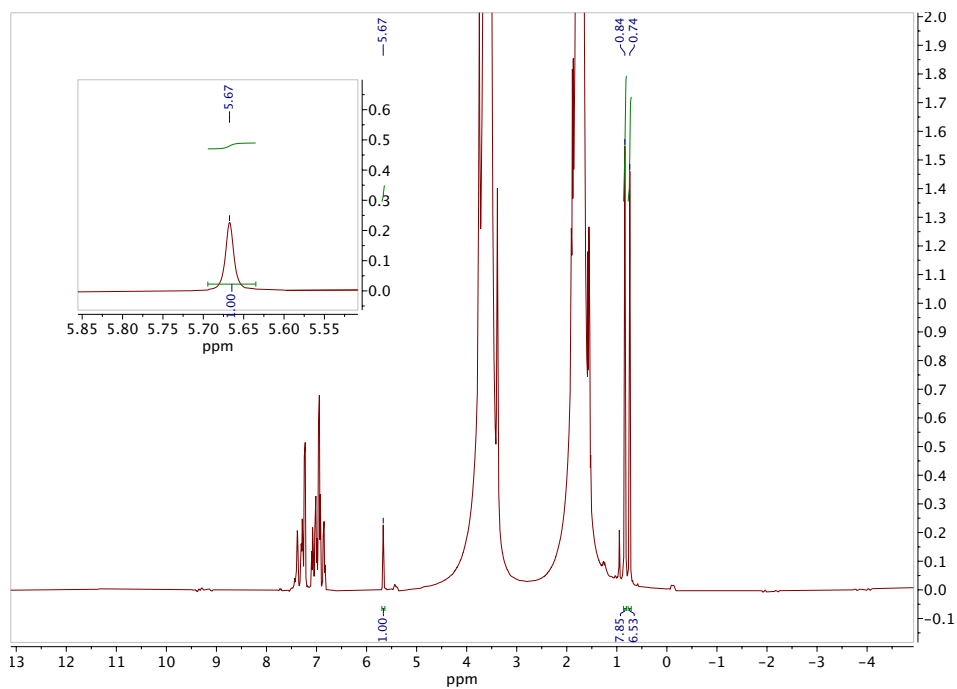


**Figure 2.27**  $^1\text{H}$  NMR HBPInCF<sub>2</sub>Ph K(18-crown-6) with benzophenone in THF

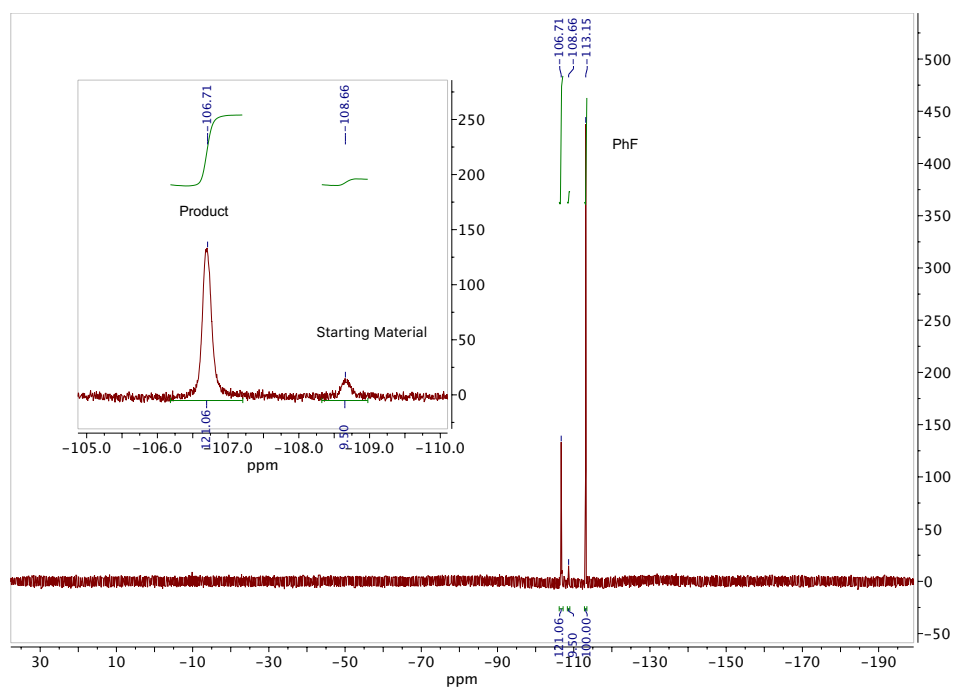
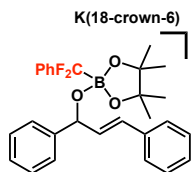


**Figure 2.28**  $^{19}\text{F}$  NMR HBPInCF<sub>2</sub>Ph K(18-crown-6) with benzophenone in THF

## Chalcone



HBPi<sub>n</sub>CF<sub>2</sub>Ph K(18-crown-6) (0.01 mmol, 5.4 mg) was dissolved in 0.3 mL of THF in a 20 mL scintillation vial. A stock solution was made by dissolving chalcone (0.025 mmol, 5.3 mg) in 0.5 mL of THF. A 0.2 mL aliquot of chalcone solution was transferred to the vial containing HBPi<sub>n</sub>CF<sub>2</sub>Ph. After 30 minutes, the reaction was monitored by <sup>1</sup>H, <sup>11</sup>B and <sup>19</sup>F NMR. A set of three interrelated peaks appeared by <sup>1</sup>H NMR 6.34 ppm (dd,  $J_{H-H} = 16.0, 5.6$  Hz), 6.05 ppm (d,  $J_{H-H} = 15.9$  Hz) and 5.34 ppm (d,  $J_{H-H} = 6.0$  Hz) indicating 1,2-insertion of the hydride into the carbonyl. Two sets of doublets by <sup>19</sup>F NMR (-105.5 ppm, -106.3 ppm, -107.6 ppm, -108.4 ppm) accompanied by a tetrahedral borate resonance <sup>11</sup>B 1.99 ppm (*unreferenced*).

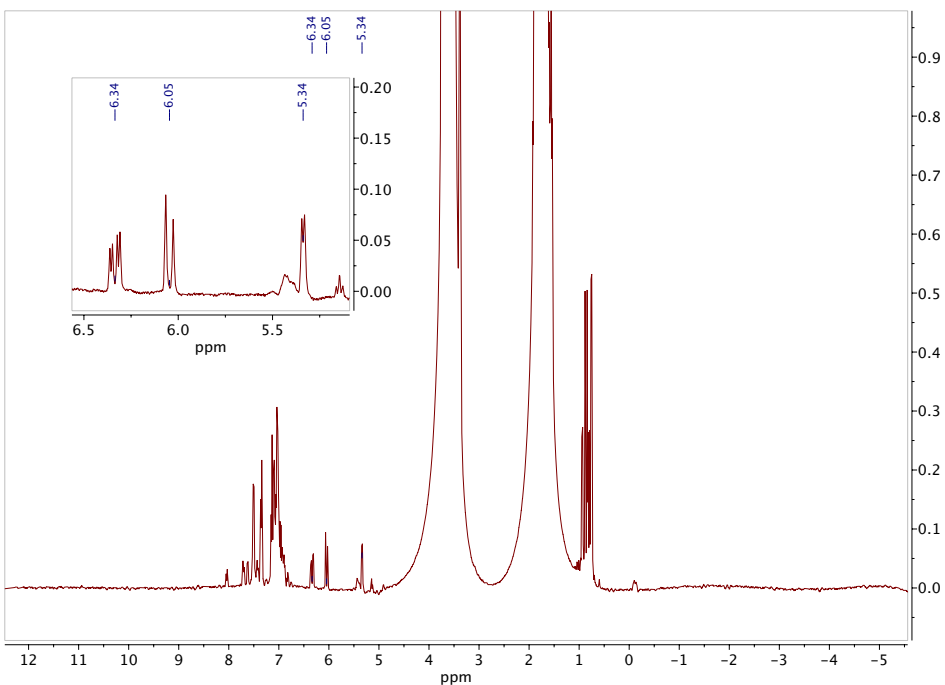


**Figure 2.29**  $^1\text{H}$  NMR of HBPInCF<sub>2</sub>Ph K(18-crown-6) with chalcone in THF

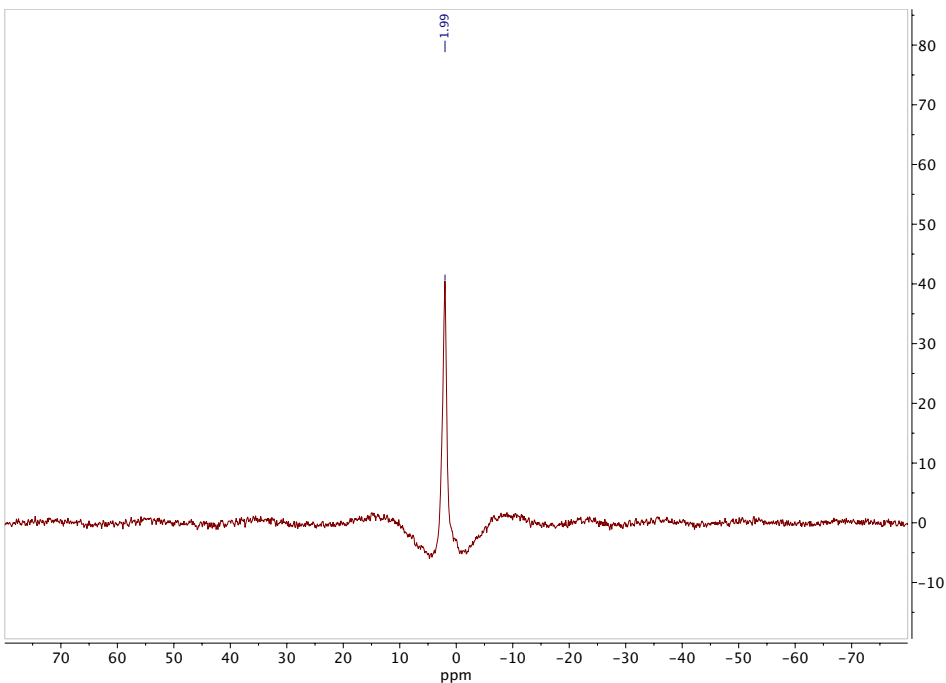


**Figure 2.30**  $^{11}\text{B}$  NMR of HBPInCF<sub>2</sub>Ph K(18-crown-6) with chalcone in THF (unreferenced)

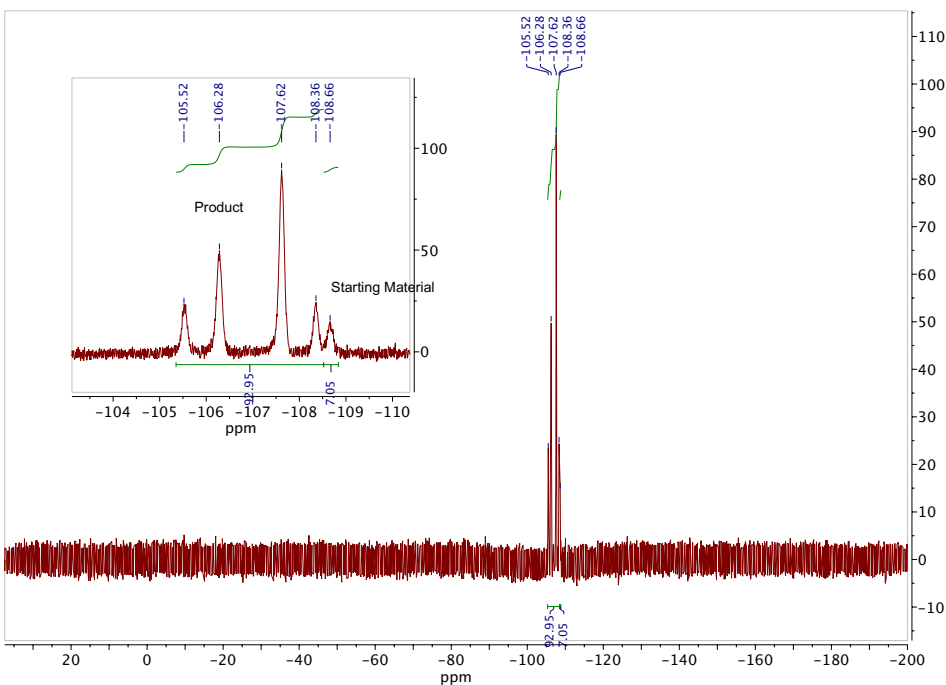
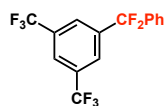


**Figure 2.31**  $^{19}\text{F}$  NMR of HBPInCF<sub>2</sub>Ph K(18-crown-6) with chalcone in THF  
**Pd(II)Br(3,5-(CF<sub>3</sub>)<sub>2</sub>Ph)(PPh<sub>3</sub>)<sub>2</sub>**



In a screwcap NMR tube, HBPInCF<sub>2</sub>Ph K(18-crown-6) (0.02 mmol), Pd(II)Br(3,5-(CF<sub>3</sub>)<sub>2</sub>Ph)(PPh<sub>3</sub>)<sub>2</sub> (0.04 mmol), KO<sup>t</sup>Bu (0.02 mmol) and fluorobenzene (0.04 mmol) were dissolved in 1 mL of THF and heated to 65 °C for 70 hours. The reaction yield was monitored by <sup>19</sup>F NMR displaying the formation of PhCF<sub>2</sub>(3,5-(CF<sub>3</sub>)<sub>2</sub>Ph) in 6% as a singlet at -89.42 ppm.

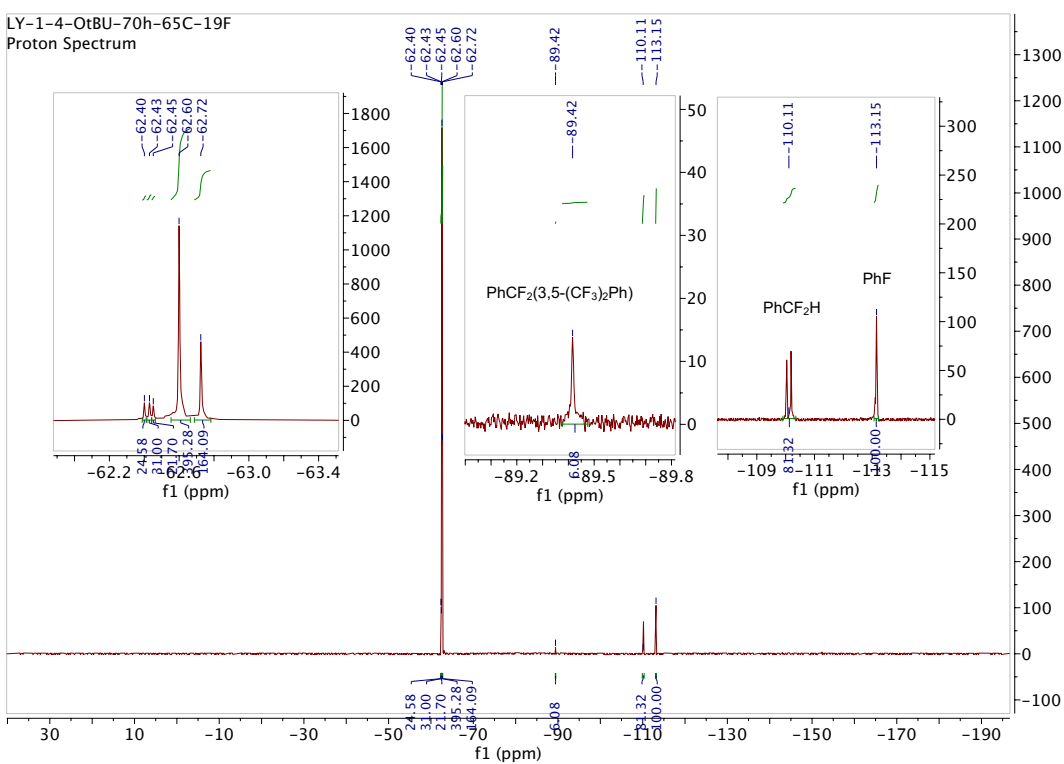
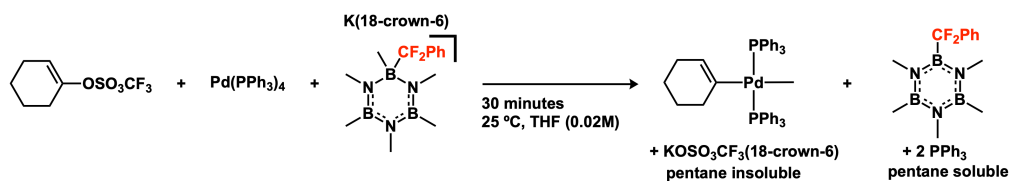


**Figure 2.32** <sup>19</sup>F NMR of HBPInCF<sub>2</sub>Ph K(18-crown-6) with Pd(II)Br(3,5-(CF<sub>3</sub>)<sub>2</sub>Ph)(PPh<sub>3</sub>)<sub>2</sub> in THF

## 2.8.6 Synthesis and Characterization of Pentamethylborazine-*CF*<sub>2</sub>Ph



Hexamethylborazine-*CF*<sub>2</sub>Ph K(18-crown-6) (0.30 mmol, 179 mg) and Pd(PPh<sub>3</sub>)<sub>4</sub> (0.30, 348 mg) were weighed into a 20 mL scintillation vial. Cyclohexenyl triflate (0.30 mmol, 69.4 mg) was dissolved in 15 mL of THF. The cyclohexenyl triflate solution was rapidly transferred to the vial containing the other two reagents. The reaction stirred for 30 minutes, and then the solvent was removed in vacuo. The crude mixture was washed with 3 x 5 mL of pentane affording a green flakey solid (pentane insoluble material, 341.4 mg) and an orange solution which became orange and white crystalline solid upon evaporation (pentane soluble material, 187.3 mg). The products were analyzed by NMR spectroscopy in C<sub>6</sub>D<sub>6</sub>. The pentane insoluble material contained a vinylic resonance at -5.54 ppm indicating the fate of the cyclohexenyl group as part of the Pd complex. Moreover, the <sup>31</sup>P signal at 34.82 ppm indicated that the Pd species was likely Pd(II) rather than Pd(0).

<sup>1</sup>H-NMR (C<sub>6</sub>D<sub>6</sub>): 0.39 (H<sub>a</sub>, 6H, s), 2.70 (H<sub>b</sub>, 3H, s), 2.87 (H<sub>c</sub>, 6H, t, *J*<sub>H-F</sub> = 2.0 Hz), 7.11 (H<sub>d</sub>, 2H, OL), 7.13 (H<sub>e</sub>, 1H, OL), 7.64 (H<sub>f</sub>, 2H, m). <sup>19</sup>F-NMR: -93.27 (2F, broad).

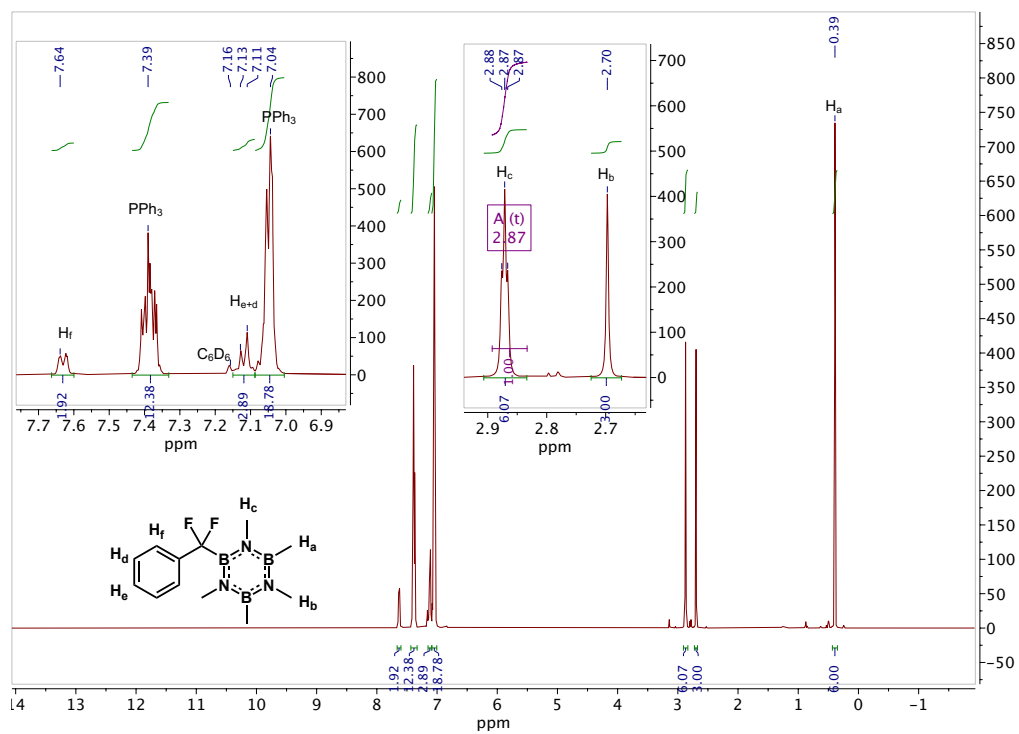


Figure 2.33  $^1\text{H}$  NMR of difluorobenzyl pentamethylborazine in  $\text{C}_6\text{D}_6$

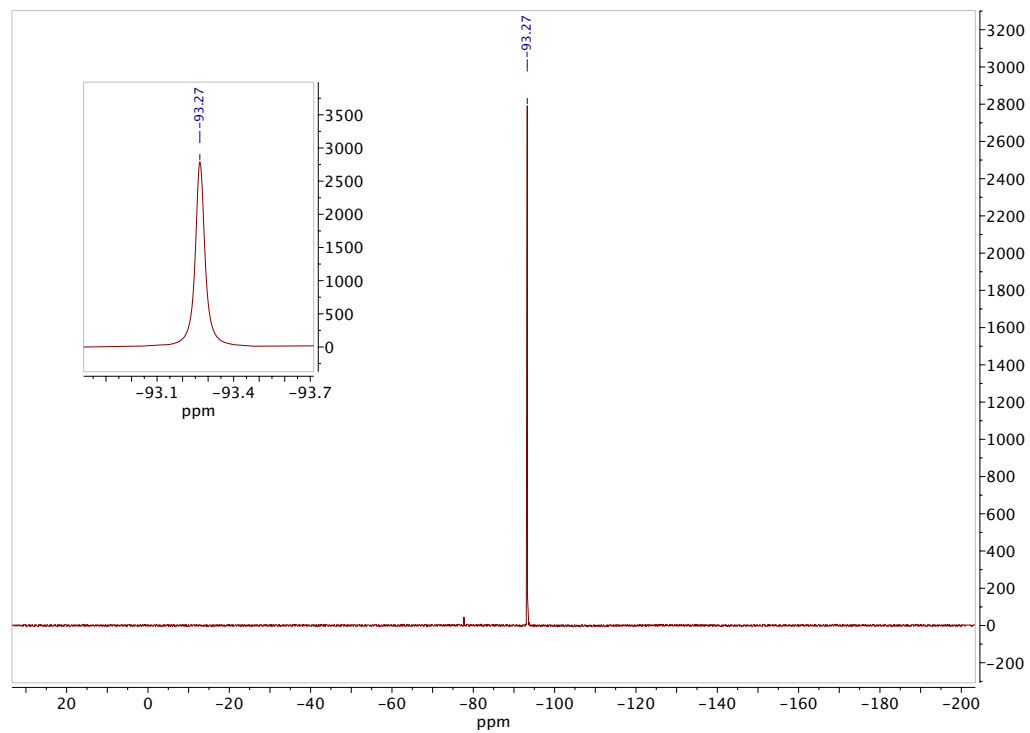


Figure 2.34  $^{19}\text{F}$  NMR of difluorobenzyl pentamethylborazine in  $\text{C}_6\text{D}_6$



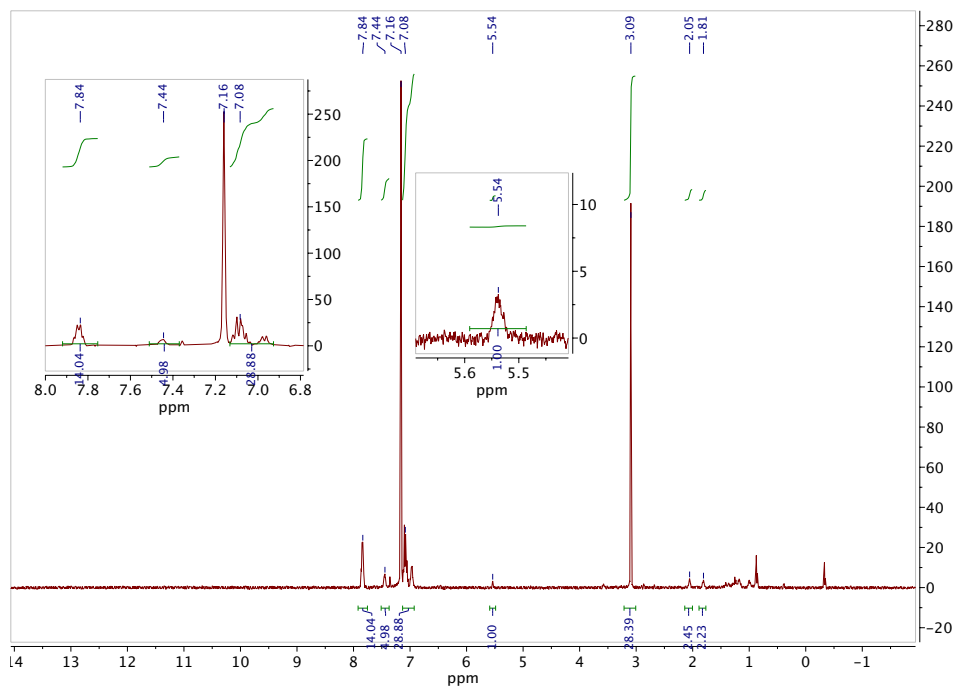


Figure 2.35  $^1\text{H}$  NMR of pentane insoluble material in  $\text{C}_6\text{D}_6$

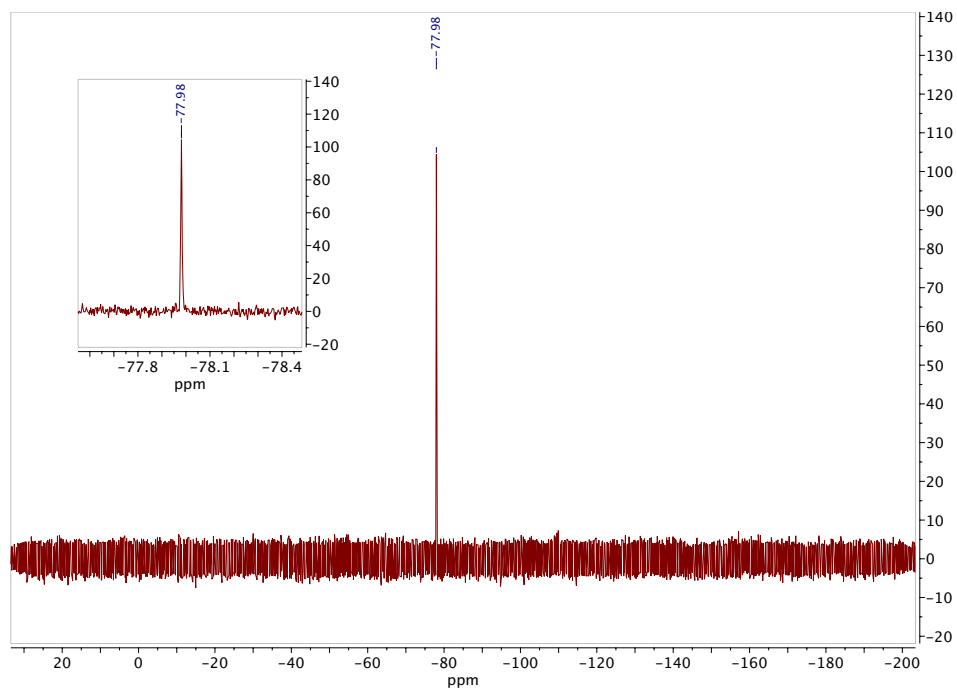
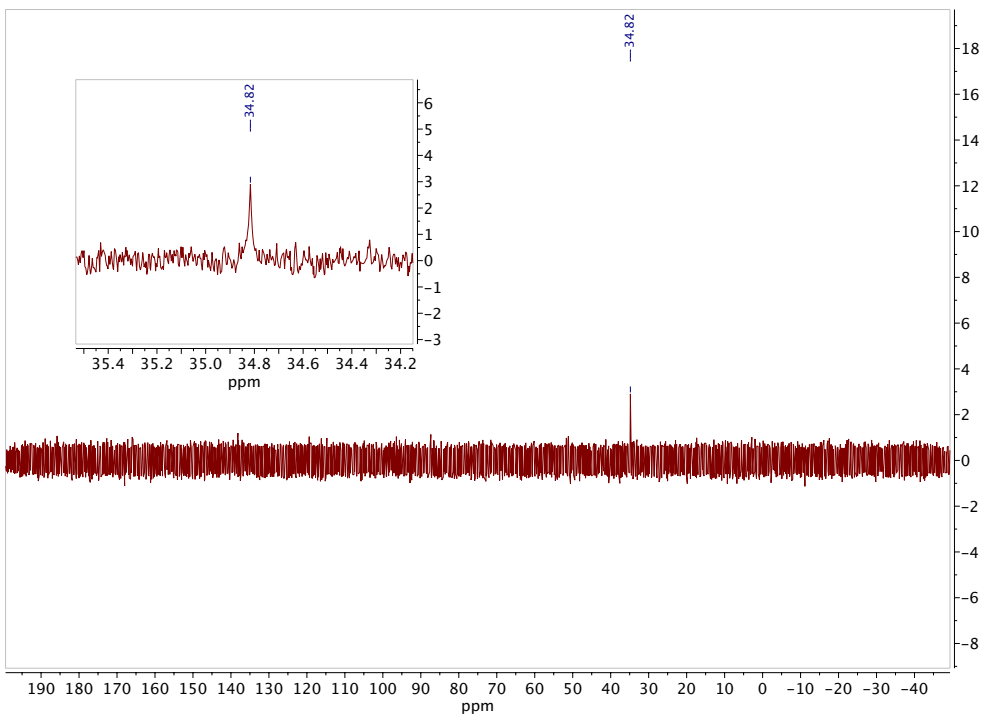
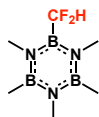


Figure 2.36  $^{19}\text{F}$  NMR of pentane insoluble material in  $\text{C}_6\text{D}_6$



**Figure 2.37**  $^{31}\text{P}$  NMR of pentane insoluble material in  $\text{C}_6\text{D}_6$

### 2.8.7 Synthesis and Characterization of Pentamethylborazine- $\text{CF}_2\text{H}$



Hexamethylborazine- $\text{CF}_2\text{H}$  K(18-crown-6) (0.02 mmol, 10.5 mg) and  $\text{Pd}(\text{PPh}_3)_4$  (0.02, 22.8 mg) were weighed into a 20 mL scintillation vial. Cyclohexenyl triflate (0.02 mmol, 5.1 mg) and fluorobenzene (0.04 mmol, 3.8  $\mu\text{L}$ ) were dissolved in 1 mL of THF. The cyclohexenyl triflate solution was rapidly transferred to the vial containing the other two reagents and after 15 minutes, the reaction was assessed by NMR spectroscopy. Pentamethylborazine- $\text{CF}_2\text{H}$  exhibited a upfield  $^{19}\text{F}$  NMR resonance at -134.30 ppm (d,  $J_{\text{H-F}} = 47.0$  Hz) along with corresponding  $^1\text{H}$  NMR triplet at 6.33 ppm (t,  $J_{\text{H-F}} = 47.0$  Hz). The corresponding  $^{19}\text{F}$  and  $^1\text{H}$  NMR resonances in the starting material appear at -128.23 and 5.20 ppm respectively.<sup>21</sup> Importantly, two new resonances appear

in the trigonal region of the  $^{11}\text{B}$  NMR at 34.12 and 25.34 ppm (*unreferenced*) at roughly a 2:1 ratio.

$^1\text{H}$ -NMR (THF): 0.48 ( $\text{H}_a$ , 6H, s), 2.88 ( $\text{H}_b$ , 3H, s), 2.96 ( $\text{H}_c$ , 6H, s), 6.33 ( $\text{H}_d$ , 1H, t,  $J_{\text{H-F}} = 47.0$  Hz).  $^{19}\text{F}$ -NMR: -134.30 (2F, d,  $J_{\text{H-F}} = 47.0$  Hz).

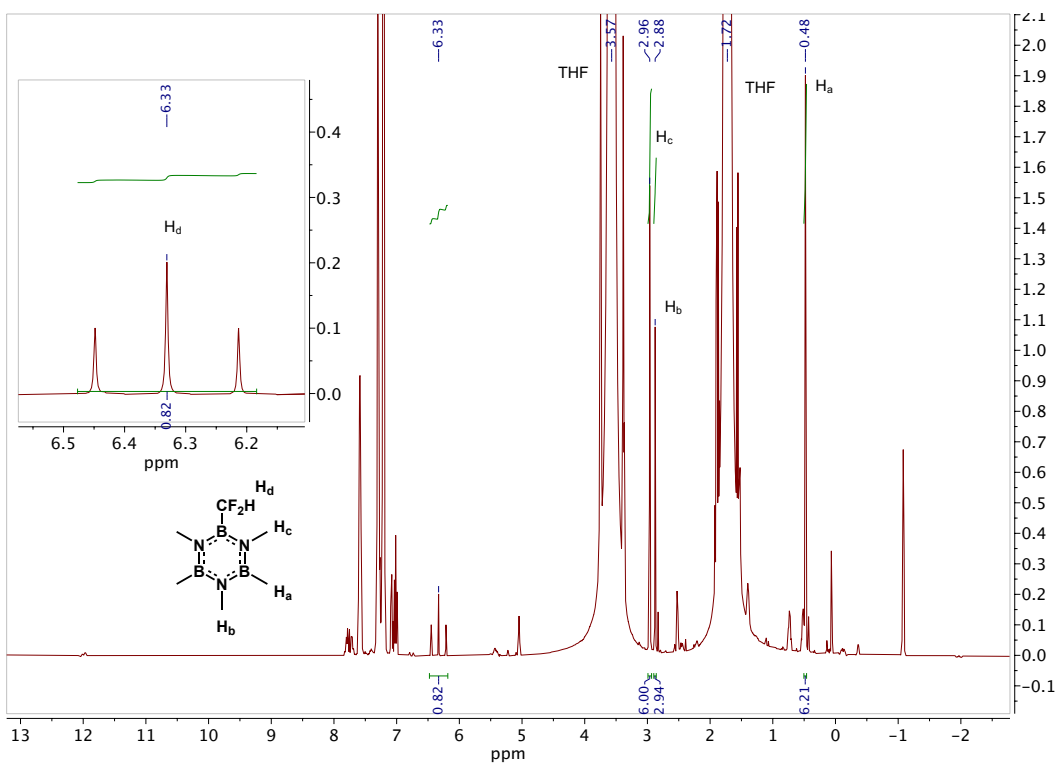


**Figure 2.38**  $^1\text{H}$  NMR of pentamethylborazine- $\text{CF}_2\text{H}$  in THF

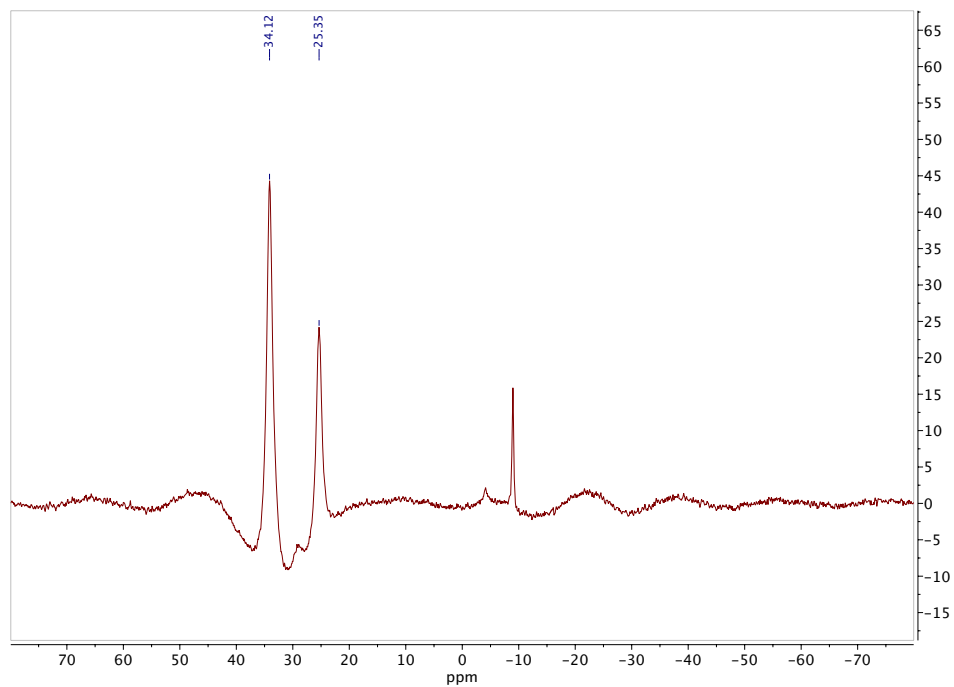


**Figure 2.39**  $^{11}\text{B}$  NMR of pentamethylborazine- $\text{CF}_2\text{H}$  in THF

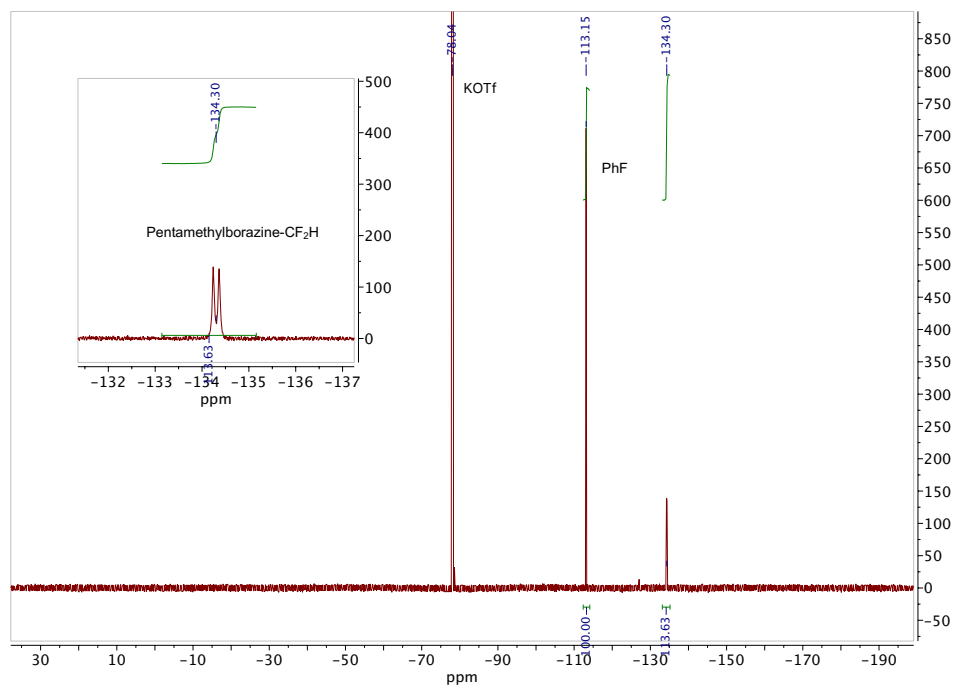
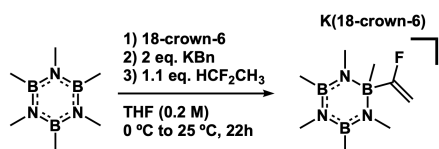


**Figure 2.40**  $^{19}\text{F}$  NMR of pentamethylborazine- $\text{CF}_2\text{H}$  in THF

## 2.8.8 Synthesis and Characterization of Hexamethylborazine-CF=CH<sub>2</sub> Adduct



Hexamethylborazine (1.00 mmol, 166 mg) and 18-crown-6 (1.00 mmol, 266 mg) were dissolved in 5 mL of THF. The solution was cooled to 0 °C in an ice bath and benzyl potassium (1.98 mmol, 258 mg) were added. After 10 minutes, 1,1-difluoroethane gas (1.12 mmol, 25 mL) were bubbled through the THF solution and PhOCF<sub>3</sub> (0.10 mmol, 13.2 μL) were added. The reaction mixture was allowed to stir at 25 °C for 22 h and the in situ yield was assessed by <sup>19</sup>F NMR (26%). The solvent was removed under vacuum and the resulting precipitate was washed with pentane, leaving 122.4 mg of crude product. The crystalline material was dissolved in DMSO-d<sub>6</sub> for <sup>1</sup>H NMR analysis.

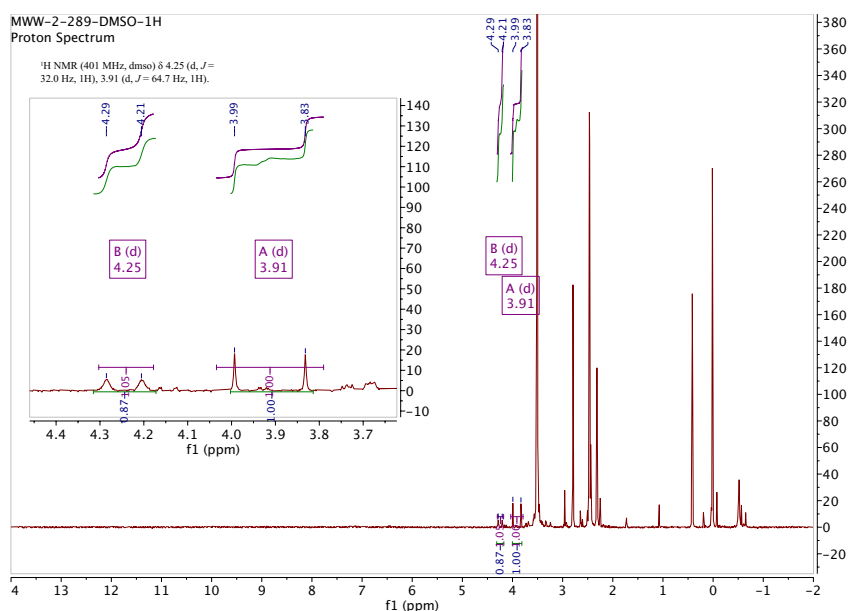


**Figure 2.41** <sup>1</sup>H NMR of the hexamethylborazine-CF=CH<sub>2</sub> adduct in DMSO-d<sub>6</sub>

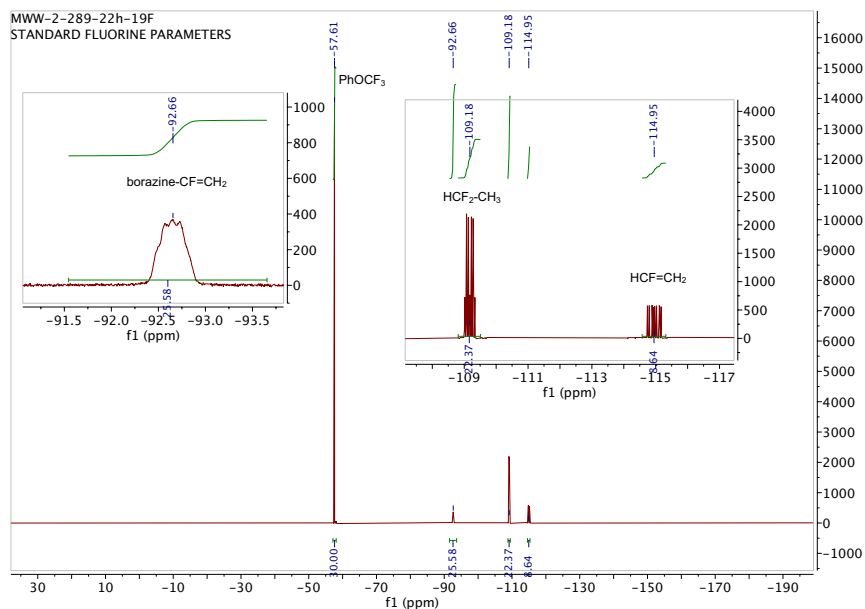
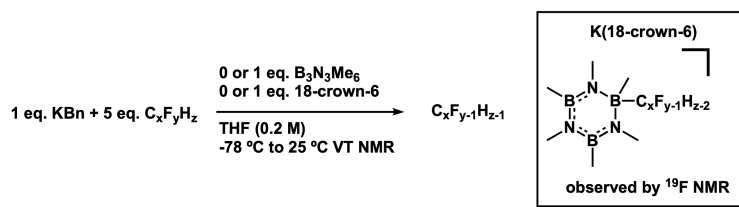


**Figure 2.42**  $^{19}\text{F}$  NMR of the hexamethylborazine- $\text{CF}=\text{CH}_2$  adduct in THF

### 2.8.9 Deprotonation of Polyfluoroethane and Polyfluoropropane Substrates



Two reactions were set up side-by-side to include or exclude hexamethylborazine and 18-crown-6 from the reaction mixture.

Reaction A: Benzyl potassium (0.20 mmol, 26 mg) was dissolved in 1 mL of THF at  $-78\text{ }^\circ\text{C}$ . Fluoroalkane gas (1.0 mmol, 22 mL) were bubbled through the THF solution, and fluorobenzene (0.12 mmol, 11.3  $\mu\text{L}$ ) were added as a  $^{19}\text{F}$  internal standard. Reaction contents were transferred to a  $-78\text{ }^\circ\text{C}$  screwcap NMR tube for further analysis.

Reaction B: Hexamethylborazine (0.20 mmol, 33 mg) and 18-crown-6 (0.20 mmol, 53 mg) were dissolved in 1 mL THF. The reaction was cooled to  $-78\text{ }^\circ\text{C}$  and benzyl potassium (0.20 mmol, 26

mg) was added. Fluoroalkane gas (1.0 mmol, 22 mL) were bubbled through the THF solution, and fluorobenzene (0.12 mmol, 11.3  $\mu$ L) were added as a  $^{19}\text{F}$  internal standard. Reaction contents were transferred to a  $-78\text{ }^{\circ}\text{C}$  screwcap NMR tube for further analysis.

Both reactions A and B were analyzed by variable temperature  $^{19}\text{F}$  NMR. The NMR spectrometer was warmed in  $15\text{ }^{\circ}\text{C}$  intervals over 20 minutes and spectra were acquired at each temperature ( $-65\text{ }^{\circ}\text{C}$  to  $25\text{ }^{\circ}\text{C}$ ). In some cases, another  $^{19}\text{F}$  NMR spectrum was acquired the next day to see if the reaction had further progressed at  $25\text{ }^{\circ}\text{C}$ .

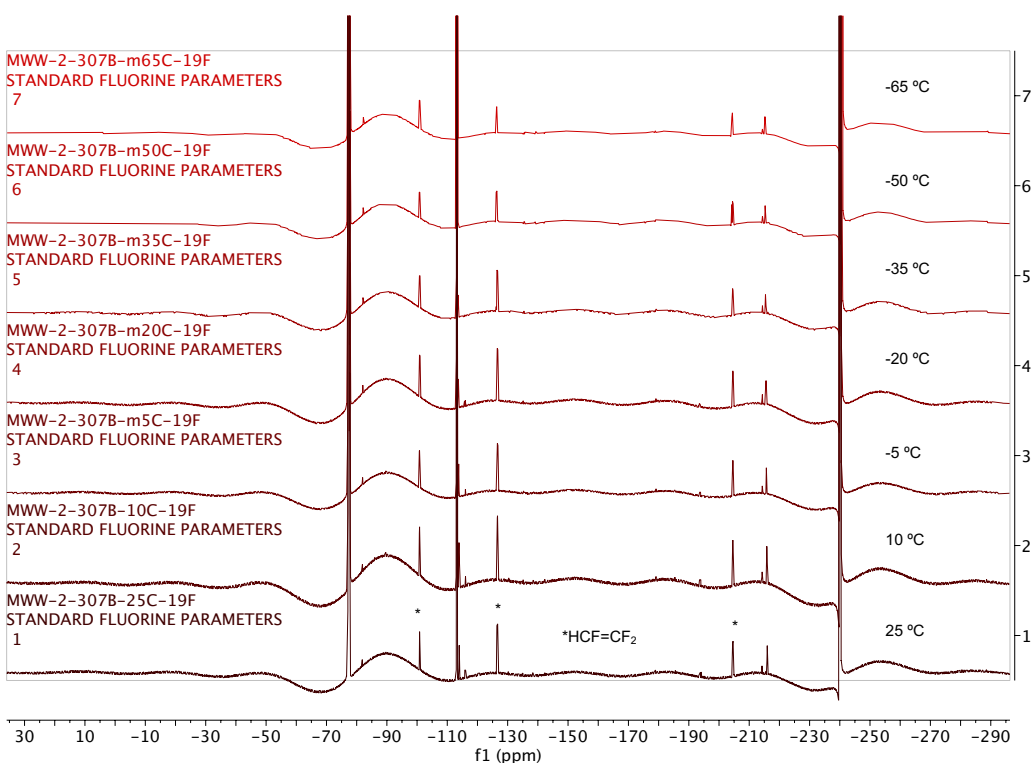


**Figure 2.43** Deprotonation of 1,1,1,2-tetrafluoroethane (no borazine)  $^{19}\text{F}$  NMR array

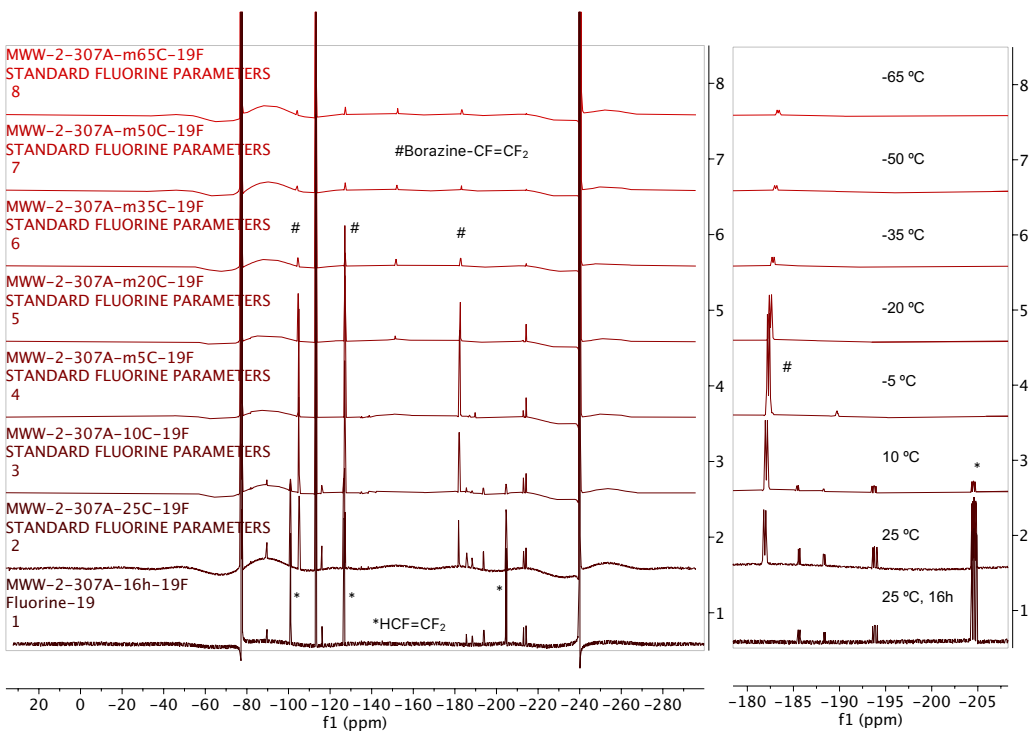


**Figure 2.44** Deprotonation of 1,1,1,2-tetrafluoroethane (with borazine) <sup>19</sup>F NMR array

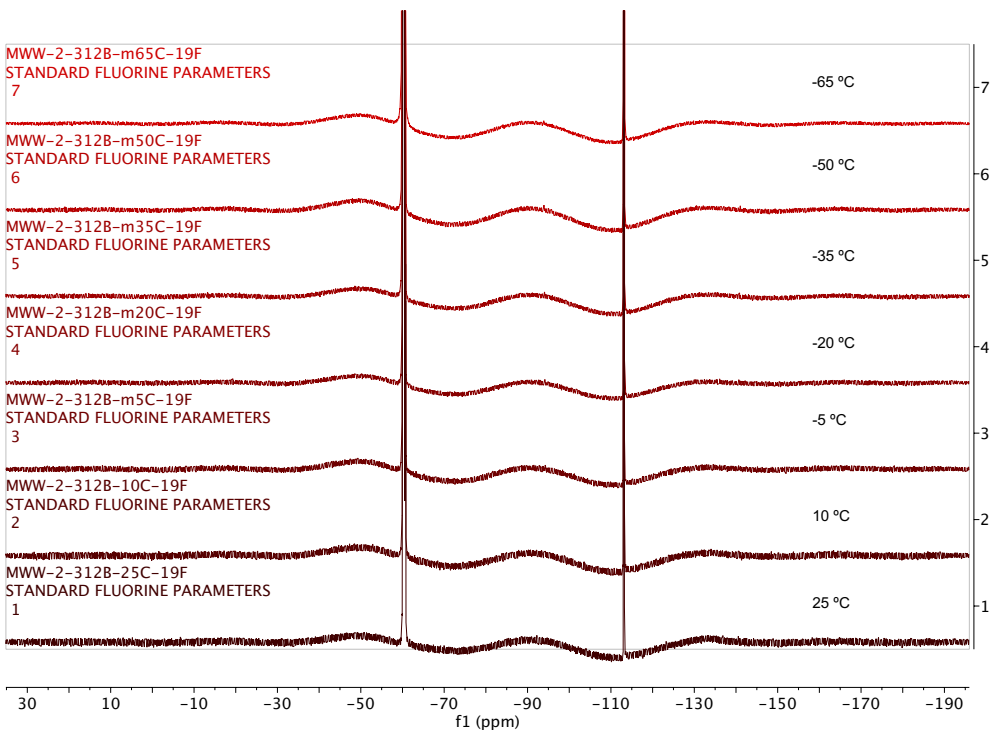


**Figure 2.45** Deprotonation of 1,1,1-trifluoroethane (no borazine) <sup>19</sup>F NMR array



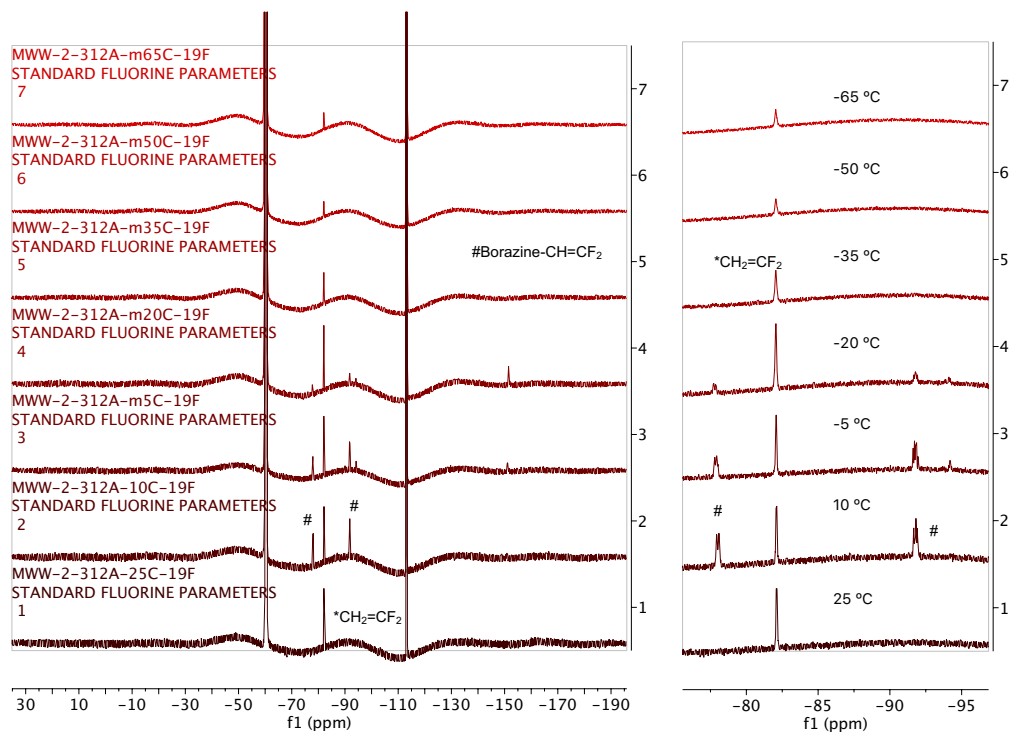


**Figure 2.46** Deprotonation of 1,1,1-trifluoroethane (with borazine)  $^{19}\text{F}$  NMR array

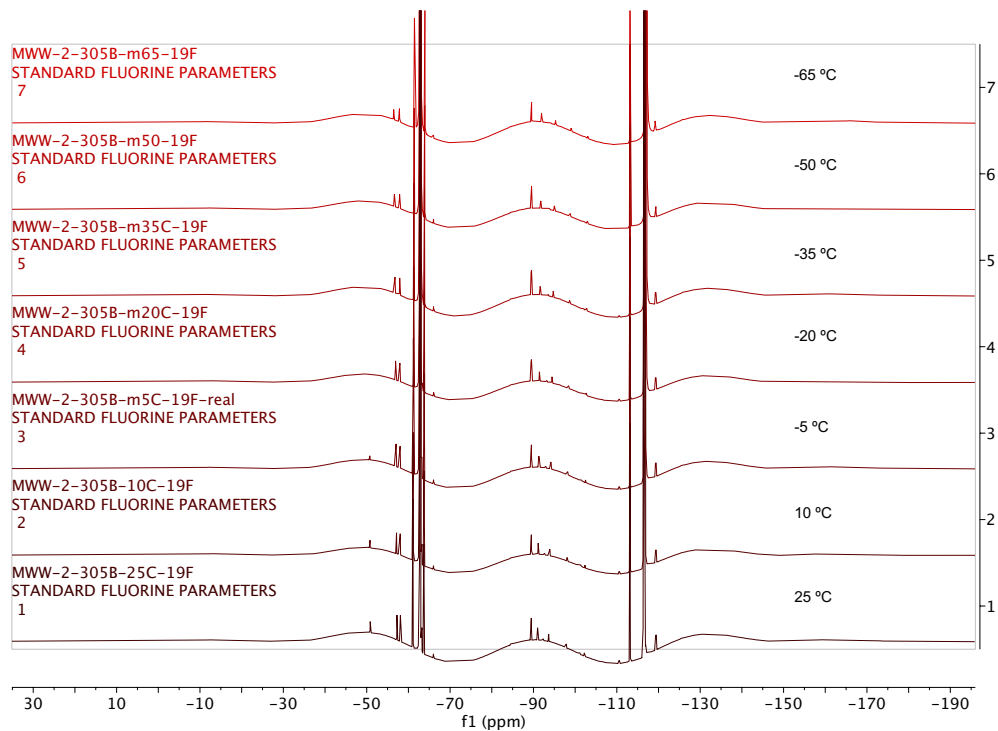


**Figure 2.47** Deprotonation of 1,1,1,3,3-pentafluoropropane (no borazine)  $^{19}\text{F}$  NMR array

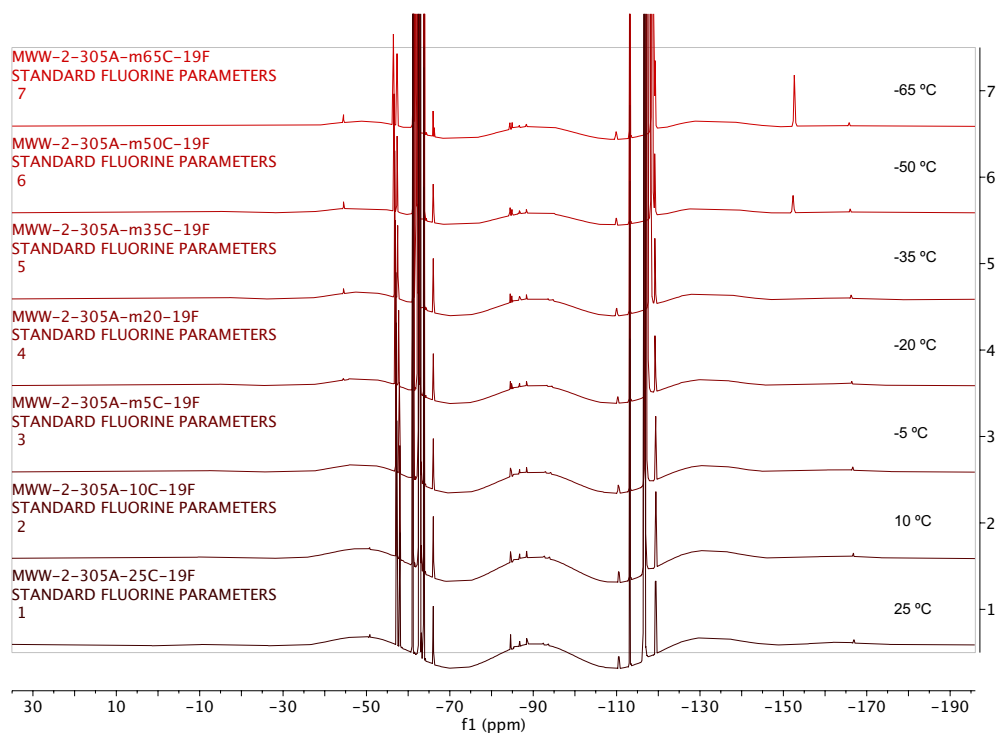


**Figure 2.48** Deprotonation of 1,1,1,3,3-pentafluoropropane (with borazine)  $^{19}\text{F}$  NMR array

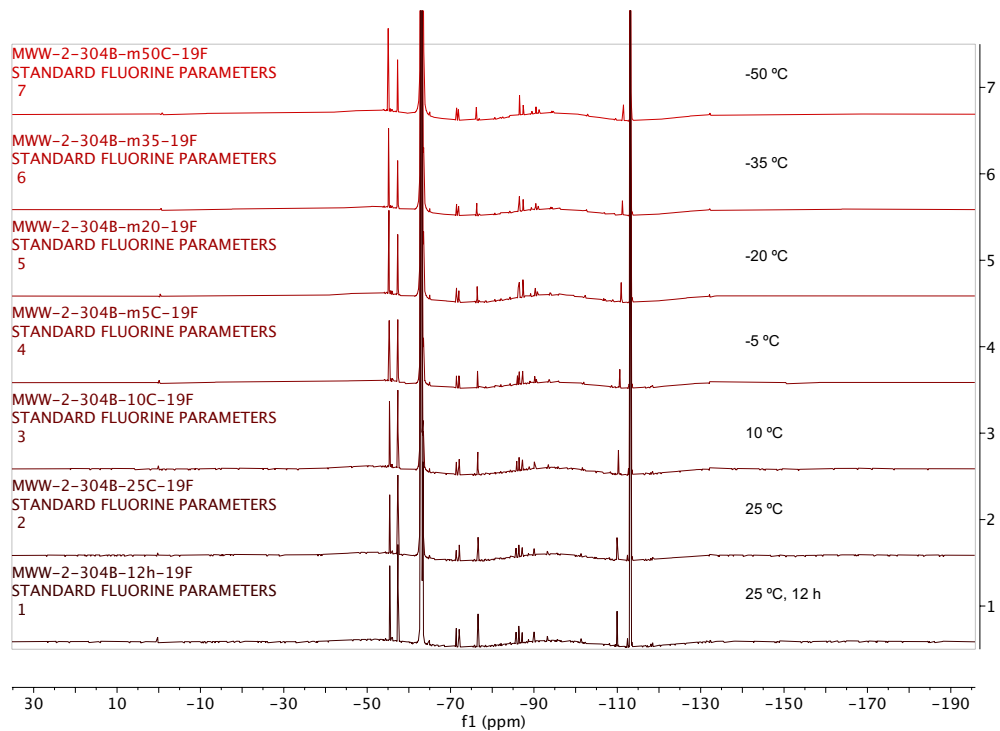


**Figure 2.49** Deprotonation of 1,1,1,3,3,3-hexafluoropropane (no borazine)  $^{19}\text{F}$  NMR array

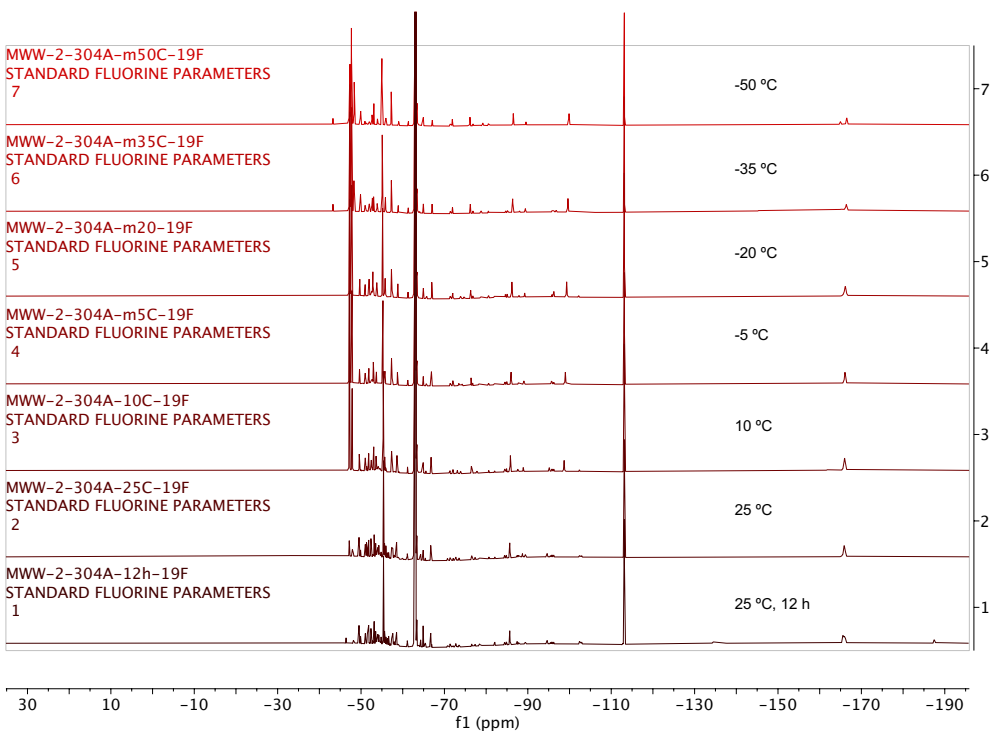


**Figure 2.50** Deprotonation of 1,1,1,3,3,3-hexafluoropropane (with borazine)  $^{19}\text{F}$  NMR array

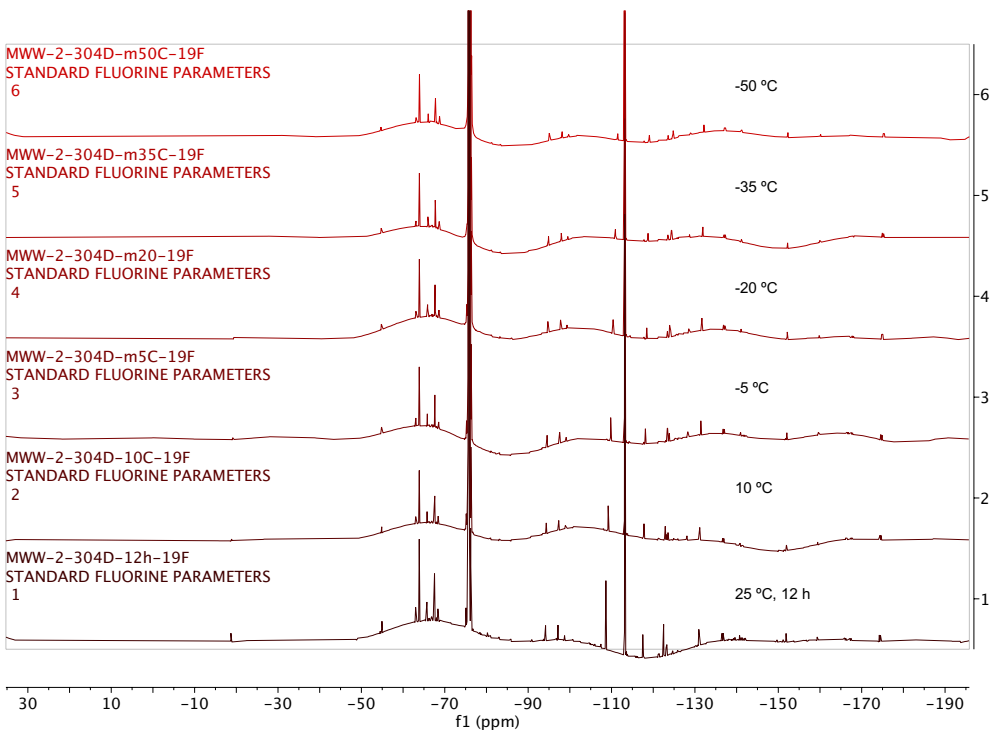


**Figure 2.51** Deprotonation of 2-H-heptafluoropropane (no borazine)  $^{19}\text{F}$  NMR array

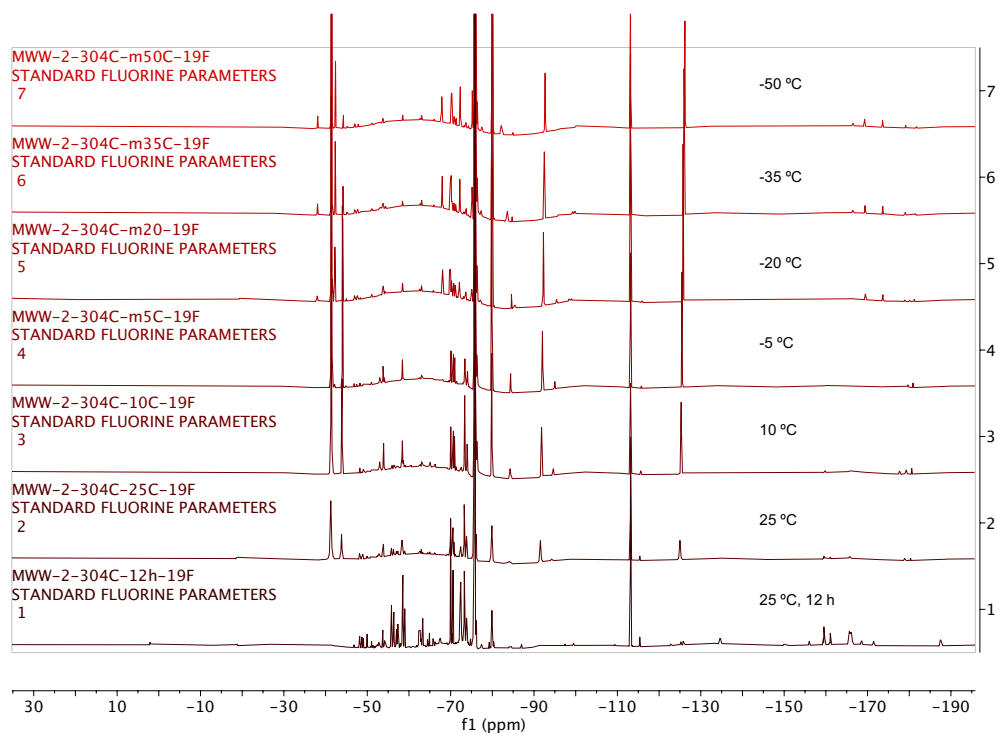
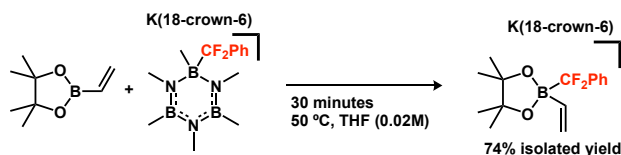


**Figure 2.52** Deprotonation of 2-H-heptafluoropropane (with borazine)  $^{19}\text{F}$  NMR array

### 2.8.10 Synthesis and Characterization of VinylBPinCF<sub>2</sub>Ph K(18-crown-6)



Hexamethylborazine- $\text{CF}_2\text{Ph}$  K(18-crown-6) (0.30 mmol, 179 mg),  $\text{PhOCF}_3$  (0.10 mmol, 13.2  $\mu\text{L}$ ) and vinylBPin (0.30 mmol, 51  $\mu\text{L}$ ) were dissolved in 15 mL of THF in a 20 mL scintillation vial charged with a magnetic stir bar. The reaction mixture was heated to 50  $^\circ\text{C}$  and stirred for 30 minutes. THF and excess vinylBPin were removed under vacuum and the remaining solid residue was washed with 3 x 3 mL of pentane to afford 184.9 mg of HBPin $\text{CF}_2\text{Ph}$  K(18-crown-6). Crystals were grown by layering pentane onto a concentrated THF solution at 25  $^\circ\text{C}$  which afforded 130.2 mg of material 74% isolated yield.

$^1\text{H-NMR}$  (THF- $d_8$ ): 1.00 ( $\text{H}_a$ , 6H, OL), 1.02 ( $\text{H}_b$ , 6H, OL), 3.63 ( $\text{H}_c$ , 24H, s), 4.94 ( $\text{H}_d$ , 1H, m), 4.94 ( $\text{H}_d$ , 1H, m), 5.07 ( $\text{H}_e$ , 1H, dd,  $J_{\text{H-H}} = 19.4, 6.1$  Hz), 6.11 ( $\text{H}_f$ , 1H, dd,  $J_{\text{H-H}} = 19.5, 13.3$  Hz), 7.04 ( $\text{H}_g$ , 1H, OL), 7.09 ( $\text{H}_h$ , 2H, OL), 7.47 ( $\text{H}_i$ , 2H, d,  $J_{\text{H-H}} = 7.5$  Hz).  $^{11}\text{B-NMR}$ : 3.46 (s).  $^{19}\text{F-NMR}$ : -106.27 (2F, broad).

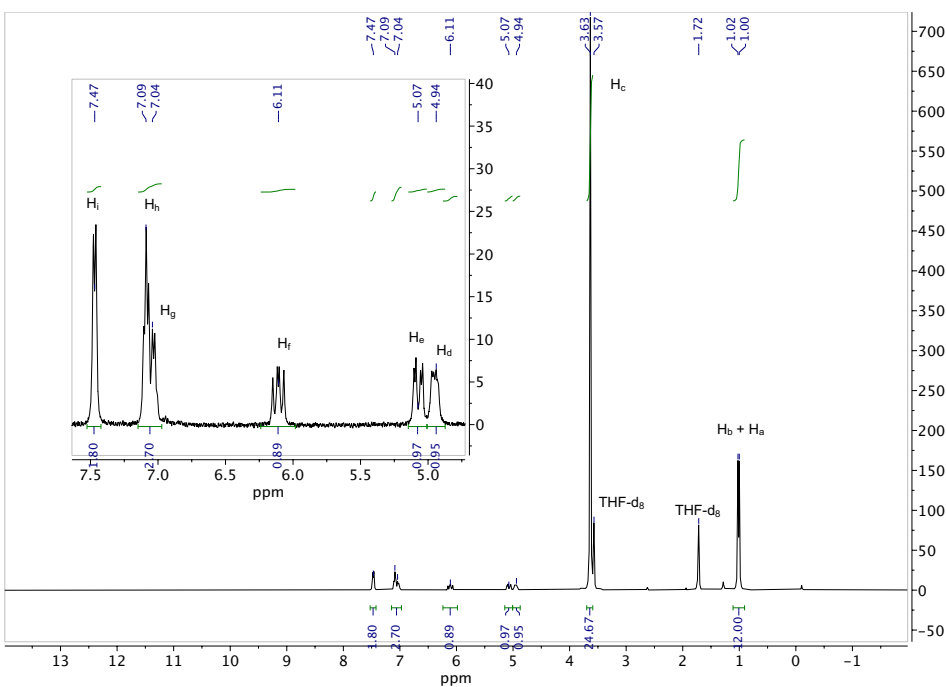


**Figure 2.53**  $^1\text{H}$  NMR spectrum of vinylBPinCF<sub>2</sub>Ph K(18-crown-6) in THF- $d_8$

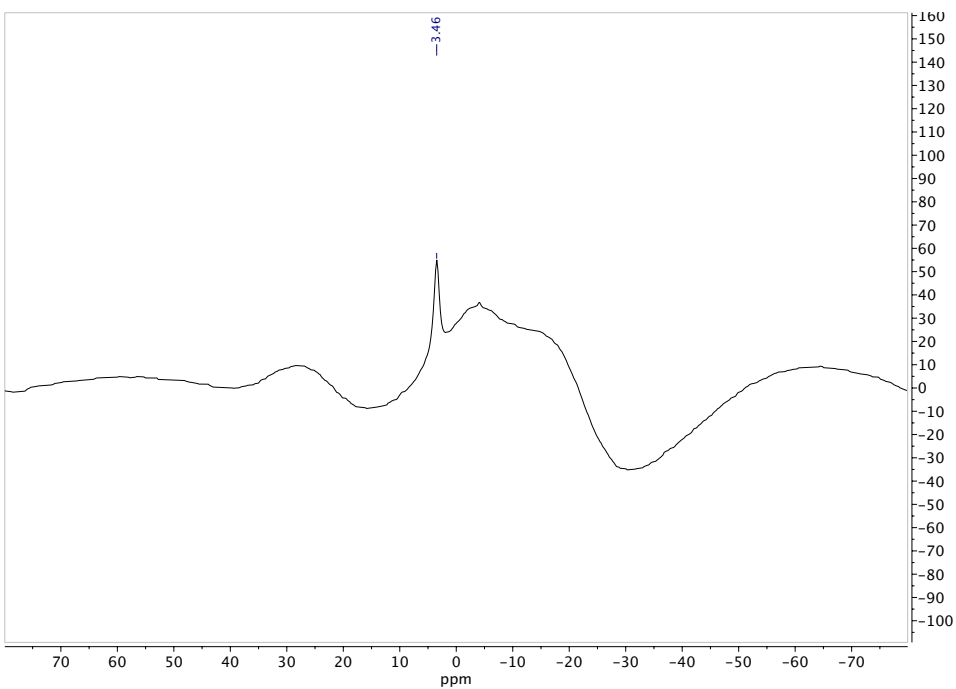


**Figure 2.54**  $^{11}\text{B}$  NMR spectrum of vinylBPInCF<sub>2</sub>Ph K(18-crown-6) in THF-d<sub>8</sub>

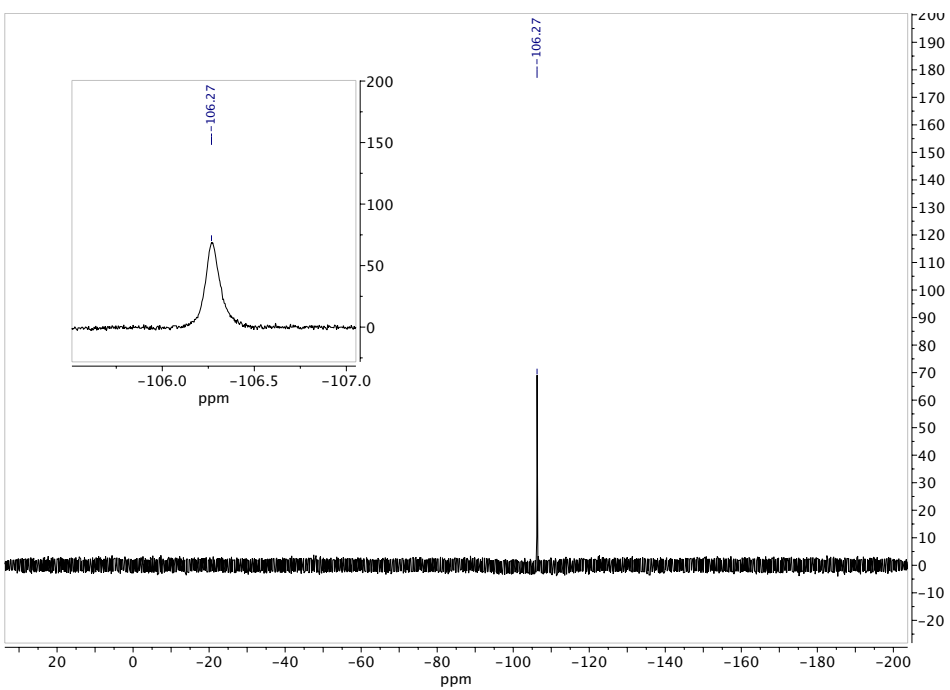
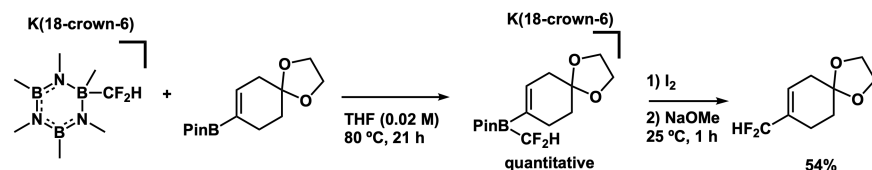


**Figure 2.55**  $^{19}\text{F}$  NMR spectrum of vinylBPInCF<sub>2</sub>Ph K(18-crown-6) in THF-d<sub>8</sub>

## 2.8.11 Zweifel Olefination Reactions

### 8-(Difluoromethyl)-1,4-dioxaspiro[4.5]dec-7-ene



Hexamethylborazane-CF<sub>2</sub>H K(18-crown-6)<sup>21</sup> (0.02 mmol, 10.2 mg), 1,4-Dioxa-spiro[4,5]dec-7-en-8-boronic acid, pinacol ester (0.02 mmol, 5.2 mg) and PhOCF<sub>3</sub> (0.04 mmol, 5.3 μL) were dissolved in 1 mL of THF in a screwcap NMR tube. The reaction mixture was heated for 21 h at 80 °C. Next, iodine (0.02 mmol, 5.1 mg) was added to the reaction mixture, and 5 minutes later sodium methoxide (0.02 mmol, 1.2 mg) was added. The contents were allowed to mix for 1 hour at 25 °C before the yield was assessed by <sup>19</sup>F NMR (54%).

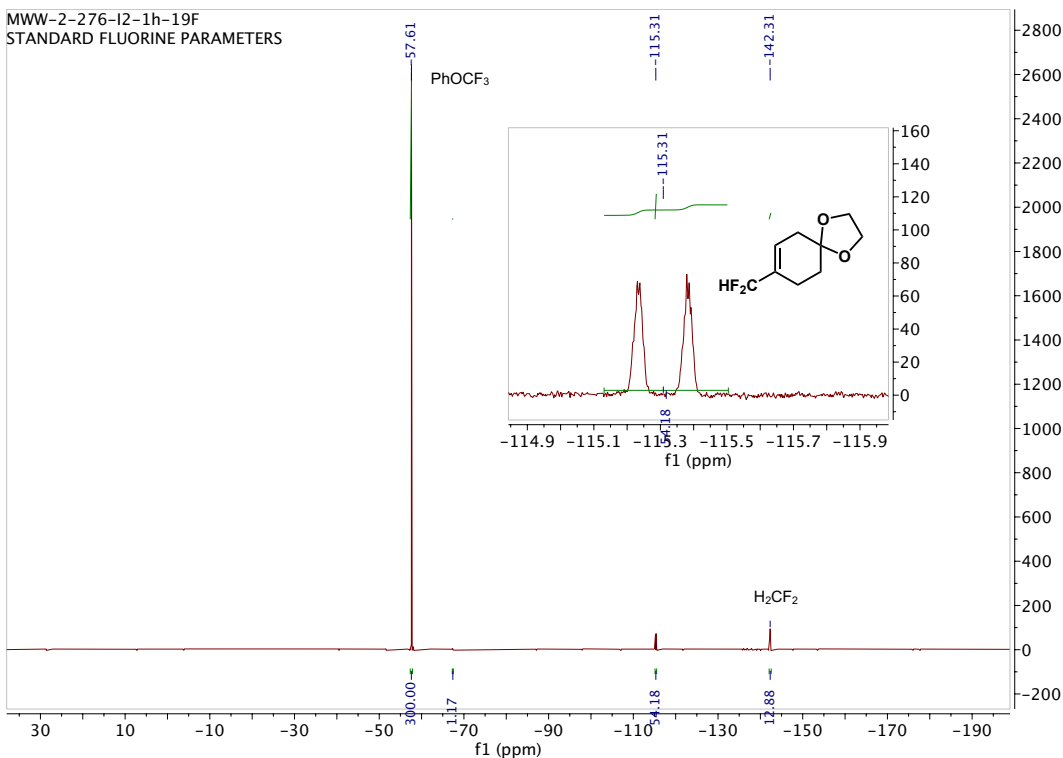
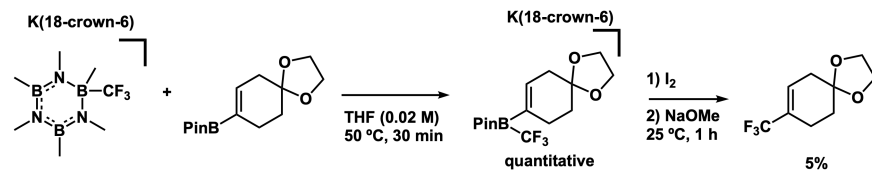


**Figure 2.56** <sup>19</sup>F NMR spectrum of 8-(difluoromethyl)-1,4-dioxaspiro[4.5]dec-7-ene (54% yield)

## 8-(Trifluoromethyl)-1,4-dioxaspiro[4.5]dec-7-ene



Hexamethylborazane-CF<sub>3</sub> K(18-crown-6)<sup>10</sup> (0.02 mmol, 100  $\mu$ L of a 0.2 M solution), 1,4-Dioxaspiro[4,5]dec-7-en-8-boronic acid, pinacol ester (0.02 mmol, 5.5 mg) and PhOCF<sub>3</sub> (0.04 mmol, 5.3  $\mu$ L) were dissolved in 0.9 mL of THF in a screwcap NMR tube. The reaction mixture was heated for 30 min at 50 °C. Next, iodine (0.02 mmol, 5.3 mg) was added to the reaction mixture, and 5 minutes later sodium methoxide (0.02 mmol, 1.3 mg) was added. The contents were allowed to mix for 1 hour at 25 °C before the yield was assessed by <sup>19</sup>F NMR (5%).

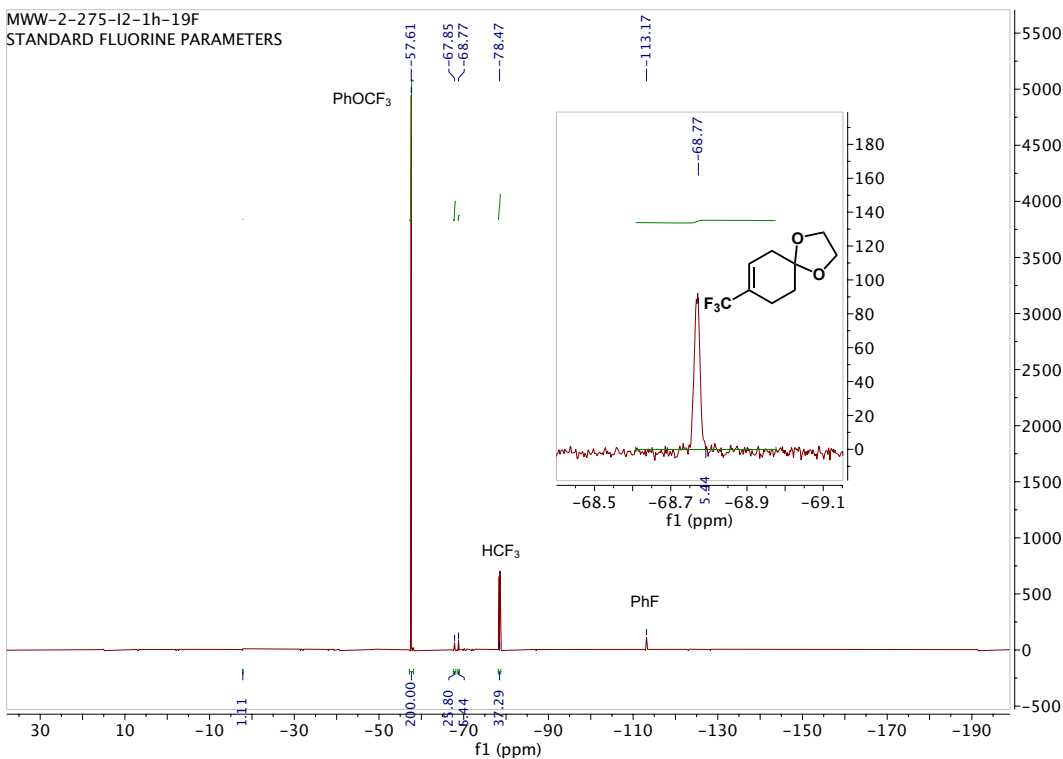
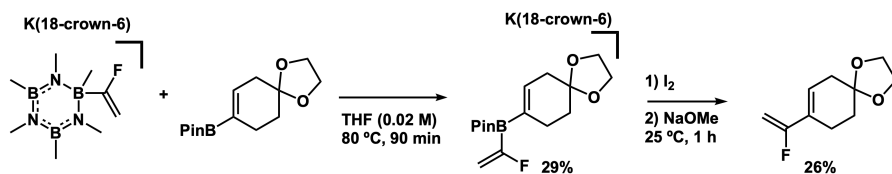


**Figure 2.57** <sup>19</sup>F NMR spectrum of 8-(trifluoromethyl)-1,4-dioxaspiro[4.5]dec-7-ene (5% yield)



## 8-(1-Fluorovinyl)-1,4-dioxaspiro[4.5]dec-7-ene

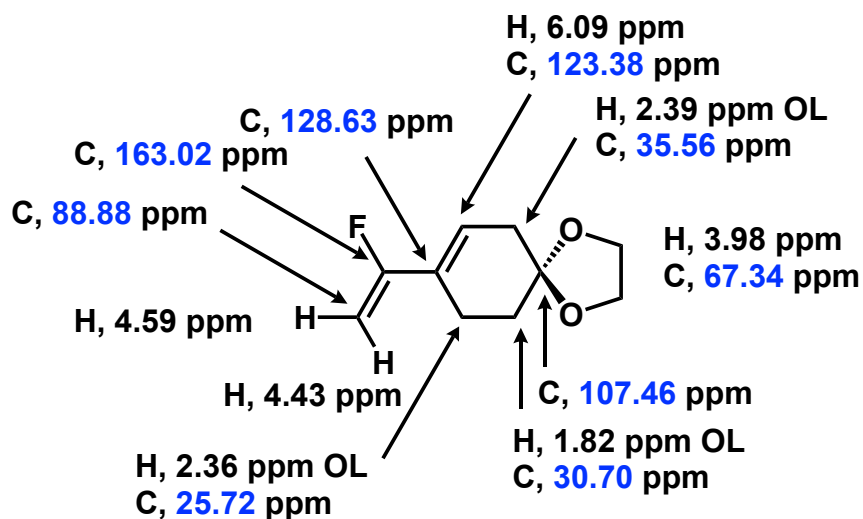


Hexamethylborazine-CF=CH<sub>2</sub> K(18-crown-6) (0.1 mmol, 500  $\mu$ L of a 0.2 M solution), 1,4-Dioxaspiro[4,5]dec-7-en-8-boronic acid, pinacol ester (0.1 mmol, 26.2 mg) and PhF (0.02 mmol) were dissolved in 4.5 mL of THF in a 20 mL scintillation vial. The reaction mixture was heated for 90 min at 80 °C. Next, iodine (0.1 mmol, 25.4 mg) was added to the reaction mixture, and 5 minutes later sodium methoxide (0.1 mmol, 5.5 mg) was added. The contents were allowed to mix for 1 hour at 25 °C before the yield was assessed by <sup>19</sup>F NMR (26%). The THF was removed under vacuum, and the pentane soluble products were analyzed by <sup>1</sup>H and <sup>13</sup>C NMR.

<sup>1</sup>H NMR (CDCl<sub>3</sub>): 1.82 (2H), 2.36 (2H), 2.39 (2H), 3.98 (4H), 4.43 (1H), 4.59 (1H), 6.09 (1H)

<sup>13</sup>C NMR (CDCl<sub>3</sub>): 25.72, 30.70, 35.56, 67.34, 88.88, 107.46, 123.38, 128.63, 163.02

GCMS: 184.1 m/z



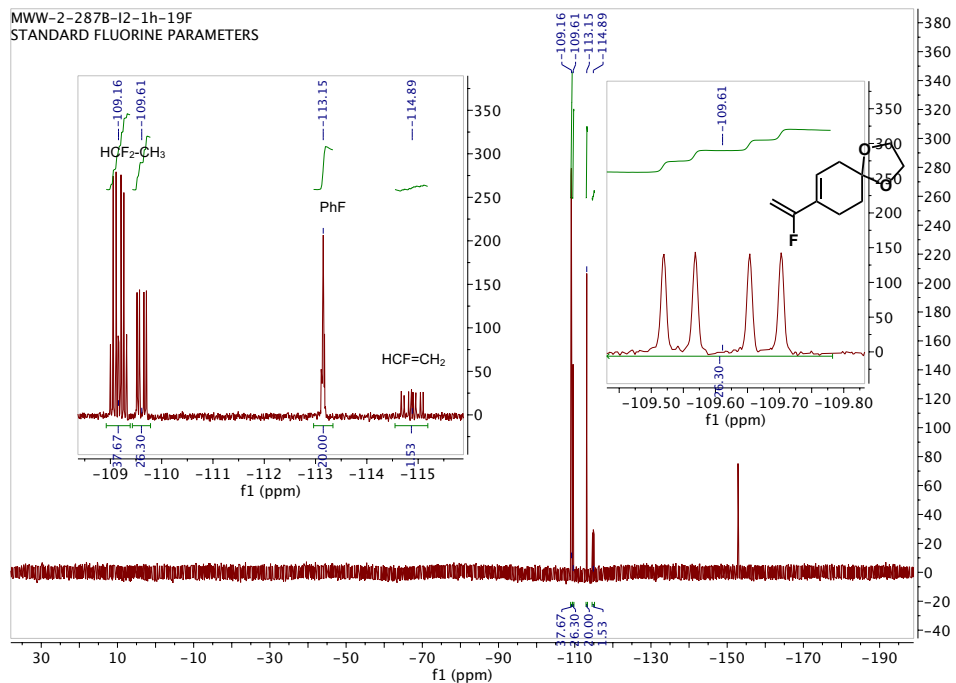


**Figure 2.58**  $^{19}\text{F}$  NMR (THF) spectrum of 8-(1-fluorovinyl)-1,4-dioxaspiro[4.5]dec-7-ene (26% yield)

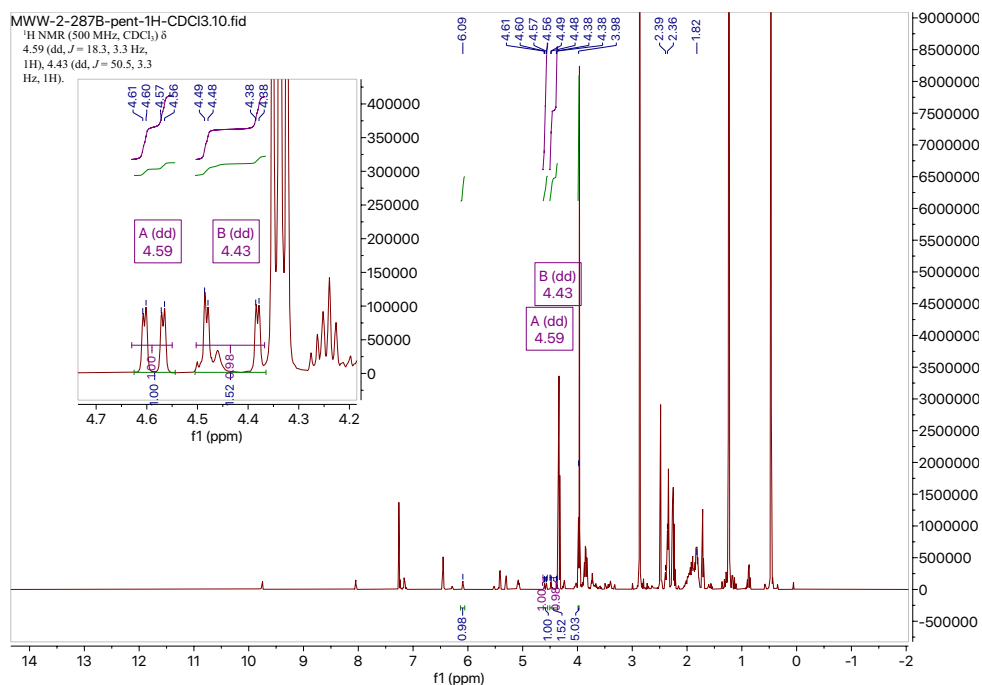


**Figure 2.59**  $^1\text{H}$  NMR ( $\text{CDCl}_3$ ) spectrum of 8-(1-fluorovinyl)-1,4-dioxaspiro[4.5]dec-7-ene

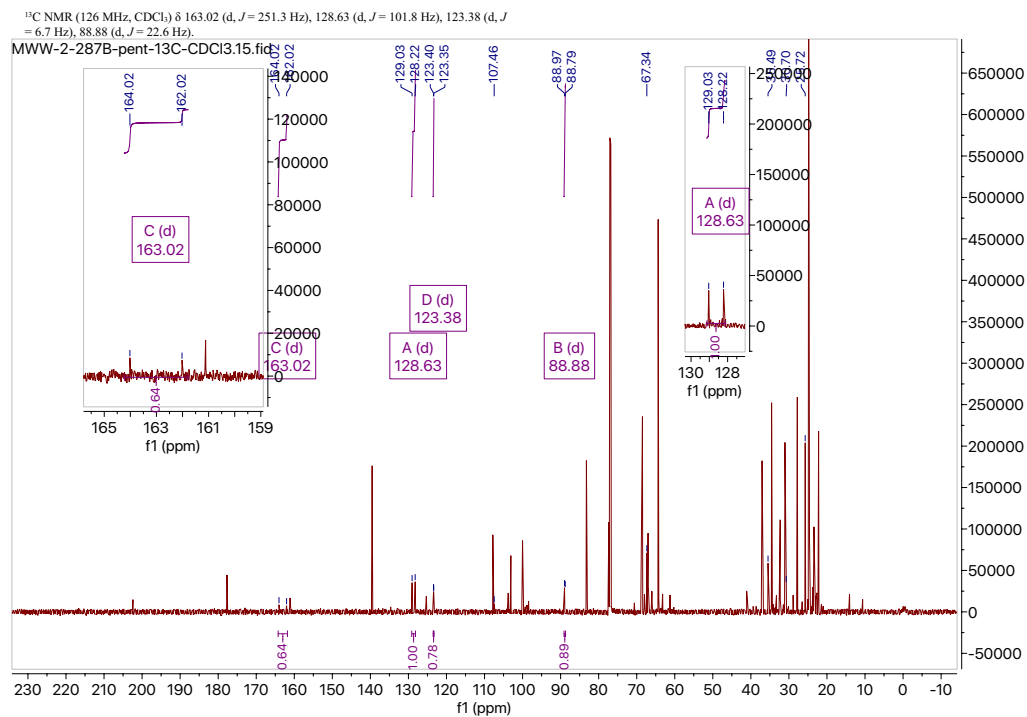


**Figure 2.60** <sup>13</sup>C NMR (CDCl<sub>3</sub>) spectrum of 8-(1-fluorovinyl)-1,4-dioxaspiro[4.5]dec-7-ene

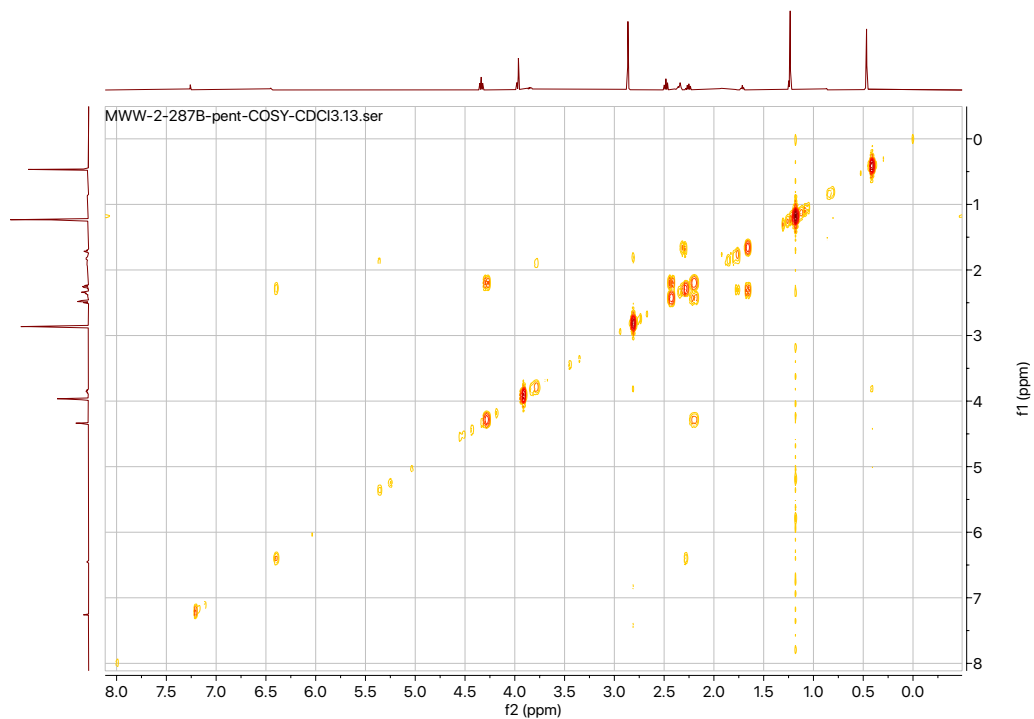


**Figure 2.61** <sup>1</sup>H-<sup>1</sup>H COSY (CDCl<sub>3</sub>) spectrum of 8-(1-fluorovinyl)-1,4-dioxaspiro[4.5]dec-7-ene

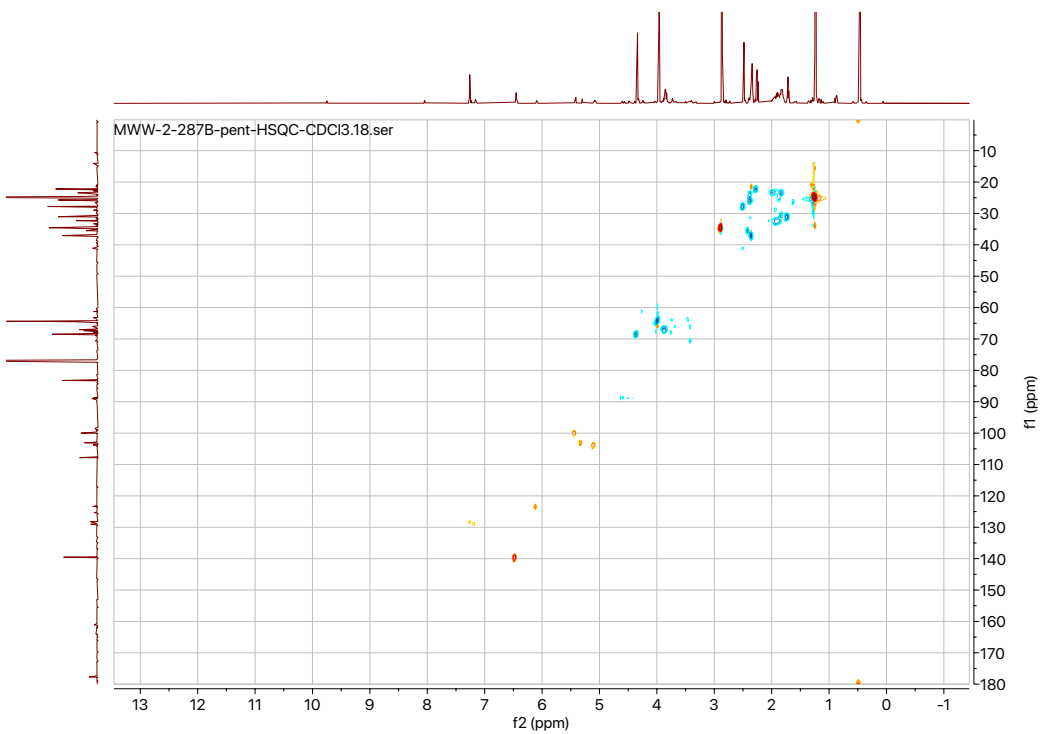


**Figure 2.62**  $^1\text{H}$ - $^{13}\text{C}$  HSQC ( $\text{CDCl}_3$ ) spectrum of 8-(1-fluorovinyl)-1,4-dioxaspiro[4.5]dec-7-ene

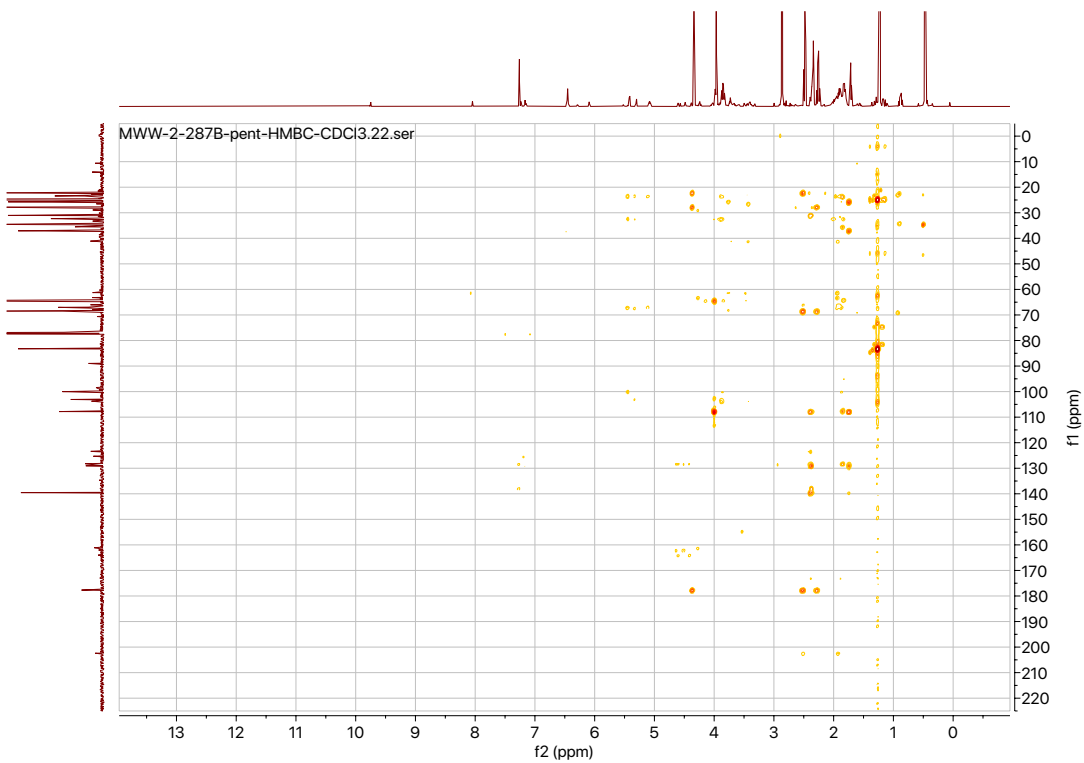
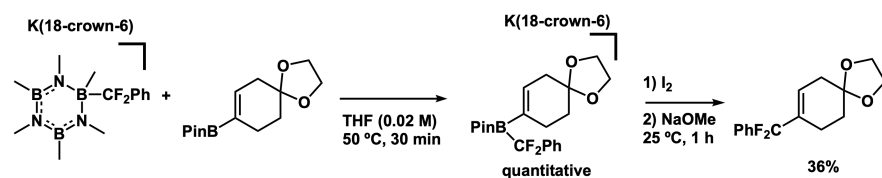


**Figure 2.63**  $^1\text{H}$ - $^{13}\text{C}$  HMBC ( $\text{CDCl}_3$ ) spectrum of 8-(1-fluorovinyl)-1,4-dioxaspiro[4.5]dec-7-ene

## 8-(Difluoro(phenyl)methyl)-1,4-dioxaspiro[4.5]dec-7-ene



Hexamethylborazine-CF<sub>2</sub>Ph K(18-crown-6)<sup>16</sup> (0.02 mmol, 12.3 mg), 1,4-Dioxaspiro[4.5]dec-7-en-8-boronic acid, pinacol ester (0.02 mmol, 5.1 mg) and PhOCF<sub>3</sub> (0.04 mmol, 5.3 μL) were dissolved in 1 mL of THF in a screwcap NMR tube. The reaction mixture was heated for 30 min at 50 °C. Next, iodine (0.02 mmol, 5.3 mg) was added to the reaction mixture, and 5 minutes later sodium methoxide (0.02 mmol, 1.2 mg) was added. The contents were allowed to mix for 1 hour at 25 °C before the yield was assessed by <sup>19</sup>F NMR (36%).

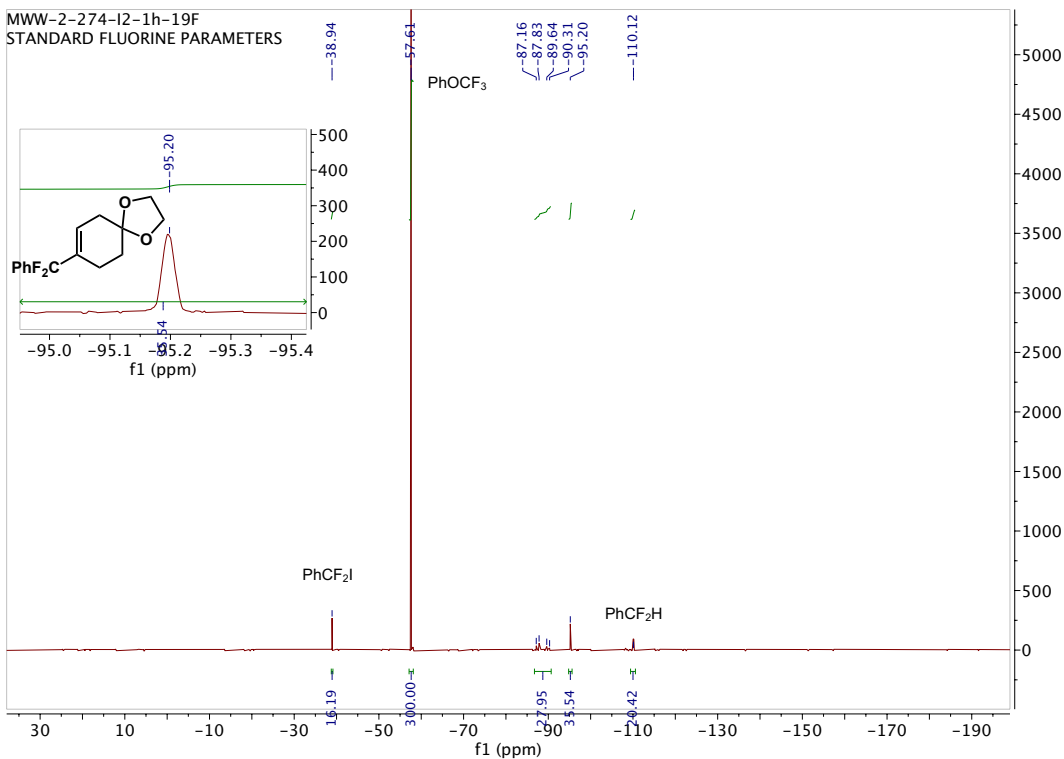
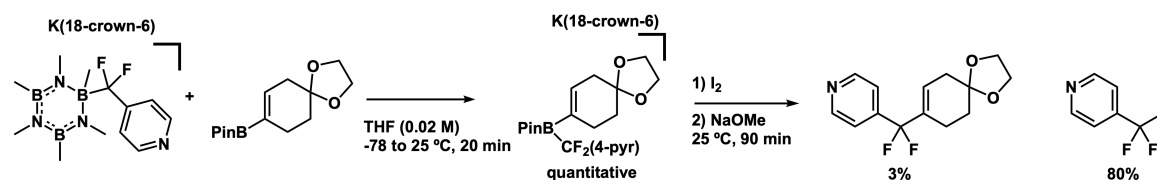


**Figure 2.64** <sup>19</sup>F NMR spectrum of 8-(difluoro(phenyl)methyl)-1,4-dioxaspiro[4.5]dec-7-ene (36% yield)

## 4-(Difluoro(1,4-dioxaspiro[4.5]dec-7-en-8-yl)methyl)pyridine



Hexamethylborazine-CF<sub>2</sub>(4-pyr) K(18-crown-6)<sup>16</sup> (0.03 mmol), 1,4-Dioxa-spiro[4,5]dec-7-en-8-boronic acid, pinacol ester (0.03 mmol, 8.4 mg) and PhF (0.06 mmol, 5.6  $\mu$ L) were dissolved in 1.5 mL of THF in a screwcap NMR tube at -78 °C. The reaction mixture was warmed to 25 °C for 20 min. Next, iodine (0.03 mmol, 8.2 mg) was added to the reaction mixture, and 5 minutes later sodium methoxide (0.03 mmol, 1.9 mg) was added. The contents were allowed to mix for 90 min at 25 °C before the yield was assessed by <sup>19</sup>F NMR (3%).

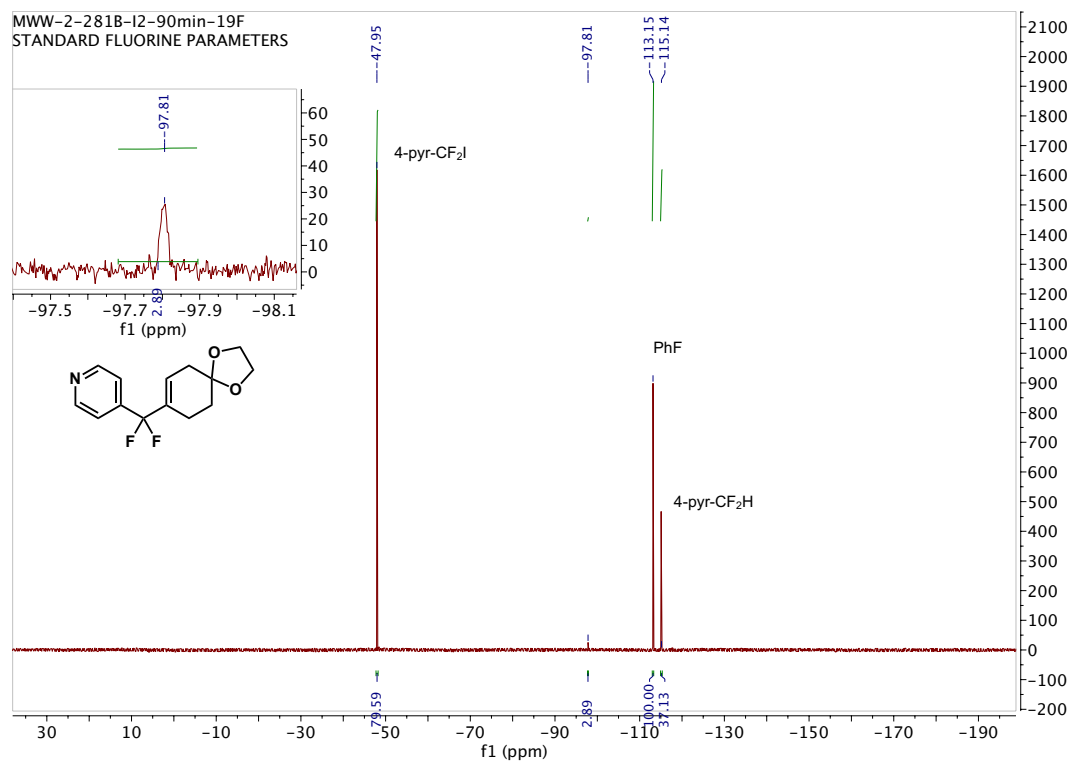
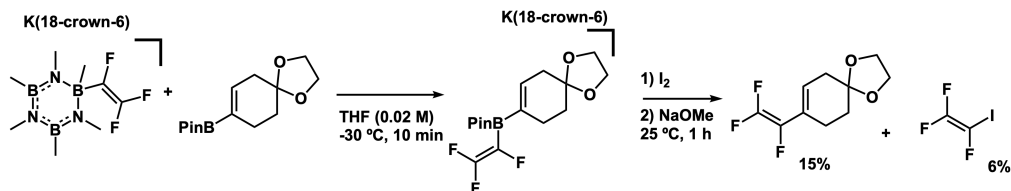


**Figure 2.65** <sup>19</sup>F NMR Spectrum of 4-(Difluoro(1,4-dioxaspiro[4.5]dec-7-en-8-yl)methyl)pyridine (3% Yield)

## 8-(1,2,2-Trifluorovinyl)-1,4-dioxaspiro[4.5]dec-7-ene



Hexamethylborazine-CF=CF<sub>2</sub> K(18-crown-6) (0.02 mmol), 1,4-Dioxa-spiro[4,5]dec-7-en-8-boronic acid, pinacol ester (0.02 mmol, 5.3 mg) and PhF (0.006 mmol) were dissolved in 1 mL of THF in a screwcap NMR tube at -30 °C. After 10 minutes, iodine (0.02 mmol, 5.3 mg) was added to the reaction mixture which then was allowed to warm to 25 °C. After 5 minutes, sodium methoxide (0.03 mmol, 1.5 mg) was added. The contents were allowed to mix for 1 hour at 25 °C before the yield was assessed by <sup>19</sup>F NMR (15%).

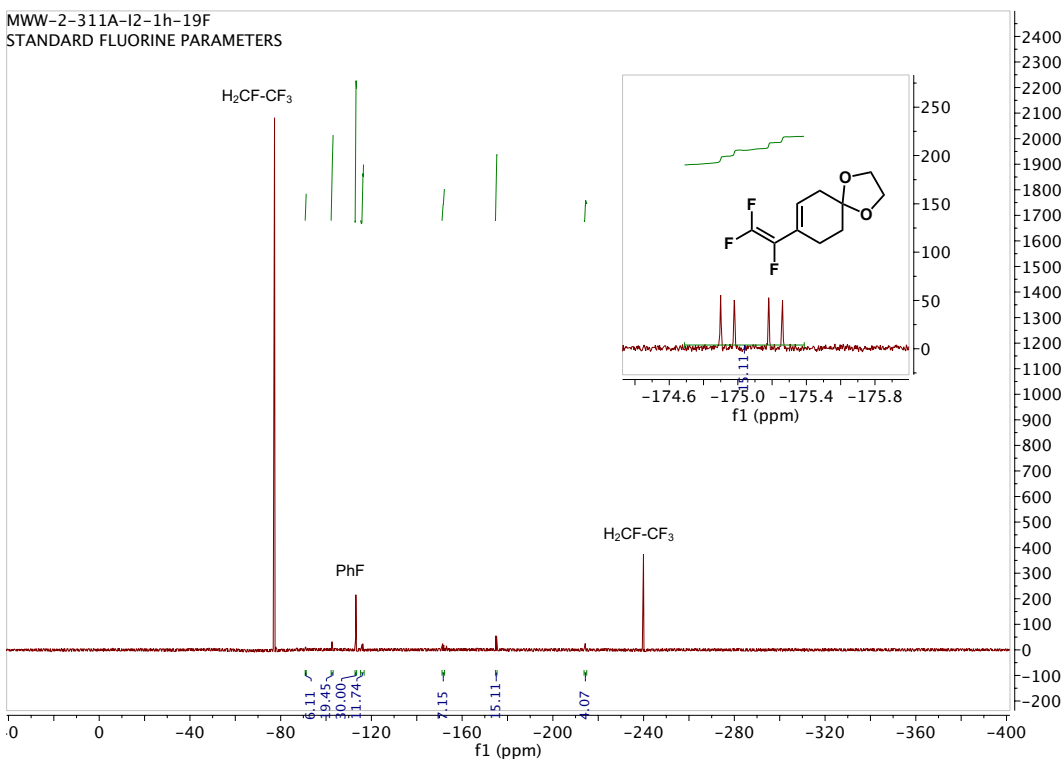


**Figure 2.66** <sup>19</sup>F NMR spectrum of 8-(1,2,2-trifluorovinyl)-1,4-dioxaspiro[4.5]dec-7-ene (15% yield)

## Bibliography

1. Gillis, E. P.; Eastman, K. J.; Hill, M. D.; Donnelly, D. J.; Meanwell, N. A. *J. Med. Chem.*, 2015, 58, 8315-8359.
2. Meanwell, N. A. *J. Med. Chem.*, 2018, 61, 5822-5880.
3. Ruppert, I.; Schlich, K.; Vollbach, W. *Tetrahedron Lett.*, 1984, 25, 2195-2198.
4. Prakash, G. K. S.; Krishnamurti, R.; Olah, G. A. *J. Am. Chem. Soc.*, 1989, 111, 393-395.
5. Liu, X.; Xu, C.; Wang, M.; Liu, Q. *Chem. Rev.*, 2015, 115, 683-730.
6. Maggiarosa, N.; Tyrra, W.; Naumann, D.; Kirij, N. V.; Yagupolskii, Y. L. *Angew. Chem. Int. Ed.*, 1999, 38, 2252-2253.
7. Johnston, C. P.; West, T. H.; Dooley, R. E.; Reid, M.; Jones, A. B.; King, E. J.; Leach, A. G.; Lloyd-Jones, G. C. *J. Am. Chem. Soc.*, 2018, 140, 11112-11124.
8. Kolomeitsev, A. A.; Kadyrov, A. A.; Szczepkowska-Sztolcman, J.; Milewska, M.; Koroniak, H.; Bissky, G.; Barten, J. A.; Röschenthaler, G.-V. *Tetrahedron Lett.*, 2003, 44, 8273-8277.
9. Pietsch, S.; Neeve, E. C.; Apperley, D. C.; Bertermann, R.; Mo, F.; Qiu, D.; Cheung, M. S.; Dang, L.; Wang, J.; Radius, U.; Lin, Z.; Kleeberg, C.; Marder, T. B. *Chem. Eur. J.*, 2015, 21, 7082-7098.
10. Geri, J. B.; Szymczak, N. K. *J. Am. Chem. Soc.*, 2017, 139, 9811-9814.
11. Lishchynskiy, A.; Miloserdov, F. M.; Martin, E.; Benet-Buchholz, J.; Escudero-Adán, E. C.; Konovalov, A. I.; Grushin, V. V. *Angew. Chem. Int. Ed.*, 2015, 54, 15289-15293.
12. Levin, V. V.; Dilman, A. D.; Belyakov, P. A.; Struchkova, M. I.; Tartakovskiy, V. A. *Tetrahedron Lett.*, 2011, 52, 281-284.
13. Knauber, T.; Arikan, F.; Röschenthaler, G.-V.; Gooßen, L. J. *Chem. Eur. J.*, 2011, 17, 2689-2697.
14. Neufeld, R.; Teuteberg, T. L.; Herbst-Irmer, R.; Mata, R. A.; Stalke, D. *J. Am. Chem. Soc.*, 2016, 138, 4796-4806.
15. Geri, J. B.; Wade Wolfe, M. M.; Szymczak, N. K. *Angew. Chem. Int. Ed.*, 2018, 57, 1381-1385.
16. Geri, J. B.; Wade Wolfe, M. M.; Szymczak, N. K. *J. Am. Chem. Soc.*, 2018, 140, 9404-9408.
17. See Chapter 4 for additional information
18. Amatore, C.; Jutand, A.; Le Duc, G. *Angew. Chem. Int. Ed.*, 2012, 51, 1379-1382.
19. Suzuki, A. *J. Organomet. Chem.*, 1999, 576, 147-168.
20. Klanica, A. J.; Faust, J. P.; King, C. S. *Inorg.*, 1967, 6, 840-842.
21. Geri, J. B.; Aguilera, E. Y.; Szymczak, N. K. *Chem. Commun.*, 2019, 55, 5119-5122.
22. Using only 1 equiv. of benzyl potassium did not change the product profile.
23. Goto, Y.; Shiosaki, M.; Hanamoto, T.; Yoshida, M.; Sawada, H. *Colloid Polym. Sci.*, 2013, 291, 1211-1217.
24. Martín-Santamaría, S.; Lavan, B.; Rzepa, H. S. *J. Chem. Soc., Perkin Trans.*, 1415-1417.



25. Jeschke, P. in *Organofluorine Chemistry*, 2021, pp. 363-395.
26. Duric, S.; Schmidt, B. M.; Ninnemann, N. M.; Lentz, D.; Tzschucke, C. C. *Chem. Eur. J.*, 2012, 18, 437-441.
27. Silvi, M.; Sandford, C.; Aggarwal, V. K. *J. Am. Chem. Soc.*, 2017, 139, 5736-5739.
28. Ueda, M.; Kato, Y.; Taniguchi, N.; Morisaki, T. *Org. Lett.*, 2020, 22, 6234-6238.
29. Kischkewitz, M.; Okamoto, K.; Mück-Lichtenfeld, C.; Studer, A. *Science*, 2017, 355, 936-938.
30. Nandakumar, M.; Rubial, B.; Noble, A.; Myers, E. L.; Aggarwal, V. K. *Angew. Chem. Int. Ed.*, 2020, 59, 1187-1191.
31. Jonker, S. J. T.; Jayarajan, R.; Kireilis, T.; Deliaval, M.; Eriksson, L.; Szabó, K. J. *J. Am. Chem. Soc.*, 2020, 142, 21254-21259.
32. Armstrong, R. J.; Aggarwal, V. K. *Synthesis*, 2017, 49, 3323-3336.

## Chapter 3 Defluorinative Functionalization of Pd (II) Fluoroalkyl Complexes

Portions of this chapter have been published

Wade Wolfe, M. M.; Shanahan, J. P.; Kampf, J. W.; Szymczak, N. K. *J. Am. Chem. Soc.* **2020**, *142*, 18698-18705.

### 3.1 Introduction

Fluoroalkylated compounds are rapidly gaining prominence in materials science,<sup>1</sup> agrochemistry,<sup>2</sup> and medicinal chemistry.<sup>3</sup> For instance, nearly 30-40% of new FDA approved drugs in 2018<sup>4</sup> and 2019<sup>5-6</sup> contain an organofluorine unit, compared to 17% during the 2000's.<sup>7</sup> When compared to non-fluorinated analogues, bioactive organic compounds that contain a –C-F instead of a –C-H bond often have distinct chemical and biological properties, including higher metabolic stability and lipophilicity *in vivo*.<sup>3</sup> Consequently, the development of strategies to both install and further diversify organofluorinated compounds<sup>8-9</sup> is at the forefront of efforts within the synthetic community.<sup>10-17</sup> Routes to install the –CF<sub>3</sub> group are most numerous, likely due to the availability of Me<sub>3</sub>SiCF<sub>3</sub> as a reagent.<sup>18</sup> In contrast, significantly fewer routes are known to install other fluoroalkyl groups, such as R–CF<sub>2</sub>–R and R–CFH–R.<sup>19-26</sup> Transition metal-based cross-coupling has become a widely used strategy for assembling and reductively eliminating fluorinated alkyl groups and a coupling partner in order to broadly access organofluorinated compounds.<sup>26-28</sup>

Heterolytic C–F defluorination and subsequent attack by nucleophiles<sup>29-30</sup> is an attractive approach for building new carbon-carbon<sup>31-33</sup> and carbon-heteroatom bonds.<sup>34-37</sup> However, defluorination methods require specialized substrates that stabilize the resulting carbocation and/or

a potent Lewis acid that can *polydefluorinate*  $-CF_n$  groups.<sup>38</sup> Metal fluorocarbenes, accessible from defluorination of metal fluoroalkyl complexes,<sup>39-40</sup> offer an attractive alternative to carbocation intermediates because they are similarly susceptible to nucleophilic attack, can have increased stability, and allow preassembly of nucleophilic partners on a metal precursor. These features can be used to promote selective functionalization of  $-CF_2R$  groups.

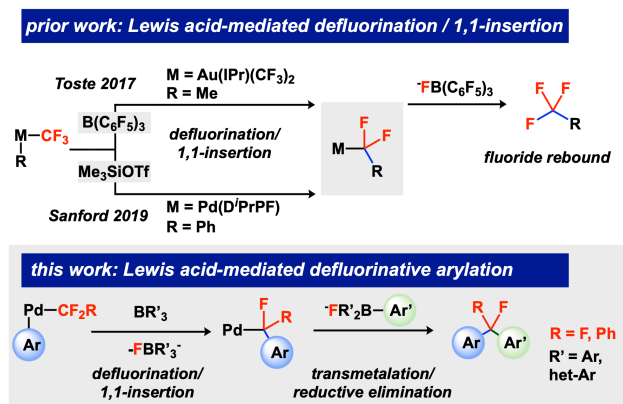


**Figure 3.1** Prior work demonstrating defluorination induced 1,1-insertion (top), and Lewis acid-mediated defluorinative arylation (bottom). In the Sanford example, CsF was added 30 min. after  $Me_3SiOTf$ .<sup>41</sup>

Defluorination of metal fluoroalkyl complexes can be promoted by introducing a Lewis acid. Acid-induced defluorination typically requires fluorophilic reagents such as boranes ( $BR_3$ ) and silylium cations ( $SiR_3^+$ ), which abstract a fluoride ( $F^-$ ) from a metal fluoroalkyl.<sup>39-44</sup> The intermediate metal fluorocarbenes that form can be susceptible to either nucleophilic attack, or alternatively, can undergo 1,1 insertions. Recent examples by Baker<sup>42</sup> as well as Fürstner<sup>45</sup> showed that a  $M=CF_2$  can react with pyridine or even weak nucleophiles to form  $M-CF_2X$  adducts ( $X =$  pyridine, OTf,  $NTf_2$ ). Complementary to exogenous nucleophilic addition to  $M=CF_2$  adducts, Sanford<sup>41</sup> and Toste<sup>46</sup> reported separate examples where an intermediate  $(R)M=CF_2$ , formed by defluorination of a  $(R)M-CF_3$ , underwent 1,1 insertion into a metal aryl or alkyl (**Figure 3.1**). In the latter case, the product reacted with exogenous  $F^-$ , which was used as a strategy to install  $^{18}F$  for radiolabeling.<sup>46</sup> Alternatively, three coordinate  $Pd-CF_3$  complexes have been shown to undergo

thermal defluorination via unimolecular  $\alpha$ -fluoride elimination en route to Ar/CF<sub>3</sub> reductive elimination. However, under stoichiometric reaction conditions, the proposed Pd(CF<sub>2</sub>)(F)(Ph)(PR<sub>3</sub>) intermediate was found to transmetalate with another equivalent of a Pd(Ph) complex to afford diphenyldifluoromethane in a competitive, but low yielding (< 22%) pathway.<sup>47</sup> Importantly, formation the difluorodiphenyl methane side product provides precedent for defluorination/transmetalation strategies at palladium to prepare difluorobenzyl linkages.

We hypothesized that, rather than reintroducing F<sup>-</sup> as a nucleophile, Pd fluoroalkyl complexes are uniquely situated to react with a variety of nucleophilic aryl reagents. We targeted a series of boron based reagents capable of promoting a defluorination reaction coupled with transmetalation of a nucleophile to enable a distinct set of functionalization reactions accessible from simple metal fluoroalkyl precursors. Our group recently disclosed a Lewis acid/base pair strategy to access anionic -CF<sub>2</sub>Ar synthons, enabling facile diversification from simple H-CF<sub>2</sub>Ar precursors.<sup>24</sup> Stoichiometric Pd-cross-coupling of the -CF<sub>2</sub>Ar reagents provided difluorodiarlylmethane products, likely through transmetalation to Pd(II), followed by reductive elimination. These reactions provide an entry point into species that may be functionalized through a net defluorinative arylation reaction.

### 3.2 Synthesis and Reactivity of the [Pd]-CF<sub>2</sub>Ph Complex

To prepare fluoroalkylated complexes amenable to rapid diversification, we targeted the isolation of (PPh<sub>3</sub>)<sub>n</sub>(Ar)Pd-CF<sub>2</sub>Ph; a likely intermediate during the cross-coupling reaction sequence. Introduction of the -CF<sub>2</sub>Ph synthon, [K(18-crown-6)][PhCF<sub>2</sub>-B<sub>3</sub>N<sub>3</sub>Me<sub>6</sub>], to (PPh<sub>3</sub>)<sub>2</sub>(3,5-(CF<sub>3</sub>)<sub>2</sub>Ph)PdBr in tetrahydrofuran (THF), at 23 °C for 22 h, suppressed reductive elimination, enabling access to the transmetalated adduct, (PPh<sub>3</sub>)(3,5-(CF<sub>3</sub>)<sub>2</sub>Ph)Pd(CF<sub>2</sub>Ph)Br (**1a**), as an isolable product in 85% yield (**Figure 3.2 a**).

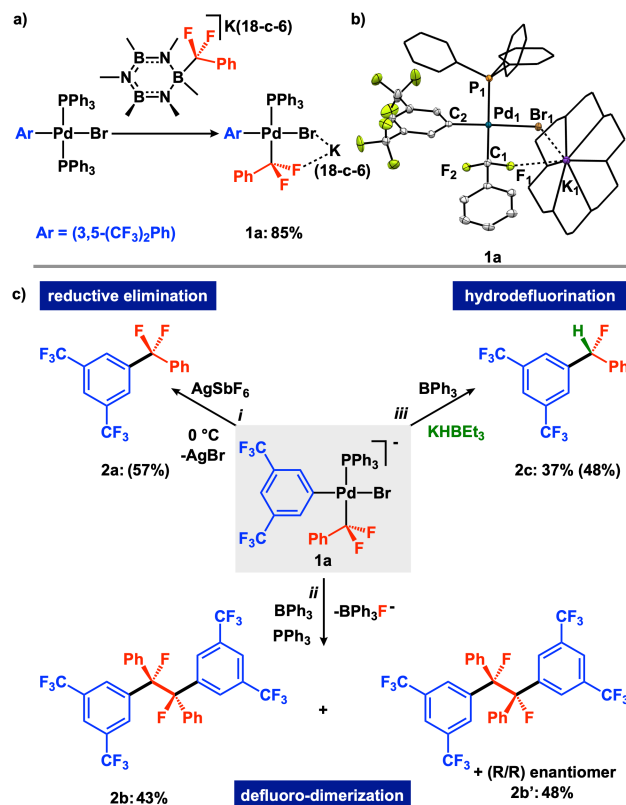


**Figure 3.2** a) Preparation of **1a**. b) X-ray structure of **1a**, Pd<sub>1</sub>–C<sub>1</sub> distance 2.0735(19) Å, ellipsoids shown at 50%, H-atoms removed and non-essential aryl rings wireframed for clarity. c) Diversification of **1a**: i) 1 eq. AgSbF<sub>6</sub> at 0 °C (1 h) affords **2a**, ii) 1 eq. BPh<sub>3</sub> (5 min), followed by 1 eq. PPh<sub>3</sub> (17 h) at RT affords **2b/2b'** and iii) 1 eq. BPh<sub>3</sub> (15 min), followed by 1 eq. KHBEt<sub>3</sub> at RT for 17 h affords **2c**.

Crystals suitable for an X-ray diffraction experiment were obtained from diethyl ether, and the structure revealed an anionic [LX<sub>3</sub>Pd]<sup>-</sup> complex (**Figure 3.2 b**). This formulation contrasts with the common L<sub>2</sub>X<sub>2</sub>Pd products of similar reactions with non-fluorinated alkyl nucleophiles.<sup>48</sup> Unlike transmetalation of an aryl group to palladium(II)aryl-bromide complexes, PPh<sub>3</sub> is displaced as opposed to bromide, forming an anionic complex with potassium 18-crown-6 as the counter cation.<sup>48</sup> **1a** exhibits a Pd<sub>1</sub>–C<sub>1</sub> distance of 2.0735(19) Å, which is similar to the Pd–C distance of the anionic Pd complex, Pd(CF<sub>3</sub>)<sub>3</sub>PPh<sub>3</sub><sup>-</sup> (2.062(5) Å).<sup>49–50</sup> The structure indicates an *associated* potassium counter ion interacting with both a fluorine atom of CF<sub>2</sub>Ph (K1–F1 = 2.8310(12) Å), as well as Br (K1–Br1 = 3.2286(4) Å).

Analysis of the  $^{19}\text{F}$  NMR spectrum in  $\text{C}_6\text{D}_6$  of **1a** revealed two resonances: a singlet at -62.16 ppm (6F) (from 3,5-( $\text{CF}_3$ ) $_2$ Ph) and a doublet at -69.08 ppm (2F) with a coupling constant of 39.3 Hz, consistent with the formation of a Pd- $\text{CF}_2$ Ph.<sup>41</sup> The  $^{31}\text{P}$  NMR spectrum contained a triplet at 18.75 ppm, also exhibiting a coupling constant of 39.3 Hz, which we assign as  $^3J_{\text{P-F}}$ .<sup>41</sup> Finally, the  $^1\text{H}$  NMR spectrum revealed aromatic resonances for the  $-\text{CF}_2\text{Ph}$  moiety (5H) that integrate 1:1 with respect to one  $\text{PPh}_3$  molecule (15H). Importantly, the  $^{19}\text{F}$  NMR splitting pattern corresponds to a single equivalent of  $\text{PPh}_3$  for each  $\text{CF}_2\text{Ph}$  unit, consistent with the uncommon anionic formulation from the solid-state structural analysis.

We investigated subsequent reactivity of **1a** with a series of Lewis acidic reagents in order to assess possible fluoroalkyl diversification routes through this single precursor. Subjecting **1a** to 50 °C for 45 h induced C(sp<sup>2</sup>)-C(sp<sup>3</sup>) reductive elimination to form [ $\text{PhCF}_2(3,5-(\text{CF}_3)_2\text{Ph})$ ] (**2a**) in 71% yield, as assessed by  $^{19}\text{F}$  NMR spectroscopy. Addition of 1 equiv.  $\text{AgSbF}_6$  had a dramatic effect: **2a** was afforded in 57% yield after just 1 hour at 0 °C (**Figure 3.2 c**, left). Another strategy to diversify **1a** is *via* the  $\alpha$ -fluorine-carbon bond, a motif that has been shown to be reactive toward strong fluorophiles in late transition metals.<sup>41,46</sup>

In contrast to the ionic Lewis acid ( $\text{Ag}^+$ ), we observed distinct product profiles when using a borane Lewis acid. Subjecting **1a** to 1 equiv.  $\text{BPh}_3$  at 25 °C in THF for 5 minutes followed by 1 equiv  $\text{PPh}_3$  for 17 h resulted in a color change from yellow to red. Analyses by GCMS ( $m/z = 321$ ) and  $^{19}\text{F}$  NMR spectroscopy (-148.87 ppm and -148.57 ppm) were consistent with formation of isomers of  $(3,5-(\text{CF}_3)_2\text{Ph}(\text{CFPh}))_2$ , formulated as **2b** and **2b'** (**Figure 3.2 c**, bottom).<sup>51</sup> The loss of fluorine in the products, relative the starting material, implies a defluorinated intermediate during the reaction. A plausible pathway to these products involves borane-mediated defluorination from **1a**, followed by 1,1-migratory insertion of the aryl group into the resulting fluorocarbene to form

a Pd-fluorodibenzyl species that undergoes C(sp<sup>3</sup>)-C(sp<sup>3</sup>) coupling (**Figure 3.3**). These products are fluorinated versions of (CHArAr')<sub>2</sub>, which have been reported as sources of carbon radicals following C-C bond homolysis and capable of forming new C-O bonds (e.g. Ph<sub>2</sub>CHOMe from (HCPH<sub>2</sub>)<sub>2</sub> and MeOH).<sup>52</sup> By extension, the formation of **2b/2b'** from **1a** provides an entry point to (CFArAr')<sub>2</sub> products, enabling access to compounds that can potentially be further diversified into medicinally relevant fluorinated ethers.<sup>53</sup>

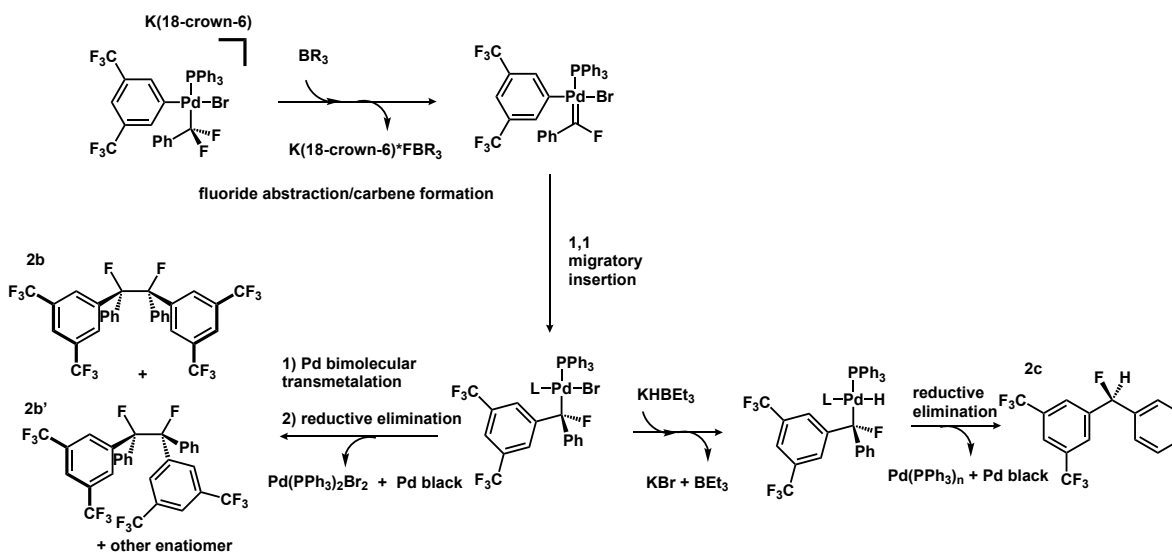


**Figure 3.3** Proposed mechanism for formation of **2b/2b'** and **2c**

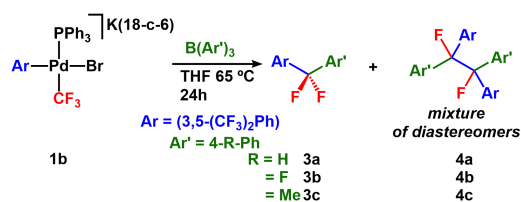
We hypothesized that, in addition to undergoing homocoupling to afford **2b/2b'**, the defluorinated intermediate might be intercepted with another nucleophile, such as H<sup>-</sup>, and undergo a subsequent reductive elimination. In support, we found that after allowing a mixture of **1a**/1 equiv. BPh<sub>3</sub> to react for 15 minutes at 25 °C, addition of 1 equiv. KHBET<sub>3</sub> resulted in a net hydrodefluorination reaction to form ((3,5-(CF<sub>3</sub>)<sub>2</sub>Ph)(Ph)CHF), **2c**, in 48% (37% isolated) yield (**Figure 3.2 c**, right). This reaction represents a simple strategy to access monofluoromethylene arenes, which are pharmaceutical targets<sup>54</sup> and are typically accessed through alternative reagents and/or precursors.<sup>19,20,23,55</sup>

### 3.3 Synthesis and Reactivity of the [Pd]-CF<sub>3</sub> Complex

To evaluate if the borane-induced defluorinative functionalization reaction is general, we prepared the Pd-CF<sub>3</sub> complex, (PPh<sub>3</sub>)(3,5-(CF<sub>3</sub>)<sub>2</sub>Ph)Pd(CF<sub>3</sub>)Br, **1b**, through an analogous route to **1a**. **1b** exhibits a similar solution structure to **1a**, as assessed by heteronuclear NMR spectroscopy. The X-ray crystal structure of **1b** confirmed the structural similarities, with a Pd<sub>1</sub>-C<sub>1</sub> bond distance of 2.068(9) Å in addition to a K<sub>1</sub>-F<sub>1</sub> distance of 2.735(5) Å for the associated K<sup>+</sup> counterion. Given these structural similarities, we hypothesized that **1b** might exhibit analogous reactivity to **1a**.

Upon addition of **1b** to 1 equiv. BPh<sub>3</sub> in THF for 24 h at 65 °C we observed difluorodiarlylmethane (**3a**) and difluorotetraarylethane (**4a**) products (**Table 3.1**). These products are either singly- (**3**) or doubly- (**4**) defluorinated and both contain an additional -Ph group. To assess the origin of the -Ph group, we repeated the experiment above with a 4-substituted triphenyl borane (B(4-R-Ph)<sub>3</sub>) where the Ph groups on B were replaced with 4-F-Ph. Similar to the product observed using BPh<sub>3</sub>, we found 4-F-Ph transfer to form **3b** and **4b**, and we propose that both B(4-R-Ph)<sub>3</sub> reagents (R= H and F) are competent for defluorination and arylation. These results illustrate a tandem sequence for select B(4-R-Ph)<sub>3</sub> reagents that is distinct from reported reactions using B(C<sub>6</sub>F<sub>5</sub>)<sub>3</sub>:<sup>46</sup> instead of F<sup>-</sup> rebound, we propose that the FB(4-R-Ph)<sub>3</sub><sup>-</sup> species generated after F<sup>-</sup> abstraction is competent for transmetalation to palladium.

**Table 3.1** Influence of (B(4-R-Ph)<sub>3</sub>) identity on the formation of **3** and **4** from **1b**. BAr'<sub>3</sub> and **1b** were allowed to react at 65 °C for 24 h. \*Yields determined by <sup>19</sup>F NMR integration with respect to C<sub>6</sub>H<sub>5</sub>F or C<sub>6</sub>H<sub>5</sub>OCF<sub>3</sub> internal standard. Entries 1-3 = 0.008 M, entries 4 and 5 = 0.01 M.





Entry	Conditions	Yield 3	Yield 4	Ratio 4/3
1	R=H	17 ± 4	28 ± 7	1.6
2	R=F	3 ± 2	41 ± 16	12
3	R=Me	12 ± 2	17 ± 2	1.4
4	2 eq. BAr' <sub>3</sub> , R=F	0.5 ± 0.5	47 ± 6	98
5	0.75 eq. BAr' <sub>3</sub> , R=F, 2 eq. PPh <sub>3</sub> ,	35 ± 9	10 ± 3	0.3

In support of this hypothesis, when the electronic environment surrounding the borane was varied, the ratio of **3** to **4** was affected. After 24 hours at 65 °C, we observed differing selectivities of **4** to **3** (B(4-F-Ph)<sub>3</sub> = 12; BPh<sub>3</sub> = 1.6; B(4-Me-Ph)<sub>3</sub> = 1.4). Our rationale for this difference in selectivity is an electronic interplay between fluorophilicity of B(4-R-Ph)<sub>3</sub> and nucleophilicity of the *-Ar* group within FB(4-R-Ph)<sub>3</sub><sup>-</sup>. We hypothesized that the double fluoride abstraction reaction could be favored by increasing the stoichiometry of B(4-R-Ph)<sub>3</sub>. In support, the reaction of **1b** with 2 equiv. of BPh<sub>3</sub> exhibited 98:1 selectivity for **4b** (entry 4; 48 % yield). Conversely, substoichiometric borane (0.75 equiv.) and 2 equiv. PPh<sub>3</sub> *switched* the selectivity for the formation of **3b** 0.3 (entry 5), consistent with favored reductive elimination from the singly defluorinated product. In contrast to these results, when B(C<sub>6</sub>F<sub>5</sub>)<sub>3</sub> was used in place of B(4-R-Ph)<sub>3</sub>, we observed no transfer of -C<sub>6</sub>F<sub>5</sub> after 16 h at 65 °C. Although fluorinated triaryl boron Lewis acids (B(C<sub>6</sub>F<sub>5</sub>)<sub>3</sub>) have been shown to defluorinate M-CF<sub>3</sub> units,<sup>42,45-46</sup> in the current system, the BAr'<sub>3</sub> unit promotes a tandem reactivity sequence not previously reported.

We hypothesized that, although B(C<sub>6</sub>F<sub>5</sub>)<sub>3</sub> would be capable of abstracting a fluoride from **1b** and undergoing subsequent 1,1-migratory insertion, the resulting transmetalation from the fluoroborate (FB(C<sub>6</sub>F<sub>5</sub>)<sub>3</sub><sup>-</sup>) would be difficult compared to B(4-R-Ph)<sub>3</sub>.<sup>56-59</sup> The combined fluoride

affinity and difficult transmetalation of the  $-\text{C}_6\text{F}_5$  group made  $\text{B}(\text{C}_6\text{F}_5)_3$  an ideal reagent to investigate the proposed defluorination/1,1-migratory insertion intermediates (**Figure 3.4**). We targeted the product of 1,1-migratory insertion by stirring **1b** with  $\text{B}(\text{C}_6\text{F}_5)_3$  for 15 min.; however, the resulting complex decomposed during workup, preventing isolation. To arrest decomposition of the proposed coordinatively-unsaturated intermediate, we introduced 1 equivalent of  $\text{PPh}_3$  after 5 min. of stirring **1b** with  $\text{B}(\text{C}_6\text{F}_5)_3$ .  $^{31}\text{P}$  and  $^{19}\text{F}$  NMR spectra exhibited triplet resonances at 30.22 ppm ( $J_{\text{P-F}} = 42.0$  Hz) and -45.36 ppm ( $J_{\text{P-F}} = 42.2$  Hz) respectively, which are consistent with *trans*-phosphines that are *cis*- to a difluoromethyl aryl ( $-\text{CF}_2\text{Ar}$ ) ligand, and the structure *trans*- $[\text{Pd}(\text{PPh}_3)_2(\text{CF}_2\text{Ar})\text{Br}]$  (**1c**). The  $-\text{CF}_2\text{Ar}$  fluorine resonance is downfield of the corresponding resonance in **1a** (-69.08 ppm), and consistent with a *cis*, rather than *trans* orientation of the  $-\text{CF}_2\text{Ar}$  with respect to the phosphine ligand.<sup>49</sup> Similar species  $(\text{PEt}_3)\text{Pd}(\text{II})\text{CF}_3\text{Br}$  and  $(\text{PEt}_3)\text{Pd}(\text{II})(\text{C}_6\text{F}_5)\text{Br}$  are known to be stable at 25 °C.<sup>60</sup>

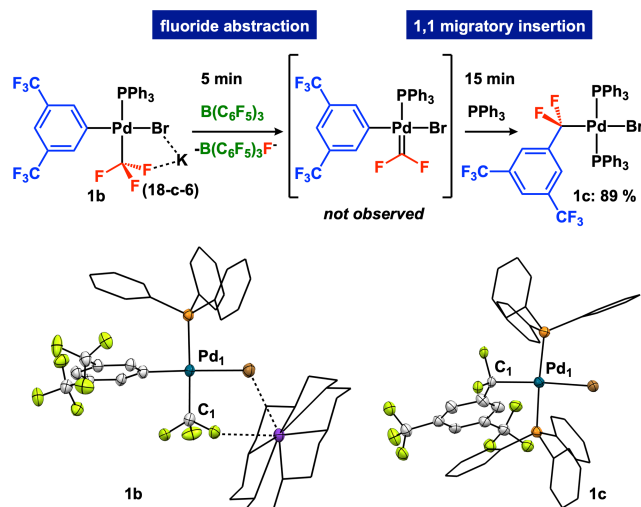


**Figure 3.4** Preparation and X-ray structure of **1c**. Elongation of  $\text{Pd}_1\text{-C}_1$  observed **1b**: 2.068(9) Å vs. **1c**: 2.176(8) Å, ellipsoids shown at 30%, H-atoms removed and non-essential aryl rings wireframed for clarity.

Isolation of **1c** proceeded in 89 % yield and the structure was confirmed by X-ray crystallography. Bond distances in the X-ray crystal structure featured an elongation of the  $\text{Pd}_1\text{-C}_1$

bond when comparing **1c** to **1a** and **1b** (2.176(8) Å, 2.0735(19) Å and 2.068(9) Å respectively). This distinction is reflective of the difference between the charges of the complexes [neutral vs. (-1)]; similar charge-dependent Pd-C bond lengths have been reported for Pd-CF<sub>3</sub> complexes.<sup>49</sup> Importantly, isolation of fluoride abstraction product **1c** supports formation of a palladium difluorocarbene intermediate and 1,1-migratory insertion upon addition of Lewis acids.

Upon learning that the 1,1-migratory insertion reaction is promoted when using an extra equivalent of PPh<sub>3</sub>, we attempted to identify a difluorocarbene intermediate without exogenous ligand at cryogenic temperatures. A stock solution was made by dissolving **1b** (0.0103 mmol, 11.0 mg) and PhOCF<sub>3</sub> (0.040 mmol, 5.3 μL) in THF (900 μL). Another solution was made by dissolving B(C<sub>6</sub>F<sub>5</sub>)<sub>3</sub> (0.0307 mmol, 15.7 mg) in THF (300 μL). These solutions were cooled to -78 °C, mixed to afford 1:1 stoichiometry and transferred to a screwcap NMR tube. The reaction was monitored by multinuclear NMR (<sup>19</sup>F and <sup>31</sup>P) starting at -80 °C and warming by 15 °C increments every 20 minutes. At -20 °C, a new set of peaks (two doublets) appeared at -54 ppm in the <sup>19</sup>F NMR spectrum (**Figure 3.5**). After reaching 10 °C, the instrument was cooled to -20 °C to reevaluate the resolution of the resonance at -54 ppm. Rather than two doublets, multiple species were observed. Finally, 25 °C spectra were acquired. These results are inconsistent with the observation of a Pd=CF<sub>2</sub> intermediate (~200 ppm). Moreover, the corresponding <sup>31</sup>P NMR data revealed a new resonance at 33 ppm at -5 °C (**Figure 3.6**). At 25 °C, this signal resolves into a triplet which is indicative of the splitting from 2 equivalent fluorine atoms from a -CF<sub>2</sub>Ar group rather than 2 chemically distinct fluorine atoms in a difluorocarbene species. Due to the difficulty of experimentally characterizing a difluorocarbene intermediate, we turned to *in silico* studies to learn about the thermodynamic profile of the defluorination/carbene formation reaction.

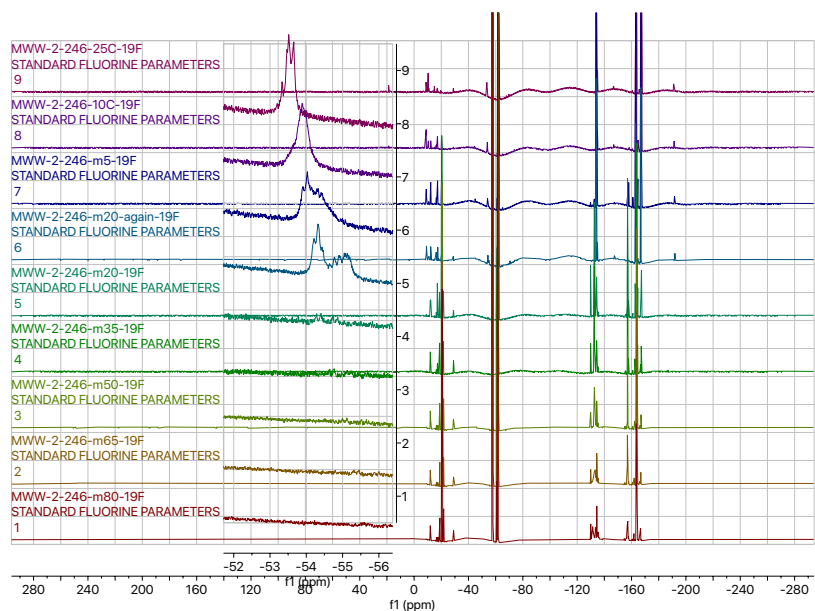
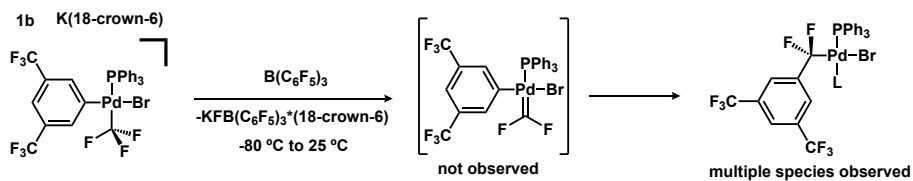


**Figure 3.5**  $^{19}\text{F}$  NMR (500 MHz, THF,  $-80$  to  $25^\circ\text{C}$ ) overlay of fluoride abstraction from **1b** ( $-80^\circ\text{C}$  bottom,  $25^\circ\text{C}$  top)

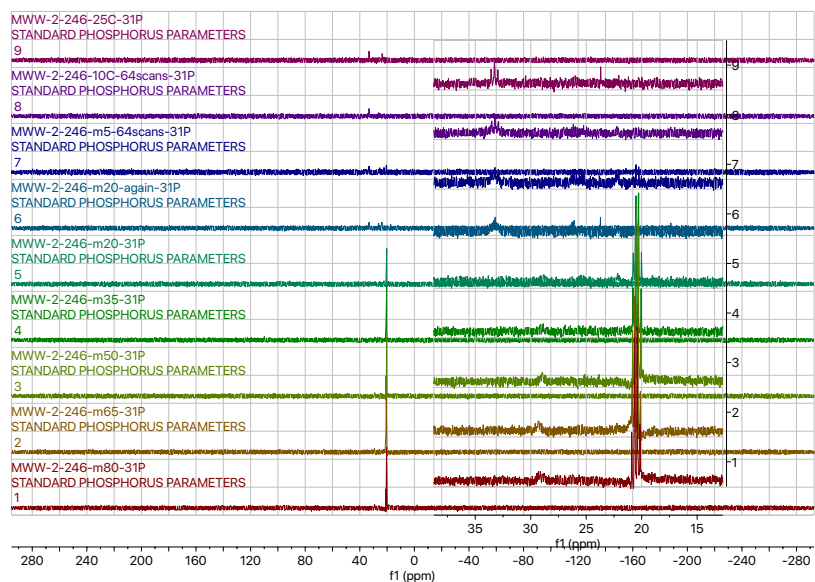


**Figure 3.6**  $^{31}\text{P}$  NMR (500 MHz, THF,  $-80$  to  $25^\circ\text{C}$ ) Overlay of Fluoride Abstraction from **1b** ( $-80^\circ\text{C}$  bottom,  $25^\circ\text{C}$  top)

### 3.4 Computational Analysis of [Pd]=CF<sub>2</sub>

Dr. James Shanahan helped contribute to this subchapter.

To understand relative trends that govern the formation of fluorocarbene intermediates by fluoride abstraction, we employed a computational assessment of borane Lewis acidity *via* Fluoride Ion Affinity (FIA).<sup>61</sup> The FIA analysis, performed at the B3LYP/6-31G(d,p)//6-311++G(d,2p) M(SDD) level of theory, was used to establish the relative fluorophilicity of Lewis acids required to initiate the reaction (**Figure 3.7**). Within a representative set of borane Lewis acids (BF<sub>3</sub>, BAr<sub>3</sub>, ArB(OH)<sub>2</sub>), the FIA spans ~40 kcal/mol, illustrating a substantial change in driving force that is possible by changing the identity of the groups surrounding boron.

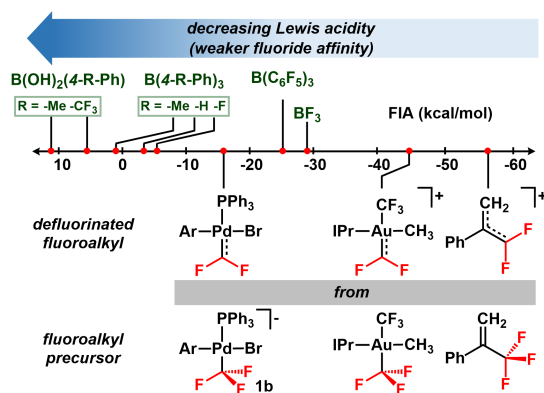


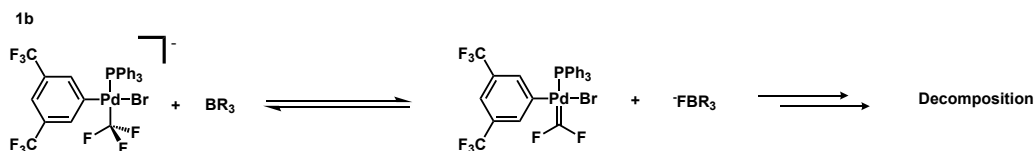
**Figure 3.7** Fluoride ion affinity (FIA) scale for Lewis acids and defluorinated fluoroalkyl products. FIA reported as the  $\Delta G$  of fluoride abstraction from CF<sub>3</sub>O<sup>-</sup> to form CF<sub>2</sub>O (i.e. CF<sub>2</sub>O FIA = 0 kcal/mol).

To provide insight into the relative abilities of Lewis acids to abstract fluoride from either M-CF<sub>2</sub>R moieties, or organofluorine compounds, we calculated FIA for the defluorinated products (i.e. fluorocarbene intermediates) as competitive Lewis acids. Relative to fluoride abstraction from (IPr)(Me)Au(CF<sub>3</sub>)<sub>2</sub> (shown to undergo F<sup>-</sup> abstraction by B(C<sub>6</sub>F<sub>5</sub>)<sub>3</sub> with F<sup>-</sup> rebound),<sup>46</sup> we found that abstraction from Pd-CF<sub>3</sub> (**1b**) was 31 kcal/mol easier. The large FIA energy difference between Au and Pd difluorocarbenes may be a consequence of the relative charges of the formed species (cationic vs neutral, respectively). Importantly, the acidity requirement of organometallic

fluoroalkyl groups is *lower* than organic -CF<sub>3</sub> groups, which typically require potent Lewis acids for fluoride abstraction.<sup>38,62-63</sup> For example, fluoride abstraction from phenyl-trifluoropropene<sup>31</sup> was found to be 41 kcal/mol more difficult than from **1b**, illustrating the intrinsic stabilization provided by using fluoroalkyl metal precursors, rather than metal-free fluoroalkyls. Overall, the mild defluorination requirements from anionic palladium fluoroalkyl complexes are due to a combination of charge effects and metal-stabilization.

### 3.5 Defluorinative Arylation of [Pd]-CF<sub>3</sub>

While BAr<sub>3</sub> compounds are attractive single use reagents that can both abstract F<sup>-</sup> and deliver an -Ar group, their use for these purposes in synthetic methodology is limited.<sup>64-65</sup> In contrast, aryl boronic acids and esters are commercially available and widely used but are only weakly Lewis acidic (*vide supra*).<sup>66</sup> As shown above, the FIAs between select BAr<sub>3</sub> reagents that perform F<sup>-</sup> abstraction are within 5 kcal/mol of the corresponding ArB(OH)<sub>2</sub> reagents. Thus, we hypothesized that ArB(OH)<sub>2</sub> compounds may be sufficiently fluorophilic to promote fluoride abstraction from **1b**. To assess these reactions, **1b** was allowed to react with 1 equiv of a given Lewis acid at room temperature for 1 hour, while monitoring by <sup>19</sup>F NMR spectroscopy (**Table 3.2**). Consumption of the Pd-CF<sub>3</sub> resonance was dependent on the Lewis acidity of the additive: B(C<sub>6</sub>F<sub>5</sub>)<sub>3</sub> and B(4-F-Ph)<sub>3</sub> (100%), B(4-Me-Ph)<sub>3</sub> (28%), (HO)<sub>2</sub>B(4-CF<sub>3</sub>-Ph) (29%), and (HO)<sub>2</sub>B(4-Me-Ph) (6%). However, the time-courses of these reactions indicate decomposition of the initially formed complex during the reaction and the amount of **1b** remaining decreases after 1 and 4 hours. Although fluoride abstraction is achievable using (HO)<sub>2</sub>B(4-Me-Ph), attempts to promote a defluorinative arylation of **1b** with 2 equivalents of (HO)<sub>2</sub>B(4-Me-Ph) afforded (3,5-(CF<sub>3</sub>)<sub>2</sub>Ph)CF<sub>2</sub>(4-Me-Ph) in low yields (21%).

**Table 3.2** Percent of **1b** remaining in the presence of 1 eq. borane

Borane	9 min	17 min	30 min	39 min	1 h	4 h
B(4-F-Ph) <sub>3</sub>	8.8%	6.6%* (20min)	3.0%		0%	0%
B(4-tol) <sub>3</sub>		78.3%	76.6%	74.6%	72%	56%
(HO) <sub>2</sub> B(4-CF <sub>3</sub> Ph)		79.0%	77.1%	73.8%	71%	52%
(HO) <sub>2</sub> B(4-tol)					94%	94%
B(C <sub>6</sub> F <sub>5</sub> ) <sub>3</sub>					0	0

We hypothesized that the two elementary steps (defluorination and –Ar transmetalation) might be separated using a pair of commercially available reagents: (1) a borane that abstracts F<sup>-</sup> but does *not* transmetalate –Ar, and (2) a boronic acid/ester with a nucleophilic activator. B(C<sub>6</sub>F<sub>5</sub>)<sub>3</sub> met the criteria for (1) because complete F<sup>-</sup> abstraction occurs within 5 min, with no incorporation of a –C<sub>6</sub>F<sub>5</sub> group, even after 16 h at 65 °C. We identified reagent-compatibility as the crucial factor needed to develop a defluorinative arylation method using two different boron reagents. To mitigate the deleterious reactions (i.e. formation of [X–B(C<sub>6</sub>F<sub>5</sub>)<sub>3</sub>]<sup>-</sup> or [Ph<sub>3</sub>P–B(C<sub>6</sub>F<sub>5</sub>)<sub>3</sub>]<sup>67</sup>; X=nucleophilic activator of Ar–B(OR)<sub>2</sub>), B(C<sub>6</sub>F<sub>5</sub>)<sub>3</sub> and **1b** were allowed to react in THF for 5 minutes (> 95 % consumption of **1b**) prior to adding other reactants. Subsequent introduction of 1 eq. of (HO)<sub>2</sub>B(4-CF<sub>3</sub>-Ph) followed by the nucleophilic activator and heating to 80 °C for 16h afforded (3,5-(CF<sub>3</sub>)-Ph)CF<sub>2</sub>(4-CF<sub>3</sub>-Ph) as the major product. Using 1 eq. of either [NMe<sub>4</sub>][F] or KO<sup>t</sup>Bu as nucleophilic activators afforded (3,5-(CF<sub>3</sub>)-Ph)CF<sub>2</sub>(4-CF<sub>3</sub>-Ph) in 12% and 41% yield

respectively. However, using 2 equiv of  $[\text{NMe}_4][\text{F}]$  improved yields to 44% while excess  $\text{KO}^t\text{Bu}$  reduced yields. Further optimization included addition of exogenous  $\text{PPh}_3$  and the use of dioxane as a solvent. The optimized protocol was to allow **1b** and  $\text{B}(\text{C}_6\text{F}_5)_3$  to react for 5 min, followed by subsequent addition of 1 eq.  $\text{PPh}_3$ , then  $(\text{HO})_2\text{B}(4\text{-CF}_3\text{-Ph})$  and 2 eq.  $[\text{NMe}_4][\text{F}]$  using dioxane as a solvent with stirring at 80 °C for 16 hours, which improved the yield to 84 %. For certain non-polar boronic acids,  $(3,5\text{-(CF}_3\text{)-Ph})_2\text{CF}_2$  formed as a side product, likely formed by transmetalation between **1b** and **1c**. This method was generalizable to a variety of pinacol boronic esters as well as boronic acids (**Figure 3.8**).

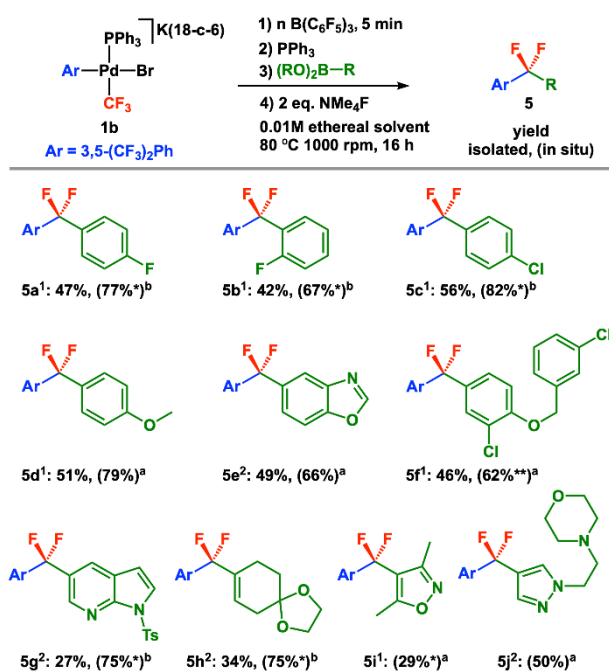


**Figure 3.8** Scope in boronic acid<sup>1</sup>/pinacol ester<sup>2</sup>. **1b** mixed with  $\text{B}(\text{C}_6\text{F}_5)_3$  for 5 min, then 1 eq.  $\text{PPh}_3$  added, followed by 1 eq.  $(\text{RO})_2\text{BR}$  and 2 eq.  $\text{NMe}_4\text{F}$  at 23 °C. Reactions were stirred at 1000 rpm at 80 °C for 16 h. Isolated reported, and (in situ) yields determined by  $^{19}\text{F}$  NMR integration against  $\text{PhOCF}_3$  internal standard. All reactions refer to 0.1 mmol scale unless otherwise noted. <sup>a</sup>: 1 eq.  $\text{B}(\text{C}_6\text{F}_5)_3$ , dioxane solvent. <sup>b</sup>: 1.1 eq.  $\text{B}(\text{C}_6\text{F}_5)_3$ , THF solvent. \*0.005 mmol scale. \*\*94 °C.

The defluorinative arylation method tolerates simple electronic and steric variations of the aryl boronic acid. We obtained similar chemical yields for electron withdrawing (4-Cl-Ph; **5c** = 82%) and electron donating (4-OMe-Ph; **5d** = 79%) boronic acids, indicating minimal electronic



influence. In contrast, *ortho*-substitution afforded a slightly decreased yield; (2-F-Ph; **5b** = 67%), compared to *para* substitution (4-F-Ph; **5a** = 77%).

To examine the broad-scope compatibility of the defluorinative arylation method, we assessed select boronic acids and pinacol boronic esters containing medicinally relevant heterocycles and commonly used protecting groups. Halogenated benzyl phenyl ethers are known to be active inhibitors of bacterial phenylalanyl-tRNA synthetase.<sup>68</sup> Use of a related chloro-substituted benzyl phenyl ether substrate afforded **5f** in good yield 46%, (62% *in situ*). Benzoxazole is a pro-nucleophilic coupling partner in the recent synthesis of a PDE4 inhibitor,<sup>69</sup> where the 2-C–H bond is a prime target for further functionalization to form drug candidates.<sup>69</sup> Thus, methods that allow the incorporation of benzoxazole motifs with retention of the 2-position C–H bond provide an additional entry point for subsequent diversification. Importantly, we found that the defluorinative arylation method is indeed mild enough to tolerate the key C–H bond at the 2-position, forming **5e** in 49% yield (66% *in situ*). Fluorination of this class of molecules represents an attractive route to generating a library of polyfluorinated benzoxazoles.<sup>70</sup> Other 5-membered heterocycles including isoxazole and pyrazole were also tolerated, forming **5i** and **5j** in 29% and 50% chemical yield, respectively. Unfortunately, **5j** decomposed during workup, preventing isolation. Although several heterocycles were tolerated, those containing N–H bonds required protection. Pyrrolo[2,3-*b*]-pyridines are attractive drug candidates since certain examples have been identified as Focal Adhesion Kinase (FAK) inhibitors, and have great potential in oncology.<sup>71</sup> After tosylation of 1-H pyrrolo pyridine, **5g** formed in high chemical yield (75%).

In addition to aryl boronic acids/esters, we found that vinyl boronic esters were also effective coupling partners. Substrate **5h** was formed in 75% chemical yield (34% isolated). This substrate contains an olefin as well as acetal-protected ketone, both of which are functional handles for

further diversification. Overall, the defluorinative arylation of aryl, heteroaryl and vinyl boronic acids and pinacol esters represents an attractive strategy to easily prepare difluoromethyl aryl compounds containing pharmaceutically-relevant moieties.

### 3.6 One-pot Strategy for Defluorinative Arylation of [Pd]-CF<sub>3</sub>

To demonstrate the synthetic utility of the defluorinative arylation methodology, we developed a sequential 4 step, 1-pot procedure to convert aryl and heteroaryl halides directly into diaryl difluoromethane compounds. We evaluated this approach by preparing **5c** in 1-pot. Following oxidative addition of 3,5-bis(trifluoromethyl)-bromobenzene with Pd(PPh<sub>3</sub>)<sub>4</sub> at 80 °C in THF, **1b** was formed after addition of 2 eq. TMSCF<sub>3</sub>, KO<sup>t</sup>Bu and 18-crown-6 in 46% chemical yield. 18-crown-6 is required to form the anionic palladium species analogous to **1b** rather than neutral Pd-CF<sub>3</sub> complexes. Although [K(18-crown-6)][CF<sub>3</sub>-B<sub>3</sub>N<sub>3</sub>Me<sub>6</sub>] was used in the reaction development (affording **1b** in 53% yield and 90% selectivity), we found that TMSCF<sub>3</sub> can also serve as a source of CF<sub>3</sub><sup>-</sup>. TMSCF<sub>3</sub> afforded lower purity **1b** with additional side products (73% selectivity), although these were not deleterious to later steps. Subsequent defluorinative arylation in the same reaction vessel afforded **5c** in 38% chemical yield over all 4 steps (**Figure 3.9**). This result compares well to the yield of the defluorinative arylation reaction from isolated **1b** (**Figure 3.8**) and indicates minimal reduction in yield between using either a 1-pot method (82 % steps 3,4) or a discretely isolated Pd-CF<sub>3</sub> complex (82 %). Note that if (PPh<sub>3</sub>)(3,5-(CF<sub>3</sub>)<sub>2</sub>Ph)Pd(CF<sub>3</sub>)<sub>2</sub><sup>-</sup> is included in the yield calculation for steps 3 and 4, the yield is 60%.

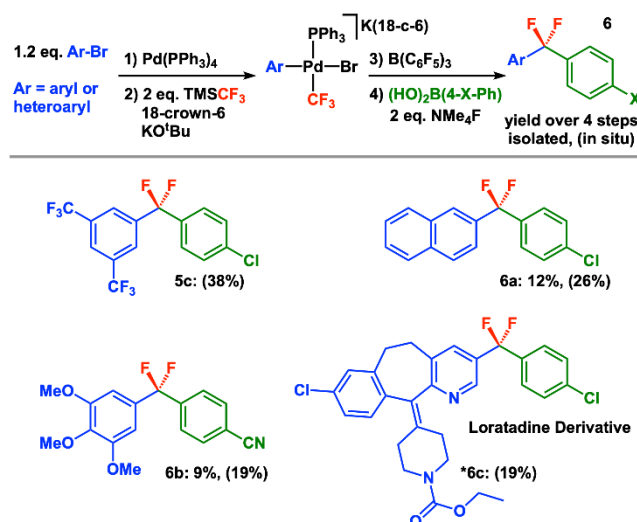


**Figure 3.9** Scope in aryl bromide. 1)  $\text{Pd}(\text{PPh}_3)_4$  was stirred with 1.2 eq. aryl bromide at  $80\text{ }^\circ\text{C}$  for 4 h in THF. 2) 2 eq.  $\text{TMSCF}_3$  added with 18-crown-6 and  $\text{KO}^t\text{Bu}$  and stirred at  $23\text{ }^\circ\text{C}$  for 2-3 h. 3)  $\text{B}(\text{C}_6\text{F}_5)_3$  added at  $23\text{ }^\circ\text{C}$  for 5 min. 4) 1 eq.  $(\text{HO})_2\text{B}(4\text{-X-Ph})$  and 2 eq.  $\text{NMe}_4\text{F}$  added and stirred at 1000 rpm at  $80\text{ }^\circ\text{C}$  for 18 h. Isolated reported, and (in situ) yields determined by  $^{19}\text{F}$  NMR integration against  $\text{PhOCF}_3$  internal standard. All reactions refer to 0.15 mmol scale unless otherwise noted. \*0.004 mmol scale with 2 eq. of  $\text{B}(\text{C}_6\text{F}_5)_3$  used in step 3.

The 1-pot method for defluorinative arylation was applied directly to a series of (hetero)aryl bromides. 2-bromonaphthalene and the electron-rich 1,2,3-trimethoxy-5-bromobenzene were both competent for the reaction sequence, generating **6a** and **6b** in 26% and 19% chemical yield, respectively, across all 4-steps. To facilitate separation for **6b**, 4-cyanophenyl boronic acid was used instead of 4-chlorophenyl boronic acid. Finally, we showcased the compatibility of the defluorinative arylation strategy with pharmaceutically-relevant precursors by preparing **6c**, a difluoromethylarylated derivative of Loratadine in 19% chemical yield over 4-steps.

In contrast to the preparation of  $\text{ArCF}_2\text{Ar}'$  compounds by Pd cross-coupling, which requires either bromodifluoromethyl- or difluoromethyl arenes, entry into these species via a  $-\text{CF}_3$  unit is an attractive alternate route that obviates the requirement for  $\text{ArCF}_2\text{X}$  reagents ( $\text{X}=\text{H}, \text{Br}$ ).<sup>3,24</sup> While useful methods exist for coupling other  $\text{RCF}_2\text{Br}$  electrophiles that include vinyl groups<sup>72</sup> and heterocycles<sup>73</sup> we propose that the defluorinative arylation method may be of particular

interest for high-throughput screening and drug discovery. Stoichiometric coupling reactions at Pd have been recently shown as a strategy to rapidly generate a library of targets for SAR studies.<sup>74</sup>

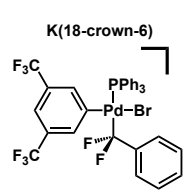
### 3.7 Conclusions

In conclusion, we have harnessed the unique reactivity of the C–F bond within anionic Pd fluoroalkyl complexes to construct molecules with new –CF<sub>2</sub>– linkages. Through analysis of Lewis acidity requirements for the defluorination reaction, we discovered a reaction sequence using mild boron-based Lewis acids that provides access to reactive Pd difluorocarbenes: species that undergo 1,1-migratory insertion into a Pd-aryl bond. The resulting Pd-CF<sub>2</sub>Ar species can be induced to form Ar'-CF<sub>2</sub>-Ar compounds by reacting with either FBAr'<sub>3</sub><sup>-</sup> (formed from defluorination with BAr'<sub>3</sub>) or using widely available Ar'-B(OR)<sub>2</sub> reagents via transmetalation/reductive elimination. This tandem reaction sequence provides access to Ar'-CF<sub>2</sub>Ar, heteroaryl-CF<sub>2</sub>Ar, vinyl-CF<sub>2</sub>Ar products that may exhibit improved pharmacokinetic properties.

### 3.8 Experimental Details

#### 3.8.1 Synthesis of Pd Fluoroalkyl Complexes (1a-1c)

##### Synthesis of 1a: (PPh<sub>3</sub>)<sub>2</sub>(3,5-(CF<sub>3</sub>)<sub>2</sub>Ph)Pd(CF<sub>2</sub>Ph)Br(18-crown-6)K

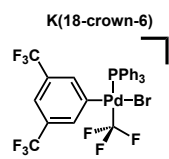
 (PPh<sub>3</sub>)<sub>2</sub>Pd(3,5-(CF<sub>3</sub>)<sub>2</sub>Ph)Br (0.499 mmol, 461 mg) was dissolved in THF 5 mL in a 20 mL scintillation vial charged with a magnetic stir bar. [Me<sub>6</sub>B<sub>3</sub>N<sub>3</sub>CF<sub>2</sub>Ph]K(18-c-6) (0.549 mmol, 327 mg) was added and the reaction was stirred at 23 °C for 22 hours. Additional [Me<sub>6</sub>B<sub>3</sub>N<sub>3</sub>CF<sub>2</sub>Ph]K(18-c-6) (0.245 mmol, 146 mg) was added to ensure reaction completion. Solvent was removed under vacuum and the crude mixture was washed with pentane (3 x 5 mL) to remove free hexamethyl borazine. The crude material was purified by either crystallization (method A) or tritration (method B).

Method A: Dissolution in minimal THF (*ca.* 1-2 mL) followed by layering with pentane afforded crystals after 1 day that were subsequently washed with diethyl ether (3 x 5 mL). Yield: 219.8 mg (40%).

Method B: Trituration of a 5 mL benzene solution with *ca.* 15 mL pentane afforded the product as a tan powder. Yield: 458.7 mg (85%), (98%, purity as assessed by  $^{19}\text{F}$  NMR spectroscopy using  $\text{PhOCF}_3$  internal standard).

$^1\text{H}$ -NMR ( $\text{C}_6\text{D}_6$ ): 3.15 ( $H_a$ , 24H, s), 6.95 ( $H_b$ , 6H, (overlap)), 6.95 ( $H_c$ , 3H, (overlap)), 7.07 ( $H_d$ , 1H, t,  $J_{1\text{H}-1\text{H}}=7.2$  Hz), 7.26 ( $H_e$ , 2H, t (apparent),  $J_{1\text{H}-1\text{H}}=7.6$  Hz), 7.34 ( $H_f$ , 1H, s), 7.48 ( $H_g$ , 2H, d,  $J_{1\text{H}-1\text{H}}=7.4$  Hz), 7.73 ( $H_h$ , 6H, m), 7.81 ( $H_i$ , 2H, s).  $^{19}\text{F}$ -NMR: -69.08 ( $F_a$ , 2F, d,  $J_{19\text{F}-31\text{P}}=39.3$  Hz), -62.16 ( $F_b$ , 6F, s).  $^{31}\text{P}$ -NMR: 18.75 (1P, t,  $J_{19\text{F}-31\text{P}}=39.3$  Hz).

### Synthesis of **1b**: $(\text{PPh}_3)_2(3,5\text{-(CF}_3)_2\text{Ph})\text{Pd}(\text{CF}_3)\text{Br}(\text{18-crown-6})\text{K}\cdot\frac{1}{2}\text{THF}$

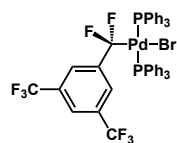
 Two parallel reactions were conducted, each in 300 mL Schlenk tubes.  $(\text{PPh}_3)_2\text{Pd}(3,5\text{-(CF}_3)_2\text{Ph})\text{Br}$  (1.50 mmol, 1.390 g) and (1.50 mmol, 1.382g) were combined, followed by diethyl ether (150 mL) and a magnetic stir bar. The reaction vessels were removed from the glovebox and heated (50 °C) with stirring (1000 rpm) for 30 min to dissolve reagents. The reaction vessels were moved back into an  $\text{N}_2$  glovebox and  $[\text{Me}_6\text{B}_3\text{N}_3\text{CF}_3]\text{K}(\text{18-c-6})$  (1.5 mmol, 2.0 M, 7.5 mL) was added dropwise to each vessel over 20 min with stirring (1000 rpm). The reactions stirred for an additional 100 min., and the combined reactions were filtered on a glass frit. The precipitate was washed with diethyl ether (5x20 mL). The filter cake was dissolved in THF (60 mL) and filtered into a 125 mL Erlenmeyer flask. The flask was placed in a 1 L jar containing pentane (250 mL) and was sealed for vapor diffusion, affording crystals over 2 days. The crystals were collected on a glass frit and washed with diethyl ether (3 x 40mL) and dried

under vacuum to afford **1b** 1.831 g, 57% yield (91%, purity as assessed by  $^{19}\text{F}$  NMR spectroscopy using  $\text{PhOCF}_3$  internal standard).

Note that **1b** obtained using this procedure contains  $\frac{1}{2}$  THF, therefore, the solvate (1070.195 g/mol) was used for calculations in subsequent reactions.

$^1\text{H-NMR}$  ( $\text{C}_6\text{D}_6$ ): 3.13 ( $H_a$ , 24H, s), 6.94 ( $H_b$ , 6H, (overlap)), 6.94 ( $H_c$ , 3H, (overlap)), 7.35 ( $H_d$ , 1H, s), 7.76 ( $H_e$ , 6H, m), 8.17 ( $H_f$ , 2H, s).  $^{19}\text{F-NMR}$ : -62.16 ( $F_b$ , 6F, s), -19.36 ( $F_a$ , 3F, d,  $J_{19\text{F}-31\text{P}}=47.4$  Hz).  $^{31}\text{P-NMR}$ : 21.18 (1P, q,  $J_{19\text{F}-31\text{P}}=47.4$  Hz).

### Synthesis of **1c**: $(\text{PPh}_3)_2\text{Pd}(\text{CF}_2(3,5\text{-(CF}_3)_2\text{Ph)})\text{Br}$

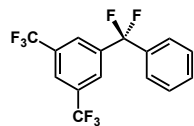


**1b** (0.049 mmol, 52.0 mg) was dissolved in THF (1.5 mL) in a 20 mL scintillation vial charged with a magnetic stir bar.  $\text{B}(\text{C}_6\text{F}_5)_3$  (0.050 mmol, 25.8 mg) dissolved in THF (3 mL) was added to the reaction mixture and stirred for 5 min.  $\text{PPh}_3$  (0.052, 13.7 mg) was then added with THF (1.5 mL) and the mixture was allowed to react for 15 min. Solvent was removed under vacuum and the solid residue was washed with diethyl ether (3 x 5mL), affording **1c** 42 mg, 89% yield.

$^{19}\text{F-NMR}$  (THF): -62.95 ( $F_b$ , 6F, s), -45.36 ( $F_a$ , 2F, d,  $J_{19\text{F}-31\text{P}}=42.2$  Hz).  $^{31}\text{P-NMR}$ : 30.22 (2P, t,  $J_{19\text{F}-31\text{P}}=42.0$  Hz).

### 3.8.2 Organic Molecules Derived from **1a**

#### Syntheses of **2a**: 1-(difluoro(phenyl)methyl)-3,5-bis(trifluoromethyl)benzene



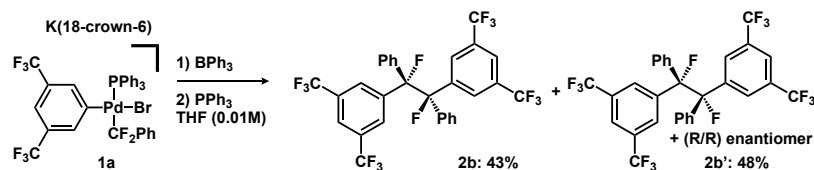
Compound **2a** was obtained by one of two methods:

Method A (thermal reaction): **1a** (0.01 mmol, 10.9 mg) was dissolved in THF (1 mL) along with (0.041 mmol, 3.8  $\mu$ L) of PhF internal standard and added to a screwcap NMR tube. The NMR tube was heated at 50 °C. After 1 h, the in situ yield was 22 %. Continued heating for 45 h afford **2a** in 71% in situ yield.

Method B (bromide abstraction): **1a** (0.097 mmol, 105.6 mg) was dissolved in THF (10 mL) and cooled to 0 °C in a 20 mL scintillation vial using the glovebox cold well. AgSbF<sub>6</sub> (0.099 mmol, 34.1 mg) was added to the reaction mixture as a solid. After the reaction stirred at 0 °C for 1 hour, AgBr was filtered and (0.100 mmol, 13.2  $\mu$ L) of PhOCF<sub>3</sub> internal standard was added. Analysis by <sup>19</sup>F NMR spectroscopy revealed 57 % yield. The reaction mixture was dried onto 500 mg of SiO<sub>2</sub> and eluted on a 100g Biotage column with 100% hexanes at the rate of 6 mL/min, 3-4 column volumes. After an additional column, the sample of **2a** (18.5 mg, 56 % yield) contained 38 % of (3-5(CF<sub>3</sub>)<sub>2</sub>Ph)<sub>2</sub> as an impurity, noted as x in <sup>1</sup>H and <sup>19</sup>F NMR spectra.

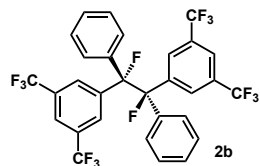
<sup>1</sup>H-NMR (CDCl<sub>3</sub>): 7.49 (*H<sub>a</sub>*, 1H, (overlap)), 7.49 (*H<sub>b</sub>*, 2H, (overlap)), 7.49 (*H<sub>c</sub>*, 2H, (overlap)), 7.97 (*H<sub>d</sub>*, 2H, s), 8.03 (*H<sub>e</sub>*, 1H, s). <sup>19</sup>F-NMR: -89.60 (*F<sub>a</sub>*, 2F, s), -62.99 (*F<sub>b</sub>*, 6F, s).

### Syntheses of **2b** and **2b'**: 1,2-difluoro-1,2-diphenyl-1,2-bis(3,5-bis(trifluoromethyl)phenyl)-ethane

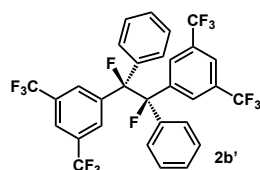


**1a** (0.100 mmol, 109.1 mg) was combined with triphenyl borane (0.100 mmol, 24.3 mg) in 10 mL THF and stirred for 5 minutes at 25 °C. Triphenyl phosphine (0.103 mmol, 27.2 mg) was added, and the reaction mixture stirred for 17 hours at 25 °C. 93% combined in situ yield was obtained (0.100 mmol, 13.2  $\mu$ L PhOCF<sub>3</sub> used as <sup>19</sup>F internal standard). The reaction mixture was dried onto 500 mg of SiO<sub>2</sub> and eluted on a 25g Biotage column with 100% pentane at the rate of 12 mL/min,

4-8 column volumes for **2b** affording 13.7 mg (43% yield) and 8-14 column volumes for **2b'** affording 15.3 mg, 48% yield.



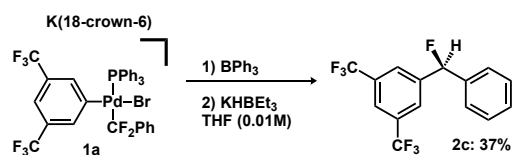
$^1\text{H-NMR}$  ( $\text{CDCl}_3$ ): 7.21 ( $H_a$ , 4H, (d,  $J_{1\text{H}-1\text{H}}=8.5$  Hz)), 7.27 ( $H_b$ , 4H, (overlap)), 7.30 ( $H_c$ , 2H, (overlap)), 7.69 ( $H_d$ , 4H, s), 7.76 ( $H_e$ , 2H, s).  $^{13}\text{C-NMR}$ : 99.23 ( $C_a$ , dd,  $J_{13\text{C}-19\text{F}}=185.5, 29.8$  Hz), 122.27 ( $C_b$ ), 123.11 ( $C_c$ , q,  $J_{13\text{C}-19\text{F}}=273.2$  Hz), 126.92 ( $C_d$ , dd,  $J_{13\text{C}-19\text{F}}=9.3, 3.6$  Hz), 127.67 ( $C_e$ ), 128.43 ( $C_f$ ), 129.20 ( $C_g$ ), 131.17 ( $C_h$ , q,  $J_{13\text{C}-19\text{F}}=33.5$  Hz), 137.30 ( $C_i$ , d,  $J_{13\text{C}-19\text{F}}=22.5$  Hz), 141.90 ( $C_j$ , d,  $J_{13\text{C}-19\text{F}}=23.2$  Hz).  $^{19}\text{F-NMR}$ : -148.87 ( $F_a$ , 2F, s), -63.05 ( $F_b$ , 12F, s). MS +APCI: 321.0510 (M/2), 623.1012 (M-F).



$^1\text{H-NMR}$  ( $\text{CDCl}_3$ ): 7.29 ( $H_a$ , 2H, (overlap)), 7.30 ( $H_b$ , 4H, (overlap)), 7.40 ( $H_c$ , 4H, dd,  $J_{1\text{H}-1\text{H}}=7.2, 1.5$  Hz), 7.50 ( $H_d$ , 4H, s), 7.76 ( $H_e$ , 2H, s).  $^{13}\text{C-NMR}$ : 99.24 ( $C_a$ , dd,  $J_{13\text{C}-19\text{F}}=186.0, 29.4$  Hz), 122.31 ( $C_b$ ), 122.99 ( $C_c$ , q,  $J_{13\text{C}-19\text{F}}=272.6$  Hz), 127.23 ( $C_d$ , (overlap)), 127.25 ( $C_e$ , (overlap)), 128.48 ( $C_f$ ), 129.10 ( $C_g$ , d,  $J_{13\text{C}-19\text{F}}=1.7$  Hz), 131.37 ( $C_h$ , q,  $J_{13\text{C}-19\text{F}}=34.1$  Hz), 137.51 ( $C_i$ , dd,  $J_{13\text{C}-19\text{F}}=21.5, 2.0$  Hz), 141.98 ( $C_j$ , d,  $J_{13\text{C}-19\text{F}}=24.5$  Hz).  $^{19}\text{F-NMR}$ : -148.57 ( $F_a$ , 2F, s), -63.23 ( $F_b$ , 12F, s). MS +APCI: 321.0511 (M/2), 623.1024 (M-F).



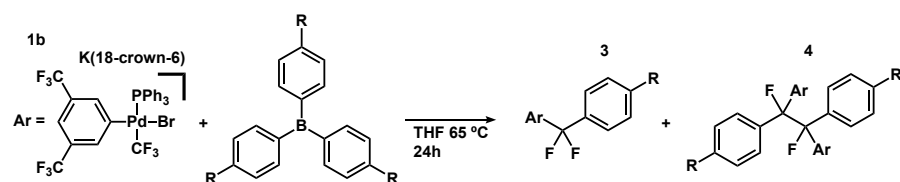
## Synthesis of 2c: 1-(fluoro(phenyl)methyl)-3,5-bis(trifluoromethyl)benzene



**1a** (0.100 mmol, 108.9 mg) was combined with triphenyl borane (0.101 mmol, 24.4 mg) in 10 mL THF and stirred for 15 minutes at 25 °C. Potassium triethyl borohydride (0.100 mmol, 100  $\mu$ L of 1M THF solution) was then added, and the reaction mixture stirred for 17 hours at 25 °C. 48% in situ yield (0.100 mmol, 13.2  $\mu$ L PhOCF<sub>3</sub> was used as <sup>19</sup>F internal standard). The reaction mixture was dried onto 500 mg of SiO<sub>2</sub> and eluted on a 25g Biotage column with 100% pentane at the rate of 12 mL/min, 4-9 column volumes, a second column was required 100% hexanes at the rate of 6 mL/min, 4-6 column volumes for **2c** affording 11.8 mg, 37% yield.

<sup>1</sup>H-NMR (CDCl<sub>3</sub>): 6.55 (*H<sub>a</sub>*, 1H, (d, *J*<sub>1H-19F</sub>=46.8 Hz)), 7.33 (*H<sub>b</sub>*, 2H, (d, *J*<sub>1H-1H</sub>=7.9 Hz)), 7.42 (*H<sub>c</sub>*, 1H, (overlap)), 7.43 (*H<sub>d</sub>*, 2H, (overlap)), 7.80 (*H<sub>e</sub>*, 2H, s), 7.86 (*H<sub>f</sub>*, 1H, s). <sup>13</sup>C-NMR: 93.30 (*C<sub>a</sub>*, d, *J*<sub>13C-19F</sub>=176.4 Hz), 122.45 (*C<sub>b</sub>*), 123.25 (*C<sub>c</sub>*, q, *J*<sub>13C-19F</sub>=272.8 Hz), 126.45 (*C<sub>d</sub>*), 127.00 (*C<sub>e</sub>*, d, *J*<sub>13C-19F</sub>=5.8 Hz), 129.17 (*C<sub>f</sub>*), 129.61 (*C<sub>g</sub>*, d, *J*<sub>13C-19F</sub>=2.5 Hz), 132.13 (*C<sub>h</sub>*, q, *J*<sub>13C-19F</sub>=33.5 Hz), 138.01 (*C<sub>i</sub>*, d, *J*<sub>13C-19F</sub>=20.7 Hz), 142.68 (*C<sub>j</sub>*, d, *J*<sub>13C-19F</sub>=23.6 Hz). <sup>19</sup>F-NMR: -168.36 (*F<sub>a</sub>*, 1F, (d, *J*<sub>1H-19F</sub>=46.8 Hz)), -62.93 (*F<sub>b</sub>*, 6F, s). MS +APCI: 322.0591 (M<sup>+</sup>).

### 3.8.3 Selective Formation of (3a-3c) or (4a-4c) from 1b with *p*-Substituted Triaryl Boranes



A 0.02 M solution was made by dissolving **1b** (0.060 mmol, 64.4 mg) and PhOCF<sub>3</sub> (0.060 mmol, 7.9  $\mu$ L) in THF (3 mL). 0.04 M solutions of BPh<sub>3</sub>, B(4-F-Ph)<sub>3</sub> and B(4-Me-Ph)<sub>3</sub> were made by dissolving (0.040 mmol, 9.8 mg), (0.079 mmol, 23.4 mg) and (0.039, 11.2 mg) of each triaryl borane in THF (1, 2 and 1 mL) respectively. A 0.1 M solution of PPh<sub>3</sub> was made by dissolving (0.10 mmol, 26.1 mg) in THF (1 mL). Amounts of **1b**, B(4-R-Ph)<sub>3</sub> and PPh<sub>3</sub> solutions (listed as A-E below) were added to screw cap NMR tubes and heated at 65 °C for 24 hours and yields were determined by <sup>19</sup>F NMR spectroscopy.

A: **1b** (200  $\mu$ L), BPh<sub>3</sub> (100  $\mu$ L), and THF (200  $\mu$ L)

B: **1b** (200  $\mu$ L), B(4-F-Ph)<sub>3</sub> (100  $\mu$ L), and THF (200  $\mu$ L)

C: **1b** (200  $\mu$ L), B(4-Me-Ph)<sub>3</sub> (100  $\mu$ L), and THF (200  $\mu$ L)

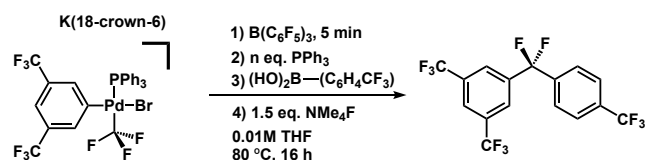
D: **1b** (250  $\mu$ L) and B(4-F-Ph)<sub>3</sub> (250  $\mu$ L)

E: **1b** (250  $\mu$ L), B(4-F-Ph)<sub>3</sub> (94  $\mu$ L), PPh<sub>3</sub> (100  $\mu$ L) and THF (56  $\mu$ L)

**Table 3.3** In situ yields of **3** and **4** across three trials

	Trial 1	Trial 1	Trial 2	Trial 2	Trial 3	Trial 3
Conditions	<b>3</b> yield%	<b>4</b> yield%	<b>3</b> yield%	<b>4</b> yield%	<b>3</b> yield%	<b>4</b> yield%
A: 1 eq. BPh <sub>3</sub>	12.2	19.4	20.3	32.6	18.6	31.6
B: 1 eq. B(4-F-Ph) <sub>3</sub>	1.3	23.1	3.5	53.3	5.6	47.7
C: 1 eq. B(4-Me-Ph) <sub>3</sub>	9.7	15.7	12.9	14.9	12.0	19.1
D: 2 eq. B(4-F-Ph) <sub>3</sub>	0.0	53.9	0.4	43.4	1.0	42.3
E: 0.75 eq. B(4-F-Ph) <sub>3</sub> , 2 eq. PPh <sub>3</sub>	44.7	12.0	28.7	6.7	31.8	9.9

### 3.8.4 Defluorinative Arylation from **1b** Optimization of Equivalents of PPh<sub>3</sub> Added



A 0.2M stock solution of PPh<sub>3</sub> was made by dissolving (0.0503 mmol, 13.2 mg) in THF (250 μL). Aliquots of the PPh<sub>3</sub> solution (0, 25, 50, 75 μL) and THF (75, 50, 25 0 μL) were added to screw cap NMR tubes corresponding to 0-3 eq. of PPh<sub>3</sub>. A stock solution of **1b** was made in a 20 mL scintillation vial by dissolving (0.0691 mmol, 73.9 mg) in THF (3.565 mL) along with PhOCF<sub>3</sub> (0.071 mmol, 9.4 μL) as a <sup>19</sup>F NMR internal standard to make a 0.02M stock solution. An aliquot of the **1b** solution (1.1 mL) was added to a vial containing B(C<sub>6</sub>F<sub>5</sub>)<sub>3</sub> (0.0221 mmol, 11.3 mg). After 5 min 250 μL of the **1b**/ B(C<sub>6</sub>F<sub>5</sub>)<sub>3</sub> solution was added to each of the 4 NMR tubes. A stock solution was made by dissolving 4-(trifluoromethyl)phenyl boronic acid (0.0590 mmol, 11.2 mg) in THF (300 μL) and 25 μL was added to each NMR tube. Finally a slurry was made with NMe<sub>4</sub>F (0.101 mmol, 9.4 mg) in THF (2 mL) and 150 μL was added to each tube. Reactions were heated for 16 hours at 80 °C and yield was assessed by <sup>19</sup>F NMR spectroscopy.

**Table 3.4** Yield dependence on equivalents of PPh<sub>3</sub> added

PPh <sub>3</sub> eq.	0	1	2	3
Yield %	33%	57%	55%	56%

### 3.8.5 Defluorinative Arylation Scope from **1b** (5a-5j)

#### Method A:

In a 20 mL scintillation vial charged with a magnetic stirbar, **1b** (0.1 mmol) was combined with B(C<sub>6</sub>F<sub>5</sub>)<sub>3</sub> (0.1 mmol) in 10 mL dioxane and stirred for 5 minutes at 25 °C. PPh<sub>3</sub> (0.1 mmol) was added, followed by aryl boronic acid/ester (0.1 mmol) and NMe<sub>4</sub>F (0.2 mmol) and the reaction

mixture stirred (1000 rpm) for 16 hours at 80 °C. PhOCF<sub>3</sub> (0.100 mmol, 13.2 μL) was added as a <sup>19</sup>F NMR internal standard.

#### **Method A\*: 0.005 mmol Scale in Dioxane**

Vial 1: An 800 μL aliquot of 0.0125M NMe<sub>4</sub>F solution (0.01 mmol) in MeCN was added to an 8 mL scintillation and the solvent was removed under vacuum, leaving a solid NMe<sub>4</sub>F residue.

Vial 2: In a separate 20 mL vial, a 300 μL aliquot of a solution containing 0.02M **1b** and 0.02M PhOCF<sub>3</sub> was allowed to mix with 60 μL of a 0.01M B(C<sub>6</sub>F<sub>5</sub>)<sub>3</sub> solution for 5 min.. 60 μL of a 0.1M PPh<sub>3</sub> solution was added, followed by 60 μL of the 0.1M boronic acid/ester solution and 120 μL dioxane (total volume = 600 μL).

A 500 μL aliquot (0.005 mmol) from vial 2 was transferred to vial 1, a magnetic stir bar was added and the reaction was stirred at 80 °C for 16 h. Yields were determined by <sup>19</sup>F NMR spectroscopy.

#### **Method B:**

**1b** (0.1 mmol) was combined with B(C<sub>6</sub>F<sub>5</sub>)<sub>3</sub> (0.11 mmol) in 10 mL THF and stirred for 5 minutes at 25 °C. PPh<sub>3</sub> (0.1 mmol) was added, followed by the aryl boronic acid/ester (0.1 mmol) and NMe<sub>4</sub>F (0.2 mmol) and the reaction mixture stirred (1000 rpm) for 16 hours at 80 °C. PhOCF<sub>3</sub> (0.100 mmol, 13.2 μL) was added as a <sup>19</sup>F NMR internal standard.

#### **Method B\*: 0.005 mmol Scale in THF**

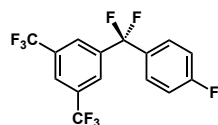
Vial 1: An 800 μL aliquot of 0.0125M NMe<sub>4</sub>F solution (0.01 mmol) in MeCN was added to an 8 mL scintillation and the solvent was removed under vacuum, leaving a solid NMe<sub>4</sub>F residue.

Vial 2: In a separate 20 mL vial, a 300  $\mu\text{L}$  aliquot of a solution containing 0.02M **1b** and 0.02M  $\text{PhOCF}_3$  was allowed to mix with 60  $\mu\text{L}$  of a 0.1M  $\text{B}(\text{C}_6\text{F}_5)_3$  solution for 5 min.. 60  $\mu\text{L}$  of a 0.1M  $\text{PPh}_3$  solution was added, followed by 60  $\mu\text{L}$  of the 0.1M boronic acid/ester solution and (120  $\mu\text{L}$  THF; total volume = 600  $\mu\text{L}$ ).

A 500  $\mu\text{L}$  aliquot (0.005 mmol) from vial 2 was transferred to vial 1, a magnetic stir bar was added and the reaction was stirred at 80  $^\circ\text{C}$  for 16 h. Yields were determined by  $^{19}\text{F}$  NMR spectroscopy.

**Note:** Many of these compounds are volatile and their isolation required attention during rotary evaporation.

#### Synthesis of **5a**: 1-(difluoro(4-fluorophenyl)methyl)-3,5-bis(trifluoromethyl)benzene

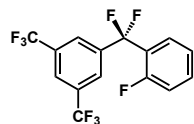


Method B was used with **1b** (0.100 mmol, 107.2 mg),  $\text{B}(\text{C}_6\text{F}_5)_3$  (0.111 mmol, 56.6 mg),  $\text{PPh}_3$  (0.101 mmol, 26.6 mg), 4-fluorophenylboronic acid (0.104 mmol, 14.5 mg),  $\text{NMe}_4\text{F}$  (0.203 mmol, 18.9 mg). With respect to  $\text{PhOCF}_3$  as  $^{19}\text{F}$  internal standard, 69% in situ yield was obtained. The reaction mixture was dried onto 500 mg of  $\text{SiO}_2$  and eluted on a 100g Biotage column with 100% hexanes at the rate of 6 mL/min, 3-5 column volumes, 2 additional columns at the same rate of 6 mL/min were required for **5a** affording 16.8 mg 47% yield.

$^1\text{H-NMR}$  ( $\text{CDCl}_3$ ): 7.16 ( $H_a$ , 2H, (t (apparent),  $J_{1\text{H}-1\text{H}}=8.6$  Hz)), 7.49 ( $H_b$ , 2H, (dd,  $J_{1\text{H}-1\text{H}}=8.9$  Hz,  $J_{1\text{H}-19\text{F}}=5.1$  Hz)), 7.95 ( $H_c$ , 2H, s), 7.98 ( $H_d$ , 1H, s).  $^{13}\text{C-NMR}$ : 116.24 ( $C_a$ , d,  $J_{13\text{C}-19\text{F}}=22.2$  Hz), 119.17 ( $C_b$ , t,  $J_{13\text{C}-19\text{F}}=243.5$  Hz), 122.96 ( $C_c$ , q,  $J_{13\text{C}-19\text{F}}=272.8$  Hz), 124.29 ( $C_d$ ), 126.28 ( $C_e$ ), 128.07 ( $C_f$ , dt,  $J_{13\text{C}-19\text{F}}=8.9, 5.6$  Hz), 132.06 ( $C_g$ , (overlap)), 132.51 ( $C_h$ , q,  $J_{13\text{C}-19\text{F}}=34.0$  Hz),

140.14 ( $C_i$ , t,  $J_{13C-19F}=30.2$  Hz), 164.09 ( $C_j$ , d,  $J_{13C-19F}=251.4$  Hz).  $^{19}F$ -NMR: -109.28 ( $F_a$ , 1F, m), -88.32 ( $F_b$ , 2F, s), -62.93 ( $F_c$ , 6F, s). MS +APCI: 358.0394 (M<sup>+</sup>).

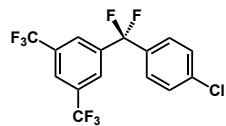
### Synthesis of **5b**: 1-(difluoro(2-fluorophenyl)methyl)-3,5-bis(trifluoromethyl)benzene



Method B was used with **1b** (0.100 mmol, 107.2 mg),  $B(C_6F_5)_3$  (0.110 mmol, 56.5 mg),  $PPh_3$  (0.100 mmol, 26.1 mg), 2-fluorophenylboronic acid (0.101 mmol, 14.2 mg),  $NMe_4F$  (0.196 mmol, 18.3 mg). With respect to  $PhOCF_3$  as  $^{19}F$  internal standard, 62% in situ yield was obtained. The reaction mixture was dried onto 500 mg of  $SiO_2$  and eluted on a 100g Biotage column with 100% hexanes at the rate of 6 mL/min, 3-5 column volumes for isolation of **5b**, 14.9 mg 42% yield.

$^1H$ -NMR ( $CDCl_3$ ): 7.12 ( $H_a$ , 1H, (dd,  $J_{1H-19F}=10.3$  Hz,  $J_{1H-1H}$  8.7 Hz)), 7.30 ( $H_b$ , 1H, (t (apparent),  $J_{1H-1H}=7.7$  Hz)), 7.51 ( $H_c$ , 1H, m), 7.72 ( $H_d$ , 1H, td,  $J_{1H-1H} = 7.7, 1.8$  Hz), 7.96 ( $H_e$ , 1H, s), 7.99 ( $H_f$ , 2H, s).  $^{13}C$ -NMR: 117.04 ( $C_a$ , d,  $J_{13C-19F}=21.1$  Hz), 117.71 ( $C_b$ , t,  $J_{13C-19F}=244.9$  Hz), 123.01 ( $C_c$ , q,  $J_{13C-19F}=272.8$  Hz), 123.69 ( $C_d$ , td,  $J_{13C-19F}=28.4, 11.2$  Hz), 124.23 ( $C_e$ ), 124.62 ( $C_f$ , d,  $J_{13C-19F}=3.7$  Hz), 126.16 ( $C_g$ ), 126.87 ( $C_h$ , td,  $J_{13C-19F}=7.2, 1.7$  Hz), 132.31 ( $C_i$ , q,  $J_{13C-19F}=34.1$  Hz), 133.27 ( $C_j$ , d,  $J_{13C-19F}=8.5$  Hz), 139.82 ( $C_k$ , t,  $J_{13C-19F}=29.3$  Hz), 159.60 ( $C_l$ , d,  $J_{13C-19F}=252.7$  Hz).  $^{19}F$ -NMR: -112.87 ( $F_a$ , 1F, m), -91.01 ( $F_b$ , 2F, d,  $J_{19F-19F}=9.6$  Hz), -63.00 ( $F_c$ , 6F, s). MS EI: 358.0396 (M<sup>+</sup>).

### Synthesis of **5c**: 1-((4-chlorophenyl)difluoromethyl)-3,5-bis(trifluoromethyl)benzene

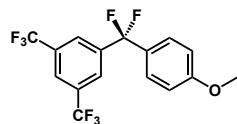


Method B was used with **1b** (0.100 mmol, 106.8 mg),  $B(C_6F_5)_3$  (0.109 mmol, 55.7 mg),  $PPh_3$  (0.100 mmol, 26.1 mg), 4-chlorophenylboronic acid (0.100 mmol, 15.6 mg),

NMe<sub>4</sub>F (0.206 mmol, 19.2 mg). With respect to PhOCF<sub>3</sub> as <sup>19</sup>F internal standard, 67% in situ yield was obtained. The reaction mixture was dried onto 500 mg of SiO<sub>2</sub> and eluted on a 100g Biotage column with 100% hexanes at the rate of 6 mL/min, 2-4 column volumes, 2 additional columns at the same rate of 6 mL/min were required for **5c** affording 20.9 mg 56% yield.

<sup>1</sup>H-NMR (CDCl<sub>3</sub>): 7.44 (*H<sub>a</sub>*, 2H, (overlap)), 7.45 (*H<sub>b</sub>*, 2H, (overlap)), 7.94 (*H<sub>c</sub>*, 2H, s), 7.98 (*H<sub>d</sub>*, 1H, s). <sup>13</sup>C-NMR: 119.11 (*C<sub>a</sub>*, t, *J*<sub>13C-19F</sub>=243.9 Hz), 122.94 (*C<sub>b</sub>*, q, *J*<sub>13C-19F</sub>=273.0 Hz), 124.35 (*C<sub>c</sub>*), 126.24 (*C<sub>d</sub>*), 127.25 (*C<sub>e</sub>*, t, *J*<sub>13C-19F</sub>=5.6 Hz), 129.41 (*C<sub>f</sub>*), 132.56 (*C<sub>g</sub>*, q, *J*<sub>13C-19F</sub>=34.0 Hz), 134.49 (*C<sub>h</sub>*, t, *J*<sub>13C-19F</sub>=28.1 Hz), 137.25 (*C<sub>i</sub>*), 139.95 (*C<sub>j</sub>*, t, *J*<sub>13C-19F</sub>=30.1 Hz). <sup>19</sup>F-NMR: -89.41 (*F<sub>a</sub>*, 2F, s), -63.01 (*F<sub>b</sub>*, 6F, s). MS EI: 374.0115 (M<sup>+</sup>).

#### Synthesis of **5d**: 1-(difluoro(4-methoxyphenyl)methyl)-3,5-bis(trifluoromethyl)benzene

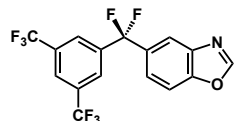


Method A was used with **1b** (0.100 mmol, 107.3 mg), B(C<sub>6</sub>F<sub>5</sub>)<sub>3</sub> (0.100 mmol, 51.3 mg), PPh<sub>3</sub> (0.101 mmol, 26.4 mg), 4-methoxyphenylboronic acid (0.101 mmol, 15.4 mg), NMe<sub>4</sub>F (0.201 mmol, 18.7 mg). With respect to PhOCF<sub>3</sub> as <sup>19</sup>F internal standard, 79% in situ yield was obtained. Dioxane was removed by diluting the reaction mixture in diethyl ether and washing 5 x 20mL of water. After residual water was removed with sodium sulfate, the reaction mixture was dissolved in 2 mL DCM and eluted on a 25g Biotage column with 0% to 10% diethyl ether in pentane at the rate of 20 mL/min, 4-10 column volumes for isolation of **5d** 18.9 mg 51% yield.

<sup>1</sup>H-NMR (CDCl<sub>3</sub>): 3.85 (*H<sub>a</sub>*, 3H, s), 6.96 (*H<sub>b</sub>*, 2H, (d, *J*<sub>1H-1H</sub>=8.9 Hz)), 7.40 (*H<sub>c</sub>*, 2H, (d, *J*<sub>1H-1H</sub>=8.9 Hz)), 7.96 (*H<sub>d</sub>*, 2H, (overlap)), 7.96 (*H<sub>e</sub>*, 1H, (overlap)). <sup>13</sup>C-NMR: 55.56 (*C<sub>a</sub>*), 114.31 (*C<sub>b</sub>*), 119.68

( $C_c$ , t,  $J_{13C-19F}=242.8$  Hz), 123.04 ( $C_d$ , q,  $J_{13C-19F}=273.2$  Hz), 124.00 ( $C_e$ , m), 126.38 ( $C_f$ , m), 127.41 ( $C_g$ , t,  $J_{13C-19F}=5.4$  Hz), 128.15 ( $C_h$ , t,  $J_{13C-19F}=28.3$  Hz), 132.30 ( $C_i$ , q,  $J_{13C-19F}=34.1$  Hz), 140.69 ( $C_j$ , t,  $J_{13C-19F}=30.5$  Hz), 161.41 ( $C_k$ ).  $^{19}F$ -NMR: -87.59 ( $F_a$ , 2F, s), -62.97 ( $F_b$ , 6F, s). MS EI: 370.0595 (M+).

### Synthesis of **5e**: 5-((3,5-bis(trifluoromethyl)phenyl)difluoromethyl)benzo[d]oxazole

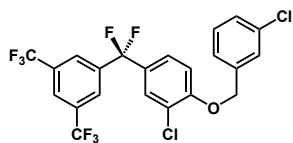


Method A was used with **1b** (0.100 mmol, 107.0 mg),  $B(C_6F_5)_3$  (0.100 mmol, 51.1 mg),  $PPh_3$  (0.101 mmol, 26.6 mg), benzooxazole-5-boronic acid pinacol ester (0.102 mmol, 24.9 mg),  $NMe_4F$  (0.204 mmol, 19.0 mg). With respect to  $PhOCF_3$  as  $^{19}F$  internal standard, 66% in situ yield obtained. Dioxane was removed by diluting the reaction mixture in diethyl ether and washing 5 x 20mL of water. After residual water was removed with sodium sulfate, the reaction mixture was dissolved with 2 mL pentane/diethyl ether (1:1) and eluted on a 25g Biotage column with 0% to 20% diethyl ether in pentane at the rate of 20 mL/min, 24-27 column volumes for isolation of **5e** 18.5 mg 49% yield.

$^1H$ -NMR ( $CDCl_3$ ): 7.56 ( $H_a$ , 1H, (dd,  $J_{1H-1H}=8.6, 2.0$  Hz)), 7.69 ( $H_b$ , 1H, (d,  $J_{1H-1H}=8.6$  Hz)), 7.94 ( $H_c$ , 1H, (broad)), 7.98 ( $H_d$ , 2H, (overlap)), 7.98 ( $H_e$ , 1H, (overlap)), 8.19 ( $H_f$ , 1H, s).  $^{13}C$ -NMR: 111.89 ( $C_a$ ), 118.85 ( $C_b$ , t,  $J_{13C-19F}=6.1$  Hz), 119.44 ( $C_c$ , t,  $J_{13C-19F}=244.2$  Hz), 122.95 ( $C_d$ , q,  $J_{13C-19F}=273.2$  Hz), 123.58 ( $C_e$ , t,  $J_{13C-19F}=5.4$  Hz), 124.30 ( $C_f$ , m), 126.35 ( $C_g$ , m), 132.53 ( $C_h$ , q,  $J_{13C-19F}=34.1$  Hz), 133.08 ( $C_i$ , t,  $J_{13C-19F}=27.9$  Hz), 140.26 ( $C_j$ , t,  $J_{13C-19F}=30.2$  Hz), 140.54 ( $C_k$ ), 151.23 ( $C_l$ ), 154.10 ( $C_m$ ).  $^{19}F$ -NMR: -87.56 ( $F_a$ , 2F, s), -62.98 ( $F_b$ , 6F, s). MS +APCI: 382.0461 (M+).



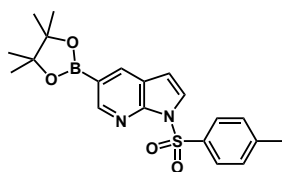
**Synthesis of 5f: 4-((3,5-bis(trifluoromethyl)phenyl)difluoromethyl)-2-chloro-1-((3-chlorobenzyl)oxy)benzene**



Method A was used with **1b** (0.100 mmol, 107.2 mg),  $B(C_6F_5)_3$  (0.100 mmol, 51.3 mg),  $PPh_3$  (0.100 mmol, 26.1 mg), 3-Chloro-4-(3'-chlorobenzyl)oxyphenylboronic acid (0.101 mmol, 29.9 mg),  $NMe_4F$  (0.204 mmol, 19.0 mg). Dioxane was removed by diluting the reaction mixture in diethyl ether and washing 5 x 20mL of water. After residual water was removed with sodium sulfate, the reaction mixture was dried onto 500 mg of  $SiO_2$  and eluted on a 25g Biotage column with hexane at the rate of 12 mL/min, 10-25 column volumes, after a second 100g Biotage column, the product coeluted with  $PPh_3$  so preparatory TLC was run 10% ethyl acetate in hexanes for isolation of **5f** 23.9 mg 46% yield.

$^1H$ -NMR ( $CDCl_3$ ): 5.17 ( $H_a$ , 2H, s), 6.99 ( $H_b$ , 1H, (d,  $J_{1H-1H}=8.6$  Hz)), 7.29 ( $H_c$ , 1H, (dd,  $J_{1H-1H}=8.7$ , 2.3 Hz)), 7.33 ( $H_d$ , 2H, (overlap)), 7.33 ( $H_e$ , 1H, (overlap)), 7.34 ( $H_f$ , 1H, (overlap)), 7.46 ( $H_g$ , 1H, s), 7.55 ( $H_h$ , 1H, (d,  $J_{1H-1H}=2.3$  Hz)), 7.95 ( $H_i$ , 2H, s), 7.98 ( $H_j$ , 1H, s).  $^{13}C$ -NMR: 70.24 ( $C_a$ ), 113.63 ( $C_b$ ), 118.87 ( $C_c$ , t,  $J_{13C-19F}=243.9$  Hz), 122.95 ( $C_d$ , q,  $J_{13C-19F}=273.2$  Hz), 124.12 ( $C_e$ ), 124.33 ( $C_f$ , m), 125.15 ( $C_g$ ), 125.58 ( $C_h$ , t,  $J_{13C-19F}=5.6$  Hz), 126.27 ( $C_i$ , m), 127.22 ( $C_j$ ), 128.14 ( $C_k$ , t,  $J_{13C-19F}=5.5$  Hz), 128.62 ( $C_l$ ), 129.59 ( $C_m$ , t,  $J_{13C-19F}=28.8$  Hz), 130.20 ( $C_n$ ), 132.50 ( $C_o$ , q,  $J_{13C-19F}=33.9$  Hz), 134.86 ( $C_p$ ), 137.92 ( $C_q$ ), 139.96 ( $C_r$ , t,  $J_{13C-19F}=30.1$  Hz), 155.78 ( $C_s$ ).  $^{19}F$ -NMR: -88.16 ( $F_a$ , 2F, s), -62.95 ( $F_b$ , 6F, s). MS EI: 514.0124 ( $M^+$ ).

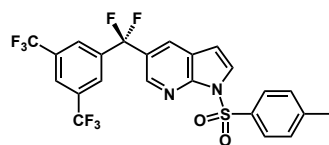
**Synthesis of 5-(4,4,5,5-tetramethyl-1,3,2-dioxaborolan-2-yl)-1-tosyl-1*H*-pyrrolo[2,3-*b*]pyridine**



7-Azaindole-5-boronic acid pinacol ester (1.00 mmol, 244.6 mg) was dissolved in 5 mL of THF in a 20 mL vial with a magnetic stir bar and the solution was stirred at 750 rpm. The reaction solution as well as a vial containing sodium hydride (1.02, 24.4 mg) and a vial containing tosyl chloride (1.01 mmol, 192 mg) and 5 mL of THF were cooled to 0°C. These components chilled for 30 minutes. NaH was rinsed into the reaction vial with 1.6mL of THF. Reaction was allowed to stir at room temp for 15 minutes and the solution went from cloudy to yellow and transparent. The solution was cooled again for 10 minutes and TsCl was washed in with 2 x 1.7mL of THF. As the solution warmed to room temperature after 15 minutes a new precipitate formed indicating metathesis of NaCl. After 24 hours, 70% conversion by <sup>1</sup>H NMR was observed. The crude mixture was loaded onto a 50g column using 2mL of DCM which was eluted with a 5-40% gradient 100ml/min over 6-9 column volumes affording 190.6 mg of product, 48% yield.

<sup>1</sup>H-NMR (CDCl<sub>3</sub>): 1.34 (*H<sub>a</sub>*, 12H, s), 2.35 (*H<sub>b</sub>*, 3H, s), 6.57 (*H<sub>c</sub>*, 1H, d, *J*<sub>1H-1H</sub>=4.0 Hz), 7.24 (*H<sub>d</sub>*, 2H, d, *J*<sub>1H-1H</sub>=8.4 Hz), 7.70 (*H<sub>e</sub>*, 1H, d, *J*<sub>1H-1H</sub>=4.0 Hz), 8.07 (*H<sub>f</sub>*, 2H, d, *J*<sub>1H-1H</sub>=8.4 Hz), 8.24 (*H<sub>g</sub>*, 1H, d, *J*<sub>1H-1H</sub>=1.6 Hz), 8.77 (*H<sub>h</sub>*, 1H, d, *J*<sub>1H-1H</sub>=1.6 Hz). <sup>13</sup>C-NMR: 21.77 (*C<sub>a</sub>*), 25.00 (*C<sub>b</sub>*), 84.24 (*C<sub>c</sub>*), 105.57 (*C<sub>d</sub>*), 122.40 (*C<sub>e</sub>*), 126.46 (*C<sub>f</sub>*), 128.26 (*C<sub>g</sub>*), 129.70 (*C<sub>h</sub>*), 135.54 (*C<sub>i</sub>*), 136.45 (*C<sub>j</sub>*), 145.27 (*C<sub>k</sub>*), 148.96 (*C<sub>l</sub>*), 151.14 (*C<sub>m</sub>*). MS ESI: 399.1543 (M+H)<sup>+</sup>.

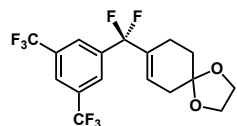
**Synthesis of 5g: 5-((3,5-bis(trifluoromethyl)phenyl)difluoromethyl)-1-tosyl-1*H*-pyrrolo[2,3-*b*]pyridine**



Method B was used with **1b** (0.100 mmol, 106.8 mg),  $B(C_6F_5)_3$  (0.110 mmol, 56.5 mg),  $PPh_3$  (0.101 mmol, 26.4 mg), 5-(4,4,5,5-tetramethyl-1,3,2-dioxaborolan-2-yl)-1-tosyl-1*H*-pyrrolo[2,3-*b*]pyridine (0.100 mmol, 39.9 mg),  $NMe_4F$  (0.204 mmol, 19.0 mg). With respect to  $PhOCF_3$  as  $^{19}F$  internal standard, 21% in situ yield was obtained. The reaction mixture was dissolved in 2 mL of DCM and eluted on a 25g Biotage column with 2 to 20% ethyl acetate in hexane at the rate of 25 mL/min, 5-8 column volumes for **5g** affording 14.3 mg 27% yield. \*\*A 16% impurity containing the tosylated pyrrolo[2,3-*b*]pyridine persists in this sample. Further purification was not possible due to COVID-19 shutdown of nonessential work.

$^1H$ -NMR ( $CDCl_3$ ): 2.39 ( $H_a$ , 3H, s), 6.66 ( $H_b$ , 1H, d,  $J_{1H-1H}=4.1$  Hz), 7.30 ( $H_c$ , 2H, d,  $J_{1H-1H}=8.1$  Hz), 7.85 ( $H_d$ , 1H, d,  $J_{1H-1H}=4.0$  Hz), 7.96 ( $H_e$ , 2H, s), 7.99 ( $H_f$ , 1H, s), 8.00 ( $H_g$ , 1H, d,  $J_{1H-1H}=2.2$  Hz), 8.09 ( $H_h$ , 2H, d,  $J_{1H-1H}=8.4$  Hz), 8.49 ( $H_i$ , 1H, d,  $J_{1H-1H}=2.3$  Hz).  $^{13}C$ -NMR: 21.83 ( $C_a$ ), 105.23 ( $C_b$ ), 124.48 ( $C_c$ , m), 126.22 ( $C_d$ , m), 127.30 ( $C_e$ , t,  $J_{13C-19F}=5.4$  Hz), 127.43 ( $C_f$ ), 128.42 ( $C_g$ ), 128.53 ( $C_h$ ), 129.95 ( $C_i$ ), 132.65 ( $C_j$ , q,  $J_{13C-19F}=34.1$  Hz), 135.10 ( $C_k$ ), 139.74 ( $C_l$ , t,  $J_{13C-19F}=29.8$  Hz), 142.54 ( $C_m$ , t,  $J_{13C-19F}=5.7$  Hz), 145.86 ( $C_n$ ), 147.87 ( $C_o$ ).  $^{19}F$ -NMR: -87.86 ( $F_a$ , 2F, s), -62.97 ( $F_b$ , 6F, s). MS ESI: 535.0729 (M+H) $^+$ .

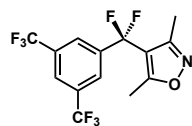
**Synthesis of 5h: 8-((3,5-bis(trifluoromethyl)phenyl)difluoromethyl)-1,4-dioxaspiro[4.5]dec-7-ene**



Method B was used with **1b** (0.100 mmol, 106.7 mg),  $B(C_6F_5)_3$  (0.110 mmol, 56.3 mg),  $PPh_3$  (0.101 mmol, 26.4 mg), 1,4-Dioxaspiro[4,5]dec-7-en-8-boronic acid, pinacol ester (0.100 mmol, 26.7 mg),  $NMe_4F$  (0.198 mmol, 18.4 mg). With respect to  $PhOCF_3$  as  $^{19}F$  internal standard, 57% in situ yield was obtained. The reaction mixture was dried onto 500 mg of  $SiO_2$  and eluted on a 25g Biotage column starting with 100% hexanes, increasing to 10% and eventually 100% ethyl at the rate of 25 mL/min, 22-24 column volumes, 2 additional columns at the same rate of 25 mL/min starting at 10% and 5% ethyl acetate were required for **5h** affording 13.7 mg 34% yield.

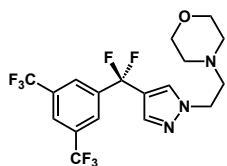
$^1H$ -NMR ( $CDCl_3$ ): 1.81 ( $H_a$ , 2H, t,  $J_{1H-1H}=6.6$  Hz), 2.34 ( $H_b$ , 2H, (overlap)), 2.37 ( $H_c$ , 2H, (overlap)), 3.98 ( $H_d$ , 4H, d (apparent),  $J_{1H-1H}=2.4$  Hz), 5.82 ( $H_e$ , 1H, m), 7.95 ( $H_f$ , 2H, (overlap)), 7.96 ( $H_g$ , 1H, (overlap)).  $^{13}C$ -NMR: 22.46 ( $C_a$ ), 30.61 ( $C_b$ ), 35.52 ( $C_c$ ), 64.71 ( $C_d$ ), 107.13 ( $C_e$ ), 119.75 ( $C_f$ , t,  $J_{13C-19F}=241.1$  Hz), 123.08 ( $C_g$ , q,  $J_{13C-19F}=272.8$  Hz), 124.05 ( $C_h$ , m), 126.53 ( $C_i$ , m), 127.78 ( $C_j$ , t,  $J_{13C-19F}=7.9$  Hz), 132.19 ( $C_k$ , q,  $J_{13C-19F}=34.1$  Hz), 133.35 ( $C_l$ , t,  $J_{13C-19F}=26.4$  Hz), 139.01 ( $C_m$ , t,  $J_{13C-19F}=29.6$  Hz).  $^{19}F$ -NMR: -95.53 ( $F_a$ , 2F, s), -62.94 ( $F_b$ , 6F, s).

**Synthesis of 5i: 4-((3,5-bis(trifluoromethyl)phenyl)difluoromethyl)-3,5-dimethylisoxazole**



Method A\* used with 3,5-dimethylisoxazole-4-boronic acid, 29% in situ yield obtained.

### Synthesis of 5j: 4-(2-(4-((3,5-bis(trifluoromethyl)phenyl)difluoromethyl)-1H-pyrazol-1-yl)-ethyl)morpholine



Method A used with 1-(2-Morpholinoethyl)-1H-pyrazole-4-boronic acid, pinacol ester, 50% in situ yield obtained.

#### 3.8.6 One-pot Defluorinative Arylation Scope in Aryl/Heteroaryl Bromide (6a-6c)

##### Method C:

$\text{Pd}(\text{PPh}_3)_4$  (0.15 mmol) was combined with aryl bromide (0.18 mmol) in 7.5 mL THF and stirred at 1000 rpm for 4 hours at 80 °C in a 20 mL vial with a Teflon cap and a magnetic stir bar.  $\text{TMSCF}_3$  (0.3 mmol) was added followed by 18-crown-6 (0.15 mmol) and  $\text{KO}^t\text{Bu}$  (0.15 mmol) along with 3 mL of THF.  $\text{PhOCF}_3$  (0.150 mmol, 19.8  $\mu\text{L}$ ) was added as a  $^{19}\text{F}$  NMR internal standard and the reaction was stirred for 3 hours at 23 °C. If possible NMR spectroscopy was acquired to find the yield of oxidative addition/trifluoromethylation steps.  $\text{B}(\text{C}_6\text{F}_5)_3$  (0.15 mmol or 0.3 mmol) was added along with 1.5 mL of THF and the reaction was allowed to stir for 5 min.. Aryl boronic acid (0.15 mmol) and  $\text{NMe}_4\text{F}$  (0.3 mmol) were added along with 3 mL THF and the reaction mixture stirred (1000 rpm) for 18 hours at 80 °C.

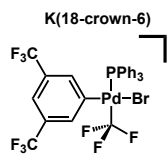
##### Method C\* 0.004 mmol Scale:

Vial 1: An 800  $\mu\text{L}$  aliquot of 0.01M  $\text{NMe}_4\text{F}$  solution (0.008 mmol) in MeCN was added to an 8 mL scintillation and the solvent was removed under vacuum, leaving a solid  $\text{NMe}_4\text{F}$  residue.

Vial 2: In a separate 8 mL vial, a 500  $\mu\text{L}$  aliquot of a solution containing 0.02M  $\text{Pd}(\text{PPh}_3)_4$  and 0.02M  $\text{PhOCF}_3$  in THF was allowed to mix with aryl bromide (0.012 mmol) solution for 4 hours at 80  $^\circ\text{C}$ . 100  $\mu\text{L}$  of a 0.2M  $\text{TMSCF}_3$  solution was added followed by 50  $\mu\text{L}$  of 0.2M 18-crown-6 and 50  $\mu\text{L}$  of 0.2M  $\text{KO}^t\text{Bu}$  solution and the reaction stirred for 3 hours at 23  $^\circ\text{C}$ . A 350  $\mu\text{L}$  aliquot of the reaction was dedicated to  $^{19}\text{F}$  NMR spectroscopy to find the yield of oxidative addition/trifluoromethylation steps. Between 50-100  $\mu\text{L}$  0.1M  $\text{B}(\text{C}_6\text{F}_5)_3$  was added, followed by 50  $\mu\text{L}$  of the 0.1M boronic acid/ester solution and (0-50  $\mu\text{L}$  THF; total volume = 500  $\mu\text{L}$ ).

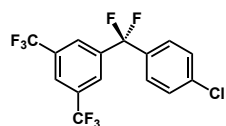
A 400  $\mu\text{L}$  aliquot (0.004 mmol) from vial 2 was transferred to vial 1, a magnetic stir bar was added and the reaction was stirred at 80  $^\circ\text{C}$  for 18 h. Yields were determined by  $^{19}\text{F}$  NMR spectroscopy.

**Formation of **1b** From  $\text{Pd}(\text{PPh}_3)_4$ , 1,3-bis(trifluoromethyl)-5-bromobenzene and  $[(\text{B}_3\text{N}_3\text{Me}_6)\text{CF}_3][\text{K}(18\text{-crown-6})]$**



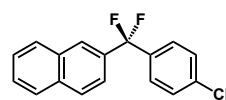
$\text{Pd}(\text{PPh}_3)_4$  (0.100 mmol, 115.7 mg) was stirred with 1,3-bis(trifluoromethyl)-5-bromobenzene (0.12 mmol, 21  $\mu\text{L}$ ) in THF (5 mL) for 4 hours at 80  $^\circ\text{C}$ . An aliquot of this stock solution (0.01 mmol, 0.5 mL) was added to an 8 mL scintillation vial along with  $\text{PhOCF}_3$  internal standard (0.040 mmol, 5.3  $\mu\text{L}$ ) and THF (150  $\mu\text{L}$ ). An aliquot of a 0.2 M solution of  $[(\text{B}_3\text{N}_3\text{Me}_6)\text{CF}_3][\text{K}(18\text{-crown-6})]$  (0.01 mmol, 50  $\mu\text{L}$ ) was added, and the reaction stirred for 3 hours at 23  $^\circ\text{C}$ . With respect to  $\text{PhOCF}_3$  as internal standard, 53% **1b** was observed with 6% formation of  $\text{Ar}(\text{PPh}_3)\text{Pd}(\text{CF}_3)_2$  as a side product.

### Synthesis of **5c** Using the One-pot Method C: 1-((4-chlorophenyl)difluoromethyl)-3,5-bis(trifluoromethyl)benzene



Method C was used with Pd(PPh<sub>3</sub>)<sub>4</sub> (0.150 mmol, 173.5 mg), 1,3-bis(trifluoromethyl)-5-bromobenzene (0.18 mmol, 31 μL), TMSCF<sub>3</sub> (0.30 mmol, 44 μL), 18-crown-6 (0.151 mmol, 40.0 mg) and KO<sup>t</sup>Bu (0.150 mmol, 16.8 mg). With respect to PhOCF<sub>3</sub> as internal standard, 46% in situ formation of **1b** was observed with 17% formation of Ar(PPh<sub>3</sub>)Pd(CF<sub>3</sub>)<sub>2</sub> as a side product. B(C<sub>6</sub>F<sub>5</sub>)<sub>3</sub> (0.151 mmol, 77.2 mg), 4-chlorophenylboronic acid (0.152 mmol, 23.7 mg), NMe<sub>4</sub>F (0.307 mmol, 28.6 mg) were used for the defluorination and arylation steps and 38% overall in situ yield was obtained.

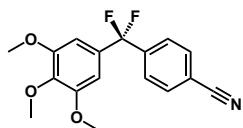
### Synthesis of **6a**: 2-((4-chlorophenyl)difluoromethyl)naphthalene



Method C was used with Pd(PPh<sub>3</sub>)<sub>4</sub> (0.150 mmol, 173.0 mg), 2-bromonaphthalene (0.182 mmol, 37.7 mg), TMSCF<sub>3</sub> (0.30 mmol, 1.5 mL of 0.2 M stock solution), 18-crown-6 (0.15 mmol, 0.75 mL of 0.2 M stock solution), KO<sup>t</sup>Bu (0.15 mmol, 0.75 mL of 0.2 M stock solution), B(C<sub>6</sub>F<sub>5</sub>)<sub>3</sub> (0.15 mmol, 1.5 mL of 0.1M stock solution), 4-chlorophenylboronic acid (0.15 mmol, 3 mL of 0.05M stock solution), NMe<sub>4</sub>F (0.305 mmol, 28.4 mg). With respect to PhOCF<sub>3</sub> as internal standard 26% overall in situ yield was obtained. The reaction mixture was dried onto 750 mg of SiO<sub>2</sub> and eluted on a 25g Biotage column with 100% hexanes at the rate of 75 mL/min, 5-10 column volumes, 3 additional columns at the rate of 12 mL/min (2x100g, 1x25g) were required for **6a** affording 9.1 mg. Due to the large amount of higher order hexanes (H-grease) accumulated in the sample, 12% true yield was found by comparison to mesitylene (8.34 μL) as a <sup>1</sup>H NMR internal standard.

$^1\text{H-NMR}$  ( $\text{CDCl}_3$ ): 7.40 ( $H_a$ , 2H, d,  $J_{1\text{H}-1\text{H}}=8.4$  Hz), 7.49 ( $H_b$ , 2H, d,  $J_{1\text{H}-1\text{H}}=8.4$  Hz), 7.52 ( $H_c$ , 1H, (overlap)), 7.55 ( $H_d$ , 1H, (overlap)), 7.56 ( $H_e$ , 1H, (overlap)), 7.86 ( $H_f$ , 1H, (overlap)), 7.88 ( $H_g$ , 1H, (overlap)), 7.89 ( $H_h$ , 1H, (overlap)), 7.98 ( $H_i$ , 1H, s).  $^{13}\text{C-NMR}$ : 120.65 ( $C_a$ , t,  $J_{13\text{C}-19\text{F}}=241.8$  Hz), 122.95 ( $C_b$ , t,  $J_{13\text{C}-19\text{F}}=4.6$  Hz), 125.64 ( $C_c$ , t,  $J_{13\text{C}-19\text{F}}=6.5$  Hz), 126.97 ( $C_d$ ), 127.53 ( $C_e$ ), 127.63 ( $C_f$ , t,  $J_{13\text{C}-19\text{F}}=5.5$  Hz), 127.89 ( $C_g$ ), 128.77 ( $C_h$ ), 128.81 ( $C_i$ ), 128.86 ( $C_j$ ), 132.58 ( $C_k$ ), 133.96 ( $C_l$ ), 134.48 ( $C_m$ , t,  $J_{13\text{C}-19\text{F}}=28.1$  Hz), 136.28 ( $C_n$ , (overlap)), 136.29 ( $C_o$ , t,  $J_{13\text{C}-19\text{F}}=28.8$  Hz).  $^{19}\text{F-NMR}$ : -88.47 (2F, s). MS EI: 288.0524 ( $\text{M}^+$ ).

#### Synthesis of **6b**: 4-(difluoro(3,4,5-trimethoxyphenyl)methyl)benzonitrile



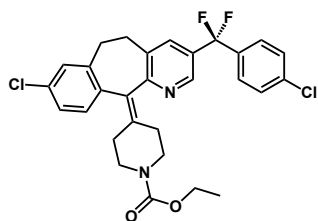
Method C was used with  $\text{Pd}(\text{PPh}_3)_4$  (0.150 mmol, 173.5 mg), 5-bromo-1,2,3-trimethoxybenzene (0.185 mmol, 45.6 mg),  $\text{TMSCF}_3$  (0.30 mmol, 44  $\mu\text{L}$ ), 18-crown-6 (0.150 mmol, 39.6 mg),  $\text{KO}^t\text{Bu}$  (0.152 mmol, 17.1 mg),  $\text{B}(\text{C}_6\text{F}_5)_3$  (0.151 mmol, 77.1 mg), 4-cyanophenylboronic acid (0.150 mmol, 22.0 mg),  $\text{NMe}_4\text{F}$  (0.301 mmol, 28.0 mg). With respect to  $\text{PhOCF}_3$  as internal standard 19% overall in situ yield was obtained. The reaction mixture was dried onto 750 mg of  $\text{SiO}_2$  and eluted on a 25g Biotage column with a gradient of 100% hexanes to 100% ethyl acetate at the rate of 75 mL/min, 8-10 column volumes. Two additional 100 g columns at the rate of 12 mL/min were required as well as a preparatory TLC (25% ethyl acetate) for **6b** affording 4.5 mg, 9% isolated yield.

$^1\text{H-NMR}$  ( $\text{CDCl}_3$ ): 3.85 ( $H_a$ , 6H, s), 3.87 ( $H_b$ , 3H, s), 6.66 ( $H_c$ , 2H, s), 7.64 ( $H_d$ , 2H, d,  $J_{1\text{H}-1\text{H}}=8.2$  Hz), 7.73 ( $H_e$ , 2H, d,  $J_{1\text{H}-1\text{H}}=8.2$  Hz).  $^{13}\text{C-NMR}$ : 56.43 ( $C_a$ ), 61.04 ( $C_b$ ), 103.21 ( $C_c$ ), 114.25 ( $C_d$ ), 118.14 ( $C_e$ ), 119.78 ( $C_f$ , t,  $J_{13\text{C}-19\text{F}}=243.9$  Hz), 126.79 ( $C_g$ , t,  $J_{13\text{C}-19\text{F}}=5.3$  Hz), 131.68 ( $C_h$ , t,  $J_{13\text{C}-$



$^{19}\text{F}$ -NMR: -28.1 Hz), 132.52 ( $C_i$ ), 139.75 ( $C_j$ ), 142.18 ( $C_k$ , t,  $J_{13\text{C}-19\text{F}}=29.6$  Hz), 153.56 ( $C_l$ ).  $^{19}\text{F}$ -NMR: -89.30 (2F, s). MS EI: 319.1024 (M<sup>+</sup>).

**Synthesis of 6c: ethyl 4-(8-chloro-3-((4-chlorophenyl)difluoromethyl)-5,6-dihydro-11H-benzo[5,6]cyclohepta[1,2-b]pyridin-11-ylidene)piperidine-1-carboxylate**



Method C was used with Pd(PPh<sub>3</sub>)<sub>4</sub> (0.150 mmol, 173.7 mg), ethyl 4-(3-bromo-8-chloro-5,6-dihydro-11H-benzo[5,6]cyclohepta[1,2-b]pyridin-11-ylidene)piperidine-1-carboxylate (0.179 mmol, 82.6 mg), TMSCF<sub>3</sub> (0.30 mmol, 44  $\mu\text{L}$ ), 18-crown-6 (0.150 mmol, 39.6 mg), KO<sup>t</sup>Bu (0.151 mmol, 16.9 mg), B(C<sub>6</sub>F<sub>5</sub>)<sub>3</sub> (0.301 mmol, 154.1 mg), 4-chlorophenylboronic acid (0.152 mmol, 23.8 mg), NMe<sub>4</sub>F (0.298 mmol, 27.8 mg). With respect to PhOCF<sub>3</sub> as internal standard 5% overall in situ yield was obtained. The reaction mixture was dried onto 750 mg of SiO<sub>2</sub> and eluted on a 25g Biotage column with a gradient of 100% hexanes to 100% ethyl acetate at the rate of 75 mL/min, 10 column volumes. After column chromatography, a basified preparatory TLC (25% ethyl acetate) was used, affording 6.7 mg of a mixture of **6c** and a -(C<sub>6</sub>F<sub>5</sub>) coupled product. The identity of **6c** was confirmed by HRMS and NMR spectroscopy. Additional purification attempts to remove the -(C<sub>6</sub>F<sub>5</sub>) containing product from the sample involved running a longer, slower column, stirring with NMe<sub>4</sub>F in MeCN, and protonating with an HCl in ether solution. Unfortunately, none of these methods resulted in a cleaner sample of **6c**.

$^1\text{H}$ -NMR (CDCl<sub>3</sub>): 1.26 (3H), 2.33 (3H), 2.49 (1H), 2.83 (2H), 3.17 (2H), 3.40 (2H), 3.78 (2H), 4.15 (2H), 7.17 (2-4H), 7.42 (2-4H), 7.51 (1H), 7.72 (1H), 8.47 (1H).  $^{19}\text{F}$ -NMR: -89.08 (2F, s). HRMS ESI: 543.1402 (M+H)<sup>+</sup>.

### Chapter 3 Bibliography

1. Berger, R.; Resnati, G.; Metrangolo, P.; Weber, E.; Hulliger, J. *Chem. Soc. Rev.* 2011, *40*, 3496-3508.
2. Fujiwara, T.; O'Hagan, D. *J. Fluor. Chem.* 2014, *167*, 16-29.
3. Gillis, E. P.; Eastman, K. J.; Hill, M. D.; Donnelly, D. J.; Meanwell, N. A. *J. Med. Chem.* 2015, *58*, 8315-8359.
4. Mei, H.; Han, J.; Fustero, S.; Medio-Simon, M.; Sedgwick, D. M.; Santi, C.; Ruzziconi, R.; Soloshonok, V. A. *Chem. Eur. J.* 2019, *25*, 11797-11819.
5. Mei, H.; Remete, A. M.; Zou, Y.; Moriwaki, H.; Fustero, S.; Kiss, L.; Soloshonok, V. A.; Han, J. *Chin. Chem. Lett.* 2020, *31*, 2401-2413
6. Not including biologics or combinations of previously approved drugs. See reference 7 for method.
7. Ilardi, E. A.; Vitaku, E.; Njardarson, J. T. *J. Med. Chem.* 2014, *57*, 2832-2842.
8. Wiles, R. J.; Phelan, J. P.; Molander, G. A. *Chem. Commun.* 2019, *55*, 7599-7602.
9. Vogt, D. B.; Seath, C. P.; Wang, H.; Jui, N. T. *J. Am. Chem. Soc.* 2019, *141*, 13203-13211.
10. Jang, Y. J.; Rose, D.; Mirabi, B.; Lautens, M. *Angew. Chem. Int. Ed.* 2018, *57*, 16147-16151.
11. Fu, X.-P.; Xue, X.-S.; Zhang, X.-Y.; Xiao, Y.-L.; Zhang, S.; Guo, Y.-L.; Leng, X.; Houk, K. N.; Zhang, X. *Nat. Chem.* 2019, *11*, 948-956.
12. Alonso, C.; Martínez de Marigorta, E.; Rubiales, G.; Palacios, F. *Chem. Rev.* 2015, *115*, 1847-1935.
13. Charpentier, J.; Früh, N.; Togni, A. *Chem. Rev.* 2015, *115*, 650-682.
14. Hu, J. Y.; Zhang, J. L. Hydrodefluorination Reactions Catalyzed by Transition-Metal Complexes. In *Organometallic Fluorine Chemistry*, Braun, T.; Hughes, R. P., Eds. Springer Int Publishing: Cham, 2015; Vol. 52, pp 143-196.
15. Hu, J.; Zeng, Y. *Rep. Org. Chem.* 2015, *5*, 19.
16. Neumann, C. N.; Ritter, T. *Angew. Chem. Int. Ed.* 2015, *54*, 3216-3221.
17. Campbell, M. G.; Ritter, T. *Chem. Rev.* 2015, *115*, 612-633.
18. Liu, X.; Xu, C.; Wang, M.; Liu, Q. *Chem. Rev.* 2015, *115*, 683-730.
19. Ni, C.; Hu, M.; Hu, J. *Chem. Rev.* 2015, *115*, 765-825.
20. Liu, W.; Groves, J. T. *Angew. Chem. Int. Ed.* 2013, *52*, 6024-6027.
21. Xia, J.-B.; Zhu, C.; Chen, C. *J. Am. Chem. Soc.* 2013, *135*, 17494-17500.
22. Luo, C.; Bandar, J. S. *J. Am. Chem. Soc.* 2019, *141*, 14120-14125.
23. Merchant, R. R.; Edwards, J. T.; Qin, T.; Kruszyk, M. M.; Bi, C.; Che, G.; Bao, D.-H.; Qiao, W.; Sun, L.; Collins, M. R.; Fadeyi, O. O.; Gallego, G. M.; Mousseau, J. J.; Nuhant, P.; Baran, P. S. *Science* 2018, *360*, 75.
24. Geri, J. B.; Wade Wolfe, M. M.; Szymczak, N. K. *J. Am. Chem. Soc.* 2018, *140*, 9404-9408.

25. Miller, E.; Kim, S.; Gibson, K.; Derrick, J. S.; Toste, F. D. *J. Am. Chem. Soc.* 2020, *142* (19), 8946-8952.
26. Nambo, M.; Yim, J. C. H.; Freitas, L. B. O.; Tahara, Y.; Ariki, Z. T.; Maekawa, Y.; Yokogawa, D.; Crudden, C. M. *Nat. Commun.* 2019, *10*, 4528.
27. Cho, E. J.; Senecal, T. D.; Kinzel, T.; Zhang, Y.; Watson, D. A.; Buchwald, S. L. *Science* 2010, *328*, 1679-1681.
28. Gu, J.-W.; Guo, W.-H.; Zhang, X. *Org. Chem. Front.* 2015, *2*, 38-41.
29. Stahl, T.; Klare, H. F. T.; Oestreich, M. *ACS Catal.* 2013, *3*, 1578-1587.
30. Amii, H.; Uneyama, K. *Chem. Rev.* 2009, *109*, 2119-2183.
31. Fuchibe, K.; Hatta, H.; Oh, K.; Oki, R.; Ichikawa, J. *Angew. Chem. Int. Ed.* 2017, *56*, 5890-5893.
32. Terao, J.; Begum, S. A.; Shinohara, Y.; Tomita, M.; Naitoh, Y.; Kambe, N. *Chem. Commun.* 2007, (8), 855-857.
33. Butcher, T. W.; Yang, J. L.; Amberg, W. M.; Watkins, N. B.; Wilkinson, N. D.; Hartwig, J. F. *Nature* 2020, *583* (7817), 548-553.
34. Zi, Y.; Lange, M.; Schultz, C.; Vilotijevic, I. *Angew. Chem. Int. Ed.* 2019, *58*, 10727-10731.
35. Sati, G. C.; Martin, J. L.; Xu, Y.; Malakar, T.; Zimmerman, P. M.; Montgomery, J. *J. Am. Chem. Soc.* 2020, *142*, 7235-7242.
36. Haufe, G.; Suzuki, S.; Yasui, H.; Terada, C.; Kitayama, T.; Shiro, M.; Shibata, N. *Angew. Chem. Int. Ed.* 2012, *51*, 12275-12279.
37. Scott, V. J.; Çelenligil-Çetin, R.; Ozerov, O. V. *J. Am. Chem. Soc.* 2005, *127*, 2852-2853.
38. Stahl, T.; Klare, H. F. T.; Oestreich, M. *ACS Catal.* 2013, *3*, 1578-1587.
39. Clark, G. R.; Hoskins, S. V.; Roper, W. R. *J. Organomet. Chem.* 1982, *234*, C9-C12.
40. Koola, J. D.; Roddick, D. M. *Organometallics* 1991, *10*, 591-597.
41. Ferguson, D. M.; Bour, J. R.; Canty, A. J.; Kampf, J. W.; Sanford, M. S. *Organometallics* 2019, *38*, 519-526.
42. Lee, G. M.; Korobkov, I.; Baker, R. T. *J. Organomet. Chem.* 2017, *847*, 270-277.
43. Richmond, T. G.; Crespi, A. M.; Shriver, D. F. *Organometallics* 1984, *3*, 314-319.
44. Leclerc, M. C.; Bayne, J. M.; Lee, G. M.; Gorelsky, S. I.; Vasiliu, M.; Korobkov, I.; Harrison, D. J.; Dixon, D. A.; Baker, R. T. *J. Am. Chem. Soc.* 2015, *137* (51), 16064-16073.
45. Tskhovrebov, A. G.; Lingnau, J. B.; Fürstner, A. *Angew. Chem. Int. Ed.* 2019, *58*, 8834-8838.
46. Levin, M. D.; Chen, T. Q.; Neubig, M. E.; Hong, C. M.; Theulier, C. A.; Kobylanskii, I. J.; Janabi, M.; O'Neil, J. P.; Toste, F. D. *Science* 2017, *356*, 1272.
47. Ferguson, D. M.; Bour, J. R.; Canty, A. J.; Kampf, J. W.; Sanford, M. S. *J. Am. Chem. Soc.* 2017, *139* (34), 11662-11665.
48. Jana, R.; Pathak, T. P.; Sigman, M. S. *Chem. Rev.* 2011, *111*, 1417-1492.
49. Grushin, V. V.; Marshall, W. J. *J. Am. Chem. Soc.* 2006, *128*, 12644-12645.
50. Note that Pd(CF<sub>3</sub>)<sub>3</sub>PPh<sub>3</sub><sup>-</sup> was prepared by disproportionation, not transmetalation, see ref. 49 for details.
51. Patrick, T. B.; Qian, S. *Org. Lett.* 2000, *2*, 3359-3360.
52. Okamoto, A.; Arnold, D. R. *Can. J. Chem.* 1985, *63*, 2341-2342.
53. Simoni, D.; Rossi, M.; Bertolasi, V.; Roberti, M.; Pizzirani, D.; Rondanin, R.; Baruchello, R.; Invidiata, F. P.; Tolomeo, M.; Grimaudo, S.; Merighi, S.; Varani, K.; Gessi, S.; Borea,

- P. A.; Marino, S.; Cavallini, S.; Bianchi, C.; Siniscalchi, A. *J. Med. Chem.* 2005, *48*, 3337-3343.
54. Purohit, A.; Benetti, R.; Hayes, M.; Guaraldi, M.; Kagan, M.; Yalamanchilli, P.; Su, F.; Azure, M.; Mistry, M.; Yu, M.; Robinson, S.; Dischino, D. D.; Casebier, D. *Bioorg. Med. Chem. Lett.* 2007, *17*, 4882-4885.
55. Sheng, J.; Ni, H.-Q.; Liu, G.; Li, Y.; Wang, X.-S. *Org. Lett.* 2017, *19*, 4480-4483.
56. Transmetalation of  $-C_6F_5$  is generally difficult (see refs. 57 - 59).
57. Barlow, G. K.; Boyle, J. D.; Cooley, N. A.; Ghaffar, T.; Wass, D. F. *Organometallics* 2000, *19*, 1470-1476.
58. Shabalin, A. Y.; Adonin, N. Y.; Bardin, V. V.; Parmon, V. N. *Tetrahedron* 2014, *70*, 3720-3725.
59. Piers, W. E. The Chemistry of Perfluoroaryl Boranes. In *Adv. Organomet. Chem.*, West, R., Hill, A., Eds., Academic Press: Cambridge, MA, 2005; Vol. 52, pp 1-76.
60. Klabunde, K. J.; Low, J. Y. F. *J. Am. Chem. Soc.* 1974, *96* (25), 7674-7680.
61. Slattery, J. M.; Hussein, S. *Dalton Trans.* 2012, *41*, 1808-1815.
62. Mandal, D.; Gupta, R.; Young, R. D. *J. Am. Chem. Soc.* 2018, *140*, 10682-10686.
63. Bayne, J. M.; Stephan, D. W. *Chem. Eur. J.* 2019, *25*, 9350-9357.
64. Carden, J. L.; Dasgupta, A.; Melen, R. L. *Chem. Soc. Rev.* 2020, *49*, 1706-1725.
65. Willcox, D.; Melen, R. L. *Trends Chem.* 2019, *1*, 625-626.
66. Partyka, D. V. *Chem. Rev.* 2011, *111*, 1529-1595.
67. Jacobsen, H.; Berke, H.; Döring, S.; Kehr, G.; Erker, G.; Fröhlich, R.; Meyer, O. *Organometallics* 1999, *18*, 1724-1735.
68. Montgomery, J. I.; Toogood, P. L.; Hutchings, K. M.; Liu, J.; Narasimhan, L.; Braden, T.; Dermeyer, M. R.; Kulynych, A. D.; Smith, Y. D.; Warmus, J. S.; Taylor, C. *Bioorg. Med. Chem. Lett.* 2009, *19*, 665-669.
69. Kuroda, K.; Tsuyumine, S.; Kodama, T. *Org. Process Res. Dev.* 2016, *20*, 1053-1058.
70. Aiello, S.; Wells, G.; Stone, E. L.; Kadri, H.; Bazzi, R.; Bell, D. R.; Stevens, M. F. G.; Matthews, C. S.; Bradshaw, T. D.; Westwell, A. D. *J. Med. Chem.* 2008, *51*, 5135-5139.
71. Heinrich, T.; Seenisamy, J.; Emmanuvel, L.; Kulkarni, S. S.; Bomke, J.; Rohdich, F.; Greiner, H.; Esdar, C.; Krier, M.; Grädler, U.; Musil, D. *J. Med. Chem.* 2013, *56*, 1160-1170.
72. Min, Q.-Q.; Yin, Z.; Feng, Z.; Guo, W.-H.; Zhang, X. *J. Am. Chem. Soc.* 2014, *136*, 1230-1233.
73. Xiao, Y.-L.; Zhang, B.; Feng, Z.; Zhang, X. *Org. Lett.* 2014, *16*, 4822-4825.
74. Uehling, M. R.; King, R. P.; Krska, S. W.; Cernak, T.; Buchwald, S. L. *Science* 2019, *363*, 405-408.

## Chapter 4 Synthetic Approaches to Construct C–CF<sub>2</sub>Ph Bonds Using a Nucleophilic Borazine–CF<sub>2</sub>Ph Reagent

### 4.1 Introduction

The development of new reagents and synthetic strategies to install fluorine into organic molecules has been a highly targeted pursuit over the past two decades.<sup>1</sup> Many recent agrochemicals<sup>2</sup> and pharmaceutical compounds<sup>3</sup> and contain C–F bonds as prominent motifs, which for the latter, often improve their properties compared to their non-fluorinated counterparts (higher metabolic stability and lipophilicity).<sup>3</sup> Among the organofluorine motifs, –CF<sub>3</sub> groups are the most common, which likely stems from available synthetic methods and the wide abundance of trifluoromethylating sources such as Me<sub>3</sub>Si–CF<sub>3</sub>,<sup>4,5</sup> and related radical<sup>6</sup> and electrophilic reagents.<sup>7</sup> In contrast, there are significantly fewer routes to install internal C–F bonds,<sup>8-16</sup> some of which require potentially explosive reagents (deoxyfluorination).<sup>17</sup> Within the last several years, transition metal catalysis has become an increasingly popular strategy to install CF<sub>2</sub>R motifs.<sup>18-23</sup> The Zhang group (**Figure 4.1 a**) has recently advanced this field by using halodifluoromethyl arenes<sup>24,25</sup> and alkanes<sup>26,27</sup> as radical/electrophilic partners in conjunction with organonucleophiles to form products with internal –CF<sub>2</sub>– linkages. The Crudden and Baran groups have investigated difluoromethyl aryl and difluoroalkyl sulfones, another class of radical/electrophilic reagents that can be further transformed into ArCF<sub>2</sub>R products.<sup>28-30</sup> Unlike the –CF<sub>3</sub> group, orthogonal nucleophilic methodologies to install –CF<sub>2</sub>Ar groups remain largely underdeveloped.<sup>31-33</sup> We

anticipated that a Lewis-acidic boron based scaffold could provide broad routes to related compounds with  $-\text{CF}_2\text{Ar}$  functionality.

Our group recently reported a strategy to access anionic  $-\text{CF}_2\text{Ar}$  reagents stabilized by a borazine Lewis acid, enabling a diverse array of chemical transformations from simple  $\text{H}-\text{CF}_2\text{Ar}$  precursors.<sup>34</sup> We previously found that hexamethylborazine Lewis-acid adducts of  $[\text{CF}_2\text{Ar}]^-$  ( $\text{Ar} = \text{Ph}$ ; **1a**) react with select electrophilic substrates through 1,2-addition (ketones, imines), C-H functionalization of electron deficient (hetero)arenes, and stoichiometric cross coupling.<sup>34</sup> In this manuscript we report additional strategies to use this reagent to construct new C-C bonds (**Figure 4.1 b**).

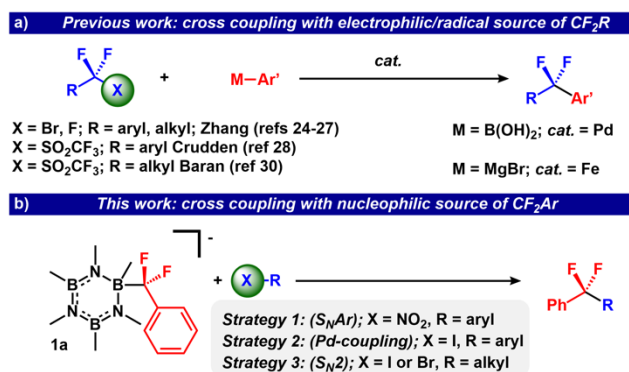


**Figure 4.1** a) Previous work: cross-coupling reactions of aryl and alkyl  $\text{CF}_2\text{X}$ . b) This work: nucleophilic strategies to form C-C<sub>F</sub> bonds

## 4.2 Difluorobenzyl C(sp<sup>2</sup>)-C(sp<sup>3</sup>) Coupling through $\text{S}_{\text{N}}\text{Ar}$ and Pd Cross-coupling

Lucy S. Yu helped contribute to this subchapter.

We targeted a series of general reactions to enable C(sp<sup>2</sup>)-C(sp<sup>3</sup>) coupling across electronically diverse arenes. Nucleophilic aromatic substitution,  $\text{S}_{\text{N}}\text{Ar}$ , is a powerful strategy that leverages the inherent reactivity of electron deficient arenes toward strong nucleophiles, including  $-\text{CF}_2\text{Ar}^-$ .<sup>34,35</sup> Importantly, the arene reactivity in these types of reactions is dominated by the strength of the electron withdrawing groups.<sup>35</sup> We first evaluated the reactivity limits of electron

deficient *para*-substituted nitro arenes using **1a** as the nucleophile to form phenyl difluoromethylene arene products. When 1 equiv. **1a** was introduced to 1.2 equiv. of 1,4-dinitrobenzene (Hammett  $\sigma$  value of *p*-NO<sub>2</sub> = 0.78) in THF solvent at room temperature, **3a** formed in 37% yield (**Figure 4.2**). In contrast, when the less electron deficient substrates, 1,4-cyanonitrobenzene ( $\sigma$  of *p*-CN = 0.66) and 4-nitrobenzotrifluoride ( $\sigma$  of *p*-CF<sub>3</sub> = 0.54) were subjected to identical conditions, **3b** and **3c** formed in only 11% and 4% yield respectively. When 1,4-bromonitrobenzene ( $\sigma$  of *p*-Br = 0.23) was used, 1% of the *S<sub>N</sub>Ar* product **3d** was formed. These results establish clear electronic limits to form C(sp<sup>2</sup>)-CF<sub>2</sub>Ar bonds using an *S<sub>N</sub>Ar* methodology.<sup>36</sup>

To access electron-neutral and rich C(sp<sup>2</sup>)-CF<sub>2</sub>Ar products, we targeted catalytic cross-coupling. Unlike *S<sub>N</sub>Ar* reactions, Pd-mediated cross coupling can functionalize even unactivated aryl-halogen bonds. For this reaction type, aryl iodides were selected as ideal substrates because they readily undergo oxidative addition. We previously reported stoichiometric cross coupling of phenyl iodide with **1a** in the presence of 1 eq. of Pd(PPh<sub>3</sub>)<sub>4</sub>,<sup>34</sup> at 0.02 M concentration. To modify these reaction conditions to be catalytic with respect to Pd(PPh<sub>3</sub>)<sub>4</sub>, we held the concentration of Pd constant (0.02 M, 10 mol%), while increasing the concentration of **1a** and Ph-I to 0.2 M.

When a THF solution containing these reagents was combined and mixed at 50 °C, **2a** formed in 35% yield after 20 h. Dilution of the concentration of **1a** and Ph-I to 0.02M resulted in an improvement to 60% yield. Unfortunately, other commonly used Pd precursors such as Pd(OAc)<sub>2</sub> and Pd<sub>2</sub>(dba)<sub>3</sub>•CHCl<sub>3</sub> in conjunction with classical Suzuki coupling ligands, such as SPhos,<sup>37</sup> P(*o*-tol)<sub>3</sub>,<sup>38</sup> DPEPhos<sup>39</sup> and diadamantyl butyl phosphine<sup>25, 40</sup> did not significantly improve yields (see **Table 4.2** for more details). In contrast, analysis of the solvent effects revealed that non-polar solvents, such as toluene and DME improved the reaction to over 80% (8 TON) yield. Finally, when the catalyst loading was reduced to 5%, we obtained 65 % yield (13 TON) in

DME or 72% yield (14 TON) in toluene. Further decreasing the catalyst loading to 2% caused a dramatic decrease in yield to 3%. We also observed that while a slight excess (1.2 equiv.) of phenyl iodide improved the yield, super-stoichiometric quantities were detrimental to productive catalysis (Table 4.1, entry 6). Finally, we observed a negligible difference at 50 °C and 25 °C.

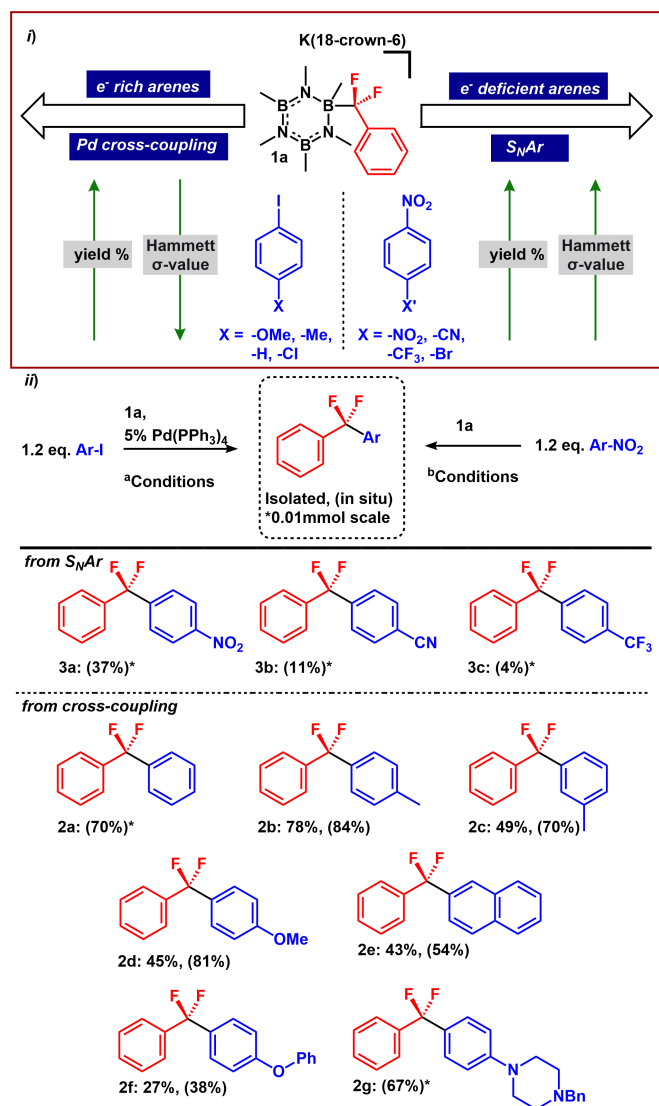
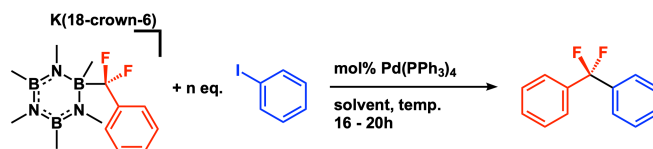


**Figure 4.2** i) Electronic trends with Pd catalyzed cross-coupling and  $S_NAr$ . ii) Scope in cross coupling and  $S_NAr$ . In situ yields measured by  $^{19}F$  NMR with respect to an internal standard, trifluoromethyl anisole. Mass purity of isolated samples measured by  $^{19}F$  NMR with respect to an internal standard, trifluoromethyl anisole. <sup>a</sup>Conditions: reactions performed in toluene (0.02M) at 25 °C, 16h with 5 mol% Pd(PPh<sub>3</sub>)<sub>4</sub>. <sup>b</sup>Conditions: reactions performed in THF (0.02M) at 25 °C, 18h.



**Table 4.1** Optimization of Pd catalyzed sp<sup>2</sup>-sp<sup>3</sup> cross coupling. In situ yields were measured by <sup>19</sup>F NMR with respect to an internal standard, trifluoromethyl anisole or by GC-FID. <sup>a</sup>Reaction run in triplicate, error bars reported as 3 standard deviations from the mean.



Entry	Solvent	(M)	Pd <sup>0</sup> %	PhI (eq.)	°C	Yield%	TON
1	THF	0.2	10	1.03	50	35	3.5
2	THF	0.02	10	1.03	50	60	6.0
3	DME	0.02	10	1.03	50	81±4 <sup>a</sup>	8.1
4	DME	0.02	5	1.03	50	65	13.0
5	DME	0.02	2	1.03	50	3	1.5
6	DME	0.02	5	3	50	28	5.6
7	<b>Tol</b>	<b>0.02</b>	<b>5</b>	<b>1.2</b>	<b>50</b>	<b>72</b>	<b>14.4</b>
8	<b>Tol</b>	<b>0.02</b>	<b>5</b>	<b>1.2</b>	<b>25</b>	<b>70</b>	<b>14.0</b>

Although a variety of soluble Pd precatalysts are routinely added in C-C cross coupling reactions, several of these reactions have been shown to operate via an active *heterogenous* catalyst.<sup>41,42</sup> Based on our observation that the solvent had a larger impact on the reaction than selection of ligand, we questioned whether in the current system, Pd(PPh<sub>3</sub>)<sub>4</sub> might actually serve as a precursor to a heterogeneous Pd catalyst. A highly used method to test for an operative heterogeneous catalyst is through the addition of catalyst poisons *after* initiation of catalysis.<sup>43,44</sup> Because Hg forms amalgams with Pd, it is often used as an inhibitor of heterogeneous Pd catalysts.<sup>45,46</sup> To examine the effect of Hg on the coupling reaction, we initiated catalysis with 4-iodoanisole as a substrate at 25 °C for 100 min, then added ~300 eq. of Hg, and continued to follow

the reaction progress. We found that the rate profiles were identical with and without added Hg, consistent with an active homogeneous catalyst (**Figure 4.3**).

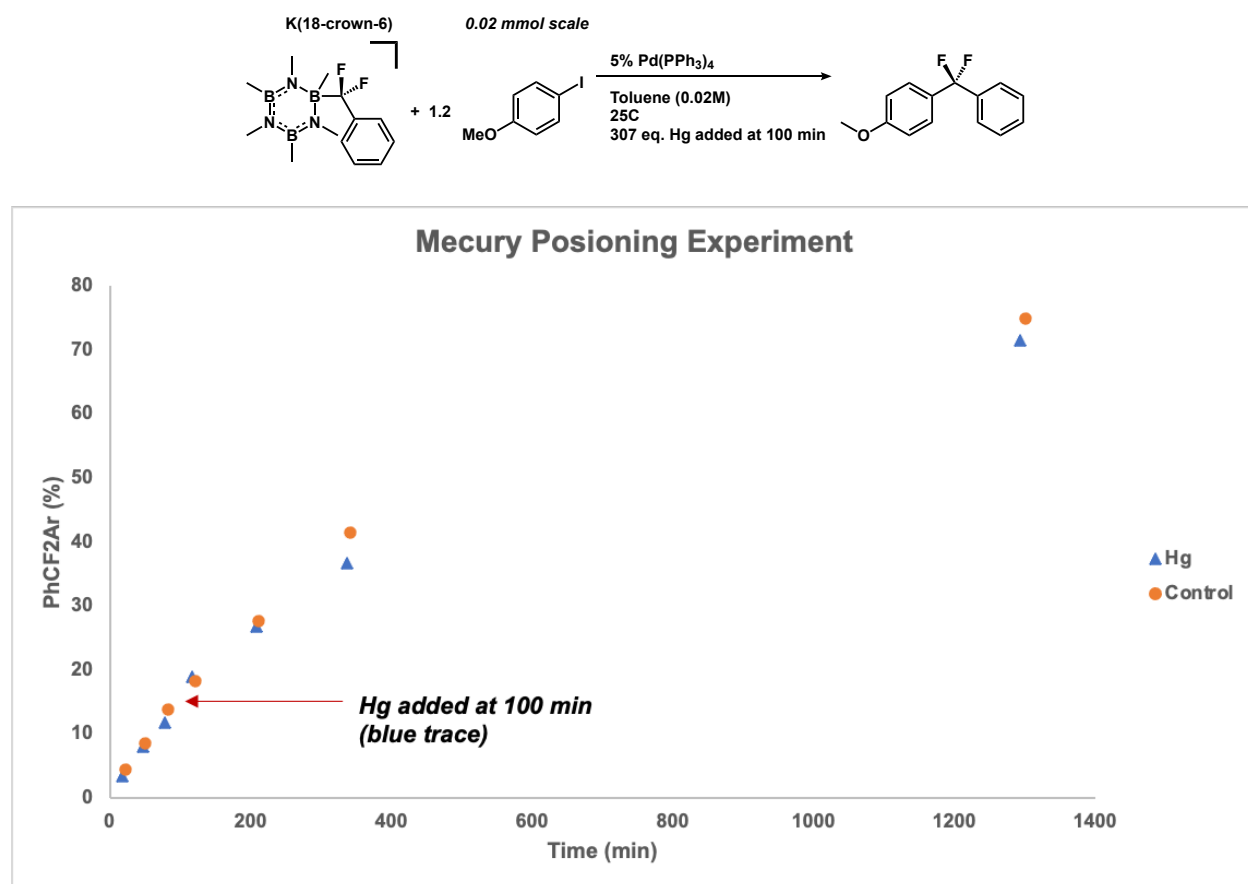


**Figure 4.3** Mercury poisoning experiment

The yield for catalytic cross coupling improved with simple electronic variations to the aryl iodide. Moderately electron-rich substrates (4-iodotoluene and 4-iodoanisole) improved the chemical yields to form **2b** and **2d** in 84% and 81% yields respectively. In conjunction with this observation, electron neutral substrates performed comparably to iodobenzene, (3-iodotoluene and 2-iodonaphthylene) forming the products **2c** (70% yield) and **2e** (54% yield). The more sterically encumbered derivatives (2-iodotoluene and 1-iodonaphthylene) performed poorly toward catalysis, (1 TON or less) in formation of **2i** and **2h**. We ascribe this steep decline in yield to the transmetalation step becoming more difficult and slower than uncatalyzed decomposition of **1a** to

difluoromethyl benzene. Larger electron rich substrates performed in moderate to good yield **2f** (38%) and **2g** (67%).

Unfortunately, electron deficient arenes such as 4-fluoroiodo benzene and 4-chloriodobenzene, provided 1 TON or less. In these cases, difluoromethyl benzene was the major product. We hypothesize that this dramatic decrease in catalytic activity is due to a combination of several detrimental factors: 1) steric accessibility for transmetalation, 2) electron-deficient Pd intermediates having lower rates of reductive elimination, 3) increased acidity of the iodoarene causing an increase in the rate of formation of difluoromethyl benzene. Overall, the  $S_NAr$  and Pd-catalyzed cross coupling reactions demonstrate that **1a** can be used to effect  $C(sp^2)$ - $C(sp^3)$  coupling reactions spanning both electron deficient ( $S_NAr$ ) and electron rich (cross-coupling) arenes.

### 4.3 Difluorobenzyl $C(sp^3)$ - $C(sp^3)$ Coupling through $S_N2$

Lucy S. Yu, Dr. Shuo Guo and Trenton Vogel helped contribute to this subchapter.

To complement the above methodology, we sought to evaluate  $C(sp^3)$ - $C(sp^3)$  bond formation with **1a**.  $S_N2$  reactions represent an attractive application of carbon nucleophiles, and although such transformations are known for select perfluorinated TMS reagents ( $CF_3$ ,  $C_2F_5$ ,  $C(CF_3)_3$ ,  $C(CF_3)_2(C_3F_7)$ ),<sup>47</sup> they have not been reported using TMS- $CF_2Ar$  reagents. We found that when either 1-iodobutane or 1-bromobutane were allowed to react with **1a** at elevated temperature (90 °C) in toluene, the corresponding C-C coupled product ((1,1-difluoropentyl)benzene; **4a**) formed in 83% and 84% chemical yield, respectively. These simple substrates demonstrate the feasibility of an  $S_N2$  pathway that outcompetes the undesired E2 pathway. Benzyl bromide proved to be more challenging as a substrate, forming 1,1-difluoro-1,2-diphenylethane (**4b**) in only 32% chemical yield. For this substrate, the remaining mass balance was difluorotoluene. We propose a competitive deprotonation pathway for this substrate at the benzylic  $CH_2$  site, noting the high

basicity of PhCF<sub>2</sub>.<sup>34</sup> For a benzyl bromide containing less acidic benzylic -CH<sub>2</sub>- groups (p-OMe-benzyl bromide), we found lower yields of the S<sub>N</sub>2 reaction to form **4c**. This result highlights a needed balance of the benzylic carbon electrophilicity compared to its acidity.

We evaluated the viability of this method in the presence of oxetanes, which are valuable motifs in drug discovery. Such units have been shown to act as a bioisostere, mimicking conformational and electronic properties of *gem*-dimethyl and carbonyl substitutions, while imparting improved physiochemical properties to target molecules.<sup>48</sup> In other applications, fluorinated oxetanes are desirable functional groups that undergo polymerization under photoinduced or cationic conditions.<sup>49</sup> We found that an oxetane is retained under the reaction conditions with substrate **4e**, which formed in 92% chemical yield. Compared to prior routes to fluorinated oxetanes (acid-promoted ring closure of fluorinated diols<sup>50</sup>), our methodology enables a 1-step route from a commercially available electrophile.

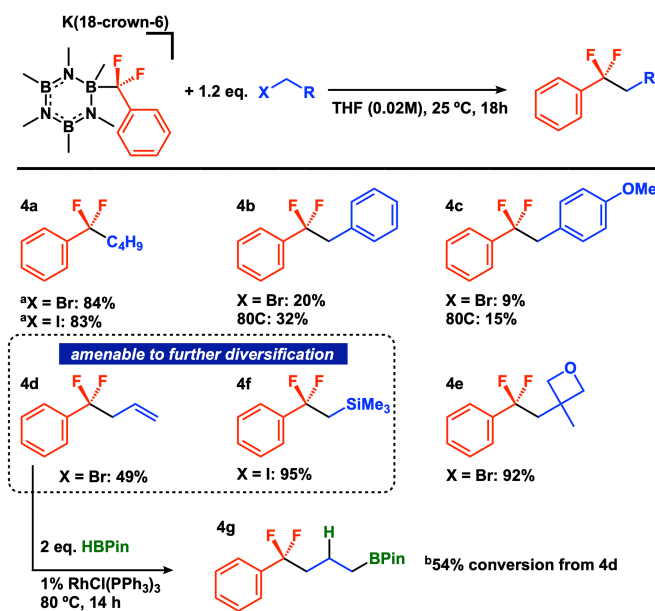


**Figure 4.4** S<sub>N</sub>2 reactions with alkyl halides. Reactions performed on 0.01-0.02 mmol scale In situ yields measured by <sup>19</sup>F NMR with respect to an internal standard, trifluoromethyl anisole. <sup>a</sup>Reaction performed at 90 °C, 30 min in toluene. <sup>b</sup>After formation of **4d**, solids removed by filtration and allyl bromide removed by vacuum. **4d** heated to 80 °C in 1.2 mL THF in the presence of pinacol borane (2eq.) and RhCl(PPh<sub>3</sub>)<sub>3</sub> for 14 h.

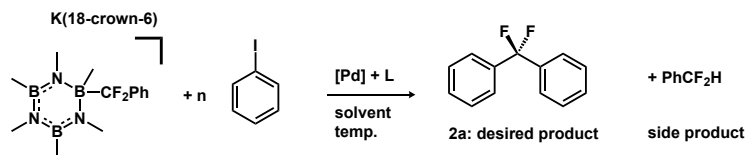
We next evaluated whether the  $S_N2$  pathway could provide access to fluoroalkylated units that are readily diversifiable.  $I-CH_2SiMe_3$  has been used as a  $-CH_2-$  linchpin in the total syntheses of Cephalotaxus esters.<sup>51</sup> We found that, even though  $I-CH_2SiMe_3$  contains a competitive  $-SiMe_3$  Lewis acidic site, it cleanly reacted with **1a** at room temperature to form (2,2-difluoro-2-phenylethyl)trimethylsilane (**4f**) in 95%. We next examined allyl bromide, which is a highly reactive electrophile whose terminal olefin product can easily undergo either reductive or oxidative functionalization reactions. We found that substrate **4d**, formed in 49% yield. To demonstrate the feasibility of a tandem reaction sequence, this product underwent hydroboration to afford **4g** in 54%. Overall, access to both of these reaction products establishes that  $S_N2$  fluoroalkylation can be used as a key intermediate step in a larger reaction sequence to form high value products from simple building blocks.

#### 4.4 Conclusions

In conclusion, we demonstrated an operationally simple approach that uses nucleophilic  $PhCF_2^-$  precursors for both Pd-catalyzed and metal-free ( $S_NAr$  and  $S_N2$ ) C-C coupling reactions. The latter approach offers a distinct advantage when compared to  $RCF_2-Br$  reagents, whose reactions require a metal mediator.<sup>27</sup> Importantly, we show that these methods tolerate substrates that are amenable to further diversification, potentially highlighting this methodology as a modular route to incorporate  $-CF_2-$  linkages within a longer reaction sequence.

## 4.5 Experimental Details

### 4.5.1 Optimization of Pd Catalysis



**General Method:** Catalyst was allowed to mix with ligand and then phenyl iodide at room temperature. **1a** and internal standard were added and the reaction was stirred (1000 rpm) in 0.5 mL of solvent in a 8 mL scintillation vial at 50 °C or 25 °C overnight. Yields were determined by GCFID with hexamethylbenzene (HMB) as internal standard, unless indicated with \*, where PhOCF<sub>3</sub> as internal standard and yields were determined by <sup>19</sup>F NMR.

<sup>a</sup>Yields are slightly inflated due to addition of internal standard by weigh paper in the glovebox.

<sup>b</sup>Reaction was performed in triplicate in order to determine reproducibility.

Blue vs. black entries annotate different batches of reactions set up.

Pd<sub>2</sub>(dba)<sub>3</sub> chloroform adduct was used

**Table 4.2** Reaction optimization for sp<sup>2</sup>-sp<sup>3</sup> coupling

Entry	Catalyst	mol %	Ligand	mol%	Temp. (°C)	Solvent	Conc. (M)	Time, (h)	PhI eq.	Yield %
1*	Pd(PPh <sub>3</sub> ) <sub>4</sub>	10	-	-	50	THF	0.2	20	1	36
2*	Pd(PPh <sub>3</sub> ) <sub>4</sub>	10	P( <i>o</i> -tol) <sub>3</sub>	15	50	THF	0.2	20	1	36
3*	Pd(PPh <sub>3</sub> ) <sub>4</sub>	10	DPEphos	10	50	THF	0.2	20	1	42
4*	Pd(PPh <sub>3</sub> ) <sub>4</sub>	10	PAd <sub>2</sub> Bu	15	50	THF	0.2	20	1	32
5*	Pd(PPh <sub>3</sub> ) <sub>4</sub>	10	SPhos	15	50	THF	0.2	20	1	34

6*	Pd(OAc) <sub>2</sub>	10	-	-	50	THF	0.2	20	1	0
7*	Pd(OAc) <sub>2</sub>	10	P( <i>o</i> -tol) <sub>3</sub>	15	50	THF	0.2	20	1	0
8*	Pd(OAc) <sub>2</sub>	10	DPEphos	10	50	THF	0.2	20	1	22
9*	Pd(OAc) <sub>2</sub>	10	PAd <sub>2</sub> Bu	15	50	THF	0.2	20	1	15
10*	Pd(OAc) <sub>2</sub>	10	SPhos	15	50	THF	0.2	20	1	3
11*	Pd <sub>2</sub> (dba) <sub>3</sub>	4.5	-	-	50	THF	0.2	20	1	0.2
12*	Pd <sub>2</sub> (dba) <sub>3</sub>	4.5	P( <i>o</i> -tol) <sub>3</sub>	15	50	THF	0.2	20	1	0.2
13*	Pd <sub>2</sub> (dba) <sub>3</sub>	4.5	DPEphos	10	50	THF	0.2	20	1	10
14*	Pd <sub>2</sub> (dba) <sub>3</sub>	4.5	PAd <sub>2</sub> Bu	15	50	THF	0.2	20	1	0.4
15*	Pd <sub>2</sub> (dba) <sub>3</sub>	4.5	SPhos	15	50	THF	0.2	20	1	0.7
16	Pd(PPh <sub>3</sub> ) <sub>4</sub>	10	-	-	50	THF	0.2	20	1.03	35
17	Pd(PPh <sub>3</sub> ) <sub>4</sub>	10	-	-	50	THF	0.1	20	1.03	51
18	Pd(PPh <sub>3</sub> ) <sub>4</sub>	10	-	-	50	THF	0.05	20	1.03	63
19	Pd(PPh <sub>3</sub> ) <sub>4</sub>	10	-	-	50	THF	0.02	20	1.03	60
20	Pd(OAc) <sub>2</sub>	10	PAd <sub>2</sub> Bu	10	50	THF	0.02	20	1	31
21	Pd(OAc) <sub>2</sub>	10	PAd <sub>2</sub> Bu	20	50	THF	0.02	20	1	41
22	Pd(OAc) <sub>2</sub>	10	PAd <sub>2</sub> Bu	30	50	THF	0.02	20	1	37
23	Pd(OAc) <sub>2</sub>	10	PAd <sub>2</sub> Bu	40	50	THF	0.02	20	1	35
24	Pd(OAc) <sub>2</sub>	10	PAd <sub>2</sub> Bu	50	50	THF	0.02	20	1	34
25	Pd(dba) <sub>2</sub>	10	PAd <sub>2</sub> Bu	20	50	THF	0.02	20	1	4
26	(PdallylCl) <sub>2</sub>	5	PAd <sub>2</sub> Bu	20	50	THF	0.02	20	1	10
27	(IrCODCl) <sub>2</sub>	5	PAd <sub>2</sub> Bu	20	50	THF	0.02	20	1	0
28 <sup>a</sup>	Pd(PPh <sub>3</sub> ) <sub>4</sub>	10	-	-	50	Toluene	0.02	20	1.03	96
29 <sup>a</sup>	Pd(PPh <sub>3</sub> ) <sub>4</sub>	10	-	-	50	DME	0.02	20	1.03	93
30 <sup>a</sup>	Pd(PPh <sub>3</sub> ) <sub>4</sub>	10	-	-	50	THF	0.02	20	1.03	84
31 <sup>a</sup>	Pd(PPh <sub>3</sub> ) <sub>4</sub>	10	-	-	50	Dioxane	0.02	20	1.03	91
32 <sup>a</sup>	Pd(PPh <sub>3</sub> ) <sub>4</sub>	10	-	-	50	DMSO	0.02	20	1.03	0

33 <sup>a</sup>	Pd(PPh <sub>3</sub> ) <sub>4</sub>	10	-	-	50	DMF	0.02	20	1.03	64
34 <sup>a</sup>	Pd(PPh <sub>3</sub> ) <sub>4</sub>	10	-	-	50	Anisole	0.02	20	1.03	90
35 <sup>b</sup>	Pd(PPh <sub>3</sub> ) <sub>4</sub>	10	-	-	50	DME	0.02	20	1.03	80
36 <sup>b</sup>	Pd(PPh <sub>3</sub> ) <sub>4</sub>	10	-	-	50	DME	0.02	20	1.03	79
37 <sup>b</sup>	Pd(PPh <sub>3</sub> ) <sub>4</sub>	10	-	-	50	DME	0.02	20	1.03	82
38	Pd(PPh <sub>3</sub> ) <sub>4</sub>	5	-	-	50	DME	0.02	20	1.03	65
39	Pd(PPh <sub>3</sub> ) <sub>4</sub>	2	-	-	50	DME	0.02	20	1.03	3
40	Pd(PPh <sub>3</sub> ) <sub>4</sub>	1	-	-	50	DME	0.02	20	1.03	0.4
41	Pd(PPh <sub>3</sub> ) <sub>4</sub>	5	-	-	50	Toluene	0.02	20	1.03	68
42	Pd(PPh <sub>3</sub> ) <sub>4</sub>	5	-	-	50	DME	0.02	20	1.03	69
43	Pd(PPh <sub>3</sub> ) <sub>4</sub>	5	-	-	50	THF	0.02	20	1.03	54
44	Pd(PPh <sub>3</sub> ) <sub>4</sub>	5	-	-	50	Dioxane	0.02	20	1.03	72
45	Pd(PPh <sub>3</sub> ) <sub>4</sub>	5	-	-	50	Anisole	0.02	20	1.03	60
46	Pd(PPh <sub>3</sub> ) <sub>4</sub>	5	-	-	50	DME	0.02	20	1	55
47	Pd(PPh <sub>3</sub> ) <sub>4</sub>	5	-	-	50	DME	0.02	20	1.2	66
48	Pd(PPh <sub>3</sub> ) <sub>4</sub>	5	-	-	50	DME	0.02	20	1.5	57
49	Pd(PPh <sub>3</sub> ) <sub>4</sub>	5	-	-	50	DME	0.02	20	2	48
50	Pd(PPh <sub>3</sub> ) <sub>4</sub>	5	-	-	50	DME	0.02	20	3	28
51*	Pd(PPh <sub>3</sub> ) <sub>4</sub>	5	-	-	50	Toluene	0.02	18	1.2	72
52*	Pd(PPh <sub>3</sub> ) <sub>4</sub>	5	-	-	25	Toluene	0.02	18	1.2	70
53*	Pd(PPh <sub>3</sub> ) <sub>4</sub>	5	-	-	25	Toluene	0.02	16	1.2	64
54*	none	-	-	-	25	Toluene	0.02	16	1.2	0



#### 4.5.2 Scope in $sp^2$ - $sp^3$ Coupling (2a-2k)

##### Method A:

In a 20 mL scintillation vial charged with a magnetic stir bar,  $\text{Pd}(\text{PPh}_3)_4$  (0.005 mmol) was combined with iodoarene (0.12 mmol) in 5 mL toluene.  $\text{PhOCF}_3$  (0.1 mmol, 13.2  $\mu\text{L}$ ) was added as an inert  $^{19}\text{F}$  NMR internal standard.  $[\text{Me}_6\text{B}_3\text{N}_3\text{CF}_2\text{Ph}]\text{K}(18\text{-c-}6)$  **1a** (0.1 mmol) was added and the reaction mixture stirred (1000 rpm) for 16 hours at 25  $^\circ\text{C}$ .

##### Method A\*: 0.01 mmol

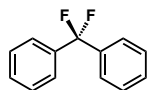
Vial 1: **1a** (0.01 mmol) was directly weighed into an 8 mL scintillation vial.

Vial 2: In a separate 20 mL scintillation vial  $\text{Pd}(\text{PPh}_3)_4$  (0.004 mmol, 0.001 M) and  $\text{PhOCF}_3$  (0.08 mmol, 10.6  $\mu\text{L}$ , 0.02 M) were dissolved in 4 mL of toluene to generate a stock solution.

Vial 3: In a separate 20 mL vial, a 1.5 mL aliquot of vial 2 solution was allowed to mix with iodoarene (0.036 mmol, 0.024 M).

A 0.5 mL aliquot from vial 3 was transferred to vial 1, a magnetic stir bar was added and the reaction was stirred (1000 rpm) at 25  $^\circ\text{C}$  for 16 h. Yields were determined by  $^{19}\text{F}$  NMR spectroscopy.

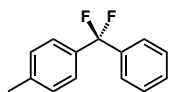
##### Synthesis of **2a**: difluorodiphenylmethane



Method A\* was used with **1a** (0.01 mmol, 5.8 mg) and iodobenzene (0.012 mmol). Reaction ran for 18 h. With respect to  $\text{PhOCF}_3$  as  $^{19}\text{F}$  internal standard, 70% in situ yield of **2a** was obtained.

Spectroscopic features were in good agreement in comparison to the compound reported in the literature.<sup>34</sup>

##### Synthesis of **2b**: 1-(difluoro(phenyl)methyl)-4-methylbenzene



Method A was used with **1a** (0.101 mmol, 60.0 mg), 4-iodotoluene (0.122 mmol, 26.5 mg), Pd(PPh<sub>3</sub>)<sub>4</sub> (0.0048 mmol, 5.6 mg). With respect to PhOCF<sub>3</sub> as <sup>19</sup>F internal standard, 84% in situ yield was obtained. The reaction mixture directly loaded onto a 100g Biotage column and eluted with 100% hexanes at the rate of 25 mL/min, 3-8 column volumes for isolation of **2b**, 17.2 mg 78% yield. After NMR analysis, **2b** was reconstituted and assessed by quantitative <sup>19</sup>F NMR with respect to PhOCF<sub>3</sub> (10.0 μL). 77% purity by mass was found (compared to 17.4 mg sample).

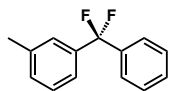
<sup>1</sup>H-NMR (CDCl<sub>3</sub>): 2.38 (*H<sub>a</sub>*, 3H, s), 7.22 (*H<sub>b</sub>*, 2H, (d, *J*<sub>1H-1H</sub>=8.1 Hz)), 7.39 (*H<sub>c</sub>*, 2H, OL), 7.41 (*H<sub>d</sub>*, 2H, OL), 7.42 (*H<sub>e</sub>*, 1H, OL), 7.51 (*H<sub>f</sub>*, 2H, (dd, *J*<sub>1H-1H</sub>=6.9, 2.7 Hz)).

<sup>13</sup>C-NMR: 21.41 (*C<sub>a</sub>*), 121.00 (*C<sub>b</sub>*, t, *J*<sub>13C-19F</sub>=241.2 Hz), 125.93 (*C<sub>c</sub>*, OL), 125.96 (*C<sub>d</sub>*, OL), 128.48 (*C<sub>e</sub>*), 129.16 (*C<sub>f</sub>*), 129.90 (*C<sub>g</sub>*, t, *J*<sub>13C-19F</sub>=2.1 Hz), 135.00 (*C<sub>h</sub>*, t, *J*<sub>13C-19F</sub>=28.2 Hz), 137.99 (*C<sub>i</sub>*, t, *J*<sub>13C-19F</sub>=28.5 Hz), 140.04 (*C<sub>j</sub>*, t, *J*<sub>13C-19F</sub>=2.4 Hz).

<sup>19</sup>F-NMR: -88.22.

MS EI: 218.0910 (M<sup>+</sup>).

### Synthesis of **2c**: 1-(difluoro(phenyl)methyl)-3-methylbenzene



Method A was used with **1a** (0.101 mmol, 60.0 mg), 3-iodotoluene (0.120 mmol, 15.4 μL), Pd(PPh<sub>3</sub>)<sub>4</sub> (0.0050 mmol, 5.8 mg). With respect to PhOCF<sub>3</sub> as <sup>19</sup>F internal standard, 70% in situ yield was obtained. The reaction mixture directly loaded onto a 100g Biotage column and eluted with 100% hexanes at the rate of 25 mL/min, 3-5 column volumes. Some of the material was subjected to a second column; (10g, 18mL/min, 3 column volumes) for isolation of **2c**, 10.8 mg

49% yield. After NMR analysis, **2c** was reconstituted and assessed by quantitative  $^{19}\text{F}$  NMR with respect to  $\text{PhOCF}_3$  (10.0  $\mu\text{L}$ ). 83% purity by mass was found (compared to 10.7 mg sample).

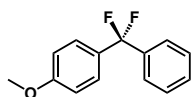
$^1\text{H}$ -NMR ( $\text{CDCl}_3$ ): 2.37 ( $H_a$ , 3H, s), 7.23 ( $H_b$ , 1H, m), 7.30 ( $H_c$ , 1H, OL), 7.30 ( $H_d$ , 1H, OL), 7.32 ( $H_e$ , 1H, s), 7.41 ( $H_f$ , 2H, OL), 7.43 ( $H_g$ , 1H, OL), 7.51 ( $H_h$ , 2H, m).

$^{13}\text{C}$ -NMR: 21.59 ( $C_a$ ), 120.89 ( $C_b$ , t,  $J_{13\text{C}-19\text{F}}=241.4$  Hz), 123.06 ( $C_c$ , t,  $J_{13\text{C}-19\text{F}}=5.7$  Hz), 125.95 ( $C_d$ , t,  $J_{13\text{C}-19\text{F}}=5.7$  Hz), 126.48 ( $C_e$ , t,  $J_{13\text{C}-19\text{F}}=5.5$  Hz), 128.42 ( $C_f$ ), 128.49 ( $C_g$ ), 129.93 ( $C_h$ , t,  $J_{13\text{C}-19\text{F}}=2.1$  Hz), 130.72 ( $C_i$ , t,  $J_{13\text{C}-19\text{F}}=2.1$  Hz), 137.74 ( $C_j$ , t,  $J_{13\text{C}-19\text{F}}=28.2$  Hz), 137.94 ( $C_k$ , t,  $J_{13\text{C}-19\text{F}}=28.5$  Hz), 138.35 ( $C_l$ ).

$^{19}\text{F}$ -NMR: -88.75.

MS EI: 218.0914 ( $\text{M}^+$ ).

### Synthesis of **2d**: 1-(difluoro(phenyl)methyl)-4-methoxybenzene



Method A was used with **1a** (0.101 mmol, 59.9 mg), 4-iodoanisole (0.118 mmol, 27.7 mg),  $\text{Pd}(\text{PPh}_3)_4$  (0.0050 mmol, 5.8 mg). With respect to  $\text{PhOCF}_3$  as  $^{19}\text{F}$  internal standard, 81% in situ yield was obtained. The reaction mixture directly loaded onto a 50g Biotage column and eluted with a gradient of 0-10% ethyl acetate in hexanes at the rate of 25 mL/min, 12-13 column volumes for isolation of **2d**, 10.5 mg 45% yield. After NMR analysis, **2d** was reconstituted and assessed by quantitative  $^{19}\text{F}$  NMR with respect to  $\text{PhOCF}_3$  (10.0  $\mu\text{L}$ ). 73% purity by mass was found (compared to 11.0 mg sample).

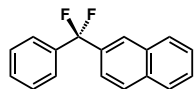
$^1\text{H-NMR}$  ( $\text{CDCl}_3$ ): 2.83 ( $H_a$ , 3H, s), 6.91 ( $H_b$ , 2H, (d,  $J_{1\text{H}-1\text{H}}=8.9$  Hz)), 7.41 ( $H_c$ , 2H, OL), 7.42 ( $H_d$ , 2H, OL), 7.42 ( $H_e$ , 1H, OL), 7.50 ( $H_f$ , 2H, (m)).

$^{13}\text{C-NMR}$ : 55.49 ( $C_a$ ), 113.79 ( $C_b$ ), 121.03 ( $C_c$ , t,  $J_{13\text{C}-19\text{F}}=240.8$  Hz), 126.02 ( $C_d$ , t,  $J_{13\text{C}-19\text{F}}=5.4$  Hz), 127.60 ( $C_e$ , t,  $J_{13\text{C}-19\text{F}}=5.4$  Hz), 128.46 ( $C_f$ ), 129.90 ( $C_g$ , t,  $J_{13\text{C}-19\text{F}}=2.0$  Hz), 130.14 ( $C_h$ , t,  $J_{13\text{C}-19\text{F}}=28.8$  Hz), 138.01 ( $C_i$ , t,  $J_{13\text{C}-19\text{F}}=28.6$  Hz), 160.81 ( $C_j$ , t,  $J_{13\text{C}-19\text{F}}=1.7$  Hz).

$^{19}\text{F-NMR}$ : -86.86.

MS EI: 234.0865 ( $\text{M}^+$ ).

### Synthesis of **2e**: 2-(difluoro(phenyl)methyl)naphthalene



Method A was used with **1a** (0.100 mmol, 59.8 mg), 2-iodonaphthalene (0.120 mmol, 30.4 mg),  $\text{Pd}(\text{PPh}_3)_4$  (0.0051 mmol, 5.9 mg). With respect to  $\text{PhOCF}_3$  as  $^{19}\text{F}$  internal standard, 54% in situ yield was obtained. The reaction mixture dry loaded onto a 25g Biotage column (using Davisil) and eluted with a 100% HPLC grade pentane at the rate of 25 mL/min, 5-10 column volumes for isolation of **2e**, 11.1 mg 43% yield. After NMR analysis, **2e** was reconstituted and assessed by quantitative  $^{19}\text{F}$  NMR with respect to  $\text{PhOCF}_3$  (10.0  $\mu\text{L}$ ). 88% purity by mass was found (compared to 11.1 mg sample).

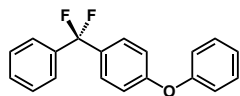
$^1\text{H-NMR}$  ( $\text{CO}(\text{CD}_3)_2$ ): 7.51 ( $H_a$ , 1H, OL), 7.52 ( $H_b$ , 2H, OL), 7.60 ( $H_c$ , 1H, OL), 7.61 ( $H_d$ , 1H, OL), 7.61 ( $H_e$ , 1H, OL), 7.62 ( $H_f$ , 2H, (OL)), 7.98 ( $H_g$ , 1H, m), 8.01 ( $H_h$ , 1H, OL), 8.02 ( $H_i$ , 1H, OL), 8.13 ( $H_j$ , 1H, s).

$^{13}\text{C-NMR}$ : 121.96 ( $C_a$ , t,  $J_{13\text{C}-19\text{F}}=241.3\text{Hz}$ ), 123.59 ( $C_b$ , t,  $J_{13\text{C}-19\text{F}}=4.8\text{ Hz}$ ), 126.03 ( $C_c$ , t,  $J_{13\text{C}-19\text{F}}=6.6\text{ Hz}$ ), 126.54 ( $C_d$ , t,  $J_{13\text{C}-19\text{F}}=5.6\text{ Hz}$ ), 127.81 ( $C_e$ ), 128.33 ( $C_f$ ), 128.61 ( $C_g$ ), 129.53 ( $C_h$ , OL), 129.54 ( $C_i$ , OL), 129.56 ( $C_j$ , OL), 130.99 ( $C_k$ , t,  $J_{13\text{C}-19\text{F}}=1.9\text{ Hz}$ ), 133.52 ( $C_l$ ), 134.75 ( $C_m$ ), 135.88 ( $C_n$ , t,  $J_{13\text{C}-19\text{F}}=28.3\text{ Hz}$ ), 138.57 ( $C_o$ , t,  $J_{13\text{C}-19\text{F}}=28.3\text{ Hz}$ ).

$^{19}\text{F-NMR}$ : -89.55.

MS EI: 254.0906 ( $\text{M}^+$ ).

### Synthesis of **2f**: 1-(difluoro(phenyl)methyl)-4-phenoxybenzene



Method A was used with **1a** (0.100 mmol, 59.7 mg), 1-iodo-4-phenoxybenzene (0.120 mmol, 35.5 mg),  $\text{Pd}(\text{PPh}_3)_4$  (0.0051 mmol, 5.9 mg). With respect to  $\text{PhOCF}_3$  as  $^{19}\text{F}$  internal standard, 38% in situ yield was obtained. The reaction mixture dry loaded onto a 25g Biotage column (using Davisil) and eluted with a gradient of 0-10% ethyl acetate in HPLC grade pentane at the rate of 25 mL/min, 9-18 column volumes for isolation of **2f**, 8.0 mg 27% yield. After NMR analysis, **2f** was reconstituted and assessed by quantitative  $^{19}\text{F}$  NMR with respect to  $\text{PhOCF}_3$  (10.0  $\mu\text{L}$ ). 81% purity by mass was found (compared to 8.0 mg sample).

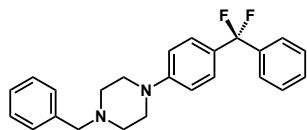
$^1\text{H-NMR}$  ( $\text{CDCl}_3$ ): 7.00 ( $H_a$ , 2H, (d,  $J_{1\text{H}-1\text{H}}=8.5$  Hz)), 7.04 ( $H_b$ , 2H, (d,  $J_{1\text{H}-1\text{H}}=8.0$  Hz)), 7.15 ( $H_c$ , 1H, (t,  $J_{1\text{H}-1\text{H}}=7.4$  Hz)), 7.36 ( $H_d$ , 2H, (t,  $J_{1\text{H}-1\text{H}}=7.7$  Hz)), 7.43 ( $H_e$ , 1H, OL), 7.44 ( $H_f$ , 2H, OL), 7.45 ( $H_g$ , 2H, OL), 7.52 ( $H_h$ , 2H, (dd,  $J_{1\text{H}-1\text{H}}=7.3, 2.3$  Hz)).

$^{13}\text{C-NMR}$ : 118.05 ( $C_a$ ), 119.74 ( $C_b$ ), 120.82 ( $C_c$ , t,  $J_{13\text{C}-19\text{F}}=241.1$  Hz), 124.16 ( $C_d$ ), 125.97 ( $C_e$ , t,  $J_{13\text{C}-19\text{F}}=5.5$  Hz), 127.78 ( $C_f$ , t,  $J_{13\text{C}-19\text{F}}=5.4$  Hz), 128.53 ( $C_g$ ), 130.01 ( $C_h$ , t,  $J_{13\text{C}-19\text{F}}=1.9$  Hz), 130.06 ( $C_i$ ), 132.35 ( $C_j$ , t,  $J_{13\text{C}-19\text{F}}=28.6$  Hz), 137.77 ( $C_k$ , t,  $J_{13\text{C}-19\text{F}}=28.6$  Hz), 156.39 ( $C_l$ ), 159.02 ( $C_m$ , t,  $J_{13\text{C}-19\text{F}}=1.9$  Hz).

$^{19}\text{F-NMR}$ : -87.36.

MS EI: 296.1018 ( $\text{M}^+$ ).

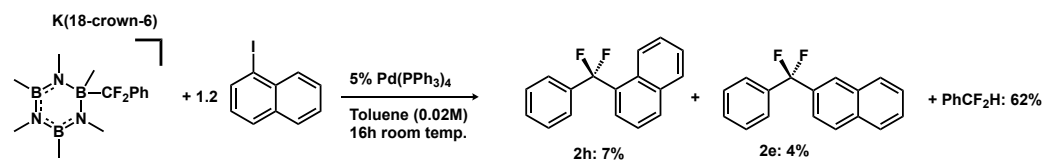
### Synthesis of **2g**: 1-benzyl-4-(4-(difluoro(phenyl)methyl)phenyl)piperazine



Method A\* was used with **1a** (0.01 mmol, 6.1 mg) and 1-benzyl-4-(4-iodophenyl)piperazine (0.012 mmol). Reaction ran for 16 h. With respect to  $\text{PhOCF}_3$  as  $^{19}\text{F}$  internal standard, 67% in situ yield of **2g** was obtained. Isolation proved to be too challenging; with normal chromatography, basified silica gel and reverse phase chromatography still not affording pure product.

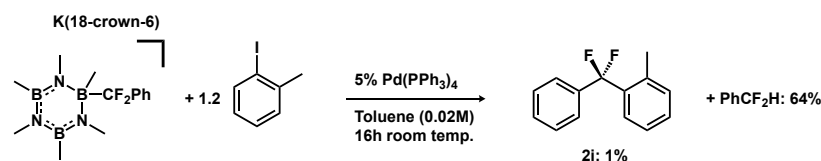
## Unsuccessful Substrates for $sp^2$ - $sp^3$ Coupling

### Synthesis Attempt of **2h**:



Method A\* was used with **1a** (0.01 mmol, 6.1 mg). Reaction ran for 16 h. With respect to PhOCF<sub>3</sub> as <sup>19</sup>F internal standard, 7% in situ yield of **2h** was obtained. **2e** was formed as a side product in 4% as well as difluoromethylbenzene in 62%.

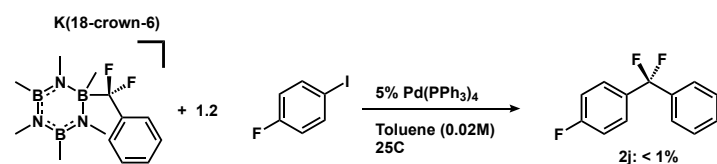
### Synthesis Attempt of **2i**:



Method A\* was used and reaction ran for 16 h. With respect to PhOCF<sub>3</sub> as <sup>19</sup>F internal standard, 1% in situ yield of **2i** was obtained with difluoromethylbenzene formed as a side product in 64%.

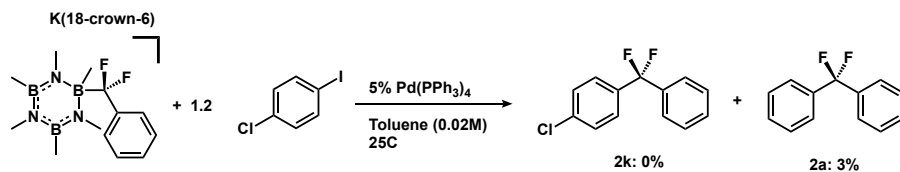
The yield was slightly improved to 5% by running the reaction at 50 °C.

### Synthesis Attempt of **2j**:



Method A\* was used and reaction ran for 16 h. With respect to PhOCF<sub>3</sub> as <sup>19</sup>F internal standard, <1% in situ yield of **2j** was obtained with difluoromethylbenzene formed as a side product in 80%.

### Synthesis Attempt of 2k:



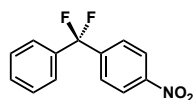
Method A\* was used with **1a** (0.01 mmol, 6.1 mg). Reaction ran for 16 h. With respect to PhOCF<sub>3</sub> as <sup>19</sup>F internal standard, 0% in situ yield of **2k** was obtained. **2a** was formed as a side product in 3% as well as difluoromethylbenzene in 49%.

### 4.5.3 Scope in S<sub>N</sub>Ar Reactions (3a-3d)

#### Method B:

In a 20 mL scintillation vial, nitroarene (0.024 mmol) was dissolved in 1 mL THF along with PhOCF<sub>3</sub> (0.04 mmol, 5.3 μL) as an inert <sup>19</sup>F NMR internal standard. [Me<sub>6</sub>B<sub>3</sub>N<sub>3</sub>CF<sub>2</sub>Ph]K(18-c-6) **1a** (0.02 mmol) was added and the mixture was halved and separated into sealed NMR tubes to further react at 25 °C or 80 °C. After 18.5 hours, in situ yields were analyzed by <sup>19</sup>F NMR.

#### Synthesis of 3a: 1-(difluoro(phenyl)methyl)-4-nitrobenzene-methane

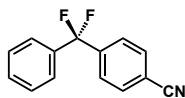


Method B was used with **1a** (0.02 mmol, 11.9 mg) and 1,4-dinitrobenzene (0.024 mmol). Reactions ran for 18.5 h at 25 °C and 80 °C. With respect to PhOCF<sub>3</sub> as <sup>19</sup>F internal standard, 37% in situ yield at 25 °C and 39% in situ yield at 80 °C of **3a** was obtained. Spectroscopic features were in good agreement in comparison to the compound reported in the literature.<sup>34</sup>

<sup>19</sup>F-NMR: -90.08 (s)



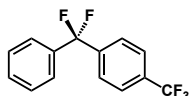
### Synthesis of **3b**: 4-(difluoro(phenyl)methyl)benzonitrile-methane



Method B was used with **1a** (0.02 mmol, 11.9 mg) and 4-nitrobenzonitrile (0.024 mmol). Reaction ran for 18.5 h at both 25 °C and 80 °C. With respect to PhOCF<sub>3</sub> as <sup>19</sup>F internal standard, 11% in situ yield at 25 °C and 80 °C of **3b** was obtained. Spectroscopic features were in good agreement in comparison to the compound reported in the literature.<sup>34</sup>

<sup>19</sup>F-NMR: -90.35 (s)

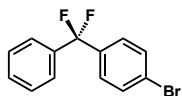
### Synthesis of **3c**: 1-(difluoro(phenyl)methyl)-4-(trifluoromethyl)benzene-methane



Method B was used with **1a** (0.02 mmol, 11.9 mg) and 4-nitrobenzotrifluoride (0.024 mmol). Reaction ran for 18.5 h at both 25 °C and 80 °C. With respect to PhOCF<sub>3</sub> as <sup>19</sup>F internal standard, 4% in situ yield at 25 °C and 80 °C of **3c** was obtained.

<sup>19</sup>F-NMR: -89.86 (s)

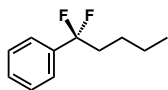
### Synthesis of **3d**: 1-bromo-4-(difluoro(phenyl)methyl)benzene-methane



Method B was used with **1a** (0.02 mmol, 11.9 mg) and 1-bromo-4-nitrobenzene (0.024 mmol). Reaction ran for 18.5 h at both 25 °C and 80 °C. With respect to PhOCF<sub>3</sub> as <sup>19</sup>F internal standard, 1% in situ yield at 25 °C and 2% in situ yield at 80 °C of **3d** was obtained.

#### 4.5.4 Scope in $S_N2$ Reactions (4a-4g)

##### Synthesis of 4a: (1,1-difluoropentyl)benzene



Two side-by-side reactions were performed. In two separate 8 mL scintillation vials with magnetic stir-bars, 1-bromobutane (0.024 mmol, 2.2  $\mu$ L) and 1-iodobutane (0.024 mmol, 2.3  $\mu$ L) were dissolved in 1 mL of toluene along with fluorobenzene (0.04 mmol, 3.8  $\mu$ L) as internal standard.  $[\text{Me}_6\text{B}_3\text{N}_3\text{CF}_2\text{Ph}]\text{K}(18\text{-c-}6)$  **1a** (0.02 mmol) was added and the mixture, and reactions were allowed to stir at 90  $^\circ\text{C}$ , 1000 rpm for 30 minutes. In situ yields of 84% (bromobutane) and 83% (iodobutane) were assessed by  $^{19}\text{F}$  NMR.

$^{19}\text{F}$ -NMR: -95.79 (t,  $J_{\text{H-}^{19}\text{F}} = 16.2$  Hz).

##### Method C:

In a 20 mL scintillation vial, alkyl halide (0.024 mmol) was dissolved in 1 mL THF along with  $\text{PhOCF}_3$  (0.04 mmol, 5.3  $\mu$ L) as an inert  $^{19}\text{F}$  NMR internal standard.  $[\text{Me}_6\text{B}_3\text{N}_3\text{CF}_2\text{Ph}]\text{K}(18\text{-c-}6)$  **1a** (0.02 mmol) was added and the mixture was halved and separated into sealed NMR tubes to further react at 25  $^\circ\text{C}$  or 80  $^\circ\text{C}$ . After 18 hours, in situ yields were analyzed by  $^{19}\text{F}$  NMR.

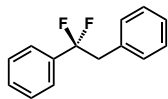
##### Method C\*: 0.02 mmol

Vial 1: Alkyl halide (0.024 mmol) was directly weighed into an 8 mL scintillation vial.

Vial 2: In a separate 20 mL scintillation vial, **1a** (0.06 mmol, 0.02 M) and  $\text{PhOCF}_3$  (0.06 mmol, 7.9  $\mu$ L, 0.02 M) were dissolved in 3 mL of THF to generate a stock solution.

A 1 mL aliquot from vial 2 was transferred to vial 1. The mixture was transferred into sealed NMR tubes to further react at 25  $^\circ\text{C}$ . After 18 hours, in situ yields were analyzed by  $^{19}\text{F}$  NMR.

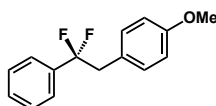
### Synthesis of 4b: (1,1-difluoroethane-1,2-diyl)dibenzene



Method C\* was used with **1a** (0.02 mmol) and benzyl bromide (0.024 mmol). Reaction ran for 18 h at 25 °C. With respect to PhOCF<sub>3</sub> as <sup>19</sup>F internal standard, 20% in situ yield at 25 °C of **4d** was obtained. With Method C at 80 °C, 32% in situ yield was obtained.

<sup>19</sup>F-NMR: -94.12 (t,  $J_{1H-19F} = 16.0$  Hz)

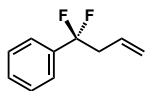
### Synthesis of 4c: 1-(2,2-difluoro-2-phenylethyl)-4-methoxybenzene



Method C was used with **1a** (0.02 mmol, 11.9 mg) and 4-methoxybenzyl bromide (0.024 mmol). Reaction ran for 18 h at both 25 °C and 80 °C. With respect to PhOCF<sub>3</sub> as <sup>19</sup>F internal standard, 9% in situ yield at 25 °C and 15% in situ yield at 80 °C of **4c** was obtained.

<sup>19</sup>F-NMR: -94.33 (t,  $J_{1H-19F} = 16.0$  Hz)

### Synthesis of 4d: (1,1-difluorobut-3-en-1-yl)benzene

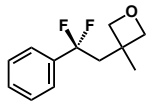


Method C\* was used with **1a** (0.02 mmol) and allyl bromide (0.024 mmol). Reaction ran for 18 h at 25 °C. With respect to PhOCF<sub>3</sub> as <sup>19</sup>F internal standard, 49% in situ yield at 25 °C of **4d** was obtained.

<sup>19</sup>F-NMR: -94.43 (t,  $J_{1H-19F} = 16.0$  Hz)

GCMS: 168 m/z

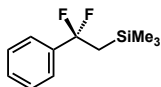
### Synthesis of 4e: 3-(2,2-difluoro-2-phenylethyl)-3-methyloxetane



Method C was used with **1a** (0.02 mmol, 11.9 mg) and 3-bromomethyl-3-methyloxetane (0.024 mmol). Reaction ran for 18 h at both 25 °C and 80 °C. With respect to PhOCF<sub>3</sub> as <sup>19</sup>F internal standard, 81% in situ yield at 25 °C and 80% in situ yield at 80 °C of **4e** was obtained. When reaction was repeated with Method C\*, ~92% in situ yield was obtained when comparing **4e** to the sole byproduct PhCF<sub>2</sub>H ~8%.

<sup>19</sup>F-NMR: -92.82 (t,  $J_{\text{H-}^{19}\text{F}} = 17.7$  Hz)

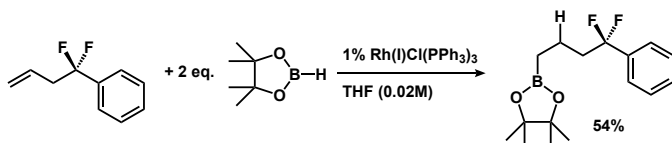
### Synthesis of 4f: (2,2-difluoro-2-phenylethyl)trimethylsilane



Method C\* was used with **1a** (0.02 mmol) and iodomethyl(trimethylsilane) (0.024 mmol). Reaction ran for 18 h at 25 °C. With respect to PhOCF<sub>3</sub> as <sup>19</sup>F internal standard, 95% in situ yield at 25 °C of **4f** was obtained.

<sup>19</sup>F-NMR: -80.18 (t,  $J_{\text{H-}^{19}\text{F}} = 20.8$  Hz)

### Synthesis of 4g: 2-(4,4-difluoro-4-phenylbutyl)-4,4,5,5-tetramethyl-1,3,2-dioxaborolane



Procedure: **4d** was formed following the above procedure (S56). Solid particulate matter was filtered through glass filter paper, and the resulting solution was concentrated under vacuum to remove unreacted allyl bromide. The solid residue was dissolved in 1mL of THF. A catalyst stock solution was made by dissolving RhCl(PPh<sub>3</sub>)<sub>3</sub> (0.01 mmol, 9.4 mg) in 1mL THF. Pinacolborane

(0.04 mmol, 5.8  $\mu$ L) was added to the reaction mixture followed by 20  $\mu$ L of Rh stock solution. The contents were transferred to a screwcap NMR tube and the vial was rinsed with  $\sim$ 200  $\mu$ L of THF. An initial 20 minute timepoint at 25  $^{\circ}$ C was acquired followed by heating to 80  $^{\circ}$ C for 14h. After heating, fluorobenzene (0.08 mmol, 7.5  $\mu$ L) was added as a new internal standard to quantify the amount of product formed by  $^{19}$ F. Comparison of remaining PhOCF<sub>3</sub> to fluorobenzene allowed for assessment of the conversion of **4d** to **4g** as 54% yield along with two other triplet products: (29%, unknown product), (17%, (1,1-difluorobutyl)benzene). The latter could be removed under vacuum and showed 170 m/z by GCMS. 1,2-difluoro-1,2-diphenylethene was also observed as a side-product.

$^{19}$ F-NMR: -95.02 (t,  $J_{\text{H-}^{19}\text{F}} = 16.3$  Hz)

HRMS ESI+: 296.2126 m/z

## Chapter 4 Bibliography

1. Mei, H.; Han, J.; Fustero, S.; Medio-Simon, M.; Sedgwick, D. M.; Santi, C.; Ruzziconi, R.; Soloshonok, V. A. *Chem. Eur. J.*, 2019, 25, 11797-11819.
2. Fujiwara, T.; O'Hagan, D. *J. Fluor. Chem.*, 2014, 167, 16-29.
3. Gillis, E. P.; Eastman, K. J.; Hill, M. D.; Donnelly, D. J.; Meanwell, N. A. *J. Med. Chem.*, 2015, 58, 8315-8359.
4. Krishnamurti, R.; Bellew, D. R.; Prakash, G. K. S. *J. Org. Chem.*, 1991, 56, 984-989.
5. Ispizua-Rodriguez, X.; Barrett, C.; Krishnamurti, V.; Prakash, G. K. S. in *The Curious World of Fluorinated Molecules*, ed. K. Seppelt, Elsevier, 2021, vol. 6, pp. 117-218.
6. Tommasino, J.-B.; Brondex, A.; Médebielle, M.; Thomalla, M.; Langlois, B. R.; Billard, T. *Synlett*, 2002, 2002, 1697-1699.
7. Charpentier, J.; Früh, N.; Togni, A. *Chem. Rev.*, 2015, 115, 650-682.
8. Vogt, D. B.; Seath, C. P.; Wang, H.; Jui, N. T. *J. Am. Chem. Soc.*, 2019, 141, 13203-13211.
9. Zhang, Y.; Lai, G.-W.; Nie, L.-J.; He, Q.; Lin, M.-J.; Chi, R.; Lu, D.-L.; Fan, X. *Org. Chem. Front.*, 2022, 9, 745-751.
10. Luo, C.; Bandar, J. S. *J. Am. Chem. Soc.*, 2019, 141, 14120-14125.
11. Levin, M. D.; O'vian, J. M.; Read, J. A.; Sigman, M. S.; Jacobsen, E. N. *J. Am. Chem. Soc.*, 2020, 142, 14831-14837.
12. Trifonov, A. L.; Dilman, A. D. *Org. Lett.*, 2021, 23, 6977-6981.
13. Yang, R.-Y.; Gao, X.; Gong, K.; Wang, J.; Zeng, X.; Wang, M.; Han, J.; Xu, B. *Org. Lett.*, 2022, 24, 164-168.
14. Rodríguez, R. I.; Sicignano, M.; Alemán, J. *Angew. Chem. Int. Ed.*, 2022, 61, e202112632.
15. Liu, C.; Shen, N.; Shang, R. *Nat. Commun.*, 2022, 13, 354.
16. Xia, J.-B.; Zhu, C.; Chen, C. *J. Am. Chem. Soc.*, 2013, 135, 17494-17500.
17. Markovskij, L. N.; Pashinnik, V. E.; Kirsanov, A. V. *Synthesis*, 1973, 1973, 787-789.
18. Xu, Z.-W.; Zhang, W.; Lin, J.-H.; Jin, C.-M.; Xiao, J.-C. *Chin. J. Chem.*, 2020, 38, 1647-1650.
19. Reina, A.; Krachko, T.; Onida, K.; Bouyssi, D.; Jeanneau, E.; Monteiro, N.; Amgoune, A. *ACS Catal.*, 2020, 10, 2189-2197.
20. Zhu, X.-L.; Huang, Y.; Xu, X.-H.; Qing, F.-L. *Org. Lett.*, 2020, 22, 5451-5455.
21. Carvalho, D. R.; Christian, A. H. *Org. Biomol. Chem.*, 2021, 19, 947-964.
22. Feng, Z.; Xiao, Y.-L.; Zhang, X. *Acc. Chem. Res.*, 2018, 51, 2264-2278.
23. Cho, E. J.; Senecal, T. D.; Kinzel, T.; Zhang, Y.; Watson, D. A.; Buchwald, S. L. *Science*, 2010, 328, 1679-1681.
24. Luo, Y.-C.; Tong, F.-F.; Zhang, Y.; He, C.-Y.; Zhang, X. *J. Am. Chem. Soc.*, 2021, 143, 13971-13979.
25. Gu, J.-W.; Guo, W.-H.; Zhang, X. *Org. Chem. Front.*, 2015, 2, 38-41.
26. An, L.; Tong, F.-F.; Zhang, X. *Huaxue Xuebao*, 2018, 76, 977-982.

27. An, L.; Xiao, Y.-L.; Zhang, S.; Zhang, X. *Angew. Chem. Int. Ed.*, 2018, 57, 6921-6925.
28. Nambo, M.; Yim, J. C. H.; Freitas, L. B. O.; Tahara, Y.; Ariki, Z. T.; Maekawa, Y.; Yokogawa, D.; Crudden, C. M. *Nat. Commun.*, 2019, 10, 4528.
29. Nambo, M.; Crudden, C. M. *Chem. Rec.*, 2021, 21, 3978-3989.
30. Merchant, R. R.; Edwards, J. T.; Qin, T.; Kruszyk, M. M.; Bi, C.; Che, G.; Bao, D. H.; Qiao, W.; Sun, L.; Collins, M. R.; Fadeyi, O. O.; Gallego, G. M.; Mousseau, J. J.; Nuhant, P.; Baran, P. S. *Science*, 2018, 360, 75-80.
31. Santos, L.; Panossian, A.; Donnard, M.; Vors, J.-P.; Pazenok, S.; Bernier, D.; Leroux, F. R. *Org. Lett.*, 2020, 22, 8741-8745.
32. Chai, J. Y.; Cha, H.; Kim, H. B.; Chi, D. Y. *Tetrahedron*, 2020, 76, 131370.
33. Khatri, H. R.; Han, C.; Luong, E.; Pan, X.; Adam, A. T.; Alshammari, M. D.; Shao, Y.; Colby, D. A. *J. Org. Chem.*, 2019, 84, 11665-11675.
34. Geri, J. B.; Wade Wolfe, M. M.; Szymczak, N. K. *J. Am. Chem. Soc.*, 2018, 140, 9404-9408.
35. Crampton, M. R. in *Organic Reaction Mechanisms · 2017*, 2020, ch. 5, pp. 213-295.
36. Hansch, C.; Leo, A.; Taft, R. W. *Chem. Rev.*, 1991, 91, 165-195.
37. Barder, T. E.; Walker, S. D.; Martinelli, J. R.; Buchwald, S. L. *J. Am. Chem. Soc.*, 2005, 127, 4685-4696.
38. Hartwig, J. F.; Paul, F. *J. Am. Chem. Soc.*, 1995, 117, 5373-5374.
39. Kranenburg, M.; van der Burgt, Y. E. M.; Kamer, P. C. J.; van Leeuwen, P. W. N. M.; Goubitz, K.; Fraanje, J. *Organometallics*, 1995, 14, 3081-3089.
40. Tewari, A.; Hein, M.; Zapf, A.; Beller, M. *Synthesis*, 2004, 2004, 935-941.
41. Phan, N. T. S.; Van Der Sluys, M.; Jones, C. W. *Adv. Synth. Catal.*, 2006, 348, 609-679.
42. Pagliaro, M.; Pandarus, V.; Ciriminna, R.; B eland, F.; Demma Car a, P. *ChemCatChem*, 2012, 4, 432-445.
43. Widegren, J. A.; Finke, R. G. *J. Mol. Catal. A Chem.*, 2003, 198, 317-341.
44. Crabtree, R. H. *Chem. Rev.*, 2012, 112, 1536-1554.
45. A recent study showed that Hg reacts with both Pd(0) and Pd(II) compounds, see: ref 46
46. Chernyshev, V. M.; Astakhov, A. V.; Chikunov, I. E.; Tyurin, R. V.; Eremin, D. B.; Ranny, G. S.; Khrustalev, V. N.; Ananikov, V. P. *ACS Catal.*, 2019, 9, 2984-2995.
47. Beier, P.; Zibinsky, M.; Prakash, G. K. S. *Organic Reactions* 2016, pp. 1-492.
48. Zhang, R.; Sun, M.; Yan, Q.; Lin, X.; Li, X.; Fang, X.; Sung, H. H. Y.; Williams, I. D.; Sun, J. *Org. Lett.*, 2022, 24, 2359-2364.
49. Vitale, A.; Bongiovanni, R.; Ameduri, B. *Chem. Rev.*, 2015, 115, 8835-8866.
50. Case, L. C.; Todd, C. C. *J. Polym. Sci.*, 1962, 58, 633-638.
51. Eckelbarger, J. D.; Wilmot, J. T.; Epperson, M. T.; Thakur, C. S.; Shum, D.; Antczak, C.; Tarassishin, L.; Djaballah, H. Gin, D. Y. *Chem. Eur. J.*, 2008, 14, 4293-4306.

## Chapter 5 Summary and Future Outlook

### 5.1 Summary

In this work, borane Lewis acids were used to stabilize fluoroalkyl anions as well as induce fluoride elimination from fluoroalkanes and palladium fluoroalkyl complexes. These principles were ultimately used to generate more chemically complex, pharmaceutically relevant molecules.

In Chapter 2, we demonstrated that nucleophilic trifluoromethyl-boron adducts operate through a dissociative mechanism. While boron Lewis acid adducts of fluoroalkanes mitigate  $\alpha$ -fluoride elimination, they induce  $\beta$ -fluoride elimination, and formation of boron fluoroalkenyl adducts is observed. These adducts are competent for fluoroalkenyl transfer and ultimately metal-free C–C<sub>F</sub> coupling reactions.

In Chapter 3, we further exploited the C–F bond-breaking reactions within anionic Pd fluoroalkyl complexes to generate new –CF<sub>2</sub>– linkages. Mild boron-based Lewis acids are sufficiently acidic to promote defluorination and form Pd difluorocarbenes which rapidly undergo 1,1-migratory insertion into a Pd-aryl bond. The resulting Pd-CF<sub>2</sub>Ar species can be subjected to transmetalation and reductive elimination to form medicinally relevant Ar'–CF<sub>2</sub>Ar, heteroaryl–CF<sub>2</sub>Ar, vinyl–CF<sub>2</sub>Ar molecules.

In Chapter 4, we further demonstrated the merit of using a nucleophilic difluorobenzyl-boron adduct by expanding the reaction scope of C–C coupling reactions. The previously established stoichiometric Pd cross-coupling reactions were amenable to catalysis. Finally, we



demonstrated metal-free nucleophilic substitution with primary alkyl halides. This powerful methodology tolerated common organic functional groups which could undergo reactions for further diversification.

## 5.2 Future Outlook

In Chapters 1 and 4, I discussed the limitations of using borazine-stabilized fluoroalkyl anions as  $\text{R}_\text{F}$  transfer reagents. Ideally, we could synthesize boron-based fluoroalkyl reagents that are robust to high temperatures and acidic protons and are competent for associative transmetalation to metal catalysts in cross-coupling. Fluoroalkyl boronic acids and esters  $[\text{B}(\text{OR})_2\text{R}_\text{F}]$  seem like ideal targets for stable reagents that are amenable to cross-coupling. Borane ( $\text{BH}_3$ ) is a simple template that can serve as a foundation for building fluoroalkyl boronic acids and esters (**Figure 5.1**).

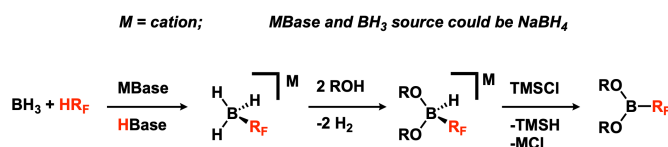


**Figure 5.1** Strategy to make fluoroalkyl boronic acids and esters from  $\text{BH}_3$

$\text{BH}_3$  has the potential to act as a Lewis acid and stabilize a fluoroalkyl anion after deprotonation. Importantly, the hydridic ligands of the  $[\text{H}_3\text{BR}_\text{F}]^-$  adduct can deprotonate alcohols, which would install the desired alkoxide ligands on to boron. Finally, the resulting  $[\text{HB}(\text{OR})_2\text{R}_\text{F}]^-$  species can either be treated with another equivalent of alcohol or  $\text{TMSCl}$  to form either a trialkoxy(fluoroalkyl)borate or a dialkoxy(fluoroalkyl)borane. Sodium borohydride ( $\text{NaBH}_4$ ) is an ideal reagent to test which could potentially serve as both a base for deprotonation of the fluoroalkane and a Lewis acid to stabilize the fluoroalkyl adduct. This strategy can be applied to generate a wide variety of fluoroalkyl borates and boranes of varying stability and nucleophilicity.

The stoichiometric Pd coupling methodology discussed in Chapter 3 can be made catalytic for hydrodefluorinative aryl coupling. This can be achieved via two possible strategies. First is the more ambitious approach of using a similar  $[\text{HB}(\text{OR})_2\text{CF}_2\text{Ph}]^-$  reaction to facilitate hydride transfer, fluoroalkyl transfer and fluoride abstraction. This would only require Pd, aryl halide, and perhaps exogenous phosphine in addition to  $[\text{HB}(\text{OR})_2\text{CF}_2\text{Ph}]^-$ . Second is the safer option of using a bromodifluoromethyl arene to initiate catalysis, followed by  $\text{BAr}_3$  to abstract fluoride and transfer an aryl group, as previously demonstrated. Finally  $\text{KHBET}_3$  or even  $\text{KH}$  can be used as the hydride source and terminal reductant which will ultimately reductively eliminate  $\text{ArCFHPh}$  as the product (**Figure 5.2**).

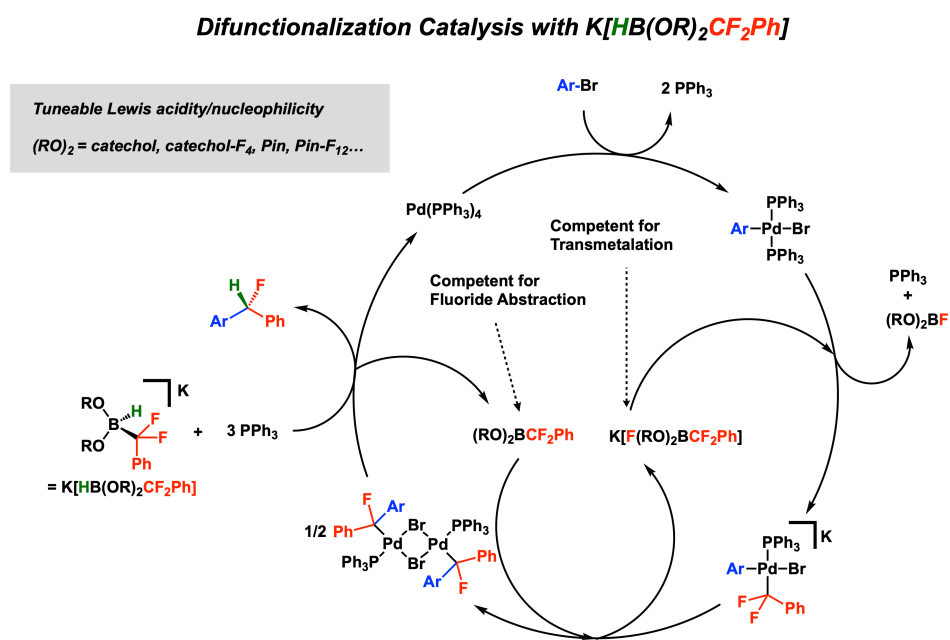


**Figure 5.2** Difunctionalization catalysis with  $\text{K}[\text{HB}(\text{OR})_2\text{CF}_2\text{Ph}]$

The challenge with the first strategy is that the borane reagent must be competent for *three* separate reactions ( $\text{H}^-$  transfer,  $^-\text{CF}_2\text{Ph}$  transfer and  $^-\text{F}$  abstraction). The fluorophilicity of a given aryl-boron reagent and the nucleophilicity of the related aryl-borate are *inversely correlated*. Thus, it is possible to tune both modes of reactivity of the boron-based reagent by modifying the R-group on the bidentate ligand. One can modify this ligand to make the boron more fluorophilic by

substitution of CH<sub>3</sub> groups on Pin with CF<sub>3</sub> or use of catechol or perfluorocatechol instead of Pin. TMSCl can be used to selectively abstract <sup>-</sup>H from to form the neutral (RO)<sub>2</sub>BCF<sub>2</sub>Ph reagents to be tested towards productive fluoride abstraction and transmetalation. The nucleophilicity of (RO)<sub>2</sub>BCF<sub>2</sub>Ph can be evaluated using <sup>-</sup>F as activator to transfer CF<sub>2</sub>Ph to ArPdBr(PPh<sub>3</sub>)<sub>2</sub>. The fluorophilicity of (RO)<sub>2</sub>BCF<sub>2</sub>Ph can be evaluated by monitoring fluoride abstraction from [ArPdCF<sub>2</sub>PhBrPPh<sub>3</sub>]<sup>-</sup>, one of the complexes reported in manuscript. The key requirement is for the reagent to be sufficiently fluorophilic to have <sup>-</sup>F abstraction outcompete reductive elimination of ArCF<sub>2</sub>Ph. Once an optimal reagent, capable of both reactions is found, a catalytic method can be developed by screening for different solvent and temperature additive requirements. It is possible that substoichiometric B(C<sub>6</sub>F<sub>5</sub>)<sub>3</sub> and/or TMSCl may be needed to initiate catalysis via <sup>-</sup>F or <sup>-</sup>H abstraction respectively.

The second strategy is a good fallback option, because we already have identified triaryl borane reagents that are capable of both <sup>-</sup>F abstraction and Ar transfer (Chapter 3). Use of BrCF<sub>2</sub>R reagents will eliminate compatibility issues between nucleophilic CF<sub>2</sub>R sources and Lewis acidic boranes. Since all 3 key reactions have been shown to work *separately* using this set of reagents, the main challenge will be optimization of ligand donor characteristics (donor strength/steric properties), aryl borane, and hydride source to achieve a productive catalytic cycle. These strategies will enable the development of catalytic reactions to convert either [HB(OR)<sub>2</sub>CF<sub>2</sub>Ph]<sup>-</sup> or RCF<sub>2</sub>Br into pharmaceutically important RCF(H)Ar units.